Fall 10-18-2012

Molecular mechanisms of spermine on its synergistic effect with beta-lactams against Staphylococcus aureus

Xiangyu Yao
Georgia State University

MOLECULAR MECHANISMS OF SPERMINE ON ITS SYNERGISTIC EFFECT WITH BETA-LACTAMS AGAINST *STAPHYLOCOCCUS AUREUS*

by

XIANGYU YAO

Under the Direction of Dr.Chung-Dar Lu

ABSTRACT

Spermine (Spm), a potent bactericidal polyamine, exerts a strong synergistic effect with β-lactams against methicillin-resistant *Staphylococcus aureus* (MRSA) in a pH-dependent manner. At high pH (>8) Spm is a potent nucleophile, and able to form Spm-β-lactam adduct. At physiological pH (or lower), Spm carries positive charges, and can bind to DNA through charge interactions. The potential of Spm interfering with cell wall was first investigated. A spontaneous mutant of MRSA Mu50 selected for Spm resistance conferred resistance to Spm/β-lactam synergy. This phenotype was due to the presence of a 7-bp deletion in *pbpB* as identified by genome resequencing and confirmed by complementation. Analysis of cell wall composition by HPLC revealed the combination of Spm and β-lactam can reduce the cross-linkage of peptidoglycan. These two lines of evidence suggest Spm may perturb cell wall integrity in favor of β-lactam efficacy with PBPs as a promising target. However, from the results of microarray analysis and fluorescent Bocillin labeling, Spm did not appear to suppress the PBPs expression or alter their interactions with β-lactams. Next, transcriptome analyses reveal the genes responsive to the synergy effect overlap extensively with those to high Spm challenge, implying the enhanced detrimental effect of

Spm facilitated by β-lactams in inhibition on cell growth. In particular the induction of iron transport and reduction of energy production under synergy were depicted in this study, and high dose Spm was found to turn off the SigB regulon. Of interest, the *tetM* gene encoding a ribosomal protection protein for tetracycline (Tc) resistance exhibited the most significant fold change and high signals by both high and low dose Spm. Further analysis by qRT-PCR demonstrated the *tetM* expression was specifically induced by Tc and Spm to a comparable level but not by other polyamines, suggesting a similar mode of action by Spm and Tc in interactions with the ribosome to initiate *tetM* induction. Collectively, these data indicated the role of Spm could be multifarious with more than one target, and a combination of Spm and β-lactams may inhibit growth of MRSA in a more complicated manner than just potentiating β-lactam inhibition on PBPs.

INDEX WORDS: Spermine, MRSA, Synergy, β-lactams

MOLECULAR MECHANISMS OF SPERMINE ON ITS SYNERGISTIC EFFECT WITH BETA-LACTAMS AGAINST *STAPHYLOCOCCUS AUREUS*

by

XIANGYU YAO

A Dissertation Submitted in Partial Fulfillment of the Requirements for the Degree of

Doctor of Philosophy

in the College of Arts and Sciences

Georgia State University

2012

MOLECULAR MECHANISMS OF SPERMINE ON ITS SYNERGISTIC EFFECT WITH BETA-LACTAMS AGAINST *STAPHYLOCOCCUS AUREUS*

by

XIANGYU YAO

Committee Chair: Dr. Chung-Dar Lu

Committee: Dr. Phang-Cheng Tai

Dr. Zehava Eichenbaum

Dr. Adam Wilson

Electronic Version Approved:

Office of Graduate Studies

College of Arts and Sciences

Georgia State University

November 2012

DEDICATION

To my parents Yan Yao, Hongtao Zhao and my brother Xiangwei Yao, with love.

ACKNOWLEDGEMENTS

Though only my name appears on the cover of this dissertation, a great many people have contributed to its production. I owe my gratitude to all those people who have made this dissertation possible and because of whom my graduate experience has been one that I will cherish forever.

My deepest gratitude is to my advisor, Dr. Chung-Dar Lu. I have been amazingly fortunate to have an advisor who gave me the freedom to explore on my own and at the same time the guidance to the right path. I am grateful to him for holding me to a high research standard and enforcing strict validations for each research result, and thus teaching me how to do research. I hope that one day I would become as good an advisor to my students as Dr. Lu has been to me.

I would give a heartfelt, special thanks to Dr. Phang-Cheng Tai. I feel very lucky to be recruited in GSU by him. I am always inspired and encouraged by his passion on science, full of energy and hard work. Most of all his continuous encouragement, guidance and genuine caring enabled me to attend to life while also earning my Ph.D. Thank you Dr. Tai!

My committee members, Dr. Zehava Eichenbaum and Dr. Adam Wilson, their insightful comments and constructive criticisms at different stages of my research were thought-provoking and they helped me focus my ideas.

I am thankful to the people in Core Facility, especially Sonja R. Young, Hyuk-Kyu Seoh, Ping Jiang, for their technical assistance, expertise, and most importantly, friendship. My gratitude is also extended to LaTesha Warren. She was one of the first friendly faces to greet me when I began this doctoral program and has always been a tremendous help no matter the task or circumstance.

I would like to acknowledge all my lab mates especially Dr. Congran Li, Dr. Weiqing He, Dr. Hsiuchin Yang, Dr. Chun-Kai Yang, Dr. Jinshan Jin, Dr. Ying-Hsin Hsieh, Yu-Chih Peng, Jeng-Yi Li, Sai Madhuri Indurthi, for their valuable discussions, support and friendship.

A very special thank you to my friends Jing Wang, Jie Xu, Lei Zhong, Nan Zhao, Wen Li. They have been always supportive and caring. I am very glad we share so many precious memories along the way. Another stanch supporter Yanjia Zhao, he not only helped me sort out the GeneChip data of my work, but has always been encouraging with full belief. For all these, I am eternally grateful.

Most importantly, none of this would have been possible without the love and patience of my family. I would like to express my heart-felt gratitude to them, for their complete faith in me, their tolerance of my willfulness, and their great love beyond comparison in the world. This dissertation is dedicated to my parents Yan Yao and Hongtao Zhao, my brother Xiangwei Yao, my sister-in law Yu Zhang and a twinkle in my eye, my little niece Zining Yao.

TABLE OF CONTENTS

LIST OF TABLES

LIST OF FIGURES

CHAPTER 1: GENERAL INTRODUCTION

Spermine, a ubiquitous biogenic polyamine, has been widely studied for its biological roles in the regulation of DNA/RNA binding (15), modulation of ion channel activity (76, 108), and as a second messenger in cellular signaling (108). In humans, polyamines in circulation were significantly higher in cancer patients, and spermine released from damaged or dead cells at inflammatory sites plays a role in regulation of macrophage activation (2, 124). Unlike in human, bacteria in general do not make spermine. Many Gram-negative bacteria possess active uptake systems for polyamines (including spermine) and specific catabolic pathways to utilize polyamines as nutrients for growth. But if left in excess and unmodified, spermine is toxic to the cells (97). Therefore, my dissertation project focused on elucidating the spermine-based antibacterial targets in the model pathogen *Staphylococcus aureus*. Particularly in Project I (Chapter 2, 3, and 4), I was interested in how spermine could potentiate β-lactams against methicillin-resistant *S. aureus* (MRSA), and provided evidence to support the idea that spermine may perturb cell wall integrity through its interactions with penicillin binding proteins (PBPs). In project II (Chapter 5), I performed the transciptome analysis and characterized how MRSA responds to the antibacterial activity of spermine *per se*.

1.1 DISTRIBUTION AND PHYSIOLOGICAL FUNCTIONS OF POLYAMINES

Polyamines are a group of organic cations (Figure 1.1) essential for cell growth in all living organisms. In general, diamine putrescine (Put) and triamine spermidine (Spd) are the two most common polyamines in all organisms while tetra-amine spermine (Spm) exists in eukaryotes but not in most bacteria. Some bacteria are capable of making other polyamines (e.g. diaminopropane, cadaverine, norspermidine) different from these three common ones. Because of the positive-charged nature, polyamines are believed

to serve as ubiquitous structural components in cells through interactions with RNA and DNA macromolecules (19).

In humans, considerable attention has been paid to polyamine biosynthesis as a target for anti-tumor therapy because an elevated level of intracellular polyamine pools is a unique character of tumor cells (113). Many compounds have been reported to serve as inhibitors of biosynthesis, as inducers of catabolism, or as competitors of polyamine uptake. Spm also participates in regulation of innate immunity. The tissue level of Spm is significantly increased at the inflammatory sites of infection. Released from dying cells, Spm can restrain macrophage activation in the anti-inflammatory process by inhibiting pro-inflammatory gene expression (124).

In bacteria, it has been reported that mutant strains of *Escherichia coli* and *Pseudomonas aeruginosa* defective in polyamine biosynthesis exhibited a retarded growth phenotype (17, 73). Based on the studies in polyamine-requiring mutant strains of *E. coli*, the concept of "polyamine modulon" was proposed by Igarashi and Kashiwagi (44), referring to a group of genes whose expression requires intracellular polyamines for translational initiation. Exogenous polyamines may serve as environmental cues and participate in many other aspects of bacterial physiology including inhibition of swarming ability and chemotaxis (26), resistance to nitrosative stress (14), activation of biofilm formation (50), anti-mutagens activity (81, 82), and SOS induction of RecA and UvrA (52). As described below, exogenous polyamines and the cognate uptake systems also play roles in bacterial virulence and drug resistance. However, molecular mechanisms for many of these multifaceted polyamine effects remain unknown.

1.2 THE TWO MODE ACTION MODEL OF SPERMINE/POLYAMINE

Many of the activities of the polyamines depend on their donation of free electron pairs. On one hand, the amine can accept a proton to form positively charged ion, rendering the ability to interact with different

polyanionic molecules (mainly DNA and RNA). On the other hand, in addition to the basicity of the amines, defined by the removal of a proton, aliphatic amines are also characterized by their reactions with nitrous acid, the addition of alkyl groups, and their conversion into amides (e.g. N-acetylation) (19). Hence, spermine, and polyamine in general, may potentially serve as nucleophile (the primary amino groups are considered most reactive) (49) to form conjugates with organic compounds or a variety of biomolecules. According to the pKa values (Table 1.1), under physiological pH or lower, spermine could acts as a base (mode I) while higher pH allows for its reactions using free amino group(s) with the nucleophilic property (mode II) (Figure 1.2).

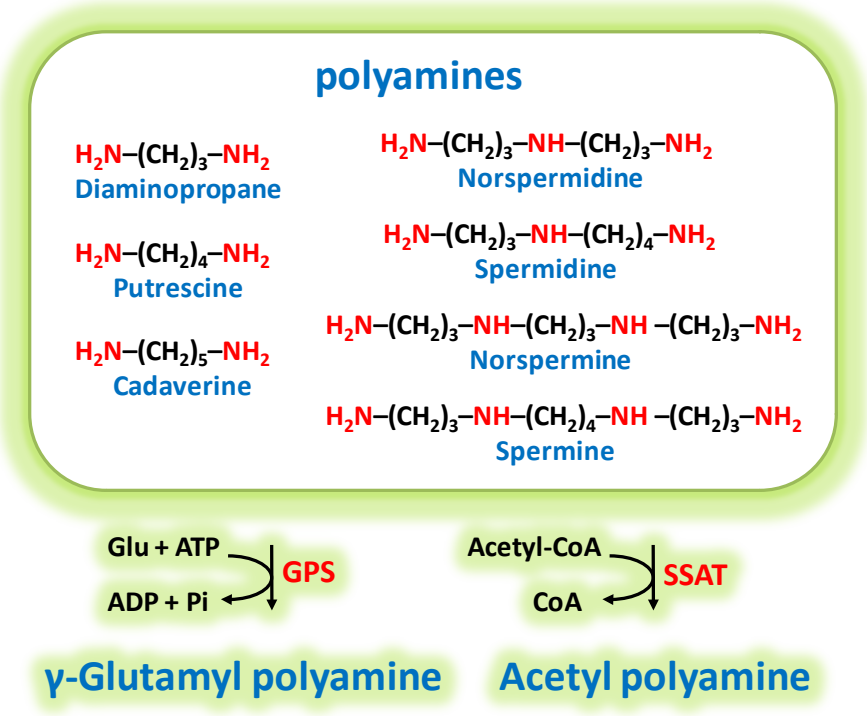

Figure 1. 1Schematic presentation of common polyamines and two polyamine modification reactions.

GPS, glutamylpolyamine synthetase;
SSAT, spermine/spermidine acetyltransferase

Table 1. 1 pKa values of polyamines.

Polyamine	pKa
Spermine[a]	10.80. 10.02, 8.85, 7.96
Spermidine[b]	10.89, 9.81, 8.34
Putrescine[c]	10.80, 9.63

[a] Adapted from Palmer and Powell (1974) in 0.1M NaCl
[b] Adapted from Gold and Powell (1976) in 0.1M NaCl
[c] Adapted from Barbucci et al. (1970) in 0.5M $NaNO_3$

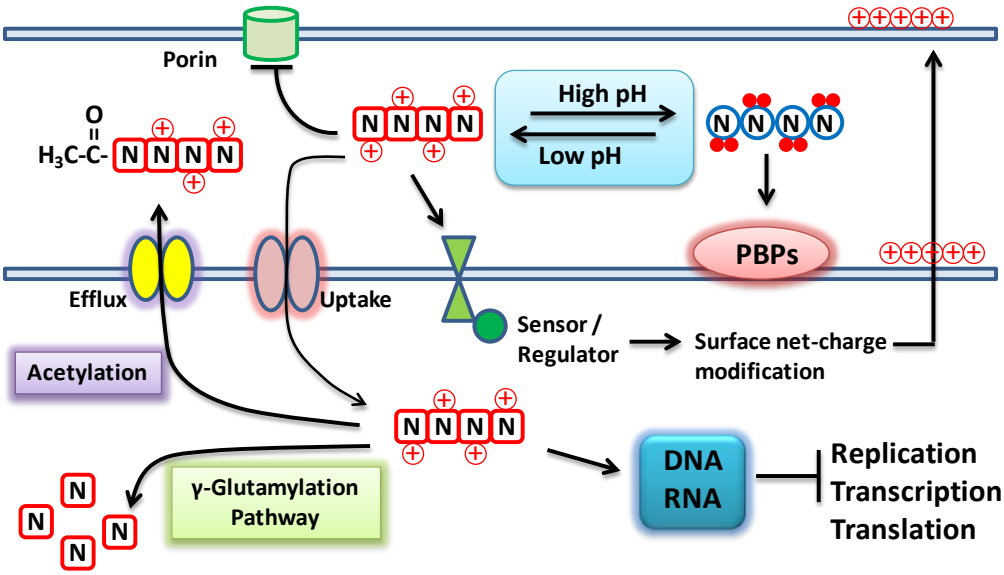

Figure 1. 2 Summary of the ''two mode action'' model of polyamines.

The tetra-amine spermine was used as representative.
PBPs, penicillin-binding proteins.

1.3 TOXICITY AND METABOLISM OF SPERMINE

Although polyamines are required for cell growth, these compounds in excess could be lethal to the cells if left unchecked. Among common polyamines in humans, spermine is the most potent bactericidal agent (33, 38, 97). To avoid the potential lethal effects, the cells need to maintain spermine homeostasis through coordinated regulation on catabolism, biosynthesis, and uptake.

Spermine catabolism

In both human and some bacteria, spermine catabolism can quickly attenuate the toxicity through modification on the amine groups, and ultimately degrade the compound. To initiate degradation, polyamines are subjected to acetylation by Spd/Spm acetyltransferase (SSAT) or γ-glutamylation by γ-glutamylpolyamine synthetases (GPS) (Figure 1.1, Figure 1.2). Human cells take the SSAT route to degrade and recycle spermidine and spermine, or pump acetylated products out of the cells. In bacteria, the function of SSAT has been reported in *E. coli* (*speG)*(31, 68), *B. subtilis* (*bltD)*(115), and a specific strain lineage of *S. aureus(speG)* (48). *P. aeruginosa* and related bacteria do not seem to have an apparent SSAT homologue based on sequence comparison. Instead, our recent report (120) and preliminary data demonstrate the presence of a specific GPS, PauA2, that is absolutely required for Spm and Spd catabolism. Therefore, Spm modification enzymes are the major defensive players against spermine toxicity inside the cell.

Spermine uptake

Since most bacteria do not make spermine through *de novo* synthesis, besides catabolism, homeostasis of this polyamine would be also be controlled by uptake. Most bacteria are capable of transporting exogenous polyamines into the cells through specific ABC transporters which in general consist of a substrate-binding protein (in the periplasm for Gram-negative bacteria), two channel-forming proteins and a membrane-associated ATPase that is involved in energy supply(45). In *E. coli*, *potABCD* and *potGHIF*

are demonstrated as spermidine-preferential and putrescine-specific uptake systems, respectively (51). In *P. aeruginosa*, the *spu*EFGH transporter is essential for Spd and Spm uptake and utilization (70). In Gram-positive *Streptococcus pneumonia*, the extracellular protein PotD encoded within the *potABCD* operon for a putative spermine/putricine transporter also showed capability of binding polyamines (114).

1.4 SPERMINE/POLYAMINE EFFECTS ON β-LACTAMS SUSCEPTIBILITY IN BACTERIA

Several interesting effects of exogenous polyamines on antibiotics (61, 63) have been reported by our group. In particular, spermine was shown to increase the susceptibility of both Gram-negative *P. aeruginosa* and *E. coli* and Gram-positive MRSA to β-lactam antibiotics.

A number of mechanisms have evolved in bacteria to increase resistance against β-lactams, such as a decreased permeability of the outer membrane, export of the antibiotics (these two mechanisms are restricted to Gram-negative bacteria), degradation of the antibiotic by β-lactamases or utilization of penicillin-binding proteins (PBPs) with low affinities to β-lactams. From the results of a series of studies in Gram-negative bacteria, the possibilities of spermine exerting its sensitization effect through β-lactamases, outer membrane permeability, or efflux pumps(62) have been ruled out. Beyond that, alteration of antibiotic target, in this case PBPs may provide another way to mediate β-lactam susceptibility.

1.5 PENICILLIN BINDING PROTEINS AND β-LACTAM RESISTANCE

β-lactam antibiotics, with the β-lactam ring as a shared feature, inactivate the enzymes (PBPs) which are involved in the final stage of cell wall synthesis. As the major component of bacterial cell wall, peptidoglycan (PG) is made of glycan chains of alternating N-acetylglucosamine (GlcNAc) and N-acetylmuramic acid (MurNAc) cross-linked by short stem peptides attached to the MurNAc (Figure 1.3A). The synthesis of PG occurs mainly through the action of PBPs. PBPs catalyze the polymerization of the

glycan strand (transglycosylation) and the cross-linking between glycan chains (transpeptidation). Some PBPs can hydrolyze the last D-alanine of stem pentapeptides (DD-carboxypeptidation) or hydrolyze the peptide bond connecting two glycan strands (endopeptidation, reverse activity of transpeptidation)(94).

While the primary sequence may be quite different, all PBPsshare a common penicillin-binding domain (PB domain) harboring the SXXK motif. The serine residue of the SXXK motif attacks the carbonyl of the second-to-last D-Ala of the stem peptide, which releases the last D-Ala from the donor peptide and forms a covalent acyl-enzyme complex. In the transpeptidation reaction, the D-Ala carbonyl-Ser ester linkage undergoes an attack from a primary amine of the third residue Lys of a second 'acceptor' stem peptide (in *S. aureus* through the amine group of penta-Gly attached to Lys of stem peptide). A peptide bridge is then created between two stem peptides, forming a link between glycan strands (Figure 1.3B). In DD-carboxypeptidation reaction, the acyl-enzyme intermediate is hydrolyzed, thereby preventing the side chain from serving as a donor in the formation of a peptide cross-link.

β-Lactams mimic the D-Ala-D-Ala dipeptide and act as inhibitors (Figure 1.3C, D). The active site serine attacks the carbonyl of the β-lactam ring, resulting in the opening of the ring and formation of a covalent acyl-enzyme complex. This complex is hydrolyzed very slowly, thus effectively preventing further reactions (123).

PBPs have been categorized as high molecular mass (HMM) and low molecular mass (LMM) PBPs. HMM PBP contains multi modules: a cytoplasmic tail, a transmembrane anchor, an N-terminal domain, a β-rich linker and a C-terminal transpeptidase (TPase) domain. Depending on the catalytic activity of the N-domain, HMM PBPs belong either to Class A (HMMA)with N-domain as transglycosylase (TGase), or class B (HMMB)with N-domain interacting with other proteins and playing roles in cell morphogenesis. The LMM PBPs have commonly been found to possess DD-carboxypeptidase activity and/or TPase activity (99).

In *S. aureus*, there are four native PBPs (PBP1-3 as HMM PBPs and PBP4 as LMM PBP) and one acquired PBP2a (HMM PBP) attributive to MRSA (Table 1.2). PBP1 is a mono-functional transpeptidase (HWWB) essential for cell viability and required for cell separation at the end of cell division. It localizes to the division septum in a way that is independent of its substrate-bindng ability (79, 80) . PBP2 is an essential bi-functional transglycosylase and transpeptidase (HMMA) that plays a central role in the ability of bacteria to express their resistance to antibiotics. It localizes to the division septum through a mechanism that is dependent on its ability to recognize the substrate (88). PBP3 and PBP4 are non-essential (85, 116). PBP3 is a mono-functional transpeptidase (HMMB) whose localization and substrate reorganization have not yet been studied in detail. PBP4, the single LMM PBP, which has been shown to have a low affinity for most β-lactams, is unique among LMM PBPs in that it possesses TPase and DD-carboxypeptidase activities(37). Like PBP1 and PBP2, PBP4 can be found at the septum of *S. aureus*. Particularly, PBP4 was shown to make high-degree cross-linking in concert with PBP2 and other cell wall components (e.g. wall teichoic acid, WTA), and was important for resistance to antibiotics (6).

In addition to the four native PBPs, MRSA strains have acquired another HMMB PBP, PBP2a, encoded by *mecA* situated in the chromosome in a genomic island designated staphylococcal cassette chromosome *mec* (SCC*mec*). Unlike native PBPs, PBP2a has a remarkably low affinity for all β-lactams, thus enabling the protein to continue cell wall synthesis in the presence of these antibiotics(36). PBP2a and PBP2 function cooperatively in the presence of β-lactam, possibly as a multi-enzyme complex (together with other PBPs and other enzymes used for PG synthesis and cell division), to ensure orderly peptidoglycan synthesis at the septum with no delocalization of PBP2 (67, 84).

Besides *mecA*, some additional factors that inactivate β-lactams or interfere with cell wall architecture orsynthesis also have the potential to modulate β-lactam resistance: the production of β-lactamase encoded by an extrachromosomal gene *blaZ* (another major resistance mechanism to β-lactams, but not

present in all MRSA), the TGase-catalyzed elongation of glycan chains (84), the abnormal configuration of stem peptide (9), the imbalance between PG synthesis and autolysis (111), etc.

1.6 RESEARCH OVERVIEW

My research throughout the Ph.D program is focused on (i) elucidating the mechanisms of resistance and stress response against polyamine toxicity in two pathogens, *S. aureus* and *P. aeruginosa;* and (ii) polyamine utilization pathways in *P. aeruginosa.* These two seemingly separate subjects unite together in the sense that both help us better understand bacterial physiology and ultimately control infections in humans. The major content of the dissertation is only concentrated on the *S. aureus* part, with the *P. aeruginosa* part enclosed in Appendix C as two published articles (120).

S. aureus is an opportunistic pathogen responsible for hospital- and community-acquired infections ranging from localized benign skin infections to life-threatening conditions such as osteomyelitis, pneumonia, sepsis and endocarditis. Staphylococcal infections are becoming increasingly difficult to treat because of the rapid emergence of MRSA, which have developed resistance to virtually all β-lactam antibiotics. They are intrinsically resistant to β-lactams by virtue of newly acquired low-affinity PBP2a, with the ability to build the cell wall when other PBPs are blocked by β-lactams. Considering the acquisition and horizontal dissemination of resistant genes are evolved with the clinical use of antibiotics in excess, instead of developing new drugs, exploring compounds that can restore the efficacy of previously ineffective antibiotics may have more potential to combat the evolving resistance.

In this context, we are examining the anti-staphylococcal potential of spermine, a polyamine found in abundance in human beings especially at inflammation. At low concentration, spermine has negligible intrinsic antibacterial activity but able to sensitize β-lactam antibiotics in a β-lactamase-independent manner. At high concentration, spermine *per se* can inhibit bacterial growth. Therefore in **Project I.**

Exploring the target(s) of spermine-dependent synergy with β-lactams in MRSA, to understand the mechanisms involved in the profound changes of β-lactam susceptibility engendered by spermine, different strategies were employed: 1) Selection of spermine/β-lactam resistant mutant and identification of the responsible mutation site(s); 2) Characterization of spermine effects on cell wall synthesis, via genetic and biochemical approaches; 3) Depiction of spermine/β-lactam mediated transcriptomic alterations through microarray analysis. Studies on those aspects will be described in Chapter 2 (121) , Chapter 3, and Chapter 4, accordingly. In **Project II**. **Elucidation of *S. aureus* responses to spermine toxicity**, to reveal new information regarding the stress response to Spm, the transcriptome analysis on MRSA Mu50 was conducted upon exposure to high dose Spm by time course, and some candidate genes with significant levels of induction were subjected to further characterization through genetic and biochemical experiments. Studies on this project are reported in Chapter 5.

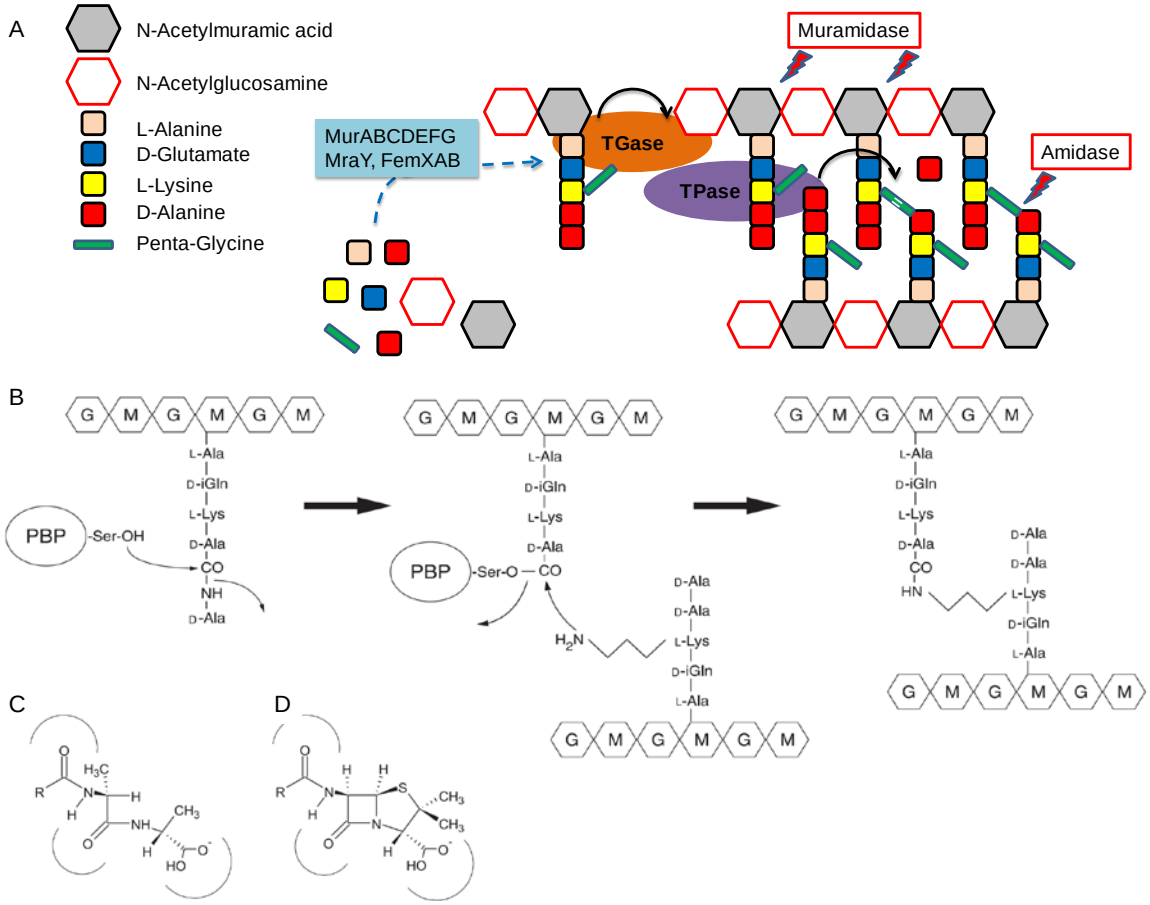

Figure 1. 3 PG synthesis and β-lactam antibiotics.

A. Schematic representation of basic structure and synthesis of cell wall in *S. aureus*.
B. Catalysis of transpeptidation during PG synthesis. Fragments of glycan strands are represented by chains of hexagones standing for GlcNAc(G) and MurNAc(M). The 'donor' stem peptide is depicted on the upper glycan strand, whereas the 'acceptor' is attached on the lower strand. The composition of stem peptide may differ in various species. Note that in *S. aureus*, penta-Gly is attached to the third residue of the acceptor peptide, and provide the free amine that attacks the acyl-enzyme intermediate.
C, D. Structural similarity between the natural substrate of the PBPs and β-lactams. (C) N-Acyl-D-Alanyl-D-Alanine peptide. (D) Penicillin backbone. The regions of negative electrostatic potential are indicated by arcs. B-D, adapted from *Andr´e Zapun, et al. (2008) FEMS Microbiol Rev*

Table 1. 2 PBPs in MRSA

	PBP class*	Function *in vivo*	Essentiality in *S.aurues*
PBP1	HMMB	transpeptidase	essential
PBP2	HMMA	transglycosylase, transpeptidase	essential
PBP3	HMMB	transpeptidase	non-essential
PBP4	LMM	carboxypeptidase, transpeptidase	non-essential
PBP2a	HMMB	transpeptidase	non-essential

*HMMA, high molecular mass class A; HMMB, high molecular mass class B; LMM, low molecular mass

CHAPTER 2: A PBP2 MUTANT DEVOID OF THE TRANSPEPTIDASE DOMAIN ABOLISHES SPERMINE / β-LACTAM SYNERGY IN *STAPHYLOCOCCUS AUREUS* MU50

2.1 INTRODUCTION

β-Lactam antibiotics function by irreversibly occupying the serine residue at the active site of penicillin binding proteins (PBPs), and formation of this stable ester-linked acyl enzyme inhibits the transpeptidation step during cell wall cross-linking (32). In *S. aureus*, there are four native PBPs (PBP1-4) and one acquired PBP2a attributive to MRSA. In contrast to other PBPs, PBP2a encoded by the *mecA* gene shows low affinity to β-lactams due to inefficient formation of the acyl-PBP intermediate, and thus ensures continued cell wall synthesis when normal PBPs are inactivated by β-lactams (36). Besides *mecA*, additional factors affecting cell wall architecture or synthesis are believed to have the potential to perturb or modulate β-lactam resistance in *S. aureus*, such as glycan chain length (87), stem peptide configuration (25), pentaglycine cross-bridge (10), coordinated activity of peptidoglycan (PG) biosynthesis and autolysis (5), etc. Particularly, one of the native PBPs, PBP2, is essential for the high level of methicillin resistance in MRSA. PBP2 belongs to the high-molecular-weight class-A PBPs with a transglycosylase (TG) domain and a transpeptidase (TP) domain. When exposed to β-lactams, PG synthesis in MRSA can be achieved at the division septum mediated by the cooperative functioning of the TG domain of PBP2 and the TP domain of PBP2A, possibly as part of a multi-enzyme complex in cell wall synthesis (87, 88).

In the current study, we isolated a MRSA strain derivative (MuM) conferring spermine resistance by serial passages *in vitro*, and compared its genetic basis as well as the phenotypic profiles with those of its parental strain Mu50. We found that this mutant not only possesses 32-fold increase in tolerance of growth inhibition by spermine, it also loses completely the spermine/β-lactam synergy. Furthermore, a 7-bp deletion within the *pbpB* gene which encodes the essential PBP2 was revealed by genome resequencing, through which the transpeptidase activity was deprived. Complementation of plasmid-borne wild-type *pbpB* to the mutant can restore its sensitivity to both spermine and the synergy. In

addition, the reduced tolerance of cell wall to hydrolysis and decreased autolytic activity were observed in this mutant, which may be due to changes on cell wall metabolism as a result of this *pbpB* lesion. This mutation also posted a pleiotropic effect on gene expression as revealed by transcriptome analysis. Taken together, our results lend support to the idea that exogenous spermine may affect cell wall synthesis through its interactions with PBP2 and/or PBP2-assoicated multi-enzyme machineries to enhance the killing effect of β-lactam antibiotics.

2.2 MATERIALS AND METHODS

Bacterial strains, plasmids, and growth conditions

S. aureus Mu50 (ATCC700699), COL (obtained from NARSA), RN4220 (kindly provided by R. P. Novick) and *E. coli* DH5α (Bethesda Research Laboratories) were employed in this study. Plasmid pCN38 (ampicillin and chloramphenicol resistance), a shuttle vector of *E. coli* and *S. aureus* (16), was used for gene cloning. Both *E. coli* and *S. aureus* strains were routinely grown and maintained in the Luria-Bertani (LB) medium. When required, the LB medium was buffered with 20mM Tris-HCl of indicated pH. Antibiotics were added to the media as necessary at the following concentrations: ampicillin, 100μg/ml (for *E. coli*); chloramphenicol, 10μg/ml (for *S. aureus*).

Isolation of spermine-resistant mutants

Spontaneous mutants of the MRSA Mu50 (oxacillin MIC of 512 μg/ml and spermine MIC of 1 mM at pH8.0) were isolated by spreading 1×10^8 CFU of log-phase cells onto spermine-containing plates (2-8 mM, pH8.0) and incubated overnight at 37 ºC. One independent colony recovered from plates with 8 mM spermine, and it remained resistant to spermine (up to 32 mM) in broth and on plates. This mutant strain was designated as MuM in this study.

Genotypic characterization of spermine-resistant mutant MuM

The chromosomal mutation in MuM was identified by pyrosequencing carried out using the 454 Life Sciences Technology at the University of Florida. Genomic DNA from both Mu50 and MuM were sent for sequencing, assembled, and compared to the published genomic sequence of *S. aureus* Mu50 (GeneBank Accession BA000017.4). The mutation unique to MuM identified in the *pbpB* gene was confirmed by PCR amplification and DNA sequencing by the following two primers: 5'-GGTTTAGTTGCTATATCTGGTGG-3' and 5'-CGCGTTGTTATAAGTACCACCG-3'.

Spermine and antibiotic susceptibility tests

Minimal inhibition concentrations (MICs) of antibiotics or spermine were determined by a liquid micro-dilution method according to the guidelines of the Clinical and Laboratory Standards Institute(18). Serial two-fold dilutions of tested compounds were prepared in a 96-well microtiter tray, and fresh overnight cultures of each bacterial strain were diluted and inoculated with approximate 10^5 CFU/well. Cells were incubated without shaking at 37 ºC for 24h (or up to 36h as specified). The lowest concentration of antimicrobial agent at which cells were not able to grow was defined as its MIC.

Transcriptome analysis

Mu50 and MuM were grown in Tris-buffered LB (pH7.5), and cultures in the exponential phase (OD_{600} around 1.0) were immediately treated with the RNAprotect Bacteria ReagentRNA protection reagent (QIAGEN) before harvesting. RNA samples were extracted from cells by phenol (Fisher), digested by RNase-free DNase I (Roche) to remove genomic DNA, and purified with RNeasy mini columns (QIAGEN). cDNA synthesis, fragmentation and terminal labeling were carried out according to the protocols by the manufacturer (Affymetrix). Labeled cDNA was hybridized to GeneChip *S. aureus* Genome Array. After scanning, the images were processed with GCOS 1.4 software (Affymetrix). Data

consisting of three independent biological experiments were analyzed by comparing gene expression of MuM to Mu50 with fold change over 2.5, and signal intensity value 200 as threshold.

Complementation of *pbpB*

The *pbpB* gene was reported to transcribe independently or as a polycistronic RNA from its upstream *prfA* promoter (86). To ensure optimal expression, a 3.2-kb fragment covering both *prfA* and *pbpB* was amplified by PCR from the Mu50 genomic DNA with the following two primers:5'- CGCGGATCCACA CATACTTGTACTTGCCTC-3' and reverse primer 5'-CGCGGCGCCGAGTGGATTAGTTGAATATACCTGTTAATCCACCGCTG-3'. The resulting PCR product was cloned into *Bam*HI and *Nar*I sites of the shuttle vector pCN38. The recombinant plasmid pYX9 was first cloned into and extracted from *E. coli* and then electroporated into *S. aureus* RN4220 by GenePulser Xcell (Bio-Rad) with parameters as described previously (60). Plasmid DNA isolated from recombinant strains of RN4220 was subsequently introduced into Mu50 and MuM by electroporation.

PBPs profiling

Membrane fractions were prepared as described previously (75) for detection of PBPs. Protein samples (50μg) were incubated with 5μM Bocillin FL (Invitrogen) for 30min followed by SDS-PAGE on a 10% gel. The fluorescent Bocillin covalently bound to the PBPs were detected with excitation at 488nm and emission at 520nm (Typhoon 9400). Due to its low affinity to Bocillin, PBP2a was detected by immunoblots with mouse anti-PBP2a antibodies (Abnova; 1: 5000 dilution), followed by rabbit anti-mouse IgG antibodies conjugated with alkaline phosphatase (Sigma; 1:30,000 dilution) and chromogenic substrates.

Triton X-100-induced autolysis assays

This assay was conducted by following a protocol as described previously (22) with minor modifications. Briefly, cells were harvested, washed twice with ice-cold water, and then re-suspended in the same

volume of 50mM Tris-HCl (pH 7.2) containing 0.05% Triton X-100. Cells were incubated at 30°C with shaking (~250rpm) and checked for lysis by measuring the progressive decrease in absorbance (OD_{600}). Autolysis was quantified as a percentage of the initial OD_{600} remaining at each sampling point.

Preparation of autolytic enzyme extracts

Cellular extracts enriched with autolytic enzymes were prepared as previously described (56) with some modifications. Briefly, the cells were grown to mid-exponential phase in 20ml of LB (20mM Tris-Cl, pH7.5) at 37°C with aeration to OD_{600} of 1, chilled on ice, harvested by centrifugation, and washed twice with ice-cold 50 mM Tris-HCl (pH 7.5) buffer with 150 mM NaCl. The pellet was directly suspended in 80 µl of 4% SDS for 30min at room temperature or 400 µl of a solution containing 3 M LiCl and 0.1% TX-100 for 30 min at 4°C with stirring. After centrifugation at 10,000 x g for 10min, the supernatants were collected as SDS extracts or LiCl extracts, which were used in zymographic analysis or *in vitro* enzymatic hydrolysis of crude cell walls, respectively.

Enzymatic hydrolysis of crude cell walls *in vitro*

This assay was performed as previously described (5). Briefly, crude cell walls were prepared from cells (10ml) grown to mid-exponential phase (OD_{600} around 1). Cell pellets were boiled in 8% SDS for 30min and washed three times with hot water to remove SDS. The obtained pellets as crude cell walls were suspended in 50 mM Tris-HCl (pH 7.5) to an OD_{600} of 0.6, and LiCl extracts as described above were added to start hydrolysis. The reaction was conducted at 37°C with shaking (~250rpm), and the hydrolysis rate was measured as a decrease of OD_{600}.

Zymographic analysis

Heat-killed cells of *S. aureus* RN4220 were prepared as the substrate for hydrolytic enzymes. Briefly, the cells in mid-exponential phase were harvested, and the pellet was suspended in 2× Laemmli SDS sample buffer and heated for 5 min at 100°C. The heat-inactivated cells (with OD_{600} equivalent to 10) in 1/10

volume of the resolving-gel (10%) solution was added to cast the gel, and the SDS-extracts as described above were applied to such SDS-PAGE to detect the hydrolytic activities. After electrophoresis, the gel was soaked for 30 min in distilled water at room temperature, then transferred into the renaturing buffer (25 mM Tris-HCl, 1% [vol/vol] Triton X-100, pH 8.0) with gentle shaking for 16 h at 37°C to allow for renaturation. The renatured autolysins appear as clear translucent bands on the opaque background, and the contrast can be enhanced for photography by staining the gels in 1% (wt/vol) methylene blue with 0.05% KOH.

Preparation and analysis of extracellular protein fraction

For the preparation of extracellular protein extracts, bacteria were grown in LB medium to exponential phase. After centrifugation, extracellular proteins in the supernatant (2 ml) were precipitated by 0.02% sodium deoxycholate at 4°C for 30min followed by 10% (w/v) trichloroacetic acid at -20°C overnight. The precipitates were harvested by centrifugation at 4°C, 16,000 x g for 20min, washed with 100% ice-cold acetone twice and dried. The protein pellet were resolved in an appropriate volume of Laemmli SDS sample buffer, boiled and separated on 10% SDS-PAGE. Bands showing different intensities between MuM and Mu50 samples were identified by MALDI-TOF MS/MS.

Electrospray ionization mass spectrometry (ESI-MS)

Solutions of spermine and oxacillin (2mM), either alone or in combination, were prepared in the ammonium acetate buffer (5mM), and the final pH was adjusted by formic acid or ammonium hydroxide. All solutions were directly injected for ESI-MS analysis. Mass spectral acquisition was done in the positive ion mode using the following parameters: capillary voltage 3000V, sample cone voltage 35, extraction cone voltage 2.5, source temperature 120 ^{o}C, desolvation temperature 150 ^{o}C, gas flows desolvation 500 l/h, pump flow rate 5 µl/min.

2.3 RESULTS

Growth inhibition of Mu50 by spermine is pH-dependent

While spermine and β-lactams exert a strong synergy effect on MRSA (61), spermine *per se* can cause growth inhibition on all tested strains of *S. aureus* (Mu50, N315, COL, RN4220 with MICs of 1mM, 1mM, 0.5mM, and 2mM, respectively, at pH 8.0). To further understand the adverse effect of spermine, we first tested whether this effect is growth phase-dependent. As shown in Figure. 2.1, growth of Mu50 in the buffered LB broth (20mM Tris-Cl, pH 8.0) was immediately inhibited by the addition of spermine (10X MIC; 10mM) regardless of the growth stage.

Spermine is a tetra-amine, and its four pKa values were reported as 10.80, 10.02, 8.85, and 7.96 (11). At pH 7.4, the relative abundance of +4/+3 species was 3/1, and the ratio could be 1/1 at pH 8.0. If not protonated, the amino group would serve as nucleophile for potential chemical reactions. To analyze the possible effect of spermine net charge on growth inhibition, spermine MIC was determined in Mu50 suspended in buffered growth media of different pH values as shown in Figure. 2.2 A. When pH is at 7.0 or lower, fully positive-charged spermine did not post a strong inhibitory effect on growth as reflected by MICs of 32-64 mM. Interestingly, MIC was reduced to 2 mM at pH 7.5, and was decreased further to 0.125 mM at pH 9.0 or higher. Since the net positive charge of spermine is reduced when the pH value is increased, these results strongly suggest that the growth inhibition effect of exogenous spermine may not be related to its positive charges, and instead its nucleophilic property may be the cause.

Table 2. 1 MICs of oxacillin, vancomycin, and spermine in Mu50 and MuM.

Antibiotic reagent	MIC* for							
	Mu50		MuM		Mu50/pYX9		MuM/pYX9	
	-	0.5mM Spm	-	0.5mM Spm	-	0.5mM Spm	-	0.5mM Spm
Oxacillin (μg/ml)	512	<1	1024	1024	512	<1	1024	<1
Vancomycin (μg/ml)	4	4	2	<0.03	8	4	8	4
Spermine (mM)	2		64		2		2	

* MICs were determined in LB broth with pH adjusted to 7.5.
Plasmid pYX9 carries the wild-type *pbpB* gene

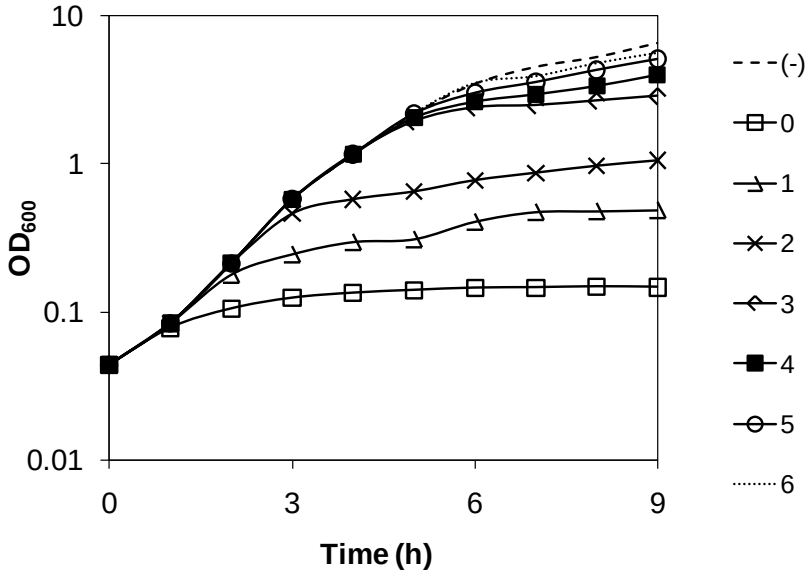

Figure 2. 1 Growth inhibition by exogenous spermine.

Cells from a fresh overnight seed culture were inoculated into pre-warmed LB broth (pH8.0). Spermine (Spm; 10mM) was added at indicated time points after inoculation, and OD_{600} was monitored at every 1-hr intervals.

Effects of pH on oxacillin/spermine synergy of Mu50

Meanwhile, we also analyzed the pH effect on oxacillin / spermine synergy by measuring oxacillin MIC in the presence of spermine at different pH (1/4 of MIC for pH 7.5 to 9.5; 0.5mM for pH 6 to 7). Like spermine *per se*, such synergy also followed the same trend of pH dependence (Figure 2.2B), but only when pH was equal to or lower than 8.0. Unexpectedly, at pH 8.5 and higher, oxacillin MIC took a reversed trend and increased 16-fold from that of pH 8.0, and a further 32-fold increment was observed if recorded after 24 more hours of incubation. These results led us to propose oxacillin inactivation by a possible chemical reaction between nucleophilic spermine and the β-lactam ring of oxacillin (77).

To test this hypothesis, possible formation of spermine-oxacillin conjugates was analyzed by ESI-MS in the positive-ionization mode as shown in Figure 2.3. In comparison to the mass spectra for spermine and oxacillin (2mM), a new peak corresponding to the proposed spermine-oxacillin conjugate (m/z 604.5) appeared in the mass spectrum of an equamolar mixture (2mM) of spermine and oxacillin at pH 9.0, but not in that of a mixture at pH 7.0. These data support pH-dependent formation of chemical conjugates between spermine and β-lactams, and were consistent with patterns of MIC readings in Figure 2.2.

Selection and preliminary characterization of a spermine-resistant mutant MuM

Strain MuM, a spermine-resistant mutant of Mu50, was isolated through selection on high concentrations of spermine as described in Materials and Methods. MuM exhibited resistance to spermine, with an MIC 32-fold higher than that of the parental Mu50 (Table 2.1). The genetic modification(s) in MuM was specific for spermine as MICs of several tested antibiotics (streptomycin, tetracycline, gentamicin, erythromycin, chloramphenicol, kanamycin, spectinomycin) on MuM were the same as those of Mu50. However, we observed significant changes on the growth behavior of MuM. In comparison, colonies of MuM on LB plates were homogeneously smaller than those of the parent strain, and these colonies required over 18h to recover from the lag phase at 37°C when inoculated into the LB broth. Once in the

logarithmic phase, the doubling time of MuM was over 3.5-fold longer than that of Mu50 (127 min v.s. 35 min; Figure 2.4A). However, fast-growers started to appear after continuous passage of MuM on LB plates, suggesting the rise of compensatory mutations from growth impairment (4). To maintain a stable MuM, we found that glucose supplement in the LB medium was indeed helpful as evidenced by a reduced doubling time to 70 min with a shortened lag phase (Figure 2.4A), and the spermine-resistance phenotype as well as homogeneous colony size remained after passages. Another interesting phenotype of MuM was that this strain is a temperature-sensitive mutant; no apparent growth can be detected at 42^{o}C.

Growth limitation of MuM by pH

To examine the pH dependence of spermine effects in MuM, MIC measurements of spermine were conducted under different pH conditions. Contrary to the pH-dependent trend in its parental strain Mu50 (Figure 2.2A), spermine MIC in MuM was estimated to be 64 mM at pH 6.0-8.0, but surprisingly was dropped to an undetectable level at pH 8.5 or higher. This prompted us to monitor the growth of MuM and Mu50 in the buffered LB broth of pH 6.0-9.5 in the absence of exogenous spermine. Strain Mu50 grew comparably at pH 6.0-8.5, and the growth rate was significantly reduced at pH 9 and 9.5 (Figure 2.4C). In comparison, MuM exhibited its optimal growth at pH 7.5-8.0 and basically showed no growth at pH 9.0 and higher (Figure 2.4B).

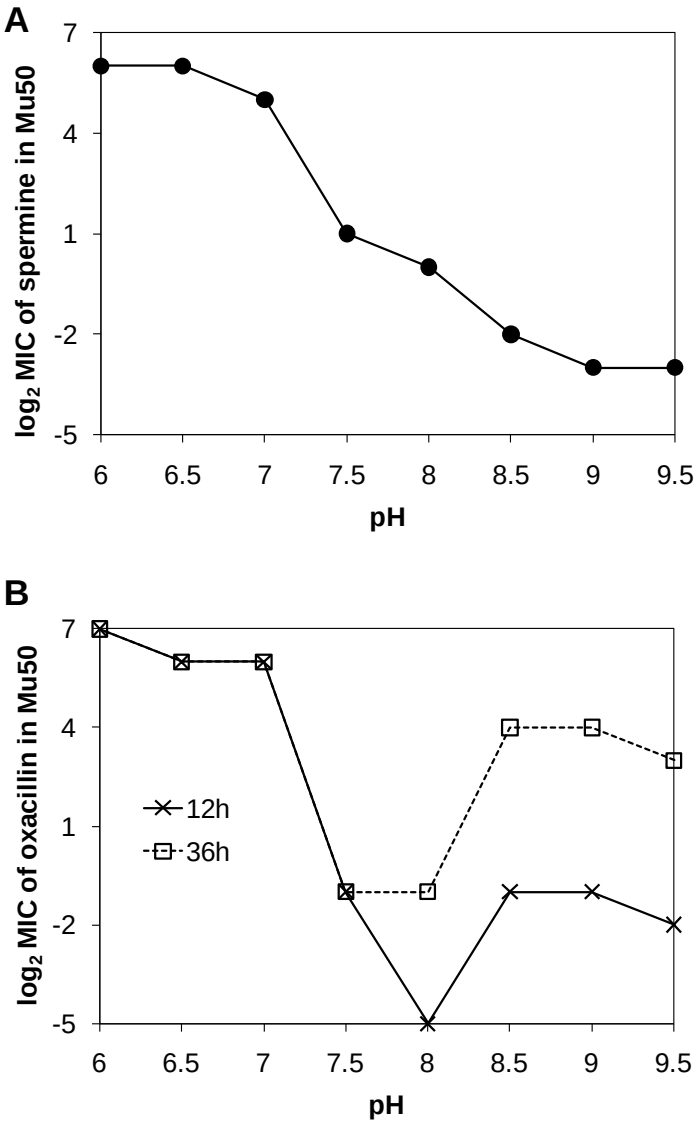

Figure 2. 2 pH-dependent effects of spermine or spermine/β-lactam synergy.

(A)MIC of spermine *per se* (B) MIC of oxacillin in the presence of spermine.
MICs of spermine or oxacillin were determined at different pH in Mu50. For measurements of oxacillin MICs, 0.25-fold MIC (for pH 8.0-9.5) or 0.5mM (for pH 6.0-7.5) of spermine was included.

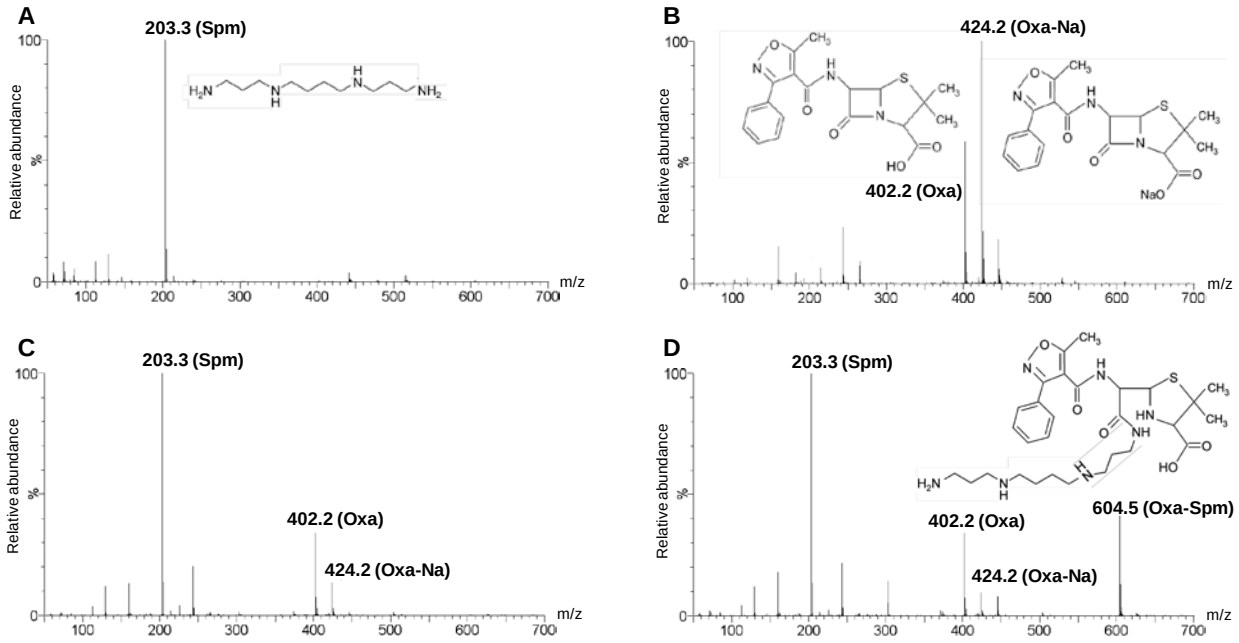

Figure 2. 3 ESI mass spectrum analysis.

All compounds were dissolved in ammonium acetate buffer (5mM), and mass spectra were acquired in positive ionization mode. (A) spermine; (B) oxacillin; (C) equal-molar mixture of spermine and oxacillin at pH 7; (D) equal-molar mixture of spermine and oxacillin at pH 9.

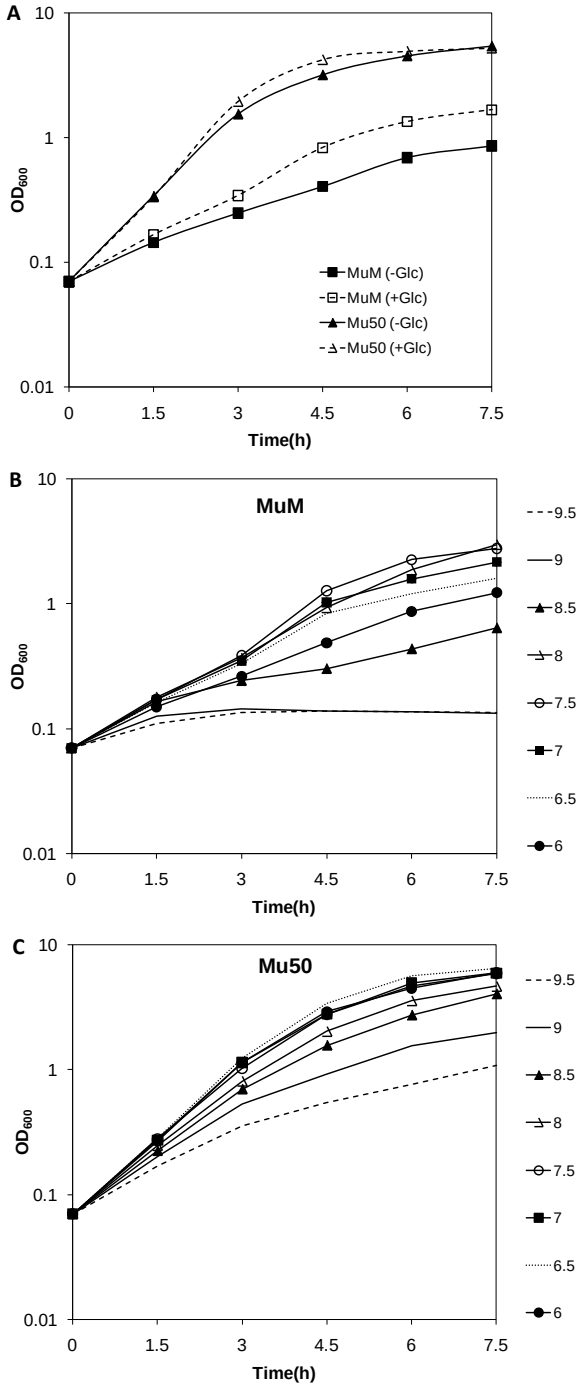

Figure 2. 4 Growth behaviors of Mu50 and MuM.

Growth of the cells in LB broth at 37°C with aeration was monitored by OD measurements. (A) Growth in the presence or absence of 0.4% glucose; (B) Growth of MuM in LB buffered with 20 mM Tris-HCl of indicated pH; (C) Growth of Mu50 in LB buffered with 20 mM Tris-HCl of indicated pH.

Loss of spermine/β-lactam and gain of spermine/vancomycin synergy in MuM

MICs of oxacillin and several different types of antibiotics in the presence and absence of spermine were determined in MuM and its parental stain Mu50. The results indicated that while spermine posted its synergy effect exclusively on β-lactams in Mu50, MuM behaved differently from Mu50 only on oxacillin (β-lactams in general) and vancomycin. As shown in Table 2.1, MICs of oxacillin in the absence of exogenous spermine were comparable in MuM and Mu50. In the presence of 0.5 mM spermine, over 500-fold reduction of MIC to oxacillin was observed in Mu50, whereas this sensitization effect was completely compromised in MuM. In the case of vancomycin, while its MIC was not affected by the presence of spermine in Mu50, MuM exhibited a considerable increase of susceptibility to this antibiotic when spermine (0.5 mM) was supplemented (Table 2.1). As a inhibitor of cell wall synthesis, vancomycin works by binding to the D-Ala-D-Ala moiety, and subsequently blocking cross-linkage, of the murein monomers during the transpeptidation reactions by PBPs (92). Such opposite responses of MuM to β-lactam and vancomycin in the presence of spermine raised the possibility that spermine may directly or indirectly inhibit cell wall synthesis.

Genome resequencing of MuM and Mu50 identified a genetic defect in *pbpB*

To identify the mutation(s) responsible for spermine resistance, genome resequencing of MuM and Mu50 was conducted by the 454 Sequencer FLX System. On average, total base-pair reads exceeded over six times of the genome size, and the generated contigs covered more than 98% of the published genome sequence of Mu50. Through sequence comparison, only one sequence variation was identified between Mu50 and MuM: a 7-bp deletion in MuM which was located at nt 1366-1372 within the *pbpB* gene encoding an essential penicillin binding protein (PBP) in *S. aureus*, PBP2 (Figure 2.5A). The presence of this deletion in MuM was confirmed by sequencing of a 461-bp fragment covering this region by PCR amplification from the genomic DNA of Mu50 and MuM.

The PBP2 protein is composed of 727 amino acids (Mr of 80,236) with an N-terminal transglycosidase domain spanning residues 82-258, and a C-terminal transpeptidase domain spanning residues 361-629 (Figure 2.5A; UniProtKB/TrEMBL:Q99U39). All PBPs share a common penicillin-binding (PB) domain which binds β-lactam antibiotics due to the structural similarity between β-lactams and the D-Ala-D-Ala moiety of the nascent peptidoglycan, the natural substrate of PBPs. The PB domain is composed of two subdomains, and three motifs broadly conserved in PBPs lie at the interface of these two subdomains. In the case of *S. aureus* PBP2, these three motifs comprise $SSLK_{401}$, SFN_{456}, and KTG_{585}, with S_{398} being the primary active residue (98). In MuM, a frame-shift by the 7-bp deletion in *pbpB* incurs an immediate stop codon that truncates the translated product from N_{456}, right at the 2nd consensus motif, and deprives the C-terminal transpeptidase domain of PBP2 (Figure 2.5A). As a result, the mutated PBP2 was expected to lose its formation of an acyl linkage with β-lactams. To test this hypothesis, we conducted PBP labeling with Bocillin, a fluorescent derivative of penicillin. As shown in Figure 2.5B, PBP2 was not detectable in the membrane preparation of MuM, supporting the presence of a truncated PBP2 in this mutant.

Complementation of the spermine-resistant MuM by *pbpB*

Plasmid pYX9 carrying *pbpB* of Mu50 was constructed for complementation tests. As shown in Table 2.1, MuM carrying pYX9 restores spermine sensitivity and the synergy effect of spermine and β-lactams. Plasmid pYX9 also restores the tolerance of MuM to vancomycin to the wild-type level in the presence of spermine. Meanwhile, empty vector (pCN38) does not rescue those phenotypes in MuM (data not shown). For growth kinetics, MuM/pYX9 grows much faster than MuM, with an estimated generation time comparable to that of Mu50 (data not shown). In addition, the pH sensitivity of growth was diminished in MuM/pYX9, indicating a correct form of PBP2 is required for the buildup of a rigid and strong cell wall to resist diverse environmental challenges.

It was suggested that different PBPs may work in concert or form a complex to coordinate the PG synthesis (66). In order to see whether the sophisticated regulation of different PBPs can be affected by

the addition of PBP2, PBPs profiles were compared in Mu50 and MuM with or without pYX9. As shown in Figure 2.5B, introduction of plasmid-borne wild-type PBP2 did not have apparent effects on the production of other PBPs. MuM with empty vector (MuM/pCN38) shows same PBPs patterns as observed in MuM (data not shown). Moreover, a similar level of PBP2a was detected in MuM and Mu50 by immunoblots (Figure 2.5B), suggesting that the genetic lesion of *pbpB* did not affect *mecA* expression in MuM. As described below, we also conducted transcriptome analysis in MuM and Mu50; consistent to the results of Bocillin labeling and PBP2a immunoblots, we found comparable levels of expression for all genes encoding penicillin-binding proteins in these two strains (Table S2).

Effects of the truncated PBP2 in MuM on cell wall hydrolysis

The mutated *pbpB* gene of MuM may result in perturbation of cell wall synthesis and change the PG structure. To test this hypothesis, sensitivity of MuM and Mu50 cell walls to hydrolytic enzymes was analyzed by incubation with a common source of autolytic enzyme extracts from strain COL. Degradation of the MuM cell wall materials was significantly faster than the control of Mu50 (Figure 2.6A), suggesting cell walls of MuM may be less cross-linked and/or more susceptible to hydrolysis due to the defects on PBP2.

It has been reported that enzymes for cell wall synthesis and hydrolysis may be co-regulated, and that the decreased expression of *pbpB* could repress the autolytic system in *S. aureus* (5). Here a similar situation may occur in the case of MuM. Whole-cell autolysis was assessed following exposure of MuM and Mu50 cells to Triton X-100. As shown in Figure 2.6B, the rate of Mu50 autolysis was significantly faster than that of MuM. Since the cell wall of MuM was more susceptible for degradation than that of Mu50 (Figure 2.6A), the slower rate of autolysis in MuM may be related to a decreased activity and /or quantity of autolytic enzymes, in addition to possible alterations on cell wall composition.

We also conducted zymographic analysis of autolytic enzymes from Mu50 and MuM. Taking crude cell walls of RN4220 as substrate, a couple of bacteriolytic bands of cell wall hydrolysis by the enzyme

extract from MuM were less intense than those from Mu50 (Figure 2.6C). Although the exact identify of these affected hydrolytic enzymes cannot be determined from this experiment, they may include the autolysin ATL of 138 kDa and its proteolytic products of 62 and 51 kDa (57). In addition, the secreted protein profiles from the spent medium of MuM and Mu50 in the logarithmic phase of growth were compared following SDS-PAGE. As shown in Figure 2.6D, one polypeptide appeared preferentially in the protein sample of Mu50 but was completely absent in that of MuM, and this peptide was identified as autolysin ATL by MALDI-MS-MS.

While the results of Figure 2.6C suggest a reduced activity of cell wall hydrolytic enzymes in MuM, surprisingly transcriptome analysis (Table S2) reveals no apparent difference in MuM and Mu50 on expression of the major hydrolytic enzymes encoded by *atl, sle, lytM,* and *SA0620/SAV0665* (5). Since autolysin ATL requires proteolytic processing to reach its maximal activity, these somewhat contradictory results may be explained by a decreased level of ATL proteolytic processing and a greater degree of ATL retention within the cell wall of MuM, perhaps as the consequence of possible alterations on the PG composition due to the *pbpB* lesion.

Transcriptome analysis

Multiple phenotypic changes of MuM prompted us to evaluate the transcriptional profiling imposed by the defective PBP2. The logarithmic-phase cells of MuM and Mu50 grown in LB alone without spermine supplement were subjected to transcriptome analysis as described in Materials and Methods. A total of 250 genes showing up-regulation and 7 genes showing down-regulation in MuM were identified and listed in Table S2. In order to see whether the unique pattern of gene expression in MuM was due to the *pbpB* lesion, we also conducted transcriptome analysis of Mu50 and MuM carrying wild-type *pbpB in trans.* When sorted against MuM/pYX9 and Mu50/pYX9 expression profiles, majority of the changes observed in MuM were greatly attenuated in MuM/pYX9, suggesting that the truncated PBP2 is responsible for the complicated transcriptional adaptations in MuM. Nonetheless, it is worth noting that

there are 10 genes (including *czrAB, vraDE, gntPK, oppF, mtlF, SAV0069, SAV0190*) showing up- or down-regulation in MuM regardless of complementation by pYX9, and the fold change of these genes in MuM/pYX9 was even greater than that in MuM.

While one might expect that the *pbpB* lesion of MuM could affect cell wall synthesis and trigger a specific stress response, the gene list in Table S2 shows no overlap with the reported signature genes of the cell wall stress stimulon (58, 109). Instead, one intriguing observation was the up-regulation of 67 genes associated with amino acid biosynthesis and transport that are members of the CodY regulon (71, 91). In *S. aureus*, like in many low G+C Gram-positive bacteria, CodY is a central regulator mediating amino acid biosynthesis, nitrogen utilization and transport of macromolecules.

Surprisingly, 67 genes residing in several genomic islands (GIs) were found activated in MuM (Table S2), and this list could be expanded further if a less stringent factor of fold-change was applied in data analysis. These GIs include SCCmec, IS1181-1, SaPIm2, SaGlm, ϕMu50B, SaPIm3, and ϕMu50A (59). Although little was known about the nature of GI activation, similar activation of GI was observed in a *murF* conditional mutant (103), in which the cell wall synthesis was perturbed in muropeptide maturation. Other than the CodY regulon and GIs, genes that were differentially up-regulated in MuM were clustered into potential operons – *ureABCEFGD* for urease synthesis, *sbnABCDRFGHI* for iron metabolism, *kdpABCDE* for an inducible potassium uptake system, and *SAV2094-thiDME* for vitamin B2 and *bioFABD* for vitamin H biosynthesis. Specifically, degradation of urea by urease in *S. aureus* was thought to neutralize acidic microenvironments by generating NH_3 and CO_2 under acid stress (13). In addition, MuM also hosts the induced *arcABCD* operon for the arginine deiminase pathway, a major role of which is to alkalinize the medium by generating NH_3 and CO_2 as well as to energize the cells by production of ATP (104, 125). All together, it strongly suggests that MuM is primed to adjust its metabolic activities to increase the internal pH, which would imply that the defective cell wall may alter the membrane potential and somehow exert a mild acid stress on MuM.

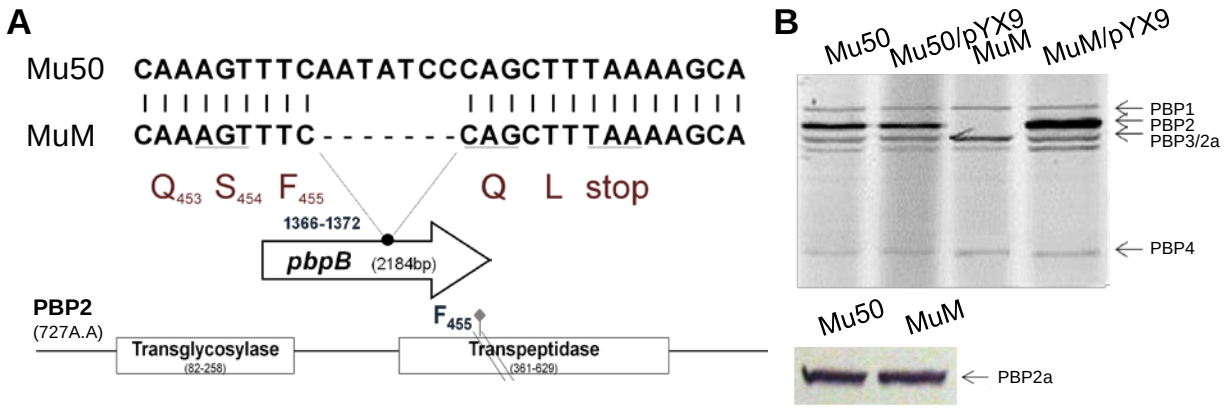

Figure 2. 5 Identification of the *pbpB* lesion in spermine-resistant mutant MuM.

(A) Sequence alignment of the *pbp*B gene from Mu50 and MuM at the mutation site. Also shown were the location of the 7-bp deletion (nt 1366-1372) in the *pbpB* gene of 2184 bp, the amino acid sequence of the truncated PBP2 of MuM, and the sizes and locations of the transglycosidase and transpeptidase domains of PBP2. (B) Absence of PBP2 in MuM and the presence of other penicillin-binding proteins were revealed by Bocillin labeling (top panel) or immunoblot (bottom panel).

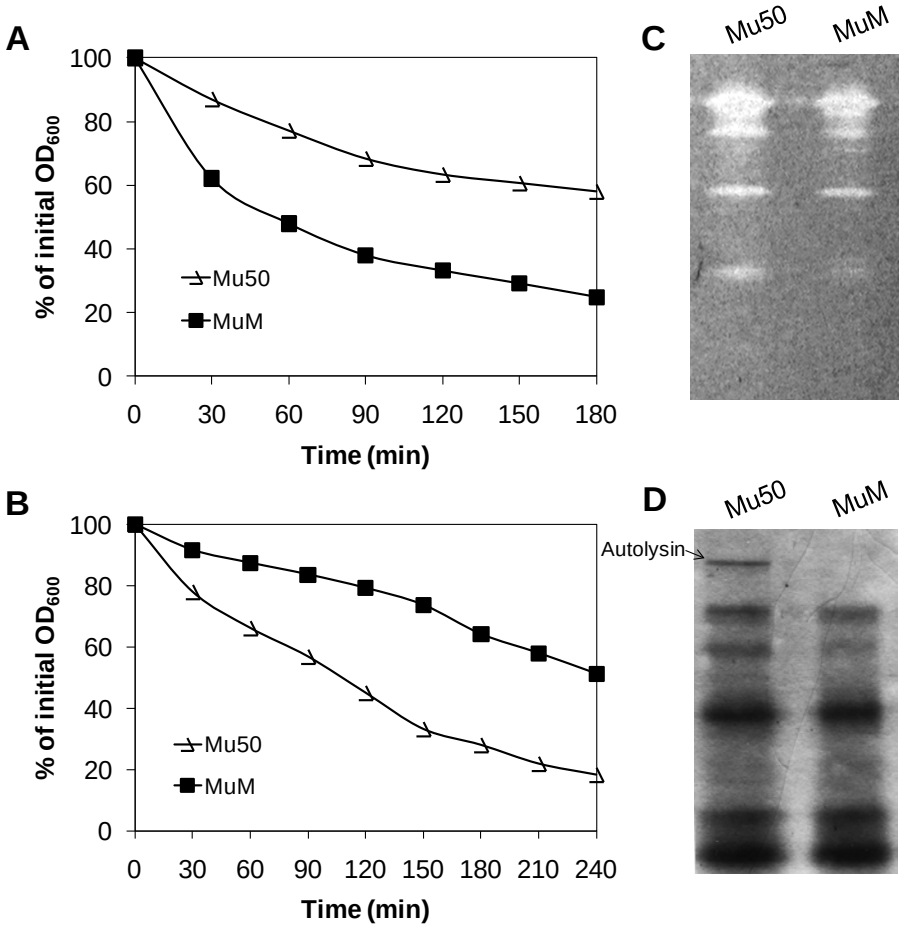

Figure 2. 6 Analysis of cell wall hydrolysis.

(A) In vitro susceptibility of cell walls. Crude cell walls of Mu50 (open triangle) and MuM (closed square) were subjected to degradation by autolytic enzymes from *S. aureus* COL. Preparations of these samples were described in Materials and Methods. The experiments were reproduced several times, and data from a one single experiment were shown here as representatives.
(B) Triton X-100 induced autolysis of Mu50 (open triangle) and MuM (closed square) cells. Values indicate the average of two independent experiments.
(C) Zymographic analysis of the autolysins in SDS cell extracts from Mu50 (left) and MuM (right). Samples were analyzed in a 10% resolving gel containing heat-killed RN4220 cells. Lytic activity was detected by incubation of the gel with gentle agitation at 37°C in renaturing buffer. Equivalent amounts of protein samples were loaded.
(D) Protein profiles in culture supernatants. Extracellular proteins from Mu50 (left) and MuM (right) were prepared as described in Materials and Methods. The gel was stained with Coomassie Blue to detect the total secreted protein profile, and the protein band of autolysin was identified by MALDI-TOF MS/MS.

2.4 DISCUSSION

Unique phenotypic behaviors and transcriptional adaptations of MuM

A spontaneous suppressor mutant of MRSA Mu50 conferring resistance to β-lactams in the presence of spermine was isolated through spermine selection. This mutant possesses a unique *pbpB* lesion, in which a 7-bp deletion generates a truncated PBP2 without the C-terminal transpeptidase (TP) domain while the transglycosidase (TG) domain at the N-terminus remains intact. Although this *pbpB* mutant MuM still confers β-lactam resistance, its physiological properties are very different from those of the parental strain Mu50, a clinical isolate of MRSA in several aspects – gain of spermine resistance, loss of spermine/ β-lactam synergy, gain of spermine/vancomycin synergy, a slower growth rate, temperature-sensitive growth phenotype, a narrow pH range for growth, changes of cell wall composition and turn-over, and a lower level of cell wall hydrolase activity. Furthermore, transcriptome analysis reveals a distinct pattern of gene expression, showing no overlap with that of the cell wall stress stimulon (58, 109)

Physiological functions of PBP2

Our results indicate that the TP domain of PBP2 is not essential for growth and β-lactam resistance of MRSA. These conclusions are consistent with a previous report (83) that a $Ser_{398}Gly$ mutation at the TP domain leads no effect on MIC to methicillin, but loss of the TG activity by a $Glu_{114}Gln$ mutation causes a more than 100-fold decrease on methicillin MIC. On the contrary, the TP activity of PBP2 is essential for the growth of MSSA (89), and specific mutations at the TP domain ($Pro_{458}Leu$) can make MSSA resistant to β-lactam antibiotics (67). This discrepancy is due to the presence of a β-lactam insensitive PBP2a encoded by the *mecA* gene of MRSA. The TP activity of PBP2a is able to sustain cell growth when that of PBP2 is not available. Investigations from that study provide direct evidence that a mutated PBP2 without the TP activity results in altered cell wall composition with reduced amounts of highly cross-linked oligomers. This is consistent with the increased cell wall degradation rate of MuM observed in our study.

In addition to the intrinsic TP and TG activities, PBP2 may serve as scaffold for a multi-enzyme complex in cell wall synthesis. The presence of multi-enzyme complex in cell wall synthesis was first proposed from studies in *E. coli* (39, 40). Later, Tomasz and coworkers (67, 83) reported evidence to support that PBP2 forms a complex with PBP2a, PBP4, and perhaps other enzymes to coordinate cell wall synthesis and hydrolysis. Along this line, one hypothesis was that the TG and TP activities of PBP2 are subjected to allosteric regulation within the complex, and the conformation of this complex could be affected by changes on the supporting scaffold of PBP2. Built upon this model, we propose a working hypothesis for spermine effects on cell wall synthesis in *S. aureus* as described below. This model may also provide an explanation of a somewhat contradictory report that insertion of a transposon at the 3' end of *pbpB* (i.e. intact TG domain and truncated TP domain) made the affected MRSA susceptible to β-lactams (90).

The proposed model of spermine/β-lactam synergy in *S. aureus*

Spermine was reported to exert a strong synergy effect with β-lactams on MRSA (61). In the current study, we present evidence that spermine *per se* also posts a pH-dependent antibacterial activity against strains of *S. aureus* (MRSA and MSSA), and this activity is most likely mediated by the nucleophilic property instead of positive charges of spermine. In search of the potential target of spermine by the genetic approach, the observed spermine-related phenotypes of MuM led us to propose that PBP2 itself or enzymatic activities associated with the PBP2-dependent complex in cell wall synthesis could be good candidates.

The working model we envisioned was: cell wall synthesis requires coordinated functions of a multi-enzyme complex to catalyze elongation of glycan chains and cross-linkage of peptide chains, and binding of spermine to this complex via PBP2 elicits a conformational change to weaken interactions among enzymes in the complex and/or inhibit the TG activity of PBP2. Given that a specific *pbpB* lesion confers resistance to spermine and spermine/oxacillin synergy on MuM, one would expect the TP domain of

PBP2 as potential target of spermine. However, we did not favor this hypothesis because TP-PBP2 is not essential for growth of MRSA in the presence of PBP2a. Moreover, the possibility of PBP2a *per se* as target of spermine could also be excluded because the spermine effects also exist in MSSA in which PBP2a is absent, and MuM possessing PBP2a is resistant to spermine. Studies to elucidate the molecular mechanism for spermine effects based on the proposed model are currently in progress.

pH sensitivity of MuM

By truncating the TP domain of PBP2, MuM can only grow in a very limited pH range. The most striking difference between Mu50 and MuM in response to pH was under alkaline conditions (Figure 2.4), which may be related to the cell wall turnover rate by the following rationale. It has been reported that the murein hydrolase exhibits a much lower level of activities in acidic conditions (119). Therefore, it is anticipated that alkaline conditions can speed up murein hydrolysis, which could have a more severe impact on MuM due to its weakened cell wall structure.

On the other hand, MuM also shows sensitivity to acidic pH. It is known that the trans-membrane pH gradient is essential for the uptake of amino acid in *S. aureus* (74). The ability of MuM to adjust trans-membrane pH gradient may be reduced due to the PBP2 mutation and concurring cell wall anomaly, which could be a possible reason for its reduced growth rate when pH is lower than 7. One explanation can be derived from the fact that PBP2a is not detectable when grown at pH 5.2 (36, 65), and therefore MuM without a functional TP of PBP2 would encounter severe cell wall defects at acidic conditions.

In summary, several lines of evidence support PBP2 as the potential target of spermine in sensitization of *S. aureus* to β-lactams. Absence of the TP domain in spermine-resistant MuM may liberate PBP2 from spermine interference, and concomitantly cooperate with PBP2a to continue functional on exposure to β-lactams. The altered phenotypic properties and transcriptional adaptations could be the compensatory effects triggered by mutated PBP2 on cell wall composition. Future studies on the molecular mechanism

of spermine interactions with the proposed PBP2-associated multi-enzyme complex in cell wall synthesis hold great potentials on the development of new therapeutics for MRSA infections.

PBP2 is not the only Spm-resistant determinant for Spm-resistant (Spm^R) mutants

Besides MuM, nine more independent Spm^R mutants were also isolated and characterized (Table B.1). Although displaying different genotypic and phenotypic properties from MuM (Figure B.1, B.2), those Spm^R all show resistance to both Spm and Spm/ β-lactam synergy (Table B.2). Notably, in the mutants derived from RN4220, each strain has more than one mutation with some of which shared in two strains (Table B.3). Therefore, products of those mutated genes may act cooperatively to counteract the Spm effect. Meanwhile, concerning the scope of mutated genes, we may infer that instead of locating a single and defined target, the role of Spm to *S. aureus* could be multifarious and complex. Details for characterization of these mutants are included in Appendix B.

CHAPTER 3: ANALYSIS OF SPERMINE-DEPENDENT SYNERGY WITH β-LACTAMS ON CELL WALL SYNTHESIS

3.1 INTRODUCTION

As described in Chapter 2, an MRSA mutant may become Spm-resistant with no Spm/β-lactam synergy by a specific mutation on PBP2 that possesses an intact N-terminal TGase domain but no C-terminal TPase domain. It strongly supports the hypothesis that Spm may interfere with PBP(s) or the coordinated complex in cell wall synthesis. Therefore, experiments were designed to test this hypothesis in the following aspects with cells upon challenge by Spm or β-lactam alone or in combination: 1) the cell wall composition; 2) expression of PBPs on transcriptional level and translational levels. Meanwhile, the recombinant PBPs of *S. aureus* were constructed, purified, and analyzed via biochemical approaches to test the possible interactions between Spm and PBPs.

3.2 MATERIALS AND METHODS

Bacterial strains, plasmids, and growth conditions

S. aureus Mu50 (ATCC700699), *E. coli* DH5α (Bethesda Research Laboratories) and Top10 (Invitrogen) were employed in this study. The plasmids used in this study are listed in Table 3.1, and primers are listed in Table S1. Both *E. coli* and *S. aureus* strains were routinely grown and maintained in the Luria-Bertani (LB) medium. When required, the LB medium was buffered with 20mM Tris-HCl at the indicated pH. For *E. coli*, ampicillin was added to the medium as necessary at 100μg/ml.

Analysis of cell wall composition

MRSA strain Mu50 was grown in LB broth (pH 8.0, w/ 20mM Tris-Cl) at 37°C with aeration. At OD_{600} of 0.5, cultures were supplemented with 0.5 mM spermine (Spm) and/or 1 ng/μl oxacillin (Ox), and cell growth was continued for 4 hours before harvest. Isolation of cell wall peptidoglycans and the analysis of

the muropeptides by reverse-phase HPLC were carried out by CeCo Labs from Tubingen University, Germany (www.cecolabs.de).

Protein cloning, expression, and purification

The *pbp1 (*or *pbpA), pbp3 (*or *pbpC), pbp4 (*or *pbpD)* gene lacking the sequence forthe N-terminal signal peptide and the putative transmembrane (TM) domain (at N-terminus of PBP1 and PBP3 andC-terminus of PBP4)was amplified from gDNA of MRSA Mu50 using Phusion polymerase (NEB). The resulting PCR product was digested with *Pst*I/*Eco*RI and cloned into the corresponding sites in the expression vector pBAD/HisD, giving rise to pH6N-PBP1, pH6N-PBP3, and pH6N-PBP4. The constructs encode the fusion of a hexa-histidine tag to the N-terminus of PBP1, PBP3, or PBP4. The resulting plasmids express the recombinant proteins which cover residues M37-D744 for PBP1), Q44-K691 for PBP3), and T25-H400 for PBP4, respectively.

Recombinant plasmids were also constructed to express the periplasmic polyamine-binding protein PotD without signal peptide) and the transcriptional regulator PotR of the *potABCD* operon.The PCR products for these constructs were digested with *Hin*dIII and *Eco*RI, respectively, and cloned into *Sma*I/*Hin*dIII and *Sma*I/*Eco*RI sites of pBAD/HisD (5' blunt end of PCR product ligating to *Sma*I site on the vector), obtaining pH6NnSP-PotD and pH6N-PotR with a hexa-histidine tag fused to N-terminus of PotD and PotR.

Recombinant strains of *E. coli* Top10 harboring plasmid of interest were grown at 30°C in LB medium containing 100 μg/ml ampicillin. When OD_{600} reached 0.6 to 0.8, the cultures were supplemented with 0.2% arabinose followed by an additional 4 hours of growth. Cells were harvested by centrifugation, resuspended in buffer A (20 mM sodium phosphate [NaPi] buffer, pH 7.4, 500mM NaCl) containing a cocktail of EDTA-free protease inhibitors (Roche), and disrupted by French press at 17,000 psi. After centrifugation at 20,000 × g for 30min at 4°C, the soluble fraction was applied to a HisTrap HP column

(GE) pre-equilibrated with Buffer A. Unbound proteins were washed off the column with 5 column volumes of Buffer A, and the bound proteins were then eluted by increasing conc. of imidazole (final conc. 500 mM) in a gradient manner. The target fractions were pooled together and concentrated using an Aminco Ultra-4 centrifugal filter unit (Millipore) and change the buffer to 20 mM Tris-HCl (pH 7.6).

For PBP2, the *pbp2* (or *pbpB*) gene was PCR amplified (Phusion, NEB) from Mu50 genomic DNA with primer pairs see Table S1. The region encodes amino acids W59 to S716 omitting the N-terminal cytoplasmic tail, transmembrane domain, and 11 amino acids from the C-terminus. The PCR product was digested with *Bsp*HI/*Sma*I and subcloned into *Nco*I/*Sma*I sites of the expression vector pBAD-HisE. The resulting plasmid pH6C-PBP2 was introduced into in *E. coli* Top10 for expression for a recombinant PBP2 with a C-terminal hexa-histidine tag.

PBP2 was expressed after induction of a log-phase culture with 0.2% arabinose for 4 hours at 30°C. The cells were broken with a French press at 17,000 psi in Buffer A with Complete EDTA-free protease inhibitors (Roche) as described above. After centrifugation at 20,000g × for 30min, freely soluble proteins were decanted, and the pellet was resuspended in Buffer A containing 20mM CHAPS, 10% glycerol, 0.1% Sarkosyl (as detergent-containing His Buffer) and adjust pH to 9.0 by 1N NaOH with stirring at 4°C. The solublized fusion protein was then loaded onto HisTrap HP column (GE) which was washed extensively with the detergent-containing Buffer A and then eluted in a stepwise manner using detergent-containing Buffer A with 500mM imidazole. The target fractions were pooled together and concentrated using an Aminco Ultra-4 centrifugal filter unit (Millipore) to change the buffer to 20 mM Tris-Cl (pH7.6).

For PBP2a, the *mecA* gene lacking the first 69 bases for its N-terminal anchoring region of 23 amino acids was amplified from Mu50 gDNA and cloned into *Nco*I/*Hin*dIII site of pBAD/HisA. The resulting plasmid pPBP2a encoding no hexa-histidine tag, was further transformed into *E. coli* Top10 for overexpression. PBP2a was expressed after induction of a log-phase culture with 0.2% arabinose for 4

hours at 30°C. Cells were suspended in Q buffer (20mM Tris-Cl, pH7.6) containing complete EDTA-free protease inhibitors (Roche), and disrupted by French press at 17,000 psi. After centrifugation at 20,000g × for 30min, the supernatant was subjected to ammonium sulfate fractionation. The fraction precipitated by 30% saturation was dissolved in Q buffer, and desalted by Aminco Ultra-4 centrifugal filter unit (Millipore). The concentrated protein sample was diluted with Q buffer and applied to HiTrap Q HP column (GE) equilibrated with same buffer. Following gradient elution with Q buffer containing 1M KCl, fractions containing target protein were combined and desalted again with Aminco Ultra-4 centrifugal filter unit to change the buffer to 20 mM Tris-HCl (pH 7.6).

Construction of expression-vector pBAD-HisE

The primer pairs hisF-5' GGGCATCATCATCATCATCATTGAATTCTGC 3' and hisR-5' GCAGAATTCAATGATGATGATGATGATGCCC 3' were annealed and digested by *Sma*I/*Eco*RI, to replace the *Sma*I-*Eco*RI region of pQF50. The resulting plasmid pQF53 was further digested with *Nco*I/*Eco*RI to release the partial MCS carrying the His6 region, which was used for replacing the *Nco*I-*Eco*RI region of expression vector pBAD-HisC (Invitrogen). The derived construct pBAD-HisE contains the translational initiation site (at *Nco*I site) followed by MCS (*Sal*I, *Xba*I, *Bam*HI, *Sma*I) and the sequence for a hexa-histidine tag.

Bocillin labeling of PBPs

For labeling of purified PBPs, the protein samples (0.04 µg in 20 µl of 20mM Tris-Cl pH8.0) were incubated with Bocillin of indicated conc. for 30 min at 37 °C with gentle shaking. For labeling with bacterial lysates, the culture of log-phase *S. aureus* (10 ml) was harvested and the cell pellet was suspended in 200 µl the lysis buffer (50mM Tris pH7.5, 50mM NaCl, 5-10 µl of lysostaphin (10mg/ml), 5µl of DNaseI (10 U/µl), 5 ul of RNase A (200 µg/ml) with gentle shaking for 15-20 min at 37 °C, followed by the addition of Bocillin to a final concentration of 5µM and incubated at 37 °C for 30 min.. For the concentration-dependent experiments, the Bocillin conc. ranges from 0.25-16µM. If needed,

samples were pre-incubated with Spm for 30 min at 37 °C prior to Bocillin labeling. After Bocillin labeling, samples were mixed with Laemmli sample buffer and boiled for 5 min prior to SDS-PAGE. The gel was rinsed with water immediately after electrophoresis and scanned with Typhoon scanner with excitation wavelength at 488 nm and emission wavelength at 530 nm. The intensity of the bands was quantified by Image Quant software.

In vivo ^{14}C Spm labeling of *S. aureus* lysate

The cells from a 10-ml culture of mid-log phase *S. aurues* in LB medium (pH8.0) were immediately collected by centrifugation and resuspended in 100 µl of Tris buffer (20mM ,pH8.0). A cocktail of 2 µl of 0.5M cold Spm and 1µl of 1mM ^{14}C Spm (0.1mCi/ml, 100mCi/mmol) were immediately added, followed by a 30 min incubation at 37 °C. Lysostaphin (2 µl; 10mg/ml) was then added and the samples were incubated at 37°C for an additional 20 min; samples were also treated with of DNase I (1 µl; 10U/µl) and of RNase A (1 µl; 200 µg/ml) in some experiments. After lysis, Laemmli sample buffer was added and the samples were boiled for 10 min, followed by electrophoresis on 10% SDS-PAGE. The gels were dried and subjected to autoradiography.

^{14}C Spm labeling of overexpressed proteins *in vivo*

Aliquots of *E. coli* culture (1.5 ml) of overexpressed recombinant proteins were harvested by centrifugation. The resulting pellet was resuspended in 30 µl of Tris buffer (20mM; pH8.0), added with a mix of 2 µl ^{14}C Spm (1 mM) / 2 µl cold Spm (2.5 mM) and incubated at 37°C for 30 min with gentle shaking, followed by the addition of lysozyme (3 µl ; 20ng/µl), DNase I (1 µl ; 10U/µl) and RNase A (1 µl; 2 mg/ml) for additional incubation of 30 min. The lysates were then added with Laemmli sample buffer and boiled for 5 min prior to SDS-PAGE analysis. After electrophoresis, the gels were dried and subjected to autoradiography.

^{14}C Spm labeling of purified proteins *in vitro*

The purified protein (10 µl of 0.04 µg/µl in 20mM Tris-Cl, pH8.0) was incubated with a mix of ^{14}C Spm (1mM; 2 µl) and cold Spm (2.5mM; 2 µl) for 30 min with gentle shaking at 37°C. Then the samples were added with Laemmli sample buffer and boiled for 5min prior to SDS-PAGE. After electrophoresis, the gels were dried and subjected to autoradiography.

DARTS (Drug Affinity Responsive Target Stability)

The purified protein (1 µg in 20 µl of 50mM Tris-Cl, pH8.0, 50mM NaCl, 10 mM $CaCl_2$) was incubated at 37°C with or without 1 mM Spm for 25 min, then subjected to trypsin digestion (0.075 µg) at 25°C for a specified period of time as indicated in results. The reaction was stopped by immediate addition of Laemmli sample buffer and boiled for 10min, followed by SDS-PAGE.

Table 3. 1 Plasmids used in Chapter 3

Plasmids	Relevant characteristics	Source or reference
pBAD/HisA	Expression vector, Amp^r	Invitrogen
pBAD/HisD	Expression vector for producing N terminal His tag fusion, Amp^R	(69)
pBAD/HisE	Expression vector for producing C-terminal His fusion, Amp^R	This study
pH6N-PBP1	pBAD/HisD expressing N-His-PBP1	This study
pH6C-PBP2	pBAD/HisE expressing C-His-PBP2	This study
pH6N-PBP3	pBAD/HisD expressing N-His-PBP3	This study
pH6N-PBP4	pBAD/HisD expressing N-His-PBP4	This study
pPBP2a	pBAD/HisA expressing no tag PBP2a	This study
pH6NnSP-PotD	pBAD/HisD expressing N-His-no signal peptide PotD	This study
pH6N-PotR	pBAD/HisD expressing N-His-PotR	This study

3.3 RESULTS

Synergy between spermine and oxacillin reduces the degree of cross linkage on cell wall

To determine the composition and degree of cell wall cross-linkage in spermine/oxacillin-grown cells, peptidoglycan was digested with M1 muramidase and the fragments were analyzed by HPLC. Examination of MRSA Mu50 grown in the presence of Spm (0.5mM) alone, Ox (1ng/μl) alone, or their combination, revealed no major changes on the biochemical composition of PG (Figure 3.1). However, differences were noted in the degree of cross-linking between glycan chains within the samples. The combination treatment results in a more depressed hump (retention time 110min and after) in this sample while samples of Spm- or Ox-alone do not cause any significant changes on the chromatograms (data not shown). A chromatogram with a depressed humpalso occured when *S. aureus* encounters high dose β-lactams that block the biochemical functions of PBPs(23). Since PG cross-linking is catalyzed by PBPs, this result strongly suggests an enhanced PBP inactivation by Oxa/Spm synergy.

The overall contribution of PBPs in cell wall synthesis in the case of Oxa/Spm synergy can be affected in multiple levels: 1) transcription and translation; 2) the binding affinity with β-lactams; 3) the enzymatic activity, which may result from irregular conformation, incorrect localization, masked active sites, etc. To clarify if PBP2a or the PBPs complex is involved in the synergism, we tested a) whether Spm suppresses PBPs' expression; b) whether Spm enhances the PBPs-β-lactam binding; c) whether Spm can directly interact with PBPs to influence their activities. We did not evaluate whether Spm can delocalize PBP(s) or prevent their recruitment to the septum due to some technical limitations.

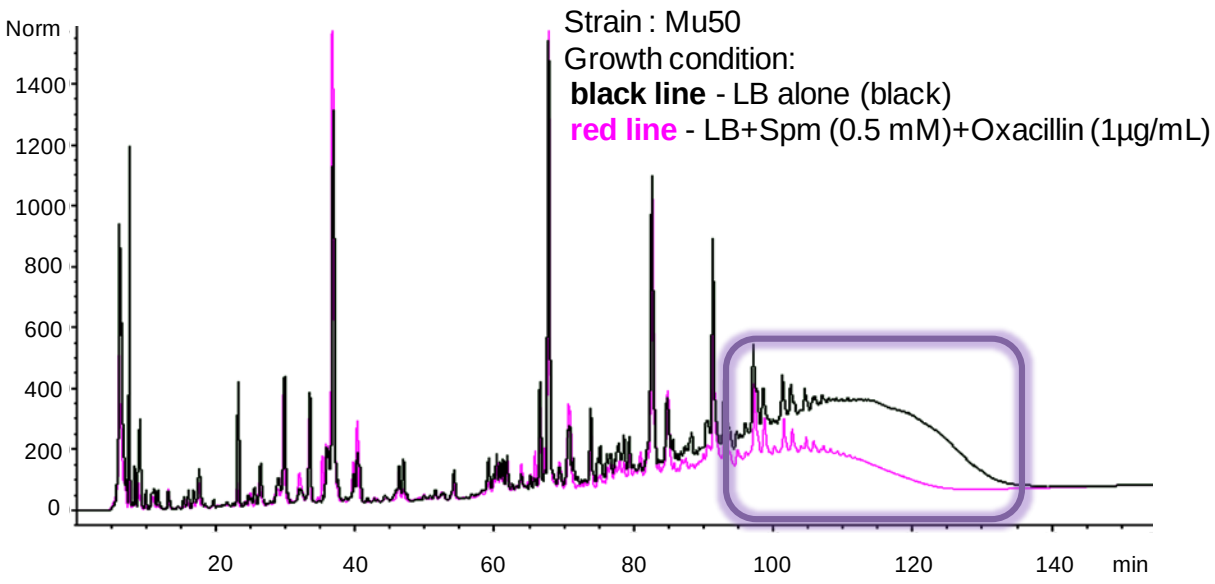

Figure 3. 1 Chromatograms of peptidoglycan analysis by HPLC.

Effect of Spm/β-lactam on the muropeptide composition and degree of cross-linking of peptidoglycan extracted from *S. aureus* Mu50. Purified peptidoglycan preparations from cells grown in the presence or absence of Spm or oxacillin or their combo were digested with muramidase and the digestion products separated by HPLC.

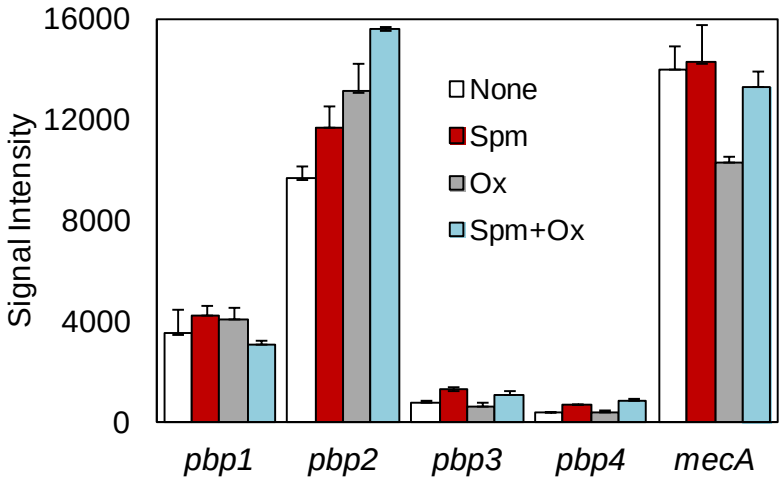

Figure 3. 2 Transcript levels of *pbp* genes exposed to Spm and Ox alone or in combination.

Spm(1mM spermine), Ox (16ng/μl oxacillin), Spm+Ox (1mM spermine + 16ng/μl oxacillin), recorded by GeneChip (Affymetrix)

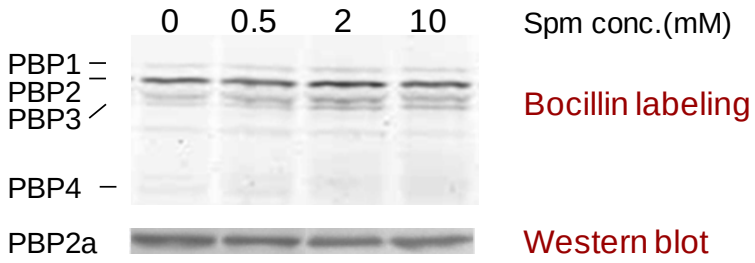

Figure 3. 3 PBPs profiles of *S. aureus* exposed to Spm during growth.

Mu50 was grown in the presence of various concentrations of spermine. Cell lysates were labeled with Bocillin to identify PBP1-4, or subjected to Western blot to detect PBP2a.

Spm does not affect PBPs expression

To determine the gene expression of PBPs upon Spm or synergy, we performed microarray analysis in MRSA Mu50 treated with Spm (1mM), Ox (16ng/μl), or in combination for 2 hours. Figure 3.2 shows the signal intensities of different *pbp* expression under the tested conditions. No significant differences can be detected between untreated and treated transcripts, suggesting low-dose Spm by itself or in combination with β-lactams may not affect the *pbp* transcription. Next, to examine whether Spm can influence the PBPs production, lysates from Mu50 grown in the presence of different concentrations of Spm (0.5mM, 2mM, 10mM) were subjected to Bocillin labeling (for detection of PBP1-4) or Western blot (for detection of PBP2a). Again, no significant changes in the quantities of any PBPs can be observed (Figure 3.3). These results indicated Spm may not affect PBPs expression either at the transcriptional or translational level.

Spm does not affect acylation of PBPs by Bocillin

To evaluate whether Spm can enhance binding of β-lactams toPBPs binding during synergy, PBPs in *S. aureus* lysate or purified PBPswere incubated with Bocillin, a fluorescent β-lactam derivative, with or without Spm treatment. The binding affinities were estimated by measuring the fluorescence intensities of acylated PBPs by Bocillin. To be specific, firstly the lysates from Mu50 grown in the medium free of Spm or Oxa were pre-incubated with 0.5mM Spm and subjected to labeling by Bocillin of indicated concentrations. The binding kinetics of Bocillin to PBPs, as illustrated in Figure 3.4A, were unaffected by the presence of Spm.

Next, purified PBPs were used to study the β-lactam-PBP binding affinity, individually or in combination. From the monophasic saturation curve obtained by the binding of Bocillin at different concentrations, the affinity of Bocillin for different PBP was calculated (Figure 3.4B). The notably higher dissociation constant (Kd) of PBP2a than those of other PBPs is consistent with its low affinity to β-lactams and the

resultant high β-lactam MIC for MRSA. Moreover, when comparing the individual Kd values between Spm treated and untreated samples, no significant variations can be detected. Coomassie staining of the same gel ensured no variations in protein amount between samples (data not shown). Collectively, these two lines of data both suggest Spm may not affect PBP acylation by β-lactams.

Formation of Spm-PBPs conjugates

Spm is a potent nucleophile at high pH, as evidenced by the formation of a Spm-Ox adduct in our recent report (121) (Figure 2.3 in Chapter 2). At the same time, growth inhibition by Spm and the synergy effect of Spm and β-lactams become more effective when pH is increased (Figure 2.2 in Chapter 2). Since PBPs of *S. aureus* reside outside of the cells where the electron numbers of amine are readily affected by environmental pH to make Spm become a nucleophile, we tested if Spm can form chemical conjugates with PBPs. Crude extracts of *E. coli* expressing recombinant PBPs were mixed with ^{14}C Spm as described in Materials and Methods, followed by SDS-PAGE and exposure to the phospoimage plate. A carboxyl esterase Est30 was used as control. As shown in Figure 3.5A, unexpectedly, all of the tested proteins were labeled with radioactivity, indicating the formation of non-specifi Spm-protein conjugates.

To further verify these results, similar experiments were performed on each purified PBP. Much less amount of purified PBPs was used compared to that in the extracts (as demonstrated with Commassie staining of the same gel), and no visible radioactive-labeled protein band can be detected (Figure 3.5B). These negative results suggest low efficiency in the formation of Spm-protein conjugates; alternatively, it is possible that the formation of conjugates requires cooperation with other factors which are present in cell extract but absent in purified protein solutions.

Also, we tried to use ^{14}C Spm to directly label *S. aureus* lysate (Figure 3.5C), and no distinct band can be detected with the lysate pre-treated with DNase and RNase. However, radioactive signals appeared as a

smeared block of high molecular weights when the lysate without nuclease treatment was used in the reaction. These results may imply possible interactions of Spm with DNA or RNA.

No change in the trypsin digestion pattern of purified PBPs by the presence of Spm

In comparison to PBPs alone, binding of Spm to PBPs may cause conformational changes, and hence the sensitivity of ligand-protein complexes against protease digestion. So, we looked for possible conformation changes of PBPs due to Spm interaction by the DARTS (drug affinity responsive target stability) method. Purified PBP was pre-incubated with or without Spm, subjected to trypsin digestion following a time course, and separated by SDS-PAGE. The unrelated carboxylesterase Est55 served as control. As shown in Figure 3.6, for all tested proteins, no significant difference on the digestion pattern can be observed regardless of Spm treatment. Although these results imply the inability of Spm to change the protein conformation *in vitro* (under test conditions), we may not rule out the possibility that other unknown factors may be required to facilitate the Spm-protein interaction, as observed in Figure 3.5A.

A

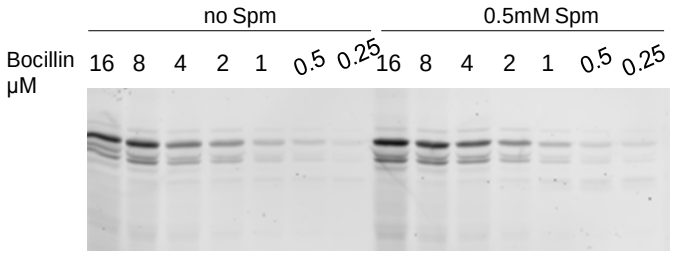

B

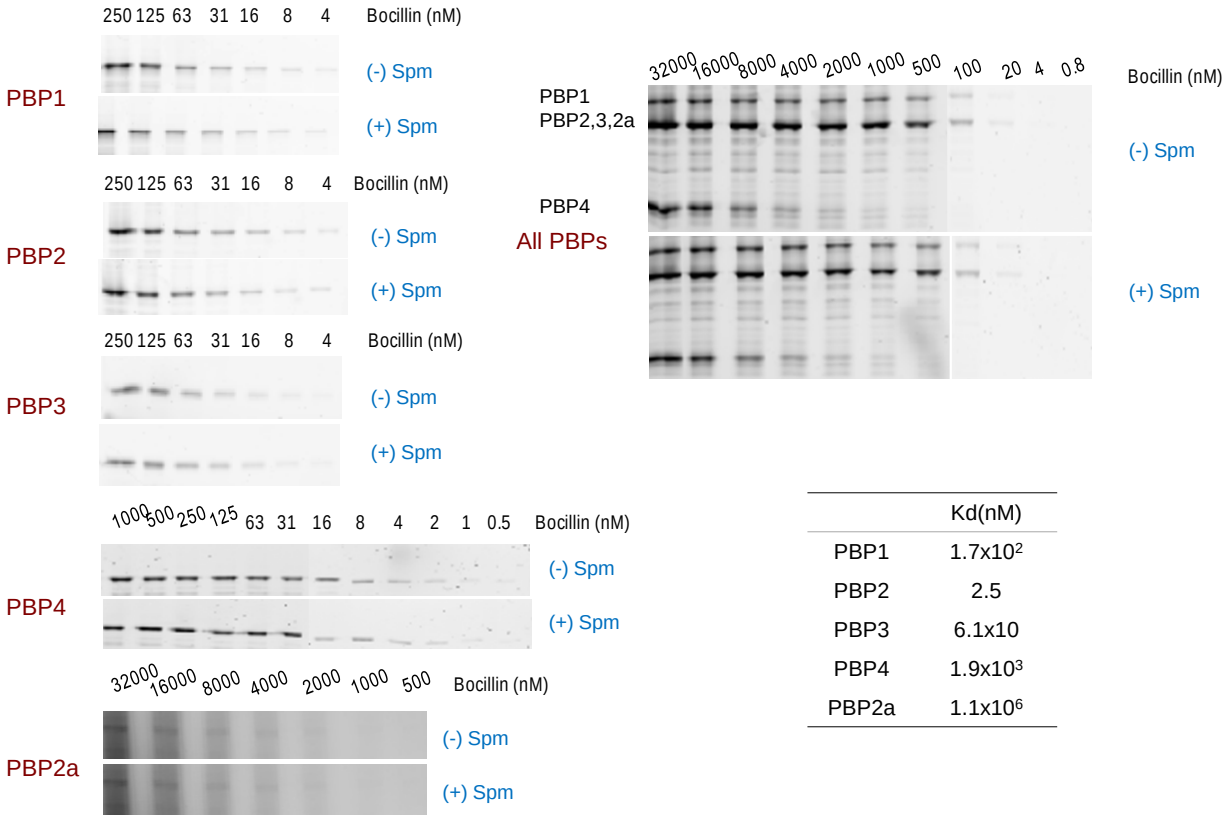

	Kd(nM)
PBP1	$1.7x10^2$
PBP2	2.5
PBP3	6.1x10
PBP4	$1.9x10^3$
PBP2a	$1.1x10^6$

Figure 3. 4 Binding kinetics of Bocillin to PBPs in the presence or absence of Spm.

(A) *in vivo* analysis using PBPs of *S. aureus* lysate. Mu50 was grown in Spm-free medium. The lysates were pre-incubated with or without Spm, and labeled by various amount of Bocillin.
(B) *in vitro* analysis using purified PBPs, for determination of PBPs - Bocillin affinity in the presence or absence of spermine. Purified PBPs (alone or in cocktail) were pre-incubated with or without Spm (1mM) and labeled by various amounts of Bocillin

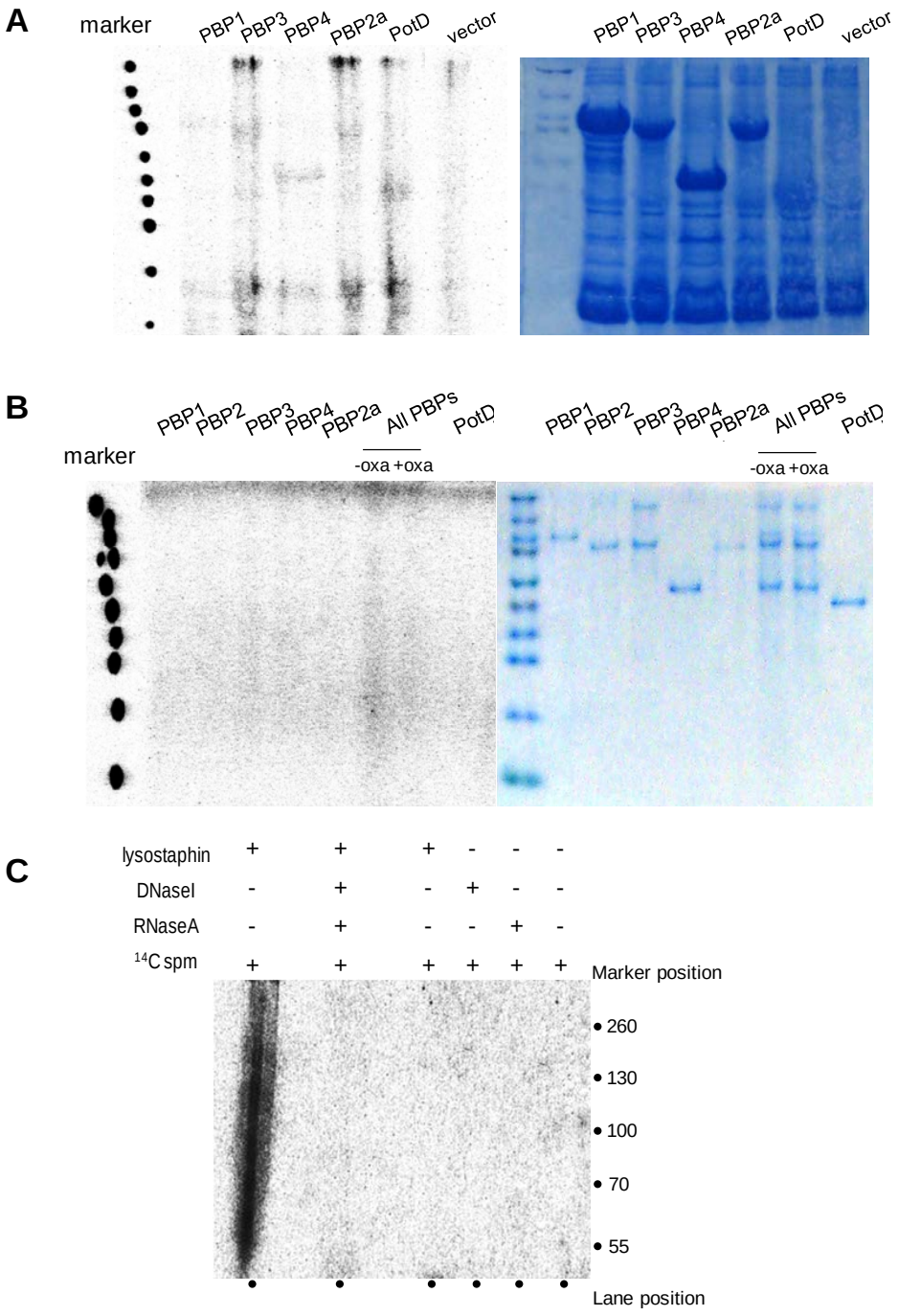

Figure 3. 5 ^{14}C Spm labeling of proteins

(A)proteins *in vivo (E.coli* lysate with overexpressed protein);
(B)proteins *in vitro* (protein after purification);
(C)cell lysate of *S. aureus.*
Samples were incubated with ^{14}C spermine and separated on SDS-PAGE; dried gel was exposed to phosphor image plate for radioisotope detection

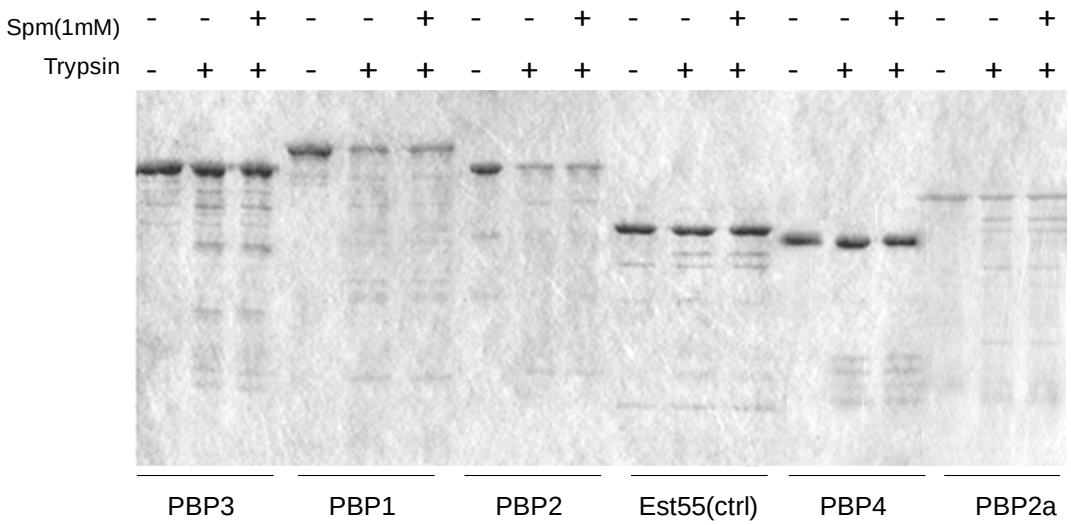

Figure 3. 6 DARTs analysis with pure PBPs.

Purified PBP or control (Est55) was incubated with or without spermine and digested with trypsin. The period of time for trypsin digestion differed among proteins: PBP1, 4min; PBP2, 10min; PBP3, 10min; PBP4, 10min; PBP2a, 20min; Est55, 10min.

3.4 DISCUSSION

Spm may potentiate β-lactam efficacy by perturbing the functional cooperation of PBPs

The PBP2 mutant strain MuM became Spm-resistant and showed no Spm/β-lactam synergy, suggesting PBPs could be the target for Spm. In line with this, the reduced PG crosslinking by a combination of low dose Spm and oxacillin further supports the hypothesis of Spm perturbing cell wall integrity in favor of β-lactam efficacy. However, a series of experiments investigating Spm effects on PBPs, the β-lactam targets, implies that Spm does not appear to suppress the PBPs expression or alter their interactions with β-lactams. Even so, these results can not rule out the possibility that the enzymatic activities of PBP-associated multi-enzyme complexes might be modulated directly by binding of Spm to the complexes or indirectly through delocalization or reconfiguration of the complexes on the membrane.

Spm may perturb other cell wall related factors (instead of PBPs) to achieve the Spm/β-lactam synergy

As described in Chapter 2 and Appendix B, in addition to strain MuM, we also characterized several other Spm-resistant mutants. Like MuM, these mutants lose the synergy effect of Spm and β-lactams, but genome resequencing identified mutations (on more than one locus per strain) other than *pbp2* in these strains. Therefore, it is possible that other mutation(s) may confer similar impacts as that of PBP2 defect in MuM to block the Spm target. In other words, other factors which can influence the cell wall turnover also have the potential to affect synergy. Three hypothetical mechanisms were described below.

1) One thought is that Spm may behave like vancomycin and other glycopeptides antibiotics, which inhibit the PG synthesis by binding to the D-Ala-D-Ala region of the stem peptide, and thus blocking both TGase and TPase activities of PBPs(112). If Spm works in this way, the resistant mutant may conquer the drug action by increasing intact D-Ala-D-Ala-carboxyl termini in the PG layer. These dipeptides may in

turn bind to and trap Spm in the layer and prevent it from reaching the target sites in the cell wall biosynthetic machinery at the cytoplasimic membrane.

This hypothesis was supported by the significant induction of *pbp4* under challenge of high dose Spm (Figure 5.5, Table S4). PBP4, which has both carboxypeptidase and transpeptidase activities *in vitro*, was hypothesized being an efficient carboxypeptidase over a transpeptidase *in vivo*. It is known the degree of cross-linking in cell wall is largely dependent on the ratio of cross-linked over free-stem peptides (100), with the latter primarily produced by the carboxypeptidase activity of PBP4 in *S. aurues*. Therefore, we speculate if Spm bind to the D-Ala-D-Ala of the stem peptide, the resultant shortage of cross-linking level and/or the excess of D-Ala-D-Ala may become a signal to induce *pbp4* expression.

2) Spm-mediated perturbation of cell wall cross-linking may be related to changes in the secretion of autolysins. Autolysins are cell wall hydrolytic enzymes that play key roles in PG turnover, and the activity and retention of which are greatly influenced by the pH/charge characteristics of cell wall (95, 111). The combination treatment of Spm andβ-lactam may decrease the net positive charge of the cell surface, e.g. reducing D-alanylation of cell wall-associated teichoic acid, which in turn reduces the autolysin processing and PG turnover, and ultimately the cell wall integrity.

3) In dividing cells, PBPs-mediated transpeptidation and transglycosylation occur predominantly at the division septum, at which the substrate of PBPs for PG synthesis was restricted. Therefore, the number of PBPs on the cell membrane could be a crucial factor in determining the rate of cell wall synthesis. As such, we speculate that Spm may intercalate into the cell membrane, interfere with the trafficking of membrane-anchored PBPs or the associated enzymes, and delocalize cell wall synthetic machinery from the septum. By doing so, the adverse effect of Spm on cell wall synthesis may be further compounded by the presence of β-lactam.

CHAPTER 4: TRANSCRIPTOME ANALYSIS OF *S. AUREUS* IN RESPONSE TO THE SYNERGISTIC EFFECT OF SPERMINE AND OXACILLIN

4.1 INTRODUCTION

Combination of two drugs may inhibit bacterial growth in more complicated ways than the single drug does. As for our case, there are various possible mechanisms by which Spm/β-lactam synergy can arise: (i) they both inhibit a common biochemical pathway-cell wall synthesis; (ii) Spm inhibits the protective enzyme against β-lactams, which is PBP2a in MRSA; (iii) β-lactam enhances the uptake of Spm to intensify its toxicity to the cell; (iv) Spm amplifies the secondary effects imposed by β-lactams, e.g. producing ROS and triggering oxidative-damage cellular death pathway. In short, the synergy of Spm and β-lactams may function by Spm facilitating β-lactams or β-lactam enhancing Spm attack on unknown targets, or the formation of a new structural configuration that makes the common target more vulnerable to attack by Spm or β-lactams. Therefore, besides exploring how Spm could affect β-lactam sensitivity in *S. aureus*, monitoring the global changes in gene expression patterns over a range of conditions, in our case Spm or Ox alone and Spm/Ox combination, may provide us a better insight of how two agents might affect each other to enhance the antibacterial effectiveness.

4.2 MATERIALS AND METHODS

Transcriptional profiling conditions (for low concentration of Spm, Ox, or Spm/Ox)

Overnight grown cultures of *S. aureus* Mu50 were used to inoculate 50ml LB broth (pH8.0) and grown at 37 ºC with shaking at 250rpm. The cultures in log-phase ($OD6_{00}$ of 0.5) were exposed to the following compounds for 2 hour exposure before harvest: Spm (1mM), Ox (16ng/µl), and a combination of Spm and Ox. The working concentrations of Spm and Ox were chosen based on the noticeable synergistic

effect at which they gave rise to. Cultures free of exogenous Spm and Ox served as control. Experiments were carried out in two independent batches of cultures.

RNA isolation

The cells from fresh cultures were harvested by centrifugation at 20 ºC for 2 min with 12,000 rpm. Cell pellets were suspended with 1 ml of suspension buffer (20mM Tris-Cl, pH7.5, 50mM NaCl, 10mM EDTA) and 2 ml of RNAprotect Bacteria Reagent (QIAGEN), and mixed immediately by vortexing for 5 seconds. The cell suspensions were then incubated for 5min at room temperature followed by centrifugation for 10min at 12,000 rpm. After decanting the supernatant, the cell pellets were resuspended in 3 ml of suspension buffer and added with 10 µl of lysostaphin (10mg/ml) to weaken cell wall. RNA extraction was then carried out using hot phenol extraction method. Contaminated genomic DNA was removed using RNase-Free DNase I (Pierce) coupled with DNase I buffer (USB). The treated sample was applied to an RNeasy Mini column (QIAGEN) to recover RNA. The quality of these RNA samples was monitored by agarose gel electrophoresis, and RNA quantity was measured by UV spectrophotometry.

DNA Microarrays

The purified RNA sample was subjected to cDNA synthesis through random priming, reverse transcription, and removal of RNA. The purified cDNA was treated with DNase I for fragmentation, followed by terminal labelling with biotinated dUTP. The labelled cDNA sample was hybridized to GeneChip® of *S. aureus* Genome Arrays (Affymetrix), which were subsequently washed, stained and scanned. All the procedures followed the GeneChip® Expression Analysis Technical Manual. For qualitative presentation, the processed and normalized signals from the array were subdivided into four categories according to the range of intensities, and were represented as follows accordingly (Table S3, S4 of Appendix A): •100-500, •• 500-1500, ••• 1500-4500, •••• 4500-50000.

4.3 RESULTS

To gain insight into the cellular responses to the synergistic effects of Spm and β-lactam, DNA microarrays experiments were conducted in MRSA Mu50 growing in the LB medium with following supplements as Experimental Group: 1mM Spm (sample S), 16 ng/μl Ox (sample O), 1mM Spm+16ng/μl Ox (sample SO). The cultures in the exponential phase were exposed to the indicated supplements for two hours before harvest for RNA purification, and the culture without exposure to any supplement (sample N) served as Control Group.

Once the signals of gene expression from each sample were obtained as described in Materials and Methods, data analysis was conducted by comparing three samples in the Experimental Group with sample N in the Control Group to identify genes of statistically significant changes in expression levels. The following criteria were applied: (1) p value ≤ 0.05, (2) absolute fold change ≥ 2, and (3) signal intensity > 100 on either the experimental set (for up-regulation sorting) or control set (for down-regulation sorting). By comparing S with N, O with N, and SO with N, a total of 507 probes was identified that showed changes of statistical significance. After removing those probes without assigned ORF ID (compiled from genome annotations of four strains: Mu50, N315, COL, NCTC8325), the number of ORFs trimmed down to 460, with 174 from S/N, 74 from O/N, and 408 from SO/N, respectively.

Quantitative analysis of ORFs influenced by Spm, Ox, Spm+Ox

Cross examinations of the S/N, O/N, and SO/N gene lists revealed seven possible overlaps, as illustrated by the Venn diagram in Figure 4.1A. In the Experimental Group SO imposed the broadest impact on gene expression among three treatments, followed by S and O in this order (Figure 4.1B). Although it was anticipated that the SO gene list overlaps most genes in the S list and O list, a substantial number of genes was identified exclusively in response to the combination of Spm and Ox (236 out of 408 genes in the

'SO-only' category of Figure 4.1B). Considering the drastic killing effect brought by Spm/Ox synergy, it is reasonable to speculate that this group of 236 genes holds up the most useful information regarding the primary target(s) or secondary effects elicited by Spm/Ox synergy. In addition, it is interesting to note that S and SO co-regulated 128 genes while O and SO only co-regulated 21 genes. Furthermore, genes in the SO-only category do not overlap with those in the reported list of cell wall stress (110). These results strongly implied that the Spm/Ox synergy does not amplify the adverse effect of Ox to a degree that triggers cell wall stress. Contrarily, this synergy might impose a stronger damage by Spm in the presence of Ox than Spm alone, or alternatively a new type of stress response that has never been reported before.

Functional classification of ORFs influenced by Spm and/or Ox

These 460 genes were further classified according to the COG functional categories (http://www.ncbi.nlm.nih.gov/COG/) (Figure 4.2). In general, Spm induced a number of genes involved in amino acid and carbohydrate metabolism as well as ion transport. Besides, several SigB-mediated virulence factors were down-regulated upon Spm addition. Moreover, DNA repair-related genes also appeared in Spm regulated group, suggesting the potential interactions of Spm with nucleic acids through its charge property. For the 74 genes altered by Ox, one of the characteristics was the induction of translation-related genes, most of which encoding ribosomal units. Functional grouping of the 408 Spm/Ox regulated genes revealed pleiotropic responses; nevertheless, as described above, those genes affected only by Spm/Ox combination but not by Spm or Ox alone could be more informative. The characteristics of the 236 genes cluster include: 1) induction of metal transport, including both regulators and transporters; 2) induction of heat shock signature proteins (30), like Hrc, chaperone, protease; 3) reduction of energy metabolism pathways, involving glycolysis, fermentation, TCA cycle; 4) reduction of pigment production (*crtMNOPQ*); 5) reduction of amino acid metabolism, e.g. aspartate family, branched-chain amino acids, and histidine; 6) reduction of *de novo* synthesis of pyrimidine and purine nucleotides. Detailed description of these genes listed in Table S3.

A

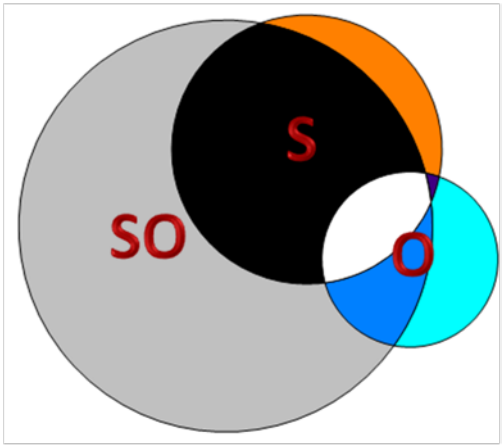

B

regulate by 1mM Spm (S)	regulate by 16ng/μl Ox (O)	regulate by 1mM Spm+16ng/μl Ox (SO)
174	74	408

Category	Regulated Gene #
only in S	22
only in O	29
only in SO	236
in S and O	1
in O and SO	21
in S and SO	128
in S, O, and SO	23
Total	460

Figure 4. 1 Quantification and overlaps of different treatment regulated transcriptional profiles.

A) Venn diagram of genes with significantly altered transcription (>2 fold) by 1mM spermine (S), 16ng/μl oxacillin(O) or their combination (SO).
B) All 7 possible intersections between three independent comparison sets revealed by A. Numbers in the table indicate the amount of genes regulated in each intersection.

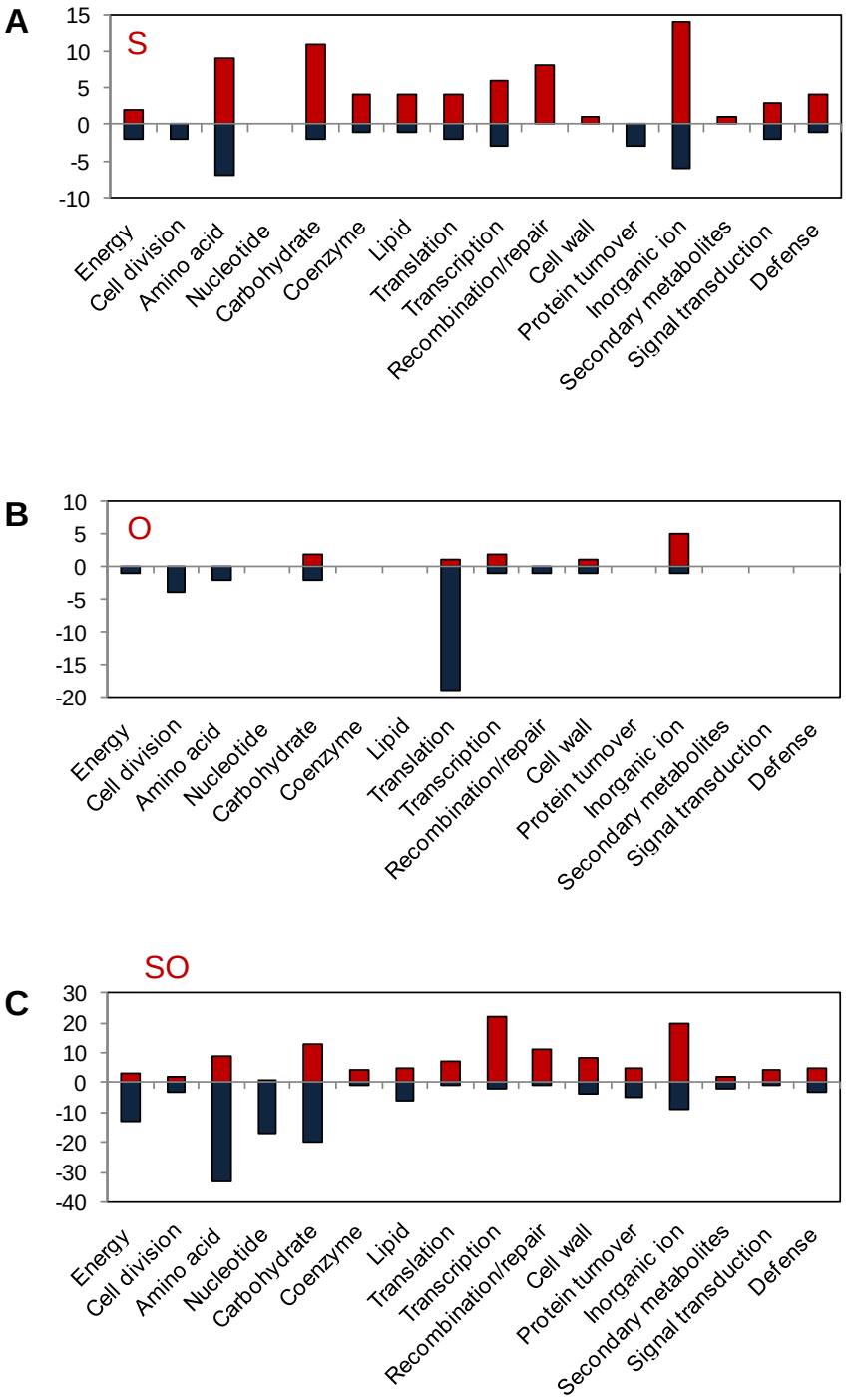

Figure 4. 2 Biological processes that are regulated in response to Spm and Ox alone or in combination.

(A) spermine, (B) oxacillin, (C)spermine+oxacillin**.** y axis represents the number of genes in each functional class. Red, up-regulation; blue, down-regulation. Genes with unknown functions were not included.

4.4 DISCUSSION

From analysis of gene expression profiling, we gained more insights into the molecular mechanisms responsible for the synergistic effect of Spm/Ox combination. The first conclusion drawn from the experiment is that the combination deregulated a significantly higher number of genes as compared with Spm or Ox alone (Figure 4.1). This means a completely different array of genes and related pathways are implicated in the cell-killing effect by Spm/Ox synergy.

Genes regulated by low dose Spm

Down-regulation of surface-associated virulence factors and *sigB* controlled genes

Transcriptome analysis revealed that low dose Spm results in down-regulation of genes for several virulence factors, including protein A (*spa*) and fibronectin binding proteins (*sdrDE, fbnB*) for host tissues attachment. Although exogenous Spm was supposed to cause some stress on cells, it did not trigger the sigma factor B (SigB) regulon in response to general stress. Contrarily, the *asp23*, *clpL*, and *csbD* genes which are generally considered as signatures of the SigB-dependent stress regulon in *S. aureus* (78) were in fact down-regulated. There results indicate that the stress response to Spm is independent of SigB, and may even cause suppression of SigB. It is known that in *S. aureus* SigB controls a large regulon extending from multiple cellular processes to fine-tuning metabolism and virulence upon different environmental stresses (12, 78). In particular, SigB positively regulates adhesion to host cells, which is in agreement with the reduction of surface-associated virulence factors as described above.

Up-regulation of iron/heme-acquisition pathways

One major category of Spm-induced genes was related to iron/heme transport (35), including *htsABC, fhuAVG, fer*, etc. Heme or/and iron availability is essential for bacterial survival and virulence. Iron homeostasis is usually linked with oxidative stress; however in current study, no typical detoxifying enzymes against oxidative stress (e.g. *katA, sodA*) were affected by Spm, suggesting the need of heme

acquisition may not result from oxidative stress. In *S. aureus*, one essential function of heme is for the biosynthesis of cytochrome as component of the electron transport chain. Therefore, it would be interesting to speculate some connections may exist between Spm and heme-related respiration chain. One hypothesis is that Spm may cause damage on the electron transport chain through cytochrome destruction, which then turns on heme uptake to compensate for cytochrome deficiency.

Gene regulated by low dose Ox

It has been reported in *S. aureus* that high dose β-lactams trigger the cell-wall stimulon of a well-defined set of genes (110). However, transcriptome analysis with low dose Ox treatment in my study revealed a completely distinct pattern: the majority of representative genes in the cell wall stimulon were absent except for the induction of *lrgAB*. Instead, there was down regulation of 21 genes in ribosomal protein synthesis. This striking feature is unusual because in general the suppression of protein synthesis apparatus is associated with lower growth rate; however, neglectable effects on growth can be observed by low dose Ox (Figure 5.3). What is more, such reduction on ribosome synthesis was alleviated by Spm/Ox combinational treat under which the growth was severely inhibited. It would be interesting to find out why low-dose Ox can down-regulate ribosomal synthesis without inhibiting the growth while supplementing Spm, on the contrary, reverses the trend with a drastic adverse effect on growth.

Genes regulated by the Spm/Ox combination

A combination of low dose Spm and Ox may result in enhanced adverse effects by Spm, which could be similar to exposure to high dose Spm. As described in Chapter 5, DNA microarrays experiments were also conducted in Mu50 following exposure to 10 mM Spm. A total of 581 genes were identified exhibiting significant changes on the expression levels by high dose Spm. For simplicity, the list of 460 genes described in this chapter was named Array I, and the one from Chapter 5 was named Array II. By comparing Array I and II, it was found that 207 genes were present in both arrays, of which 122 genes were exclusively responsive to the Spm/Ox combination (category 9 of Figure 4.3, not regulated by single

agent). In other words, genes responsive to the synergy effect overlap extensively with those to high Spm challenge. This observation prompted us to reconsider how the synergy effects occur: Spm enhancing β-lactam effect or β-lactam enhancing Spm effect? It has been reported that high dose Ox induces cell-wall stress stimulon as primary effect and triggers oxidative stress as secondary effect. If Spm facilitated the primary action of Ox on cell wall, one would expect up-regulation of cell wall stimulon by the Spm/Ox combination, which does not appear to be the case in our data. However, the induced expression of iron uptake genes (Table S3) drew our attention: iron and H_2O_2 or its precursor superoxide (O_2^-) are required for the Fenton reaction to generate highly-destructive hydroxyl radicals (·OH), which trigger a common oxidative damage cellular death pathway (53, 54). Bactericidal antibiotics including β-lactams can trigger superoxide production through destabilization of the electron transport chain (54); in our transcriptome data, iron/heme acquisition was highly stimulated by both high dose (Table S4, Array II) and low dose Spm (Table S3, Array I). Therefore, one possibility was that the enhanced ferrous iron uptake by Spm, together with superoxide generated by β-lactams, significantly intensifies the Fenton reaction and subsequently causes cell death.

On the other hand, it is still possible β-lactams augment Spm effects during the synergy. The extensively affected energy production pathways (glycolysis, fermentation, TCA cycle) by Spm may also perturb the electron transport chain. If so, one presumption is: β-lactam inhibited cell wall synthesis will disturb membrane potential, which cooperates with the possible deficiency on the electron transport chain endowed by Spm effect, to kill the bacteria.

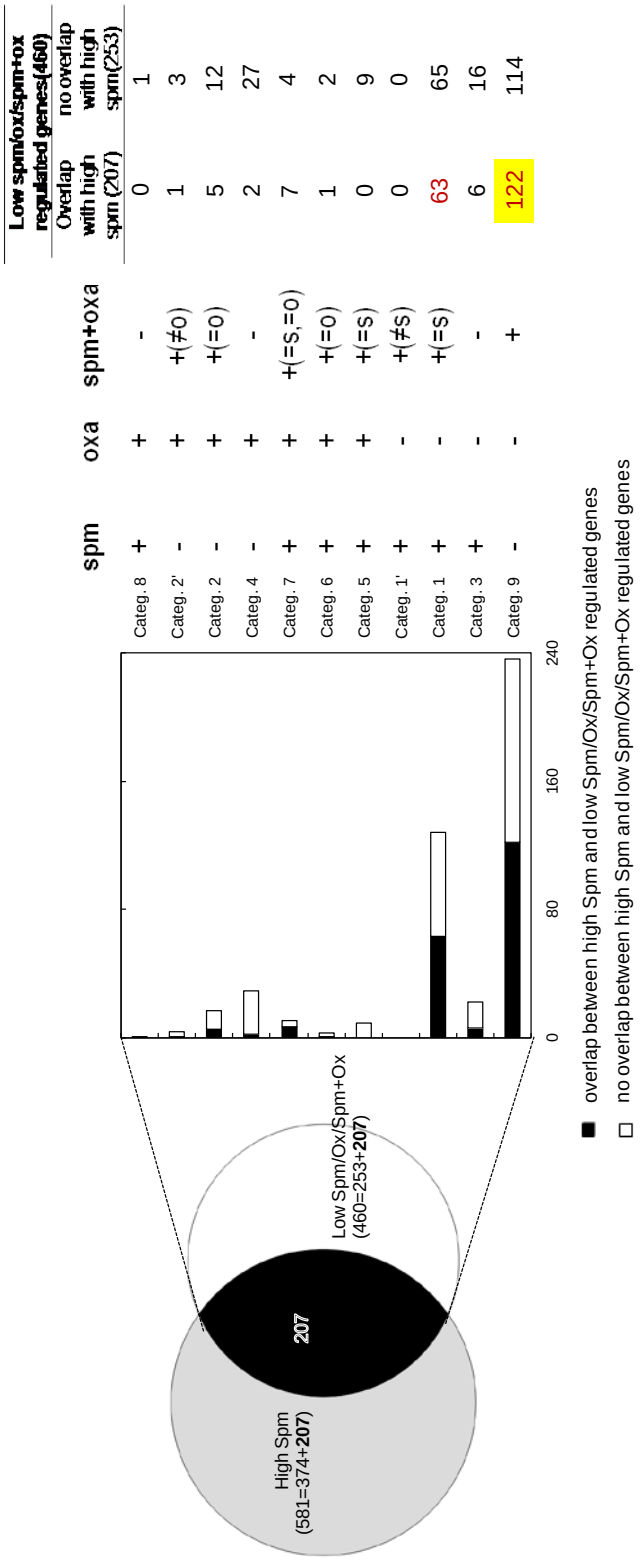

Figure 4. 3 Summary of transcriptome from Array I and Array II.

CHAPTER 5: CHARACTERIZATION OF *S. AUREUS* RESPONSE TO SPERMINE TOXICITY

5.1 INTRODUCTION

Modulation of Spm tolerance

Among common polyamines, spermine is the most potent bactericidal agent if left unmodified; thus, the intracellular concentration of Spm is tightly regulated at many control levels. In bacteria, Spm toxicity can be alleviated by degradation or uptake blockage. For degradation, Spm catabolic enzymes modify the amine groups and ultimately degrade the compound. Two common mechanisms have been reported to initiate Spm degradation: γ-glutamylation by γ-glutamylpolyamine synthetases (GPS) (Figure 1.1, Figure 1.2) in *P. aeruginosa* and acetylation by Spd/Spm acetyltransferase (SSAT) in *E. coli*, *B. subtilis*, and a specific strain lineage of *S. aureus*. In P. aeruginosa, the presence of a specific GPS PauA2 is absolutely required for Spm catabolism. It works by converting the primary amine into carboxylic acid with the release of ammonium and recycling of glutamate. In *S. aureus*, the SSAT activity of SpeG from USA-300 clones converts toxic Spm to non-toxic *N*-1 acetyl-Spm through acetylation, thus affording complete resistance to Spm. But in non-USA 300 lineage strains, like Mu50, they do not possess the *speG* gene encoding SSAT, hence being sensitive to Spm. As for uptake, polyamine transport has been characterized in more detail in Gram-negative bacteria. *E. coli* contains three different polyamine transport pathways. One of them is an ABC transporter (PotABCD), displaying preference for Spd uptake. In *P. aeruginosa*, SpuDEFGH which exhibit the highest similarities to the Pot transporter of *E.coli*, was demonstrated as the major inducible Spd/Spm uptake system. In Gram-positive *S. aureus*, it contains a five-gene operon: a regulator and a four-gene encoding putative ABC transporter for polyamines with a high degree of sequence homology to the *potABCD* in *E. coli* (Figure 5.7). However in *S. aureus*, how the polyamine/Spm transport is regulated and whether the Pot system is responsible for the uptake, remain unknown.

Of note, although Spm is toxic to the cell, many bacteria, like *P. aeruginosa*, still have the capability to take up Spm from their environment and use it as nutrient. Therefore, it is conceivable an inducible uptake system exists in those bacteria to cooperate with the active Spm catabolism. On the other side, for the bacteria without the Spm catabolism, the polyamine-transport system may evolve to reduce the Spm uptake, e.g. by decreasing the binding affinity to Spm or becoming non-inducible upon Spm. Based on this hypothesis, we are interested to know: for most *S. aureus* strains which do not have an active Spm catabolic system, how the spermine transport is modulated to maximally enhance the bacterial tolerance to Spm toxicity?

The target(s) of Spm toxicity

With multiple amines, Spm is very likely to mediate cell physiology by interactions with different molecular targets. In *P. aeruginosa*, blocking GPS pathway by knockout of *pauA2* will make the cell become sensitive to Spm, indicative of the intracellular target of Spm toxicity. Of note, deleting the Spm uptake system SpuDEFGH in *P. aeruginosa* also can increase the bacterial susceptibility to Spm, suggesting another Spm-dependent cytotoxic target may exist in the periplasm. In fact, it was demonstrated before polyamine (cadavarine) can facilitate the structural linkage between peptidoglycan and the outer membrane .in *Selenomonas ruminantium*(55), substantiating the hypothesis that potential target of polyamine/Spm may exist in the periplasm. Thus, we are interested to explore where the Spm-dependent targets locate, inside or outside of the cell; and what kind of stress responses can be triggered by the Spm toxicity in *S. aureus*.

Taken together, in this chapter, we applied the transcriptomic approach to investigate the cellular response to Spm stress and further characterize Spm-responsive candidates to elucidate the regulation of Spm homeostasis in *S. aureus*

Table 5. 1 Bacterial strains and plasmids used in Chapter 5.

	Relevant characteristics	Source or reference
Strains		
E.coli		
DH5α	F– Φ80*lac*ZΔM15 Δ(*lac*ZYA-*arg*F) U169 *rec*A1 *end*A1 *hsd*R17 (rK–, mK+) *pho*A *sup*E44 λ– *thi*-1 *gyr*A96 *rel*A1	Bethesda Research Laboratories
Top10	F– *mcr*A Δ(*mrr-hsd*RMS-*mcr*BC) Φ80*lac*ZΔM15 Δ*lac*X74 *rec*A1*ara*D139 Δ(*ara leu*) 7697 *gal*U *gal*K *rps*L (StrR) *end*A1 *nup*G	Invitrogen
S. aureus		
RN4220	Restriction-deficient derivative of *S. aureus*NCTC832-4	R.Novick
Mu50	MRSA, VISA, wild-type strain	(60)
HG003	*S. aureus* NCTC8325 derivative, *rsbU* and *tcaR* repaired	(39)
COL	HA-MRSA	(33)
JE2	USA300 LAC (CA-MRSA) strain cured of the three plasmids	Nebraska Transposon Mutant Library, (NARSA repository)
NE658	*Bursa aurealis* mariner-based, erythromycin resistance-expressing transposon within gene encoding *potD*.	
HGΔpot::Km	HG003 *potRABCD* null mutant; Km^r	This study
Plasmids		
pCN38	Low-copy-number *E. coli-S. aurues* shuttle vector, Amp^R, Cm^R	R.Novick
pCNspeG	pCN38 with *speG* under the control of its endogenous promoter	This study
pCNtetM	pCN38 with *tetM* under the control of its endogenous promoter	This study
pUCtetM	pUC18 carrying *tetM* gene	This study
pCN56	High-copy-number *E. coli-S. aureus* shuttle vector with GFP as reporter genes for promoter-gene fusions	This study
pMAD-CM	*E. coli-S. aureus* shuttle vector with a thermosensitive origin of replication for Gram-positive bacteria; Amp^R, Em^R, Cm^R, *lacZ*	(75)
pMADCMΔpot::Km	pMAD-CM with upstream of *potR* and downstream of *potD*, linked by Km cassette from pCN34(R. Novick)	This study
pCNPpotR::gfp	pCN56 with upstream region of *potR*	This study
pCNPpotRA::gfp	pCN56 with upstream region (including *potR*) of *potA*	This study
pBAD/HisD	expression vector for producing N terminal His tag fusion, Amp^R	(69)
pPotR	pBAD/HisD expressing native PotR	This study

5.2 MATERIAL AND METHODS

Bacterial strains, plasmids, and growth conditions

The bacterial strains and plasmids used in this study are listed in Table 5.1, and primers are listed in Table S1. Both *E. coli* and *S. aureus* strains were routinely grown and maintained in the Luria-Bertani (LB) medium. When required, the LB medium was buffered with 20mM Tris-HCl at the indicated pH. Antibiotics were added to the medium as necessary at the following concentrations: ampicillin, 100μg/ml for *E. coli*; kanamycin, 25μg/ml for *E. coli*, 50μg/ml for *S. aureus*; erythromycin, 10μg/ml for *S. aureus*; chloramphenicol, 10μg/ml for *S. aureus*.

Transcriptional profiling conditions and microarray (for high concentration of Spm)

Overnight grown cultures of *S. aureus* Mu50 were used to inoculate 50 ml LB broth (pH8.0, Tris-Cl 20mM) and grown at 37ºC with shaking at 250rpm. Exogenous Spm (final conc.10mM) was added to the culture in log-phase (OD_{600} of 0.5) and RNA samples were collected in a time-course manner (15min, 30min, 60min). RNA samples from cultures without Spm exposure were served as control. The subsequent Microarray experiment was conducted as described in Chapter 4.

Microarray validation by quantitative reverse transcription-PCR (qRT-PCR)

qRT-PCR was used to validate microarray data and to analyze the effects of different polyamines on candidate genes. Total RNA was prepared as described above for transcriptional profiling at the exposure to 10mM Spm for 15 min, or 1mM Spm, 1mM Spd, 1mM Put, 2ng/μl Tetracycline (Tc) for 2h when indicated. cDNA was synthesized using VeriQuest SYBR Green One-Step qRT-PCR kit (Affymetrix). Specific primers for the genes tested and for *gyrB* (internal control) were designed using Primer 3 software (Applied Biosystems) (Table S1). qRT-PCR was performed with the ABI 7500 Fast System and SYBR Green technology using cycling conditions of 10min at 50°C, 10 min at 95°C, followed by 45 cycles of 15s at 95°C and 30s at 60°C. RT-PCRs were performed in a 50-μl reaction volume containing

1.5 µl of template RNA (10 ng/µl), 2.5 µl of gene-specific primers (9 µM), 25 µl of VeriQuest SYBR Green One-Step qRT-PCR Master Mix (2×), 0.5 µl VeriQuest RT enzyme mix (100×) and 18 µl of H_2O. Each assay was performed in duplicate. The data analysis was carried out using 7500 system software (Applied Biosystems). Differences in Ct values between tested transcripts and *gyrB* signals were used for normalization purpose and based on the drug-free condition at 2h or 15min as reference. The fold change was expressed as the fold change of the difference between LB Ct (reference) and the stress condition Ct.

PotR cloning, expression, and purification

The full-length *potR* gene was amplified from genomic DNA of *S. aureus* Mu50 by using the primer pair: potR expr-F and potR expr-R in Table S1. The expression vector pBAD/HisD was first cut open by *Nco*I, and treated with Klenow fragment to fill recessed ends, followed by further digestion with *Eco*RI. The PCR product of *potR* was digested with *Eco*RI, and ligated to the pretreated pBAD/HisD. The resulting recombinant pPotR encoding the native form of PotR was further transformed into *E. coli* Top10 for overexpression.

Native PotR was expressed after induction of a log-phase culture with 0.2% arabinose for 4h at 30°C. Cells were suspended in Q buffer (20mM Tris-Cl, pH7.6) containing Complete EDTA-free protease inhibitors (Roche), and disrupted by French press at 17,000Psi. After centrifugation at 20,000g × for 30min, the supernatant was subjected to HiTrap Q HP column (GE) equilibrated with Q buffer. Following gradient elution with Q buffer containing 1M NaCl, fractions containing target protein were combined and desalted again with Aminco Ultra-4 centrifugal filter unit (Millipore) to change the buffer to 20mM Tris-Cl (pH 7.6).

Construction of a *potRABCD* knockout mutant

DNA fragments corresponding to the upstream region of *potR* (arm1) and the downstream region of *potD* (arm2) were amplified with the primer pairs potR-arm1-F/potR-arm1-R and potD-arm1-F/potD-arm2-R (Table S1) by using the genomic DNA of *S. aureus* Mu50 as template. The PCR products were treated with *Bam*HI/*Avr*II for arm1 and *Xho*I/*Bgl*II for arm2, respectively. Meanwhile, a 1.1-kb DNA fragment containing the kanamycin resistance gene *aphA-3* was cut from pCN34 (16) by *Avr*II/*Xho*I. These purified DNA fragments were mixed with *Bam*HI/*Xho*I digested pMAD-CM vector, and ligated with DNA ligase. The recombinant pMADCMΔ*pot*::Km vector selected as blue colony which was able to grow on LB plates containing Amp (100μg/ml), Km (25μg/ml), and X-Gal.

A two-step procedure was then used for allele replacement in *S. aureus.* In the first step, the recombinant pMADCMΔpot::Km was introduced by electroporation into *S. aureus* strain RN4220. Transformants were selected after two days at 27°C on LB containing Em or Cm (10μg/ml) and X-Gal, and the antibiotic-resistant phenotypes of these transformants were confirmed in the same growth medium. Plasmid extracted from one such transformant was introduced into *S. aureus* strain HG003 by electroporation. Likewise, the obtained HG003/pMADCMΔpot::Km transformant was selected. In the second step, a single blue colony was cultivated at 27°C overnight in LB medium with Em or Cm (10μg/ml). Cultures from 27°C were inoculated into pre-warmed LB broth at 43°C without antibiotic at an OD_{600} of 0.1, and growth was continued for 4h at 43°C. Serial dilutions of this culture were plated on LB medium containing X-Gal and Km (50μg/ml) and incubated at 43°C overnight. The excision of the plasmid region in the chromosome by a double-crossover event was screened for Km-resistant, Em-sensitive and white colonies, which nine candidate clones were obtained. To confirm the gene deletion, chromosomal DNA was extracted from three candidates and used in PCRs with primer pairs potA-del-arm1 F/R or potD-del-arm1 F/R. No amplification of the region immediately downstream of *potR* or upstream of *potD* validated the authenticity of the null mutants.

Cloning of the *speG* and *tetM* genes

The *speG* gene including its regulatory region (-516nt to *speG* translation initiation site and +53 nt to *speG* stop codon) from genomic DNA of *S. aureus* JE2 (USA300) was amplified by PCR, digested with *Bam*HI-*Eco*RI and cloned into corresponding sites of pCN38. The resulting construct pCNspeG was confirmed by sequencing and introduced into *S. aureus* strain RN4220. Plasmid DNA isolated from recombinant strain of RN4220 was subsequently introduced into Mu50 by electroporation. The *tetM* structural gene as well as its upstream (-705nt with respect to *tetM* translation initiation site) and downstream (+668nt with respect to *tetM* stop codon) sequences was amplified from genomic DNA of *S. aureus* Mu50 by use of primer pair tetM del-arm1-F and tetM del-arm2-R. The PCR product was digested by *Bam*HI and *Bgl*II, ligated with *Bam*HI/CIAP treated pUC18, and screened by blue/white color selection. The obtained positive clone (blue) was confirmed by enzyme digestion and named as pUCtetM. Then *tetM* gene was cut out by *Bam*HI/*Eco*RI with correct orientation from pUCtetM and subcloned into corresponding sites of *E. coli-S. aureus* shuttle vector pCN38. The construct pCNtetM was confirmed by sequencing, and introduced into *S. aureus* strain RN4220 by electroporation.

Construction of promoter::GFP fusion for the *pot* operon

Reporter strains were constructed using the putative promoter region of the *pot* operon. Primers potR-arm1-F/PpotR-R were used for PpotR::gfp fusion, and potR-arm1-F/ potR-expr-R for PpotRA::gfp fusion, with genomic DNA from Mu50 as template. PpotR covers 836 bp extending from -790 nt upstream to +72 nt downstream of *potR* start codon. PpotRA covers 1304 bp extending from -790 nt upstream of *potR* start codon to stop codon of *potR* (-12 nt upstream of *potA* start codon). The PCR product was cloned in the *Bam*HI-*Eco*RI sites with correct orientation upstream of a promoterless *gfp* gene of the shuttle vector pCN56 and was introduced into RN4220 by electroporation and subsequently into HG003.

Measurements of promoter activities

Exponential growing bacteria carrying promoter::gfp fusion were grown in LB (pH 8.0) supplemented with or without 1mM polyamine (Spm, Spd or Put) with shaking at 37°C. After 2h, the cells were collected by centrifugation, and suspended into the same volume of Tris-Cl buffer (pH8.0). The green fluorescence was then measured with a spectrofluorometer (EnSpire® Multimode Plate Readers, PerkinElmer) by excitation at a wavelength of 485 nm and detection of emission at 515 nm, and the growth curve was monitored by measuring the OD_{600}. The promoter activity value corresponds to relative fluorescence versus OD_{600}.

Electromobility shift assays

A DNA fragment covering the regulatory region of *potR* (836 bp) was PCR amplified from pCNPpotR::gfp with primers pairs of oligonucleotide primers potR-arm1-F/PpotR-R. As a negative control, a DNA fragment of 510 bp covering the region of nt 704672-704162 on Mu50 chromosome was amplified with the following primers 704394-FP/RP (Table S1). For the binding reactions, the DNA probe at 7nM was allowed to interact with different concentrations of PotR in a mixture of 20 μl containing 150mM Tris-Cl (pH 7.5), 50mM NaCl, 1mM EDTA, 4mM dithiothreitol (DTT), 5% (vol/vol) glycerol, 3nM negative-control DNA, and 200 ng/μl acetylated bovine serum albumin. As specified, different polyamines at 20μM was added to the reaction mixtures. After incubation for 20 min at room temperature, 10 μl of each reaction mixture was loaded on a polyacrylamide gel (6%) in Tris-borate-EDTA buffer (pH 8.7). The gels were stained with SYBR Green I solution (Invitrogen) for 20 min, washed twice with deionized H_2O, and scanned with an imaging system (Omega UltraLum) with a setting for excitation at 473 nm and emission at 520 nm.

Polyamine Uptake

Radio-labeled polyamines were used for uptake assays as previously describe with slight modification. Cultures of *S. aureus* strain JE2 (wt) and its *potD* mutant (NE658) were grown in LB broth (pH8.0) to mid log-phase before harvest. The cell pellets were washed twice with 50mM Tris-HCl, 50mM NaCl, pH 7.5, and resuspended at a concentration of cell number approximate $1x10^9$ (OD_{600} = 1) in the same buffer, followed by the addition of chloramphenicol (final conc.250ug/ml). After incubation of the cell suspension for 5min in 37°C water bath, different polyamines (^{14}C Spm, ^{3}H Spd, ^{3}H Put) was added to a final concentration of 500 uM, and samples (80ul) were withdrawn at various time intervals. Cells were collected on a cellulose membrane filter (0.22 um pore size, type GS, Millipore) and washed with 5ml of above buffer. Membranes were air dried in clean scintillation vials. Incorporated radioactivity was measured using 2ml of scintillation liquid and spectrometer (Beckman). Specific activity of radioactive polyamine: ^{14}C Spm, 0.1Ci/mmol; ^{3}H Spd, 44.5Ci/mmol; ^{3}H Put, 33.6Ci/mmol.

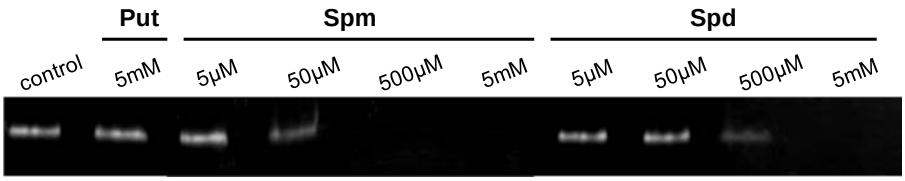

Figure 5. 1 Binding of polyamines to DNA.

Equal amounts of a DNA fragment were mixed without or with the indicated conc. of polyamines before electrophoresis. Interactions of polyamine and DNA results in the reduced intensity of DNA fragments

Table 5. 2 MICs of Spm and Ox in *speG* supplementing Mu50.

	Spm MIC (mM)	**Oxa MIC** (ng/μl)		
		No Spm	0.5mM Spm	8mM Spm
Mu50	2	256	2	NA
Mu50/*speG*	64	256	256	2

Mu50/*speG*, *S. aureus* strain Mu50 harboring pCNspeG

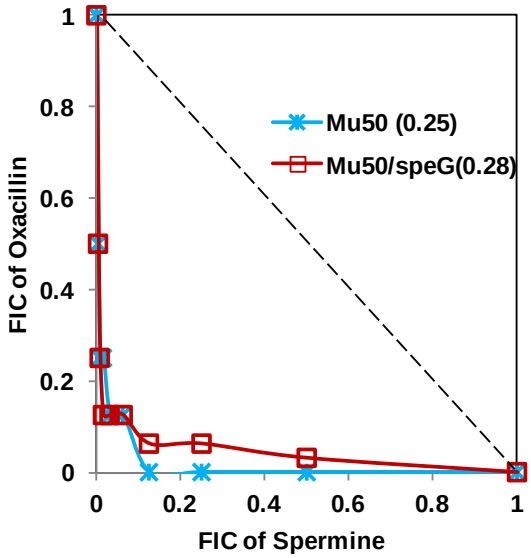

Figure 5. 2 FIC isobologram for combinations of Spm and Ox against *S.aureus* Mu50.

The FICs were determined by checkerboard assay.
The additive line is drawn in dotted line. FIC_{index} was shown in bracket.

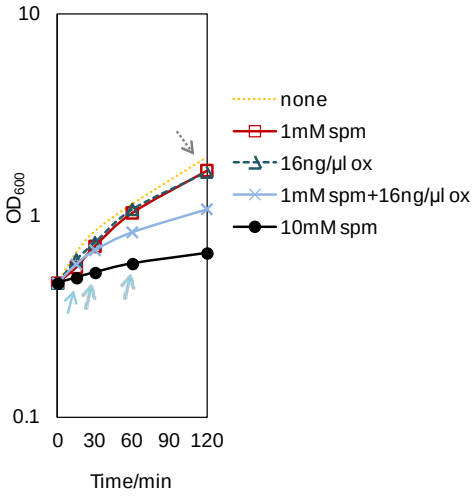

Figure 5. 3 Inhibition of growth by spermine and spermine/oxacillin combination.

5.3 RESULTS

Binding activity of Spm to DNA

The character of positive charges carried by polyamines, especially Spm and Spd, has long been considered possessing adverse effects if these essential compounds were accumulated to high concentrations inside the cell. To demonstrate the potential toxicity of polyamines by their charge interactions with nucleic acid polymers, we tested the DNA-binding activity of Spm, Spd, and Put *in vitro.* When bound to DNA, polyamines are expected to reduce overall net negative charges of DNA-polyamine complexes, thereby affecting the mobility of these complexes on the native PAGE. In other words, formation of these complexes would be reflected on decreased amounts of free-form DNA. As shown in Figure 5.1, the intrinsic DNA-binding affinity of Spm is about 10-fold higher than that of Spd, and no apparent binding by Put can be detected even at the concentration of 5mM. This trend of DNA affinity (Spm > Spd > Put) is consistent to that of toxicity of polyamine (7), suggesting the charge interaction (referred to the first mode of Spm action, as described in General Introduction and Figure 1.2) is at least partially responsible for the Spm toxicity in *S. aureus.*

Acetyltransferase SpeG affects Spm toxicity but not Spm/β-lactam synergy

Unlike *P. aeruginosa*, most strains of *S. aureus* cannot grow on Spm. However, one recent report identified the existence of a polyamine acetyltransferase (SpeG) present only in certain strain lineages (e.g. USA300 of SCC*mec* IV group) (48). The *speG* gene encoded within the ACME (arginine catabolic mobile element) island of USA300 group exhibited significant homology to SpeG from *E. coli*, and was necessary and sufficient for Spm resistance. Our data present in Table 5.2 also showed that expressing *speG in trans* in non-USA300 strains (Mu50 and RN4220) granted the complete resistance to these Spm-sensitive bacteria, supporting the existence of Spm-dependent cytotoxic effect on an intracellular target.

Besides toxicity *per se*, exogenous Spm also exerts particular effect on the sensitization of MRSA to β-lactams as characterized in Chapter 2. To examine the role of SpeG on Spm/β-lactam synergy, the checkerboard analysis was conducted in Mu50 and its *speG*-transformant. The FIC index of Spm/Ox clearly showed strong synergy in both strains (Figure 5.2). However, it needed at least 8 mM Spm to exert noticeable synergy on Mu50 harboring a recombinant clone of *speG*, while a much lower dose of Spm (0.5 mM) was sufficient to cause the same effect on the native Mu50 without *speG* (Table 5.2). These results support the hypothesis that the molecular target(s) of Spm toxicity and synergy with β-lactams may reside inside the cells.

Transcriptome analysis of *S. aureus* in response to high dose Spm

To investigate the changes in transcriptome profiles in response to high dose Spm, we conducted a series of independent microarray experiments in the absence (control group) and the presence (experimental group) of 10mM Spm upon 15, 30, and 60 min exposures (Figure 5.3). To further identify genes with statistically marked changes in expression levels, we applied the following criteria to each of the control-experimental microarray data sets: (1) p value ≤ 0.05, (2) absolute fold change in transcript level ≥ 2.5, and (3) for up-regulation, gene in experimental group has a presence of ≥ 200 signal intensity; for down-regulation sorting, gene in control group has a presence of ≥ 200 signal intensity. Of the over 3000 ORFs in the genome of *S. aureus*, a list of 581 genes showing significant changes upon Spm treatment was compiled with this approach. To examine how these genes were distributed with regard to their physiological and biochemical functions, they were further classified according to COG functional categories (Figure 5.4). Transcriptional profiles of representative genes were shown in Figure 5.5, and below described some of the major findings.

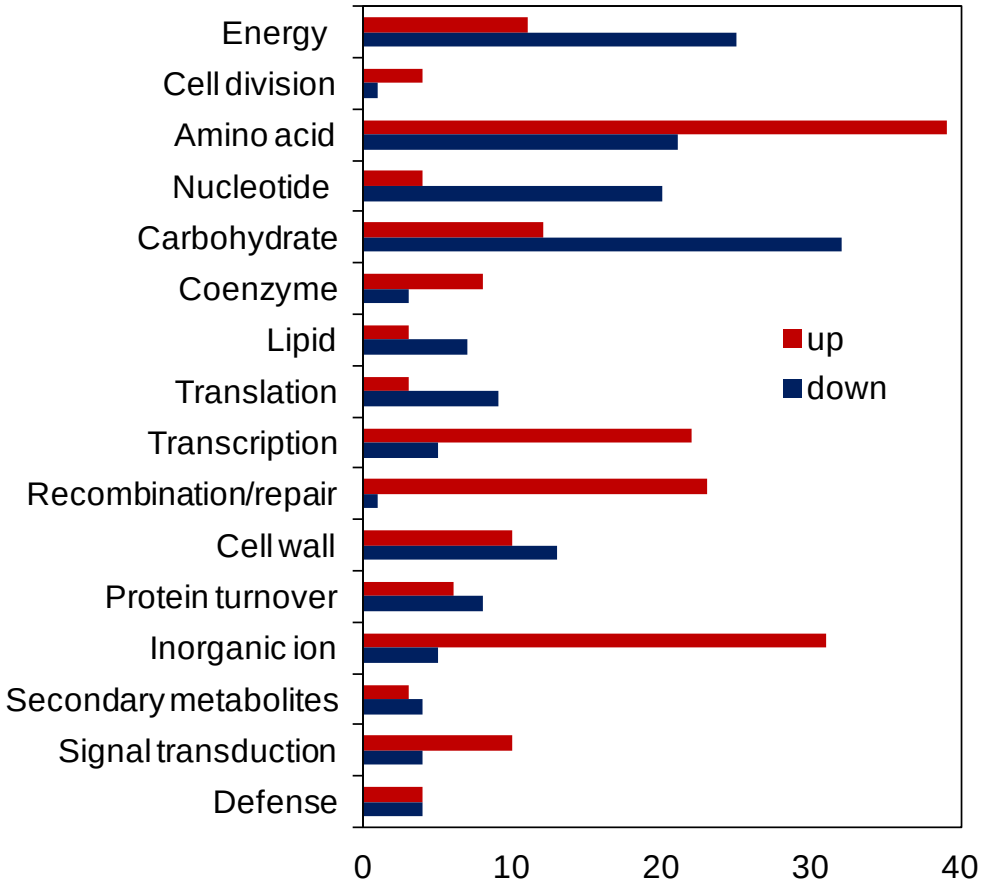

Figure 5. 4 Biological processes that are regulated in response to high dose spermine (>2.5 fold).

1) Up-regulation

Iron uptake and metal-dependent repressor

A number of genes encoding metal transporters (especially for iron) showed increased expression, indicative of possible dysregulation of metal homeostasis by Spm challenge. *S. aureus* acquires iron through siderophore or heme. It has been reported that FhuABGD (ferric hydroxymate uptake), HtsABC (heme transport system), and SirABC (staphylococcal iron regulated transporter) participate in siderophore import, while heme uptake go through Isd system and HtsBC permease. In specific, for siderophores import, staphyloferrin A is mediated by HtsABC and FhuA, staphyloferrin B by SirABC and FhuA, while xeno-siderophore by FhuABGD; Isd systems and HtsBC are responsible for heme acquisition (35). Here, the *fhuABG, htsABC, isdF* all showed 3-6 fold up-regulation by Spm. In addition, the *norA* gene encoding an iron-responsive efflux pump in *S. aureus* (28), also displayed over 2.5- fold increase. Moreover, four major metal-mediated repressors, Fur, PerR, Zur (three Fur family members) (41, 42, 64, 69) and MntR (DtxR-like protein)(43), all displayed induced expression. Although varying in DNA binding sites and dependence on metal ions, these repressors share a similar mode of action: metal binding to the regulators leads to homodimeric binding to a concensus sequence that overlaps the promoters of genes under its direct control, resulting in gene repression. In specific, upon iron limitation, dissociation of F^{2+}-Fur complex derepresses Fur regulon and activates genes in siderophore synthesis, transport, and regulation (*fur* itself)(27). Meanwhile, PerR, Zur or MntR also can directly or indirectly modulate the Fur regulon, expanding the regulatory capability on iron uptake and storage. In addition to iron-dependence, the PerR regulon (including *fur* and *perR* itself) also can be activated by peroxide, for modulation of oxidative stress resistance (41). Collectively, these observations revealed a complex regulatory network in *S. aureus* to maintain homeostasis of iron and other metal ions, which responds to possible signals of iron-restricted stress imposed by Spm toxicity.

Regulation of osmotic balance

Some Spm-induced genes likely contributed to osmotolerance, such as those encoding glycine betaine transporter (*opuD*), choline dehydrogenase (*betA*), glycine betaine/carnitine/choline ABC transporter operon (*opuCA/CB/CD*), and glycine aldehyde dehydrogenase (*gbsA*). Of interest, the *kdpABC* operon for an ABC transporter and *kdpDE* for a two-component regulatory system of potassium uptake were also induced significantly under Spm stress.

Amino acid metabolism and transport

Genes related to amino acid metabolism and transport, particularly those for arginine and urease biosynthesis, showed significant induction. Up-regulation of these amino acid synthetic pathways, despite being high consumers of ATP, infers an increased need of specific amino acids during the Spm stress. Another notable finding was the induction of an ABC transporter-the putative polyamine uptake system *potABCD*. Investigation of this operon is described below.

DNA repair or/and recombination

Some transcripts up-regulated by Spm were coding for enzymes involved in DNA repair or/and recombination, namely, *uvrC, nucC, xerD, dinB, holA*, etc. However, *recA* and *lexA*, two signature genes of standard SOS response (3), were not included in the list. It indicated that the Spm stress is different from most DNA-damaging agents, and may not trigger the SOS response.

2) Down-regulation

ATP synthesis and carbohydrate metabolism/transport

The addition of Spm to *S. aurues* decreased the expression of genes in major energy-providing central metabolic pathways to different extent, including fermentation, glycolysis, gluconeogenesis, pyruvate conversion, pentose phosphate cycle, and TCA cycle. We also noticed a down-regulation of the membrane-bound ATP synthases (F0F1-ATPases) which catalyze the synthesis of ATP by utilizing the

energy of an electrochemical gradient of protons. These data indicate an overall decreased activity or demand of energy production during Spm treatment.

Many genes in carbohydrate metabolism and transport were down regulated. In specific, expression of *ptsIH* for glucose uptake(93) was decreased, consistent with the reduction of glycolysis and pentose phosphate cycle (the alternative glucose degradation pathway), as described above. Moreover, expression of the *lacABCDFEG* operon for lactose utilization was also decreased. The assimilation of lactose or galactose by *S. aureus* accumulates galactose 6-phosphate. This phosphorylated carbohydrate is the actual intracellular signal molecule for induction of the lactose (*lac*) genes, which can be further metabolized to triose phosphates used in the glycolysis (72). Taken together, reduced expression of genes for sugar uptake and utilization was consistent with the pattern of down-regulation in ATP synthesis.

The SigB regulon

One very striking event upon Spm stress was the down-regulation of Sigma B (SigB, σ^B) regulon. A total of 251 genes was reported in the σ^B regulon of *S. aureus* (12), and 96 genes of this regulon were found responsive to high dose Spm. However, among these genes 79 ORFs positively controlled by σ^B exhibited reduced expression while 17 genes which are repressed by σ^B display an upregulated pattern in response to Spm stress (Figure S4, Figure 5.5).

The alternative sigma factor σ^B of *S. aureus* is in charge of the general stress response, expression of virulence determinants, and modulation of antibiotic resistance. It controls a large regulon, either by directly recognizing conserved σ^B promoter sequences (e.g. *asp23*, *clpL*) or indirectly via σ^B-dependent elements (e.g. RNAIII, *agrA)* (78, 101). In specific, σ^B has been shown to influence the expression of several global regulators, including up-regulation of SarA, SarS (SarH1) as well as down-regulation of RNAIII and *agr* regulatory system, all of which showed altered pattern in our study. Of note, the function of σ^B in virulence factor production is exactly the opposite from that of RNAIII/*agr* quorum sensing

circulars (the latter negatively regulates adhesins and positively regulates exoenzyme and toxins production). Therefore, the increased expression of exoprotein and toxin transcripts under Spm stress might be a consequence of lower σ^B and/or higher RNA III transcription.

From the results of transcriptome analysis, it was very clear that the σ^B regulon was turned off under Spm stress. Conserved in most bacteria, the major physiological function of the σ^B regulon was to protect the cells when under stress. However, it was surprising that Spm stress in fact shuts down the σ^B regulon. We consider this effect could be very detrimental to the cells. This novel finding warrants future investigation on the molecular mechanism of Spm effects on σ^B.

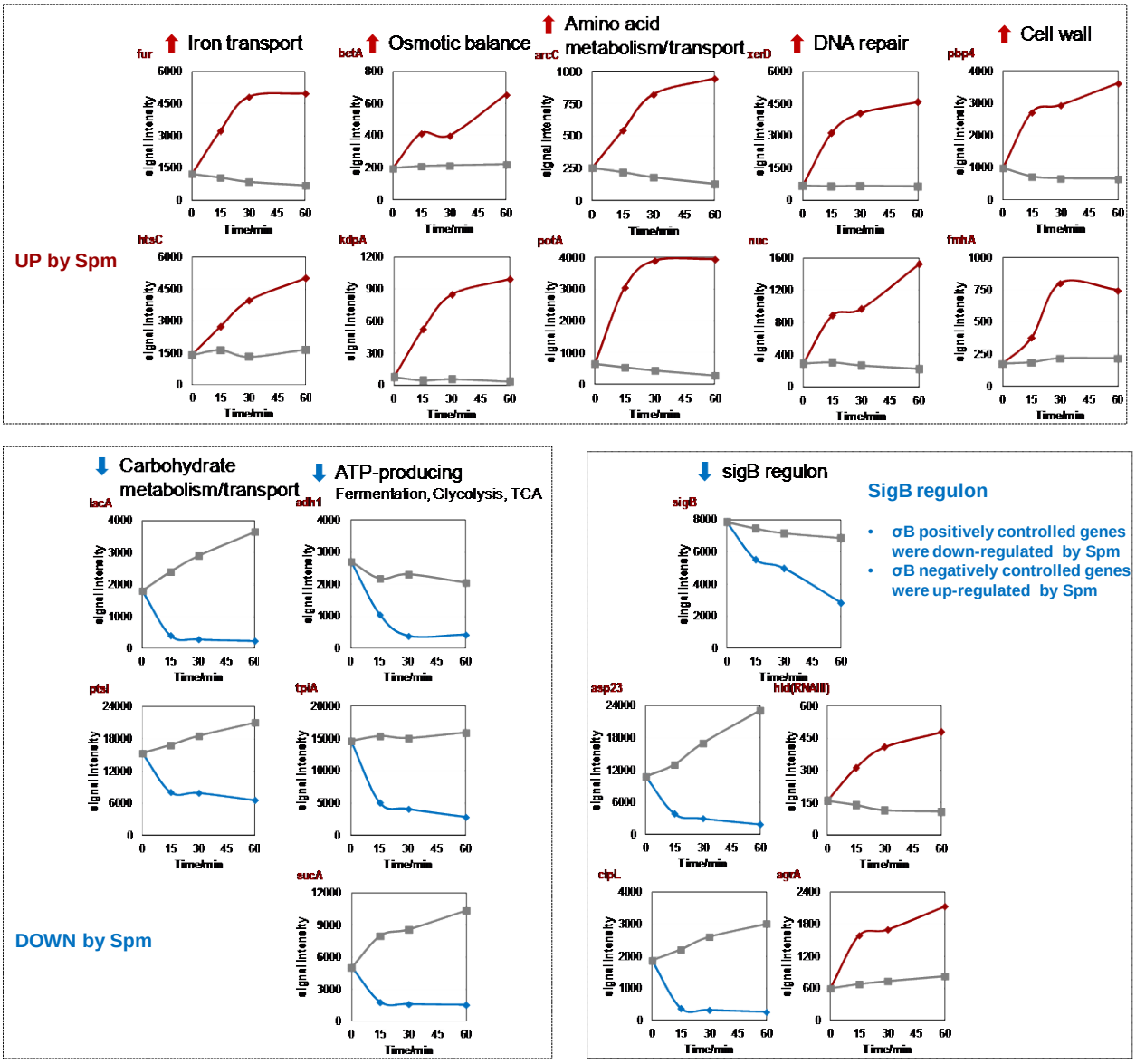

Figure 5. 5 Transcription profiles of representative genes influenced by high dose spermine.

Transcript levels sampled at different time points of growth (x axes). Data points were plotted as relative intensity value (y axes). Red line, up-regulation by Spm; blue line, down-regulation by Spm; gray line, no Spm treatment. Candidates genes were categorized according to functional class.

Among genes that were induced by 10mM Spm, the *tetM* gene for tetracycline resistance, the putative *potRABCD* operon for polyamine uptake and regulation, as well as the divergent *kdpFABCD-kdpDE* operons for a potassium uptake channel and regulation exhibited most significant fold change and high signals as confirmed by qRT-PCR. These genes were subjected to further characterization to gain insights into their potential roles in Spm toxicity and/or resistance mechanisms.

Spermine-specific induction of *tetM*

The *tetM* gene encodes a protein that confers resistance to tetracycline (Tc) by interacting with the ribosome and promoting the release of bound Tc from the ribosome (20, 107). This gene is found primarily, but not exclusively, in the Firmicutes and is known to be carried mostly by conjugative transposons of the Tn916 family(96). In *S. aurerus* Mu50, *tetM* was identified on Tn5801(59), which contains highly conserved ORFs in four functional modules: conjugation, regulation, recombination and accessory genes such as *tetM*(24).

As revealed by transcriptome analyses (Table S3,S4) and further confirmed by qRT-PCR (Figure 5.6), *tetM* in Mu50 was highly induced by both high dose and low dose Spm, It is of interest to understand why Spm can induce *tetM* transcription and whether the expression of TetM is able to confer resistant to Spm.

First, to test whether the TetM is indeed responsible for Tc resistance, the *tetM* gene including its regulatory region from Mu50 was cloned and transformed into *E. coli* (DH5α) as well as *S. aureus* strains (RN4220) where *tetM* was absent. In the subsequent drug-susceptibility test, MIC of Tc in RN4220 harboring *tetM* increased more than 30- fold in comparison to its host, equivalent to that in Mu50; similarly, *tetM* was able to raise the tolerance of *E. coli* to Tc, but to a less extent (Table 5.3).

Since Spm toxicity also applies to strains of *S. aureus* without the *tetM* gene, it is unlikely that TetM is the molecular target of Spm toxicity. However, it was possible that TetM expression might promote Spm

resistance. To test this hypothesis, Spm MIC was determined in *S. aureus* strains carrying plasmid-borne *tetM* in contrast to their individual hosts. In particular, cells grown in 1/8 MIC of Tc (able to stimulate TetM synthesis whereas not affecting bacterial growth) were used as positive control. As revealed by Table 5.3, both RN4220 and Mu50 showed no differences on the Spm sensitivity regardless of *tetM* expression, indicating the up-regulation of *tetM* by Spm is not a defensive mechanism to Spm toxicity.

Next, the response of *tetM* to different polyamines was investigated. Exponential growing cells of Mu50 were exposed to various polyamines (Spm, Spd, and Put; 1 mM), and the culture with low dose Tc (2ng/μl) served as positive control of *tetM* induction. Transcript levels were analyzed by qRT-PCR in comparison to that of the untreated sample. As shown in Figure 5.6, *tetM* expression was specifically induced by Spm and Tc to a comparable level but not by Spd or Put. Although *tetM* may not play any role in Spm toxicity, the molecular mechanism of tetM induction by Spm and its potential role in Tc resistance is exceptionally interesting and warrants further investigation in the future.

Table 5. 3 MICs of Tc and Spm in *tetM*-supplementing bacteria.

	Mu50	RN4220	RN4220/*tetM*	DH5α	DH5α/*tetM*
Tc(ng/μl)	>50	1.5	>50	1.5	25
Spm(mM)	0.5	0.25	0.5	ND*	ND

RN4220/*tetM*, *S. aureus* strain RN4220 harboring pCNtetM
DH5α/*tetM*, *E. coli* strain DH5α harboring pCNtetM
Cells were pre-grown in 1/8 MIC of Tc prior to Spm MIC measurement. * ND, not determined.

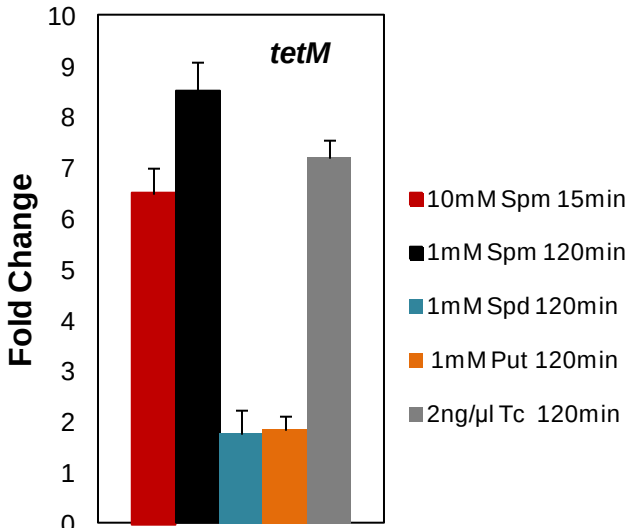

Figure 5. 6 RT-PCR analysis of *tetM* in response to different polyamines.

The fold change represents the difference between Ct of drug-free condition (reference) and Ct of the compound-supplement condition.

The *potRABCD* locus for polyamine uptake and regulation

As revealed from the transcriptome on exposure to high dose Spm (Figure 5.5, Table S3, S4) and qRT-PCR validation (Figure 5.8), the *potABCD* genes for a putative polyamine transport system were highly induced by high dose Spm but not by low dose Spm. Although PotABCD share high sequence similarities to the *E. coli* counterparts (Figure 5.7) preferential for Spd uptake(46), information about the regulation and the physiological function of this system in *S. aureus* was mainly unknown.

The *pot* operon in *S. aureus* is composed of five genes, with PotA an ATPase, PotBC channel forming unit, PotD a substrate-binding protein, as well as PotR a putative transcriptional regulator (*SAV1098* in Mu50) immediately upstream of *potABCD* which is absent in the pot loci of *E. coli* (45) and most other bacteria.

First we measured *pot* expression in the absence and presence of three different polyamines (Spm, Spd, and Put). Exponentially growing cells of Mu50 were exposed to low dose polyamines (1mM) for 2 hours and the transcript levels of *potA* were determined by qRT-PCR. As shown in Figure 5.8, both Spd and Put induced *potA* expression by 3-fold and 2.4-fold, respectively, whereas low dose Spm showed little effect.

Next, kinetic measurements of polyamine uptake were conducted in the parental strain JE2 and its *potD* mutant NE658 as described in Materials and Methods. As shown in Figure 5.9, uptake of ^{3}H-Spd or ^{3}H-Put by JE2 increased linearly from 0 to 8 min while no apparent uptake of Spm can be observed. Meanwhile, uptake of Spd and Put was abolished in the *potD* mutant. These results from uptake measurements and qRT-PCR as described above support PotABCD as the major transport system for Spd and Put in *S. aureus*. In addition, these results did not support the presence of any active or high-affinity Spm uptake system. The lack of an active Spm uptake system may be advantageous for most strains of

S. aureus that do not possess SpeG or other Spm modification enzymes as an alternative mechanism to fence off Spm toxicity.

However, it's important to note that in contrast to low Spm, high dose Spm does have the ability to induce *pot* expression (Figure 5.8). Although the uptake experiments were not conducted with high Spm as substrate, the fact that plasmid-borne *speG* does protect the cells from Spm toxicity (Table 5.2) supports that Spm is indeed taken into the cytoplasm by unknown transporter(s).

To determine whether the *potRABCD* operon has any effect on Spm sensitivity or synergy, drug susceptibility assay was conducted in parental strain HG003 and its *pot* deletion mutant (HGΔpot::Km). As shown in Table 5.4, Spm MIC in the *pot* mutant was comparable to that of HG003; likewise, the lack of *pot* also had no influence on the Spm/β-lactam synergy. These results were consistent to the conclusion that the PotABCD system is not the major transporter for Spm in *S. aureus*.

Another interesting feature for the *pot* operon is the gene which resides immediately upstream of *potA*, named as *potR* (*SAV1098* of Mu50) in this study (Figure 5.7A). PotR belongs to the Cro/Cl family of transcriptional regulators. Unlike in *E. coli* and many other human pathogens of which the *potABCD* are organized as a four-gene operon, the presence of *potR* within the *pot* cluster in *S. aureus* is suggestive of its role in modulating polyamine homeostasis. To determine the possible regulatory role of PotR on *pot* operon, two transcriptional promoter fusions were designed: 1) PpotR covering a 836-bp intergenic region upstream of *potR*; 2) PpotRA including the intact *potR* and its upstream intergenic region. These recombinant plasmids carry *gfp* as reporter gene, and the resulting pCNPpotR::*gfp* and pCNPpotRA::*gfp* were introduced into *S. aureus* HG003. The recombinant strains were grown in plain LB (pH 8.0), and the promoter activities were measured by relative fluorescence of GFP versus OD_{600}. As shown in Figure 5.10, the promoter activity in P*potR* was on average 10-fold higher than that of P*potRA*, suggesting the potential role of PotR (carried by P*potRA* but not by P*potR*) as a repressor in regulating the *pot* promoter.

In order to examine how PotR could possibly regulate *pot* operon in response to polyamines, the promoter activities were determined in strain HG003 carrying P*potRA* grown in the presence or absence of 1 mM Spm, Spd, or Put. Unexpectedly, none of the polyamine supplements can affect the promoter activity (Figure 5.10). However, the lack of regulation by polyamines in this promoter construct could be due to the nature of the vector plasmid. We have later found that because of unknown reasons even the *tetM* promoter was much less responsive to the presence of tetracycline when cloned into this vector (data not shown).

The DNA-binding activity of PotR was also tested *in vitro*. PotR was purified to homogeneity as described in Materials and Methods, and subjected to electrophoresis mobility shift assays (EMSA) using P*potR* as probe. As shown in Figure 5.11, formation was a PotR-dependent nucleoprotein complex demonstrated specific binding of PotR to the probe. When tested for effect of polyamines on PotR-DNA interactions, no apparent effect on the DNA-binding activity was detected.

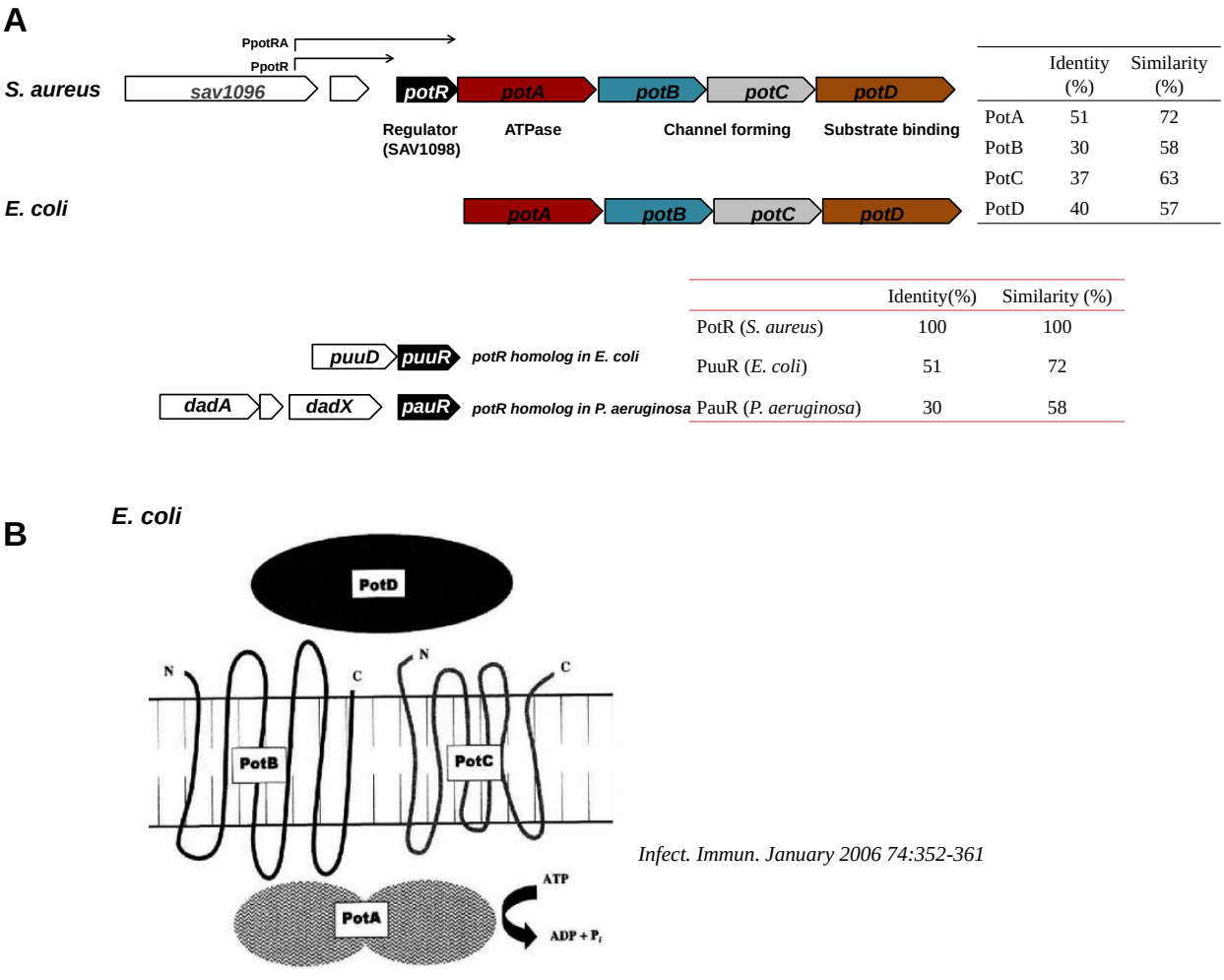

	Identity (%)	Similarity (%)
PotA	51	72
PotB	30	58
PotC	37	63
PotD	40	57

	Identity(%)	Similarity (%)
PotR (*S. aureus*)	100	100
PuuR (*E. coli*)	51	72
PauR (*P. aeruginosa*)	30	58

Infect. Immun. January 2006 74:352-361

Figure 5. 7 Schematic representations of Pot system.

(A) Organization of pot loci and neighboring regions in *S.aureus* Mu50.
Arrows indicate fragment upstream of *potR* (P*potR)* or *potA* (P*potRA*) for promoter fusion.
(B) Schematic of PotABCD structure and regulation in *E.coli*

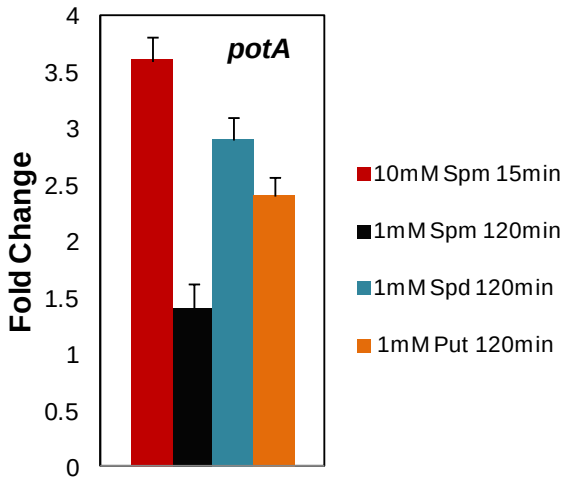

Figure 5. 8 RT-PCR analysis of *potA* in response to different polyamines.

The fold change represents difference between Ct of drug-free condition (reference) and Ct of the compound-supplement condition.

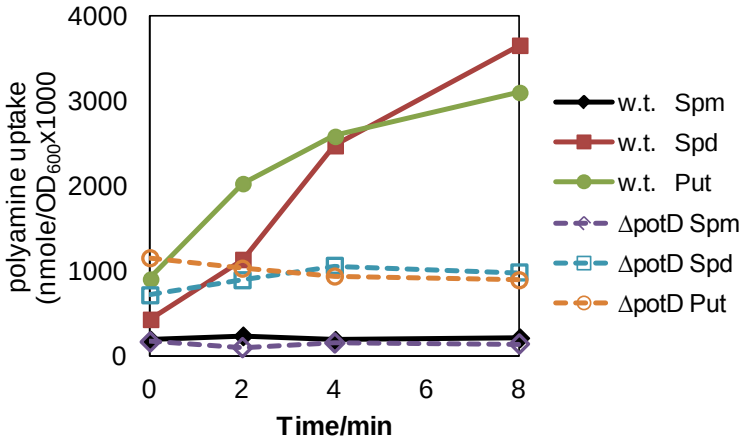

Figure 5. 9 Uptake of different polyamines in wild type and *potD* mutant

w.t. JE2; ΔpotD, NE658. Cells grown in plain LB medium (w/o polyamine) were collected and subjected to uptake assay with radiolabeled polyamine.

Table 5. 4 MICs of Spm and CFZ in wild type and *pot* mutant.

	Spm(mM)	CFZ	
		no spm	0.5mM spm
w.t.	1	16	<0.015
HGΔpot::Km	1	16	<0.015

w.t, wildtype, *S. aureus* strain HG003;
HGΔpot::Km, *pot* operon null mutant of HG003

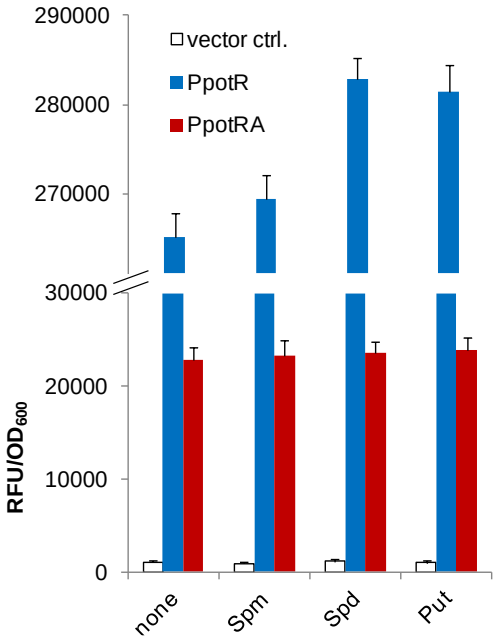

Figure 5. 10 Promoter activity of P*potR* or P*potRA*.

S. aureus strain HG003 harboring pCNPpotR::gfp or pCNPpotRA::gfp was grown for 2h in the presence or absence of polyamine. Promoter fragments are indicated as in Figure 5.7A. The promoter activities were expressed as relative fluorescence versus OD_{600} of the culture. Standard deviations are derived from at least two independent cultures.

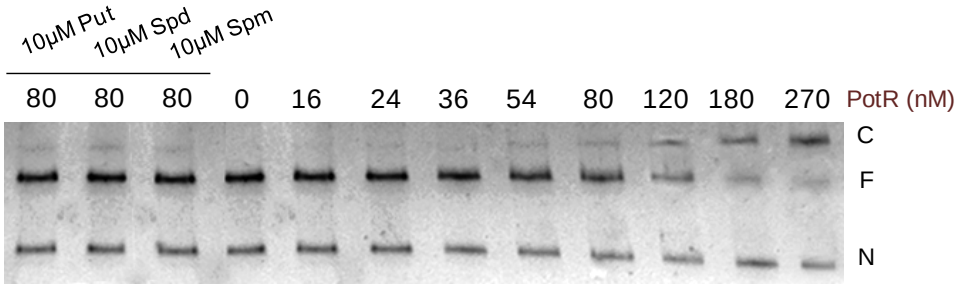

Figure 5. 11 Electromobility shift analysis of PotR-*Ppot* interaction.

The assays were conducted in the absence of polyamines, or the presence of 10μM polyamine (Put, Spd, or Spm). F, free probe; N, negative control DNA; C, PotR-DNA complex

The *kdpFABCDE* locus

The *kdp* genes for potassium uptake and regulation are widely distributed among bacteria (29) (Figure 5.12). In *E. coli*, the KdpABC is a high-affinity K^+ uptake ATPase, and its expression is regulated by the KdpDE two-component system in response to K^+ limitation or turgor pressure. This K^+ transporting ATPase shares high sequence similarities with the K^+ channel in eukaryotes (47). Given the report that Spm could enter and occlude the central K^+-channel pore (102, 117), we proposed that in *S. aureus* Spm may block the K^+ uptake in the same manner, and therefore supplement with high concentration of K^+ may increase Spm resistance by counteracting Spm obstruction on this potassium channel. Spm MIC in Mu50 was measured in LB containing 300 mM KCl. As shown in Table 5.5, KCl addition can cause 32-fold increment on Spm MIC.

Aside from K^+ limitation, it has been proposed that turgor loss (high osmolarity) serves as the regulatory signal for the *kdp* operon(8). To test whether the induction of *kdp* by Spm was due to osmolarity upshift, we also measured the Spm MIC in the presence of other osmotic-shock agents, 300mM NaCl and 600mM sucrose (Table 5.5). Surprisingly, like KCl, NaCl also enhanced the tolerance of Mu50 to Spm; nonetheless, osmotic shock with 600mM sucrose showed no effect. While these results support possible relationships between Spm and osmolarity, more work will be needed to understand induction of the *kdp* operon by Spm. Recently, *kdpDE* in *S. aureus* was reported up-regulated by the Agr/RNAIII system (118), which is consistent with our observation of highly induced *agr/RNAIII* by Spm, suggesting the role of Spm in regulating virulence with the potential coordination between K^+ sensing and Agr signaling in *S. aureus*.

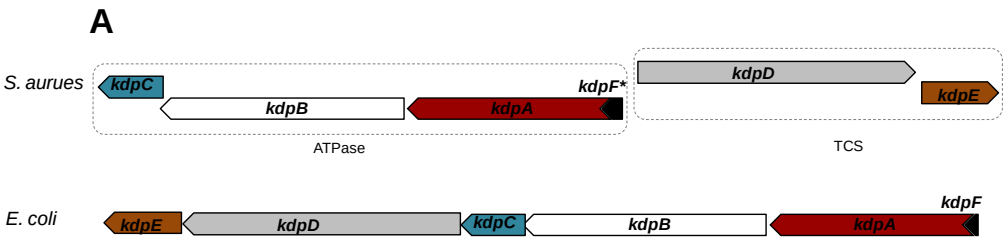

	Identity (%)	Similarity (%)
KdpF	48	67
KdpA	43	60
KdpB	55	72
KdpC	37	58
KdpD	26	49
KdpE	39	61

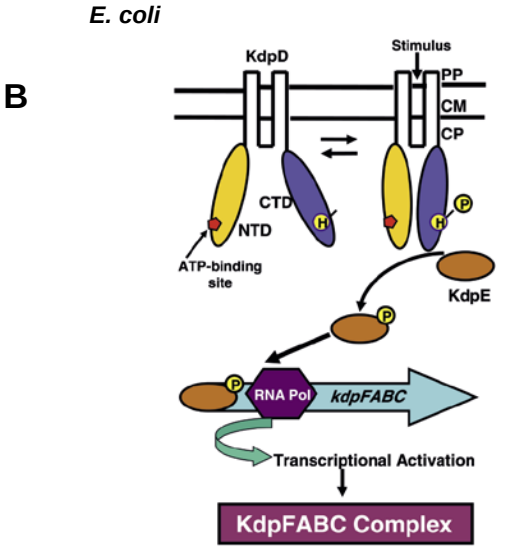

J. Biosci. 32(3), April 2007

Figure 5. 12 Schematic representation of Kdp system.

(A) Organization of *kdpFABCDE* in *S. aureus* and *E. coli.*
Identity and similarity scores correspond to similarities between the protein sequences.
(B) Schematic of KdpFABCDE structure and regulation in *E. coli*

Table 5. 5 Effects of osmotic-shock solutions on the MICs of Spm and Ox in Mu50.

		None	300mM KCl	300mM NaCl	600mM Sucrose
Spm(mM)		1	32	16	1
Oxa (ng/μl)	No spm	512	512	ND	ND
	¼ MIC spm	1	512	ND	ND

ND, not determined

5.4 DISCUSSION

Transcriptome analysis

In Chapter 4 and 5, we have analyzed changes in the transcriptome of *S. aureus* Mu50 upon Spm stress and Spm/Ox synergy. Overall, 581 genes were identified responsive to Spm while 408 regulated by Spm/Ox. Those genes of interest were placed into functional groups to define high dose Spm-dependent regulation as well as low dose Spm/Ox-affected profiles.

The stimulation of iron acquisition genes (including iron uptake and metal-specific regulators) was particularly of note. The induction was moderate under low dose Spm (*fhu*A*BG* 2-3 fold, *htsABC* 6- fold, regulators 1.5-fold), and further magnified upon Spm/Ox combination (*fhuABG* 4-fold, *htsABC* 12- fold, regulators 3.5- fold). Interestingly, high dose Spm increased iron related expression to similar levels as those by Spm/Ox synergy (*fhuABG* 3.5-4 fold, *htsABC* 4- fold, regulator 3-4 fold) (Figure S3, S4)

As known, iron is essential for bacteria due to its involvement in multiple metabolic processes, including respiration (heme-containing cytochromes, [Fe-S]-containing ferredoxins) and key enzymes in central metabolism ([Fe-S]-containing enzymes in TCA, like SdhA, CitB, CitG) (34, 35). However on the other hand, iron can also become hazardous due to the Fe2+ -triggered Fenton reaction which produces harmful ROS (21). Therefore, there is significant regulatory crosstalk between iron homeostasis and oxidative-stress resistance networks.

Collectively, we propose a model for Spm toxicity and Spm/β-lactam synergy as described below. Based on the transcriptome analysis, it seems Spm may generate iron-deplete conditions or change the intracellular iron status by some yet-unknown mechanisms. Such iron starvation signals are sensed by metal-specific regulators (Fur, PerR, MntR, Zur), which initiate derepression of iron uptake systems. The incorporation of internalized iron into iron-proteins may not catch up with the burst of Fe^{2+} within the cell,

which therefore, would promote Fenton reaction and ROS buildup. Even though low dose Spm is sufficient to induce iron uptake, the delivered impact may be sequestered by redirecting central metabolism, thus explaining why low dose Spm has no inhibition on *S. aureus*. Upon high dose Spm, the potential detrimental effect resulting from a flood of iron input might be overwhelming, which leads to the instant inhibition on cell growth. Furthermore, the fact that high dose Spm is able to turn off the SigB regulon may cause the cells even more stress to survive. Under Spm/Ox synergy, stimulation of the of H_2O_2 production by β-lactam (54) might be compounded with increased Fe^{2+} by Spm to produce a high level of deleterious hydroxyl radicals, and thereby inducing cellular death.

Spm, iron (heme) and electron-transport/energy production

A recent report shows that Spm toxicity may rely on the biosynthesis of menaquinine (48), the only electron carrier in *S. aureus*. This implies the essentiality of electron-transport during the Spm effect. Of note, as the other essential factor in electron-transport for the biosynthesis of cytochromes, heme and the associated iron-acquisition genes, showed significant induction under Spm stress, inferring a correlation between heme/iron and Spm. Therefore, both heme and menaquinine, two indispensable components for electron transport chain, seem to have connections with Spm, which indicates the possible effect of Spm on cellular respiration and energy production. In fact, the down-regulation of genes in the glycolytic pathway and the TCA cycle which require electron-transport chain to generate ATP, as shown in the transcriptomic profiles, also suggests the need of iron/heme upon Spm exposure may come from the respiration defect.

tetM

Tetracycline (Tc) functions by binding to the helix 34 and helix 31 in the 16s rRNA of 30S ribosomal subunit and preventing aminoacyl-tARNA(aa-tRNA) access in to ribosomal A site (20). The ribosomal protection protein TetM can release Tc binding and rescue the ribosome to return to the elongation cycle(106). The mechanism for *tetM* regulation has been proposed through transcriptional attenuation

(105). A ‘leader peptide’ immediately upstream of *tetM*, contains rare amino acids; therefore, the ribosome pauses at these positions due to the shortage of rare aminoacyl-tRNAs (aa-tRNAs), leading to retarded translation. The non-synchronism of RNA polymerase and ribosome makes the transcription terminated at the stem-loop termination sites which are upstream of *tetM* start codon, resulting in no expression of *tetM* when Tc is absent. When cells are exposed to Tc which retards the translation, there is a backup of charted tRNAs, including the rare ones needs within leader peptide. The increased availability of these aa-tRNAs allows coupled translation and transcription, thus able to disrupt step-loop terminator. Transcription then proceeds into *tetM*, and more TetM were expressed to protect ribosome from Tc attack.

Spm was previously reported able to bind with 16S rRNA in ribosomal 30S subunit (1). The 5’ domain, the internal and terminal loop of helix h24 as well as the upper part of h44 in 16sRNA (partially overlap with some Tc binding sites), were found as preferable binding sites for Spm. The effects of Spm interactions with 30S subunits on ribosomal functions were further characterized in many aspects: 1) Spm can enhance the binding of aa-tRNA to the A site to ribosome; 2). Spm cross-linking to rRNA reduces the translational accuracy and therefore increases the probability of using ‘wrong aa-tRNA’ for translation in the lack of right cognate aa-tRNA; 3) Spm had no impact on the peptide bond formation (1). Based on these, along with the transcriptional attenuation model for Tc regulation on *tetM*, it was reasonable to propose that a) Spm may behave like Tc by inhibiting translation to induce *tetM*; or b) Spm may facilitate aa-tRNA incorporation to 30S binding site thus bypass the transcriptional attenuation of *tetM* and enhance its expression. Considering the fact that Spm does not restrain the aa-tRNA binding as mentioned above, the former mechanism is less favorable.

How does *S. aureus* protect itself from Spm toxicity?

From this study we concluded that one way *S. aureus* protects itself from Spm toxicity is to avoid Spm uptake. We demonstrated the absence of active Spm uptake in Mu50. Although the *potABCD* operon for a

polyamine uptake system is induced by high dose Spm, several lines of evidence exclude its role in Spm uptake. However, *S. aureus* is still vulnerable to exogenous Spm, indicating Spm uptake through unknown channels. Another protection mechanism against Spm toxicity is to recruit Spm modification enzymes. Introduction of *speG* encoding a spermine acetyltransferase into Mu50 indeed rendered the recombinant strain resistant to high dose Spm. The presence of *speG* in USA300 and other strains in this lineage may be able to provide growth advantage for these strains in hosts that synthesize and release Spm in blood and tissue fluids.

CHAPTER 6: GENERAL CONCLUSION

Polyamines are ubiquitous polycationic molecules synthesized by and required for all life. Putrescine and spermidine are distributed widely in all living organisms, but spermine is primarily present in eukaryotes (and many thermophilic bacteria). The distinct distribution of this tetra-amine suggests that Spm may associate with some new activities or specific regulations during evolution. Of interest, increased Spm levels have been demonstrated at inflammatory sites of infection and in cancer cells, suggesting the significance of Spm in cell proliferation and immune functions in human body. In contrast, many studies showed that exogenous Spm may become toxic to bacteria with accumulation, the inhibition of which is especially strong in *S. aureus.* Moreover, we also found that at low concentrations, Spm by itself has negligible effects while is able to sensitize β-lactam antibiotics to kill bacteria; such synergy is most potent in *S. aureus*. In this study, we explored the targets of Spm toxicity and its synergy with β-lactams and provided insights into how Spm could possibly work alone or in combination with β-lactams to exert the antibacterial activities.

Spm toxicity

Owing to the positive charges at physiologic pH, Spm effects have been implicated through electrostatic interactions with anionic molecules (e.g. DNA/RNA). However, our pH dependent profiles revealed that the Spm-dependent inhibitory effects (both alone or with β-lactams) are effective at higher pH (≥8); in addition, the acetylated Spm had no effect on the growth of *S. aureus*, further supporting the notion that toxicity may not be correlated with net positive charge since both nontoxic acetyl-Spm and toxic Spd have the same net + 3 charge. Based on our two mode action model, the effects of Spm in bacteria may largely result from its nucleophilic activity of free amines at higher pH.

In general, Spm toxicity can be reduced by increasing Spm catabolic activity or blocking Spm uptake. Unlike in *P.aeruginosa* which can use Spm as carbon/nitrogen source through GPS, most *S. aureus* strains do not have Spm catabolic genes except the USA300 lineage. By acquiring a SSAT SpeG, those

strains can modify Spm through acetylation and remove its toxicity. For the uptake, *S. aureus* has a putative polyamine transport system *potABCD*, while deletion of which cannot confer resistance to Spm. This suggests the putative Pot transporter may not be the major Spm uptake system in *S. aureus*.

Spm/β-lactam synergy

Another effect of Spm on bacteria is to sensitize MRSA to β-lactam antibiotics. In theory, Spm/β-lactam synergy can be achieved through two possible mechanisms: 1) Spm may have the same primary target as β -lactams by attacking the cell wall; 2) Spm toxicity can be amplified by side effects of β-lactams to achieve the synergistic killing. In our study, although a spontaneous Spm-resistant mutant of MRSA containing a defected PBP2 can confer resistance to the synergy, the transcriptome and PBPs analyses in wildtype show that: Spm neither suppresses the expression of PBPs or other members in the cell-wall stress stimulon, nor affects the binding affinity of PBPs to β-lactams. It suggests that Spm may not have the same primary target as β-lactams. In contrast, Spm induces a number of genes for iron acquisition while reducing energy-producing pathways and the SigB regulon, which are remarkably distinct from β-lactam triggered profiles. More importantly, those genes also showed a similar regulated pattern under Spm/ β-lactam combinational condition; in other words, the synergy-responsive genes overlapped extensively with those to high Spm challenge.

Therefore, we contend that the Spm effects may be amplified during the synergy, via two possible mechanisms: 1) the side effect of β-lactam (e.g. production of ROS) may react with Spm triggered compounds to form some strong killing factor; 2) the side effects of β-lactam may share the same target of Spm, thus enhancing the Spm toxicity. Such hypothesis could also explain why the PBP2 deficient mutant became resistant to Spm/ β-lactam syerngy: w/o TPase domain in PBP2, β-lactams lose their primary target and are unable to engender any side effect; thus, moderate concentration of Spm by itself cannot elicit intense toxicity to bacteria, which makes the mutant able to survive under Spm/ β-lactam condition.

Collectively, our study indicates the role of Spm could be multifarious with more than one target, and a combination of Spm and β-lactams may inhibit growth of MRSA in a more complicated manner than just potentiating β-lactam inhibition on PBPs.

REFERENCES

1. **Amarantos, I., I. K. Zarkadis, and D. L. Kalpaxis.** 2002. The identification of spermine binding sites in 16S rRNA allows interpretation of the spermine effect on ribosomal 30S subunit functions. Nucleic acids research **30:**2832-2843.
2. **Amendola, R., M. Cervelli, E. Fratini, F. Polticelli, D. E. Sallustio, and P. Mariottini.** 2009. Spermine metabolism and anticancer therapy. Current cancer drug targets **9:**118-130.
3. **Anderson, K. L., C. Roberts, T. Disz, V. Vonstein, K. Hwang, R. Overbeek, P. D. Olson, S. J. Projan, and P. M. Dunman.** 2006. Characterization of the Staphylococcus aureus heat shock, cold shock, stringent, and SOS responses and their effects on log-phase mRNA turnover. Journal of bacteriology **188:**6739-6756.
4. **Andersson, D. I., and D. Hughes.** 2010. Antibiotic resistance and its cost: is it possible to reverse resistance? Nature reviews. Microbiology **8:**260-271.
5. **Antignac, A., K. Sieradzki, and A. Tomasz.** 2007. Perturbation of cell wall synthesis suppresses autolysis in Staphylococcus aureus: evidence for coregulation of cell wall synthetic and hydrolytic enzymes. Journal of bacteriology **189:**7573-7580.
6. **Atilano, M. L., P. M. Pereira, J. Yates, P. Reed, H. Veiga, M. G. Pinho, and S. R. Filipe.** 2010. Teichoic acids are temporal and spatial regulators of peptidoglycan cross-linking in Staphylococcus aureus. Proceedings of the National Academy of Sciences of the United States of America **107:**18991-18996.
7. **Bachrach, U., and A. Weinstein.** 1970. Effect of aliphatic polyamines on growth and macromolecular syntheses in bacteria. Journal of general microbiology **60:**159-165.
8. **Ballal, A., B. Basu, and S. K. Apte.** 2007. The Kdp-ATPase system and its regulation. Journal of biosciences **32:**559-568.
9. **Berger-Bachi, B., and M. Tschierske.** 1998. Role of fem factors in methicillin resistance. Drug resistance updates : reviews and commentaries in antimicrobial and anticancer chemotherapy **1:**325-335.
10. **Berger-Bächi, B., and M. Tschierske.** 1998. Role of fem factors in methicillin resistance. Drug Resistance Updates **1:**325-335.
11. **Bergeron, R. J., J. S. McManis, W. R. Weimar, K. M. Schreier, F. L. Gao, Q. H. Wu, J. Ortizocasio, G. R. Luchetta, C. Porter, and J. R. T. Vinson.** 1995. The Role of Charge in Polyamine Analog Recognition. Journal of Medicinal Chemistry **38:**2278-2285.
12. **Bischoff, M., P. Dunman, J. Kormanec, D. Macapagal, E. Murphy, W. Mounts, B. Berger-Bachi, and S. Projan.** 2004. Microarray-based analysis of the Staphylococcus aureus sigmaB regulon. Journal of bacteriology **186:**4085-4099.
13. **Bore, E., S. Langsrud, O. Langsrud, T. M. Rode, and A. Holck.** 2007. Acid-shock responses in Staphylococcus aureus investigated by global gene expression analysis. Microbiology **153:**2289-2303.
14. **Bower, J. M., and M. A. Mulvey.** 2006. Polyamine-mediated resistance of uropathogenic Escherichia coli to nitrosative stress. Journal of bacteriology **188:**928-933.
15. **Bryson, K., and R. J. Greenall.** 2000. Binding sites of the polyamines putrescine, cadaverine, spermidine and spermine on A- and B-DNA located by simulated annealing. Journal of biomolecular structure & dynamics **18:**393-412.
16. **Charpentier, E., A. I. Anton, P. Barry, B. Alfonso, Y. Fang, and R. P. Novick.** 2004. Novel cassette-based shuttle vector system for gram-positive bacteria. Applied and environmental microbiology **70:**6076-6085.
17. **Chattopadhyay, M. K., C. W. Tabor, and H. Tabor.** 2003. Polyamines protect Escherichia coli cells from the toxic effect of oxygen. Proceedings of the National Academy of Sciences of the United States of America **100:**2261-2265.

18. **CLSI.** 2011. Performance standards for antimicrobial susceptibility testing. M100-S21. 21th informational supplement. Clinical and Laboratory Standards Institute, Wayne, PA.
19. **Cohen, S. S.** 1998. A guide to the polyamines. Oxford University Press, New York.
20. **Connell, S. R., D. M. Tracz, K. H. Nierhaus, and D. E. Taylor.** 2003. Ribosomal Protection Proteins and Their Mechanism of Tetracycline Resistance. Antimicrobial Agents and Chemotherapy **47:**3675-3681.
21. **Cornelis, P., Q. Wei, S. C. Andrews, and T. Vinckx.** 2011. Iron homeostasis and management of oxidative stress response in bacteria. Metallomics : integrated biometal science **3:**540-549.
22. **de Jonge, B. L., H. de Lencastre, and A. Tomasz.** 1991. Suppression of autolysis and cell wall turnover in heterogeneous Tn551 mutants of a methicillin-resistant Staphylococcus aureus strain. Journal of bacteriology **173:**1105-1110.
23. **de Jonge, B. L., and A. Tomasz.** 1993. Abnormal peptidoglycan produced in a methicillin-resistant strain of Staphylococcus aureus grown in the presence of methicillin: functional role for penicillin-binding protein 2A in cell wall synthesis. Antimicrob Agents Chemother **37:**342-346.
24. **de Vries, L. E., H. Christensen, R. L. Skov, F. M. Aarestrup, and Y. Agerso.** 2009. Diversity of the tetracycline resistance gene tet(M) and identification of Tn916- and Tn5801-like (Tn6014) transposons in Staphylococcus aureus from humans and animals. The Journal of antimicrobial chemotherapy **64:**490-500.
25. **deJonge, B. L. M., Y. S. Chang, N. Xu, and D. Gage.** 1996. Effect of exogenous glycine on peptidoglycan composition and resistance in a methicillin-resistant Staphylococcus aureus strain. Antimicrobial Agents and Chemotherapy **40:**1498-1503.
26. **Dela Vega, A. L., and A. H. Delcour.** 1996. Polyamines decrease Escherichia coli outer membrane permeability. Journal of bacteriology **178:**3715-3721.
27. **Delany, I., G. Spohn, A. B. Pacheco, R. Ieva, C. Alaimo, R. Rappuoli, and V. Scarlato.** 2002. Autoregulation of Helicobacter pylori Fur revealed by functional analysis of the iron-binding site. Molecular microbiology **46:**1107-1122.
28. **Deng, X., F. Sun, Q. Ji, H. Liang, D. Missiakas, L. Lan, and C. He.** 2012. Expression of multidrug resistance efflux pump gene norA is iron responsive in Staphylococcus aureus. Journal of bacteriology **194:**1753-1762.
29. **Epstein, W.** 2003. The roles and regulation of potassium in bacteria. Progress in nucleic acid research and molecular biology **75:**293-320.
30. **Fleury, B., W. L. Kelley, D. Lew, F. Gotz, R. A. Proctor, and P. Vaudaux.** 2009. Transcriptomic and metabolic responses of Staphylococcus aureus exposed to supra-physiological temperatures. BMC microbiology **9:**76.
31. **Fukuchi, J., K. Kashiwagi, K. Takio, and K. Igarashi.** 1994. Properties and structure of spermidine acetyltransferase in Escherichia coli. The Journal of biological chemistry **269:**22581-22585.
32. **Ghuysen, J. M.** 1991. Serine beta-lactamases and penicillin-binding proteins. Annual review of microbiology **45:**37-67.
33. **Grossowicz, N., S. Razin, and R. Rozansky.** 1955. Factors influencing the antibacterial action of spermine and spermidine on Staphylococcus aureus. Journal of general microbiology **13:**436-441.
34. **Haley, K. P., and E. P. Skaar.** 2012. A battle for iron: host sequestration and Staphylococcus aureus acquisition. Microbes and infection / Institut Pasteur **14:**217-227.
35. **Hammer, N. D., and E. P. Skaar.** 2011. Molecular mechanisms of Staphylococcus aureus iron acquisition. Annual review of microbiology **65:**129-147.
36. **Hartman, B. J., and A. Tomasz.** 1984. Low-affinity penicillin-binding protein associated with beta-lactam resistance in Staphylococcus aureus. Journal of bacteriology **158:**513-516.
37. **Henze, U. U., and B. Berger-Bachi.** 1995. Staphylococcus aureus penicillin-binding protein 4 and intrinsic beta-lactam resistance. Antimicrob Agents Chemother **39:**2415-2422.

38. **Hirsch, J. G., and R. J. Dubos.** 1952. The effect of spermine on tubercle bacilli. The Journal of experimental medicine **95:**191-208.
39. **Holtje, J.-V.** 1998. Growth of the Stress-Bearing and Shape-Maintaining Murein Sacculus of Escherichia coli. Microbiol. Mol. Biol. Rev. **62:**181-203.
40. **Höltje, J.-V.** 1996. A hypothetical holoenzyme involved in the replication of the murein sacculus of Escherichia coli. Microbiology **142:**1911-1918.
41. **Horsburgh, M. J., M. O. Clements, H. Crossley, E. Ingham, and S. J. Foster.** 2001. PerR controls oxidative stress resistance and iron storage proteins and is required for virulence in Staphylococcus aureus. Infection and immunity **69:**3744-3754.
42. **Horsburgh, M. J., E. Ingham, and S. J. Foster.** 2001. In Staphylococcus aureus, fur is an interactive regulator with PerR, contributes to virulence, and Is necessary for oxidative stress resistance through positive regulation of catalase and iron homeostasis. Journal of bacteriology **183:**468-475.
43. **Horsburgh, M. J., S. J. Wharton, A. G. Cox, E. Ingham, S. Peacock, and S. J. Foster.** 2002. MntR modulates expression of the PerR regulon and superoxide resistance in Staphylococcus aureus through control of manganese uptake. Molecular microbiology **44:**1269-1286.
44. **Igarashi, K., and K. Kashiwagi.** 2006. Polyamine Modulon in Escherichia coli: genes involved in the stimulation of cell growth by polyamines. Journal of biochemistry **139:**11-16.
45. **Igarashi, K., and K. Kashiwagi.** 1999. Polyamine transport in bacteria and yeast. The Biochemical journal **344 Pt 3:**633-642.
46. **Igarashi, K. I., K; Kashiwagi, K.** 2001. Polyamine uptake systems in Escherichia coli. Research in microbiology **152:**271-278.
47. **Jan, L. Y., and Y. N. Jan.** 1997. Cloned potassium channels from eukaryotes and prokaryotes. Annual review of neuroscience **20:**91-123.
48. **Joshi, G. S., J. S. Spontak, D. G. Klapper, and A. R. Richardson.** 2011. Arginine catabolic mobile element encoded speG abrogates the unique hypersensitivity of Staphylococcus aureus to exogenous polyamines. Molecular microbiology **82:**9-20.
49. **Kanavarioti, A., E. E. Baird, and P. J. Smith.** 1995. Use of phosphoimidazolide-activated guanosine to investigate the nucleophilicity of spermine and spermidine. The Journal of organic chemistry **60:**4873-4883.
50. **Karatan, E., T. R. Duncan, and P. I. Watnick.** 2005. NspS, a predicted polyamine sensor, mediates activation of Vibrio cholerae biofilm formation by norspermidine. Journal of bacteriology **187:**7434-7443.
51. **Kashiwagi, K., and K. Igarashi.** 2011. Identification and assays of polyamine transport systems in Escherichia coli and Saccharomyces cerevisiae. Methods in molecular biology **720:**295-308.
52. **Kim, I. G., and T. J. Oh.** 2000. SOS induction of the recA gene by UV-, gamma-irradiation and mitomycin C is mediated by polyamines in Escherichia coli K-12. Toxicol Lett **116:**143-149.
53. **Kohanski, M. A., D. J. Dwyer, and J. J. Collins.** 2010. How antibiotics kill bacteria: from targets to networks. Nature reviews. Microbiology **8:**423-435.
54. **Kohanski, M. A., D. J. Dwyer, B. Hayete, C. A. Lawrence, and J. J. Collins.** 2007. A common mechanism of cellular death induced by bactericidal antibiotics. Cell **130:**797-810.
55. **Kojima, S., K. C. Ko, Y. Takatsuka, N. Abe, J. Kaneko, Y. Itoh, and Y. Kamio.** 2010. Cadaverine covalently linked to peptidoglycan is required for interaction between the peptidoglycan and the periplasm-exposed S-layer-homologous domain of major outer membrane protein Mep45 in Selenomonas ruminantium. Journal of bacteriology **192:**5953-5961.
56. **Komatsuzawa, H., M. Sugai, S. Nakashima, S. Yamada, A. Matsumoto, T. Oshida, and H. Suginaka.** 1997. Subcellular localization of the major autolysin, ATL and its processed proteins in Staphylococcus aureus. Microbiol Immunol **41:**469-479.
57. **Komatsuzawa, H., M. Sugai, S. Nakashima, S. Yamada, A. Matsumoto, T. Oshida, and H. Suginaka.** 1997. Subcellular localization of the major autolysin, ATL and its processed proteins in Staphylococcus aureus. Microbiol Immunol **41:**469-479.

58. **Kuroda, M., H. Kuroda, T. Oshima, F. Takeuchi, H. Mori, and K. Hiramatsu.** 2003. Two-component system VraSR positively modulates the regulation of cell-wall biosynthesis pathway in Staphylococcus aureus. Molecular microbiology **49:**807-821.
59. **Kuroda, M., T. Ohta, I. Uchiyama, T. Baba, H. Yuzawa, I. Kobayashi, L. Cui, A. Oguchi, K. Aoki, Y. Nagai, J. Lian, T. Ito, M. Kanamori, H. Matsumaru, A. Maruyama, H. Murakami, A. Hosoyama, Y. Mizutani-Ui, N. K. Takahashi, T. Sawano, R. Inoue, C. Kaito, K. Sekimizu, H. Hirakawa, S. Kuhara, S. Goto, J. Yabuzaki, M. Kanehisa, A. Yamashita, K. Oshima, K. Furuya, C. Yoshino, T. Shiba, M. Hattori, N. Ogasawara, H. Hayashi, and K. Hiramatsu.** 2001. Whole genome sequencing of meticillin-resistant Staphylococcus aureus. Lancet **357:**1225-1240.
60. **Kuwahara-Arai, K., N. Kondo, S. Hori, E. Tateda-Suzuki, and K. Hiramatsu.** 1996. Suppression of methicillin resistance in a mecA-containing pre- methicillin-resistant Staphylococcus aureus strain is caused by the mecI-mediated repression of PBP 2' production. Antimicrob. Agents Chemother. **40:**2680-2685.
61. **Kwon, D. H., and C. D. Lu.** 2007. Polyamine effects on antibiotic susceptibility in bacteria. Antimicrob Agents Chemother **51:**2070-2077.
62. **Kwon, D. H., and C. D. Lu.** 2006. Polyamines increase antibiotic susceptibility in Pseudomonas aeruginosa. Antimicrob Agents Chemother **50:**1623-1627.
63. **Kwon, D. H., and C. D. Lu.** 2006. Polyamines induce resistance to cationic peptide, aminoglycoside, and quinolone antibiotics in Pseudomonas aeruginosa PAO1. Antimicrob Agents Chemother **50:**1615-1622.
64. **Lee, J. W., and J. D. Helmann.** 2007. Functional specialization within the Fur family of metalloregulators. Biometals : an international journal on the role of metal ions in biology, biochemistry, and medicine **20:**485-499.
65. **Lemaire, S., C. Fuda, F. Van Bambeke, P. M. Tulkens, and S. Mobashery.** 2008. Restoration of susceptibility of methicillin-resistant Staphylococcus aureus to beta-lactam antibiotics by acidic pH: role of penicillin-binding protein PBP 2a. The Journal of biological chemistry **283:**12769-12776.
66. **Leski, T. A., and A. Tomasz.** 2005. Role of Penicillin-Binding Protein 2 (PBP2) in the Antibiotic Susceptibility and Cell Wall Cross-Linking of Staphylococcus aureus: Evidence for the Cooperative Functioning of PBP2, PBP4, and PBP2A. J. Bacteriol. **187:**1815-1824.
67. **Leski, T. A., and A. Tomasz.** 2005. Role of penicillin-binding protein 2 (PBP2) in the antibiotic susceptibility and cell wall cross-linking of Staphylococcus aureus: evidence for the cooperative functioning of PBP2, PBP4, and PBP2A. Journal of bacteriology **187:**1815-1824.
68. **Limsuwun, K., and P. G. Jones.** 2000. Spermidine acetyltransferase is required to prevent spermidine toxicity at low temperatures in Escherichia coli. Journal of bacteriology **182:**5373-5380.
69. **Lindsay, J. A., and S. J. Foster.** 2001. zur: a Zn(2+)-responsive regulatory element of Staphylococcus aureus. Microbiology **147:**1259-1266.
70. **Lu, C. D., Y. Itoh, Y. Nakada, and Y. Jiang.** 2002. Functional analysis and regulation of the divergent spuABCDEFGH-spuI operons for polyamine uptake and utilization in Pseudomonas aeruginosa PAO1. Journal of bacteriology **184:**3765-3773.
71. **Majerczyk, C. D., P. M. Dunman, T. T. Luong, C. Y. Lee, M. R. Sadykov, G. A. Somerville, K. Bodi, and A. L. Sonenshein.** 2010. Direct targets of CodY in Staphylococcus aureus. Journal of bacteriology **192:**2861-2877.
72. **Mcclatchy, J. R., E.** 1963. Induction of lactose utilization in Staphylococcus aureus. Journal of bacteriology **86**.
73. **Nakada, Y., and Y. Itoh.** 2003. Identification of the putrescine biosynthetic genes in Pseudomonas aeruginosa and characterization of agmatine deiminase and N-carbamoylputrescine amidohydrolase of the arginine decarboxylase pathway. Microbiology **149:**707-714.

74. **Niven, D. F., and W. A. Hamilton.** 1974. Mechanisms of energy coupling to the transport of amino acids by Staphylococcus aureus. Eur J Biochem **44:**517-522.
75. **Oku, Y., K. Kurokawa, N. Ichihashi, and K. Sekimizu.** 2004. Characterization of the Staphylococcus aureus mprF gene, involved in lysinylation of phosphatidylglycerol. Microbiology **150:**45-51.
76. **Osawa, M., M. Yokogawa, T. Muramatsu, T. Kimura, Y. Mase, and I. Shimada.** 2009. Evidence for the direct interaction of spermine with the inwardly rectifying potassium channel. The Journal of biological chemistry **284:**26117-26126.
77. **Palomo, C., and M. Oiarbide.** 2010. β-Lactam Ring Opening: A Useful Entry to Amino Acids and Relevant Nitrogen-Containing Compounds, p. 211-259. *In* B. K. Banik (ed.), Heterocyclic Scaffolds I, vol. 22. Springer Berlin / Heidelberg.
78. **Pane-Farre, J., B. Jonas, K. Forstner, S. Engelmann, and M. Hecker.** 2006. The sigmaB regulon in Staphylococcus aureus and its regulation. International journal of medical microbiology : IJMM **296:**237-258.
79. **Pereira, S. F., A. O. Henriques, M. G. Pinho, H. de Lencastre, and A. Tomasz.** 2009. Evidence for a dual role of PBP1 in the cell division and cell separation of Staphylococcus aureus. Molecular microbiology **72:**895-904.
80. **Pereira, S. F., A. O. Henriques, M. G. Pinho, H. de Lencastre, and A. Tomasz.** 2007. Role of PBP1 in cell division of Staphylococcus aureus. Journal of bacteriology **189:**3525-3531.
81. **Pillai, S. P., and D. M. Shankel.** 1998. Effects of antimutagens on development of drug/antibiotic resistance in microorganisms. Mutat Res **402:**139-150.
82. **Pillai, S. P., and D. M. Shankel.** 1997. Polyamines and their potential to be antimutagens. Mutat Res **377:**217-224.
83. **Pinho, M. G., H. de Lencastre, and A. Tomasz.** 2001. An acquired and a native penicillin-binding protein cooperate in building the cell wall of drug-resistant staphylococci. Proceedings of the National Academy of Sciences of the United States of America **98:**10886-10891.
84. **Pinho, M. G., H. de Lencastre, and A. Tomasz.** 2001. An acquired and a native penicillin-binding protein cooperate in building the cell wall of drug-resistant staphylococci. Proceedings of the National Academy of Sciences of the United States of America **98:**10886-10891.
85. **Pinho, M. G., H. de Lencastre, and A. Tomasz.** 2000. Cloning, characterization, and inactivation of the gene pbpC, encoding penicillin-binding protein 3 of Staphylococcus aureus. Journal of bacteriology **182:**1074-1079.
86. **Pinho, M. G., H. de Lencastre, and A. Tomasz.** 1998. Transcriptional analysis of the Staphylococcus aureus penicillin binding protein 2 gene. Journal of bacteriology **180:**6077-6081.
87. **Pinho, M. G., H. n. de Lencastre, and A. Tomasz.** 2001. An acquired and a native penicillin-binding protein cooperate in building the cell wall of drug-resistant staphylococci. Proceedings of the National Academy of Sciences of the United States of America **98:**10886-10891.
88. **Pinho, M. G., and J. Errington.** 2005. Recruitment of penicillin-binding protein PBP2 to the division site of Staphylococcus aureus is dependent on its transpeptidation substrates. Molecular microbiology **55:**799-807.
89. **Pinho, M. G., S. R. Filipe, H. de Lencastre, and A. Tomasz.** 2001. Complementation of the essential peptidoglycan transpeptidase function of penicillin-binding protein 2 (PBP2) by the drug resistance protein PBP2A in Staphylococcus aureus. Journal of bacteriology **183:**6525-6531.
90. **Pinho, M. G., A. M. Ludovice, S. Wu, and H. De Lencastre.** 1997. Massive reduction in methicillin resistance by transposon inactivation of the normal PBP2 in a methicillin-resistant strain of Staphylococcus aureus. Microb Drug Resist **3:**409-413.
91. **Pohl, K., P. Francois, L. Stenz, F. Schlink, T. Geiger, S. Herbert, C. Goerke, J. Schrenzel, and C. Wolz.** 2009. CodY in Staphylococcus aureus: a regulatory link between metabolism and virulence gene expression. Journal of bacteriology **191:**2953-2963.
92. **Pootoolal, J., J. Neu, and G. D. Wright.** 2002. GLYCOPEPTIDE ANTIBIOTIC RESISTANCE. Annual Review of Pharmacology and Toxicology **42:**381-408.

93. **Postma, P. W., J. W. Lengeler, and G. R. Jacobson.** 1993. Phosphoenolpyruvate:carbohydrate phosphotransferase systems of bacteria. Microbiological reviews **57:**543-594.
94. **Pratt, R. F.** 2008. Substrate specificity of bacterial DD-peptidases (penicillin-binding proteins). Cellular and molecular life sciences : CMLS **65:**2138-2155.
95. **Rice, K. C., and K. W. Bayles.** 2003. Death's toolbox: examining the molecular components of bacterial programmed cell death. Molecular microbiology **50:**729-738.
96. **Roberts, A. P., and P. Mullany.** 2009. A modular master on the move: the Tn916 family of mobile genetic elements. Trends in microbiology **17:**251-258.
97. **Rosenthal, S. M., E. R. Fisher, and E. F. Stohlman.** 1952. Nephrotoxic action of spermine. Proceedings of the Society for Experimental Biology and Medicine. Society for Experimental Biology and Medicine **80:**432-434.
98. **Sauvage, E., F. Kerff, M. Terrak, J. A. Ayala, and P. Charlier.** 2008. The penicillin-binding proteins: structure and role in peptidoglycan biosynthesis. FEMS Microbiology Reviews **32:**234-258.
99. **Sauvage, E., F. Kerff, M. Terrak, J. A. Ayala, and P. Charlier.** 2008. The penicillin-binding proteins: structure and role in peptidoglycan biosynthesis. FEMS microbiology reviews **32:**234-258.
100. **Seltmann, G.** 2002. The bacterial cell wall. Berlin ;, Springer.
101. **Shaw, L. N., J. Aish, J. E. Davenport, M. C. Brown, J. K. Lithgow, K. Simmonite, H. Crossley, J. Travis, J. Potempa, and S. J. Foster.** 2006. Investigations into sigmaB-modulated regulatory pathways governing extracellular virulence determinant production in Staphylococcus aureus. Journal of bacteriology **188:**6070-6080.
102. **Shin, H. G., and Z. Lu.** 2005. Mechanism of the voltage sensitivity of IRK1 inward-rectifier K+ channel block by the polyamine spermine. The Journal of general physiology **125:**413-426.
103. **Sobral, R. G., A. E. Jones, S. G. Des Etages, T. J. Dougherty, R. M. Peitzsch, T. Gaasterland, A. M. Ludovice, H. de Lencastre, and A. Tomasz.** 2007. Extensive and genome-wide changes in the transcription profile of Staphylococcus aureus induced by modulating the transcription of the cell wall synthesis gene murF. Journal of bacteriology **189:**2376-2391.
104. **Sonenshein, A. L., J. A. Hoch, and R. Losick.** 2002. Bacillus subtilis and its closest relatives : from genes to cells. ASM Press, Washington, D.C.
105. **Su, Y. A., P. He, and D. B. Clewell.** 1992. Characterization of the tet(M) determinant of Tn916: evidence for regulation by transcription attenuation. Antimicrobial Agents and Chemotherapy **36:**769-778.
106. **Taylor, D. E., and A. Chau.** 1996. Tetracycline resistance mediated by ribosomal protection. Antimicrob Agents Chemother **40:**1-5.
107. **Trieber, C. A., N. Burkhardt, K. H. Nierhaus, and D. E. Taylor.** 1998. Ribosomal protection from tetracycline mediated by Tet(O): Tet(O) interaction with ribosomes is GTP-dependent. Biological chemistry **379:**847-855.
108. **Tun, N. N., C. Santa-Catarina, T. Begum, V. Silveira, W. Handro, E. I. Floh, and G. F. Scherer.** 2006. Polyamines induce rapid biosynthesis of nitric oxide (NO) in Arabidopsis thaliana seedlings. Plant & cell physiology **47:**346-354.
109. **Utaida, S., P. M. Dunman, D. Macapagal, E. Murphy, S. J. Projan, V. K. Singh, R. K. Jayaswal, and B. J. Wilkinson.** 2003. Genome-wide transcriptional profiling of the response of Staphylococcus aureus to cell-wall-active antibiotics reveals a cell-wall-stress stimulon. Microbiology **149:**2719-2732.
110. **Utaida, S., P. M. Dunman, D. Macapagal, E. Murphy, S. J. Projan, V. K. Singh, R. K. Jayaswal, and B. J. Wilkinson.** 2003. Genome-wide transcriptional profiling of the response of Staphylococcus aureus to cell-wall-active antibiotics reveals a cell-wall-stress stimulon. Microbiology **149:**2719-2732.
111. **Vollmer, W., B. Joris, P. Charlier, and S. Foster.** 2008. Bacterial peptidoglycan (murein) hydrolases. FEMS microbiology reviews **32:**259-286.

112. **Walsh, T. R., and R. A. Howe.** 2002. The prevalence and mechanisms of vancomycin resistance in Staphylococcus aureus. Annual review of microbiology **56:**657-675.
113. **Wang, Y., and R. A. Casero, Jr.** 2006. Mammalian polyamine catabolism: a therapeutic target, a pathological problem, or both? Journal of biochemistry **139:**17-25.
114. **Ware, D., Y. Jiang, W. Lin, and E. Swiatlo.** 2006. Involvement of potD in Streptococcus pneumoniae polyamine transport and pathogenesis. Infection and immunity **74:**352-361.
115. **Woolridge, D. P., J. D. Martinez, D. E. Stringer, and E. W. Gerner.** 1999. Characterization of a novel spermidine/spermine acetyltransferase, BltD, from Bacillus subtilis. The Biochemical journal **340 (Pt 3):**753-758.
116. **Wyke, A. W., J. B. Ward, M. V. Hayes, and N. A. Curtis.** 1981. A role in vivo for penicillin-binding protein-4 of Staphylococcus aureus. Eur J Biochem **119:**389-393.
117. **Xie, L. H., S. A. John, and J. N. Weiss.** 2002. Spermine block of the strong inward rectifier potassium channel Kir2.1: dual roles of surface charge screening and pore block. The Journal of general physiology **120:**53-66.
118. **Xue, T., Y. You, D. Hong, H. Sun, and B. Sun.** 2011. The Staphylococcus aureus KdpDE two-component system couples extracellular K+ sensing and Agr signaling to infection programming. Infection and immunity **79:**2154-2167.
119. **Yang, S. J., P. M. Dunman, S. J. Projan, and K. W. Bayles.** 2006. Characterization of the Staphylococcus aureus CidR regulon: elucidation of a novel role for acetoin metabolism in cell death and lysis. Molecular microbiology **60:**458-468.
120. **Yao, X., W. He, and C. D. Lu.** 2011. Functional characterization of seven gamma-Glutamylpolyamine synthetase genes and the bauRABCD locus for polyamine and beta-Alanine utilization in Pseudomonas aeruginosa PAO1. Journal of bacteriology **193:**3923-3930.
121. **Yao, X., and C. D. Lu.** 2012. A PBP 2 mutant devoid of the transpeptidase domain abolishes spermine-beta-lactam synergy in Staphylococcus aureus Mu50. Antimicrob Agents Chemother **56:**83-91.
122. **Yao, X. L., C.; Zhang,J.; Lu,C.D.** 2012. (γ-Glutamyl Spermine Synthetase PauA2 as Potential Target of Antibiotic Development against Pseudomonas aeruginosa. Antimicrobial Agents and Chemotherapy,.
123. **Zapun, A., C. Contreras-Martel, and T. Vernet.** 2008. Penicillin-binding proteins and beta-lactam resistance. FEMS microbiology reviews **32:**361-385.
124. **Zhang, M., H. Wang, and K. J. Tracey.** 2000. Regulation of macrophage activation and inflammation by spermine: a new chapter in an old story. Critical care medicine **28:**N60-66.
125. **Zuniga, M., G. Perez, and F. Gonzalez-Candelas.** 2002. Evolution of arginine deiminase (ADI) pathway genes. Mol Phylogenet Evol **25:**429-444.

APPENDICES

APPENDIX A: SUPPLEMENTARY DATA

Table S1 Oligonucleotides used in this study.

Oligonucleotide	Sequence	Application
PBP1-expr-noTM-F	AAAACTGCAGCATGATTACTGGACATTCTAATGG	construction of pBAD/HisD expressing His-PBP1
PBP1-expr-R	CCGGAATTCGTTAGTCCGACTTATCCTTGTCAG	
PBP2-hisC59 -F	GCCC TCATG AGG AAAGCACCTGCTTTTACCGAAGC	construction of pBAD/HisE expressing His-PBP2
PBP2-hisC716-R	TCC CCCGGG AGATTGTTGAGATCTAGTATTGTTATTTG	
PBP3-expr-noTM-F	AAAACTGCAGACAAATCGCACAAGGCTCACATTA	construction of pBAD/HisD expressing His-PBP3
PBP3-expr-R	CCGGAATTCTTTATTTGTCTTTGTCTTTAT	
PBP4-expr-noSP-F	AAAACTGCAGTACTAACAGTGACGTAACCCCTGT	construction of pBAD/HisD expressing His-PBP4
PBP4-expr-noTM-R	CCGGAATTCTTAATGTTCTTCCCACATACTTTTAG	
PBP2A-expr-no TM-F	TAATCCATGGCTTCAAAAGATAAAGAAAT	construction of pBAD/HisA expressing PBP2a(no His-tag)
PBP2A-expr-R	TAATAAGCTTCTGTTTTGTTATTCATCTATAT	
potR-expr-F (for his & native)	AACATAGGTAATAAAATTAAAAATCTTAGAAG	construction of pBAD/HisD expression His or native PotR
potR-expr-R (for expr and promoter fusion)	CCGGAATTCCTATAAATATGAAGCTGTCGCTAC	
HisN- noSP-potD -FP	GAACAAGTGCATACAAATCAAAAAATTTACG	construction of pBAD/HisD expression His-PotD
HisN-native-potD-RP	CCCAAGCTTTTTATTTTAATGACATTTTGAA	
potR-arm1-F	CGCGGATCCCGGTGCTCAAGTAGTTGGTACTGG	construction of pCN56 carrying PpotR and PpotRA::gfp fusion; construction of potRABCDE deletion
PpotR-R	CCGGAATTCACGTTCAGCAAGTTCTTCTTGCG	construction of pCN56 carrying PpotR::gfp fusion
potR-expr-R	CCGGAATTCCTATAAATATGAAGCTGTCGCTAC	construction of pCN56 carrying PpotRA::gfp fusion
potR-arm1-R	CGACCTAGGACGTTCAGCAAGTTCTTCTTGCG	construction of pMAD/CMΔpotRABCDE
potD-arm2-F	CCGCTCGAGAATCATAAATAGTAGTTATTTACTG	
potD-arm2-R	GGAAGATCTCACATCATAATAATCATCTTTCGG	
tetM del-arm1-F	CGCGGATCCCGGACTACCAACCCAAACAGCTAG	construction pCN38/tetM
tetM del-arm2-R	GGAAGATCT TTAGAGCCGTTGGTTTAGCGATTA	
speG-F	CGCGGATCCTGCTGCTCTAGTTTTCACTTCCAAC	construction of pCN38/speG
speG-R	CCGGAATTCGAAGTAATTCAGGTTTGAACCTACC	
gyrB-F	TTAGTGTGGGAAATTGTCGATAAT	qRT-PCR
gyrB-R	AGTCTTGTGACAATGCGTTTACA	
potA-F	AATATTGTTGAAGGGCGCAT	
potA-R	TTCTGGTCGAATAACGACTTCT	
tetM-F	ACAATCCGTCACATTCCAAC	
tetM-R	TTGGGAAGTGGAATGCAGTA	
kdpA-F	ACGAGTACATCGTCATGCGT	
kdpA-R	CTGCTCCAAACCGTACCTCT	

RN1-FP	CTGCATTTAGATAATTTAGTTGGG	confirmation of mutation site, trkA
RN1-RP	CGCAACATTATGCGCAATACGTCTACCC 3’	
RN2-FP	GCTGGTAAATCCATTTCTTCACC	confirmation of mutation site, sigA
RN2-RP	CTGAATCCAAGTGATCTTAG TGCC	
RN3-FP	CCAAGACGATGTGCTAATGGTGC	confirmation of mutation site, relA
RN3-RP	GGCGAAGTAATAAATATGAATGGG	
RN4-FP	GGCACATCAATAACCAAGGCG	confirmation of mutation site, atpG
RN4-RP	GTCAGCGTTCTTGAAAACAAGCC	
RN6-FP	GCTCTCTTTACTTACCATATAATGGC	confirmation of mutation site, fbp
RN6-RP	CGAATGAATTATACAATAGTGTATAGCC	
Mu-FP	GGTTTAGTTGCTATATCTGGTGG	confirmation of mutation site, pbpB
Mu-RP	CGCGTTGTTATAAGTACCACCG	
704394-FP	CGAACAGCTGCTTCTCTTTGAACG	confirmation of mutation site, intergenic region of SAV0631-SAV0630
704394-RP	TAGCCACACTCATATGACATCGG	
XY1-F	CGCG GAT CCT AGA TAA TTT AGT TGG GGT AC	construction pCN33/(m)trkA
XY1-R	CGCGA ATT CTG TCC CAC TCC CGA TTA TCT CG	
XY2-F	CGCG GAT CCT AGT TAC CGC ATT TAA ACA AC	construction pCN33/(m)sigA
XY2-R	CGCGA ATT CGC GCT TAT TCA TGT CTT GGT ATC	
XY3-F	CGCG GAT CCA TGA AAC AGT AGA TTT AGG TCG	construction pCN33/(m)relA
XY3-R	CGCGA ATT CCA CCT CTA GTT CCA AAC TCT TG	
XY6-F	CGCG GAT CCC CTA ATA CCA AAA TCC TGC CC	construction pCN33/(m)fbp
XY6-R	CGCGA ATT CCA CGA TAC ATG CAT CAA ATG TCG	
XY4-F1	CGCG GAT CCA CCA AGC GAT TTC TGA GG	construction pCN33/(m)atpG
XY4-R11	GCG AAG CTT GTT GTA GAA ACG ACT CAT	
XY4-R12	GCG AAG CTT GAG CGG GGA TTT GTG ATC	
XY4-F2	GCG AAG CTT GCT TCT CTT AAA GAA ATA G	
XY4-R2	GCCGA ATT CAT TCC CAT GCT ATT TTC CTC	

Table S2 Transcriptome: MuM vs Mu50 (no Spm)

red font: up regulated in MuM
blue font: down regulated in MuM
gray font: PBP2-complementing strains

Remain changed in PBP2-complementing MuM	Others	CodY regulon	GI (genomic island)	Mu50 ID	Gene Symbol	signal intensity					signal intensity					JCVI Common Name(description)	JCVI sub role
						Mu50-1	Mu50-2	MuM-1	MuM-2	MuM ave/Mu50 ave	Mu50/pYX9-1	Mu50/pYX9-2	MuM/pYX9-1	MuM/pYX9-2	MM-PBP2/MP-PBP2		
				SAV0007		422	421	1226	1092	2.7	381	370	361	361	1	Predicted sugar kinase	Other
				SAV0045		87	117	365	316	3.3	52	50	97	29	1.2	unnamed protein product	Unclassified
				SAV0047		43	23	458	487	14.5	16	16	40	5	1.4	unnamed protein product	Unclassified
				SAV0058		81	35	349	399	6.4	10	12	35	14	2.2	unnamed protein product	Unclassified
				SAV0060		17	15	148	132	8.7	5	11	4	5	0.6	unnamed protein product	Unclassified
				SAV0061	ccrB	51	79	489	404	6.9	44	54	38	42	0.8	site-specific recombinase	DNA replication, recombination, and
				SAV0062	ccrA	130	150	575	659	4.4	46	43	67	69	1.5	site-specific recombinase	DNA replication, recombination, and
				SAV0063		52	34	145	183	3.8	45	26	29	35	0.9	unnamed protein product	Unclassified
				SAV0064		38	75	345	337	6.0	8	8	11	10	1.3	unnamed protein product	Unclassified
				SAV0069		215	227	713	905	3.7	99	131	241	276	2.3	conserved hypotehtical	Unclassified
				SAV0072	kdpA	204	455	1277	1000	3.5	123	116	114	100	0.9	K+-transporting ATPase	Cations and iron carrying compounds
				SAV0073	kdpB(	169	278	1333	1490	6.3	277	156	275	195	1.1	K+-transporting ATPase	Cations and iron carrying compounds
				SAV0074	kdpC(	86	91	242	205	2.5	69	54	66	63	1.1	K+-transporting ATPase	Cations and iron carrying compounds
				SAV0075		188	162	448	715	3.3	63	82	81	44	0.9	unnamed protein product	Unclassified
				SAV0076		313	317	865	941	2.9	168	211	242	239	1.3	unnamed protein product	Unclassified
				SAV0087		159	87	438	593	4.2	52	79	61	30	0.7	unnamed protein product	Unclassified
				SAV0095	plc	62	161	202	348	2.5	60	32	43	39	0.9	1-phosphatidylinositol	Degradation
				SAV0103		337	336	938	1044	2.9	570	479	896	796	1.6	Blt-like protein	Unclassified
				SAV0107		93	90	585	591	6.4	29	14	46	24	1.6	Transporter	Unclassified
				SAV0108		46	100	231	222	3.1	17	2	7	17	1.3	transcriptional regulator	Other
				SAV0115	sirA	288	216	765	667	2.8	144	117	109	85	0.7	lipoprotein	Cell envelope
				SAV0116	sbnA	143	97	681	695	5.7	31	30	14	7	0.3	SbnA	Unclassified
				SAV0117	sbnB	156	179	472	684	3.5	90	72	54	23	0.5	SbnB	Unclassified
				SAV0119		194	214	625	628	3.1	130	94	61	96	0.7	major facilitator	Transport and binding proteins
				SAV0120	sbnE	79	210	420	487	3.2	151	98	84	59	0.6	SbnE	Unclassified
				SAV0121	sbnF	210	295	668	825	3.0	163	148	66	75	0.5	SbnF	Unclassified
				SAV0122	sbnG	170	316	719	797	3.1	183	139	78	47	0.4	SbnG	Unclassified
				SAV0125		117	104	259	291	2.5	48	35	43	42	1	conserved hypothetical	Conserved
				SAV0128		106	140	312	414	2.9	48	52	57	65	1.2	NAD-dependent	Unclassified
				SAV0129		19	19	293	269	15.0	25	30	20	9	0.5	Undecaprenyl-phosphate	Biosynthesis and degradation of

JCVI sub role: belong to CodY regulon; belong to GI; others; remian changed in PBP2-complementing strains

SAV0130		102	69	515	476	5.8	23	23	63	24	1.9	glycosyltransferase	Protein modification and repair
SAV0131		100	58	422	664	6.9	56	51	31	78	1	O-Antigen Polymerase	DNA-dependent RNA polymerase
SAV0132		244	320	750	730	2.6	373	373	663	533	1.6	Polysaccharide	Biosynthesis and degradation of
SAV0140		99	147	523	367	3.6	117	49	95	70	1	phosphonates transport	Transport and binding proteins
SAV0141		117	217	362	545	2.7	84	53	15	55	0.5	phosphonates transport	Transport and binding proteins
SAV0142		182	238	495	640	2.7	45	61	57	21	0.7	transport system protein	Transport and binding proteins
SAV0143		135	96	342	293	2.7	40	36	3	12	0.2	alkylphosphonate ABC	Transport and binding proteins
SAV0144		127	285	813	866	4.1	171	137	94	112	0.7	conserved hypothetical	Conserved
SAV0148	adhE	196	218	783	796	3.8	2229	2143	1377	1584	0.7	alcohol-acetaldehyde	Unclassified
SAV0173		139	159	592	576	3.9	116	102	116	90	0.9	lipoprotein	Cell envelope
SAV0174		195	141	521	456	2.9	91	69	81	80	1	Homolog of ABC-type	Unclassified
SAV0175		304	187	682	711	2.8	246	243	236	295	1.1	conserved hypothetical	Conserved
SAV0177	fdh	210	126	442	630	3.2	58	42	64	49	1.1	NAD-dependent formate	TCA cycle
SAV0182	argB	178	179	507	587	3.1	94	128	80	119	0.9	acetylglutamate kinase	Glutamate family
SAV0183	argJ	149	115	686	597	4.9	61	91	69	76	1	arginine biosynthesis	Glutamate family
SAV0184	argC	179	207	565	625	3.1	80	91	49	83	0.8	N-acetyl-gamma-glutamyl-	Glutamate family
SAV0185	rocD	139	158	732	623	4.6	45	50	83	32	1.2	ornithine	Glutamate family
SAV0190		149	130	460	534	3.6	149	180	455	642	3.3	Bacterial protein of	Degradation of proteins, peptides,
SAV0196		68	123	317	322	3.4	39	36	64	76	1.9	conserved hypothetical	Conserved
SAV0197		88	182	274	404	2.5	17	26	38	29	1.6	SA0191/BacG-like protein	Unclassified
SAV0199		207	164	418	513	2.5	65	82	31	45	0.5	Enterococcus faecalis	Unclassified
SAV0205	oppF	211	177	728	722	3.7	106	151	338	363	2.7	oligopeptide transport	Amino acids, peptides and amines
SAV0206	trunca	54	130	429	569	5.4	8	27	44	65	3.1	Dipeptide transport	Amino acids, peptides and amines
SAV0207		76	147	518	617	5.1	36	47	51	34	1	oligopeptide ABC	Amino acids, peptides and amines
SAV0208	rlp	353	199	1231	1128	4.3	87	101	98	90	1	RGD-containing	Unclassified
SAV0209		228	289	643	743	2.7	123	118	168	97	1.1	gamma-	Biosynthesis of cofactors, prosthetic
SAV0222	uhpT	131	80	332	445	3.7	57	52	134	67	1.9	hexose phosphate	Energy metabolism
SAV0231	fadA	121	75	477	546	5.2	88	90	149	142	1.6	acetyl-CoA	Fatty acid and phospholipid
SAV0232	fadB	138	139	1056	1029	7.5	75	61	80	114	1.4	3-hydroxyacyl-CoA	Fatty acid and phospholipid
SAV0234	fadE	86	146	683	768	6.3	47	7	7	37	0.8	AMP-binding enzyme	Unclassified
SAV0235	fadX	166	190	941	881	5.1	135	49	133	127	1.4	propionate CoA-	Fermentation
SAV0237		112	178	578	673	4.3	178	112	82	83	0.6	nickel ABC transporter	Cations and iron carrying compounds
SAV0238		62	33	262	236	5.3	94	108	62	53	0.6	Protein of unknown	Unclassified
SAV0243		278	529	929	1089	2.5	541	391	488	564	1.1	inosine-uridine preferring	Purines, pyrimidines, nucleosides, and
SAV0245		153	211	391	502	2.5	65	76	62	66	0.9	PTS system	Carbohydrates, organic alcohols, and
SAV0247	gatC	370	453	1079	1075	2.6	308	341	341	295	1	PTS system	Carbohydrates, organic alcohols, and
SAV0248		239	246	755	1118	3.9	366	370	278	260	0.7	sorbitol dehydrogenase	TCA cycle
SAV0249		120	59	430	343	4.3	179	120	121	145	0.9	conserved hypothetical	Conserved

SAV0250		246	345	825	763	2.7	330	242	179	196	0.7	sorbitol dehydrogenase (L-	Unclassified
SAV0311		155	74	385	498	3.9	65	50	42	50	0.8	carbohydrate kinases	Energy metabolism
SAV0312		68	151	804	796	7.3	119	90	93	92	0.9	Erwinia chrysanthemi	Unclassified
SAV0313	nupC	58	33	228	241	5.1	29	39	30	32	0.9	nucleoside transporter	Amino acids, peptides and amines
SAV0334		113	68	389	417	4.5	74	62	78	57	1	EffD	Unclassified
SAV0336	glpT	239	286	616	712	2.5	400	603	840	877	1.7	glycerol-3-phosphate	Fatty acid and phospholipid
SAV0338		339	378	1075	816	2.6	202	179	270	309	1.5	Glyoxalase family protein	Energy metabolism
SAV0339		88	107	340	371	3.6	337	363	483	423	1.3	bacterial luciferase family	Unclassified
SAV0342		76	104	341	366	3.9	242	304	306	306	1.1	ribosomal-protein-serine	Toxin production and resistance
SAV0343		205	189	496	693	3.0	45	42	36	44	0.9	Protein ycdO	Unclassified
SAV0344		220	250	825	907	3.7	73	64	122	85	1.5	Tat-translocated enzyme	Unclassified
SAV0352		298	242	712	797	2.8	458	684	770	719	1.3	conserved hypothetical	Conserved
SAV0354		226	225	557	735	2.9	4551	4106	3338	3182	0.8	acetyl-CoA C-	Fatty acid and phospholipid
SAV0355		205	258	741	604	2.9	100	138	104	102	0.9	predicted metal-	Fatty acid and phospholipid
SAV0356	metE	142	191	682	679	4.1	155	174	130	128	0.8	5-	Aspartate family
SAV0358	metB	112	131	582	626	5.0	78	102	102	120	1.2	cystathionine beta-lyase	Aspartate family
SAV0395		67	142	268	294	2.7	79	73	90	80	1.1	conserved hypothetical	Conserved
SAV0399		166	109	534	750	4.7	114	169	59	72	0.5	TN916 ORF13 homolog	Ribosomal proteins: synthesis and
SAV0400		237	277	754	957	3.3	161	153	129	105	0.7	TN916 ORF14 and to L.	Unclassified
SAV0401		208	200	944	745	4.1	171	207	183	122	0.8	TN916 ORF15 homolog	Ribosomal proteins: synthesis and
SAV0402		456	354	1114	1232	2.9	541	536	469	513	0.9	TN916 ORF16 homolog	Ribosomal proteins: synthesis and
SAV0407		174	190	684	559	3.4	90	86	105	62	0.9	conserved hypothetical	Conserved
SAV0408		167	198	576	708	3.5	46	53	44	60	1	TN916 ORF20 homolog	Ribosomal proteins: synthesis and
SAV0409		153	115	829	880	6.4	74	64	107	89	1.4	TN916 ORF21 homolog	Ribosomal proteins: synthesis and
SAV0410		145	138	483	588	3.8	59	61	42	76	1	conserved hypothetical	Conserved
SAV0412		220	134	677	646	3.7	111	182	178	125	1	uncharacterized	Unclassified
SAV0423	set7	27	52	134	287	5.3	30	24	33	34	1.2	exotoxin 7	Toxin production and resistance
SAV0424	set8	141	212	557	660	3.5	59	43	64	56	1.2	exotoxin 8	Toxin production and resistance
SAV0425	set10	111	117	363	287	2.9	41	33	44	38	1.1	exotoxin 10	Toxin production and resistance
SAV0450		143	88	751	579	5.8	90	75	76	86	1	YciC protein	Unclassified
SAV0472	gltB	78	143	647	783	6.5	88	119	138	96	1.1	glutamate synthase large	Nitrogen metabolism
SAV0473	gltD	191	279	579	585	2.5	117	140	169	159	1.3	NADH-glutamate synthase	Glutamate family
SAV0561	sdrC	55	79	321	382	5.3	34	31	31	29	0.9	Ser-Asp rich fibrinogen-	Transport and binding proteins
SAV0562	sdrD	142	239	519	541	2.8	96	61	73	70	0.9	Ser-Asp rich fibrinogen-	Transport and binding proteins
SAV0786		111	91	361	312	3.3	39	20	34	20	0.9	transcriptional regulator	Regulatory functions
SAV0787		68	60	140	184	2.5	2	10	8	3	0.9		
SAV0788		85	90	202	446	3.7	21	14	33	38	2	conserved hypothetical	Conserved
SAV0789		23	40	110	82	3.1	2	5	11	13	3.5	Protein of unknown	Unclassified

SAV0791		94	103	415	549	4.9	30	33	74	73	2.4	prophage Lp3 protein 8	Mobile and extrachromosomal
SAV0792		131	138	431	528	3.6	64	72	143	120	1.9	conserved hypothetical	Conserved
SAV0793		105	71	440	704	6.5	66	69	129	169	2.2	conserved hypothetical	Conserved
SAV0866		154	248	681	769	3.6	70	74	100	96	1.4	77ORF018	Unclassified
SAV0868		24	43	293	343	9.5	54	34	24	27	0.6	77ORF016	Unclassified
SAV0873		296	490	816	1395	2.8	120	114	116	64	0.8	phi PVL ORF 50	Unclassified
SAV0885		44	101	161	202	2.5	2	16	5	6	0.6	small terminase	Mobile and extrachromosomal
SAV0886		89	134	326	360	3.1	36	22	44	14	1	phage terminase	Mobile and extrachromosomal
SAV0888		161	158	459	465	2.9	61	59	34	29	0.5	phi Mu50B-like protein	Unclassified
SAV0889		5	13	21	53	4.1	2	10	5	3	0.7	conserved hypothetical	Conserved
SAV0891		43	20	105	126	3.7	21	13	21	20	1.2	head protein	Degradation of proteins, peptides,
SAV0892		54	47	149	149	2.9	56	25	43	46	1.1	head protein	Degradation of proteins, peptides,
SAV0894		72	64	199	172	2.7	7	30	10	31	1.1	phi Mu50B-like protein	Unclassified
SAV0897		65	102	195	218	2.5	3	5	3	24	3.4	phi Mu50B-like protein	Unclassified
SAV0898		55	73	405	468	6.8	39	40	74	46	1.5	structural phi Mu50B	Mobile and extrachromosomal
SAV0899		220	239	605	778	3.0	79	35	82	67	1.3	conserved hypothetical	Conserved
SAV0902		33	17	257	298	11.2	6	2	7	4	1.4	phi ETA orf 54-like protein	Unclassified
SAV0903		152	261	634	604	3.0	72	60	96	81	1.3	phi ETA orf 55-like protein	Unclassified
SAV0904		145	102	515	570	4.4	17	35	60	6	1.3	phi ETA orf 56-like protein	Unclassified
SAV0906		66	110	254	287	3.1	39	32	31	25	0.8	phi105 orf 44-like protein	Unclassified
SAV0907		48	72	155	195	2.9	28	15	26	5	0.7	phage uncharacterized	Mobile and extrachromosomal
SAV0909		145	122	495	474	3.6	47	51	71	52	1.3	cell wall hydrolase	Fatty acid and phospholipid
SAV0912		53	84	306	291	4.3	23	19	27	43	1.7	holin	Mobile and extrachromosomal
SAV0913		53	68	264	153	3.4	62	39	73	36	1.1	amidase	Central intermediary metabolism
SAV1165		42	59	171	233	4.0	55	47	87	109	1.9		
SAV1166		83	34	105	199	2.6	30	18	17	35	1.1	Staphylococcal/Streptoco	Unclassified
SAV1167		73	72	225	321	3.8	46	21	33	30	0.9	Staphylococcal/Streptoco	Unclassified
SAV1168		58	68	198	232	3.4	106	87	135	103	1.2	exotoxin 12	Toxin production and resistance
SAV1169	argF	147	123	564	432	3.7	265	260	290	309	1.1	ornithine	Glutamate family
SAV1170	arcC	371	180	770	764	2.8	769	669	1358	1427	1.9	carbamate kinase	Amino acids and amines
SAV1367	trpE	118	133	282	513	3.2	27	20	42	56	2.1	anthranilate synthase	Aromatic amino acid family
SAV1368	trpG	81	74	215	244	3.0	69	46	66	52	1	anthranilate synthase	Biosynthesis of cofactors, prosthetic
SAV1370	trpC	66	29	258	261	5.4	31	38	41	32	1.1	indole-3-glycerol	Aromatic amino acid family
SAV1371	trpF	45	82	194	198	3.1	22	10	21	6	0.9	N-	Aromatic amino acid family
SAV1372	trpB	106	126	615	579	5.1	52	65	83	54	1.2	tryptophan synthase	Aromatic amino acid family
SAV1373	trpA	133	181	453	585	3.3	83	101	130	103	1.3	tryptophan synthase	Aromatic amino acid family
SAV1433	rnhA	130	63	264	265	2.7	60	47	79	93	1.6	RNase H	Degradation of RNA
SAV1434	ebhA	127	150	483	493	3.5	38	30	52	61	1.7	ATP synthase	ATP-proton motive force

SAV1435	ebhB	76	215	667	598	4.3	90	94	82	90	0.9	ebhA protein	Unclassified
SAV1436		154	124	451	388	3.0	527	624	574	571	1	Blt-like protein	Unclassified
SAV1819	lukD	77	67	229	235	3.2	27	22	8	8	0.3	leukotoxin F-subunit	Degradation of proteins, peptides,
SAV1820	lukE	95	66	234	294	3.3	14	2	27	28	3.5	leukotoxin LukE	Degradation of proteins, peptides,
SAV1821		60	62	171	201	3.0	54	53	43	64	1	conserved hypothetical	Conserved
SAV1922		106	106	327	358	3.2	88	28	85	120	1.8	conserved hypothetical	Conserved
SAV1950		28	69	161	185	3.6	57	53	79	59	1.3	conserved hypothetical	Conserved
SAV1951		125	71	245	322	2.9	161	97	122	136	1	77ORF044	Unclassified
SAV1953		138	192	604	500	3.4	50	79	102	86	1.5	phi PVL ORF 20 and 21	General
SAV1954		124	200	460	620	3.3	76	64	84	88	1.2	77ORF004	Unclassified
SAV1955		73	45	175	160	2.9	19	26	50	27	1.7	phi PVL ORF 15 and 16	General
SAV1959		66	46	147	181	2.9	27	41	31	16	0.7	77ORF029	Unclassified
SAV1960		104	41	244	246	3.4	5	30	41	29	2	phage head-tail adaptor	Mobile and extrachromosomal
SAV1961		89	64	212	270	3.1	13	27	21	43	1.6		
SAV1963		167	119	480	494	3.4	88	78	102	55	1	77ORF006	Unclassified
SAV1964		149	150	503	497	3.3	111	72	47	49	0.5	phiN315 scaffolding	Chemotaxis and motility
SAV1966		78	48	391	391	6.2	51	36	57	75	1.5	phage terminase	Mobile and extrachromosomal
SAV2053	ilvD	272	357	922	992	3.0	299	562	948	680	1.9	dihydroxy-acid	Pyruvate family
SAV2054	ilvB	150	178	499	771	3.9	184	288	351	365	1.5	acetolactate synthase	Pyruvate family
SAV2055	IlvH	73	67	197	197	2.8	81	85	131	223	2.1	acetolactate synthase	Energy metabolism
SAV2057	leuA	146	214	622	859	4.1	124	115	181	169	1.5	2-isopropylmalate	Pyruvate family
SAV2058	leuB	76	96	581	693	7.4	68	83	121	126	1.6	3-isopropylmalate	Pyruvate family
SAV2059	leuC	127	75	765	706	7.3	91	110	93	102	1	3-isopropylmalate	Pyruvate family
SAV2061	ilvA	59	56	300	292	5.1	53	58	75	73	1.3	threonine dehydratase	Pyruvate family
SAV2075	kdpC	200	227	992	1074	4.8	113	120	162	163	1.4	K+-transporting ATPase	Cations and iron carrying compounds
SAV2076	kdpB	179	206	942	864	4.7	100	100	112	92	1	K+-transporting ATPase	Cations and iron carrying compounds
SAV2077	kdpA	123	43	1194	1021	13.4	55	52	100	84	1.7	K+-transporting ATPase	Cations and iron carrying compounds
SAV2078	kdpD	138	171	1039	1041	6.7	75	61	90	79	1.2	sensor protein KdpD	Regulatory functions
SAV2079	kdpE	114	148	615	957	6.0	62	69	58	68	1	transcription regulator	Regulatory functions
SAV2091	thiE	274	302	1052	948	3.5	158	153	103	95	0.6	thiamine-phosphate	Biosynthesis of cofactors, prosthetic
SAV2092	thiM	360	304	1063	1335	3.6	161	212	147	160	0.8	Hydroxyethylthiazole	Biosynthesis of cofactors, prosthetic
SAV2093	thiD	217	389	830	924	2.9	118	203	186	144	1	phosphomethylpyrimidine	Biosynthesis of cofactors, prosthetic
SAV2094	tenA	146	132	709	522	4.4	41	52	77	54	1.4	trasncriptional activator	Unclassified
SAV2095		1547	1364	7193	5111	4.2	2444	872	462	432	0.3	SceD precursor	Unclassified
SAV2096		406	363	1170	861	2.6	937	870	869	672	0.9	Single-strand binding	Unclassified
SAV2144		940	794	2378	1915	2.5	2624	2522	3384	4011	1.4	B. subtilis YhfK protein	Degradation of proteins, peptides,
SAV2145	czrA	281	279	760	700	2.6	634	531	3835	6099	8.5	repressor protein	Regulatory functions
SAV2146	czrB	272	462	1259	1414	3.6	808	717	6391	8784	9.9	cation-efflux system	Cations and iron carrying compounds

SAV2154	glmS	170	226	526	648	3.0	149	176	153	176	1	glucosamine--fructose-6-	Central intermediary metabolism
SAV2156	mtlF	253	352	1261	1154	4.0	628	934	4595	4671	5.9	PTS system	Carbohydrates, organic alcohols, and
SAV2157		828	883	2420	2366	2.8	1469	1769	2314	2622	1.5	PRD domain protein	RNA interactions
SAV2159	mtlD	785	899	2415	1833	2.5	1775	1855	2558	2508	1.4	Mannitol-1-phosphate 5-	Sugars
SAV2160	fmtB(	210	128	924	1009	5.7	62	31	52	30	0.9	FmtB protein	Unclassified
SAV2206	budA	366	354	958	846	2.5	278	223	206	227	0.9	alpha-acetolactate	Fermentation
SAV2207	alsS	117	118	299	467	3.3	27	30	13	46	1	alpha-acetolactate	Pyruvate family
SAV2287		115	98	423	488	4.3	49	32	35	40	0.9	Urea transporter	Amino acids, peptides and amines
SAV2288	ureA	104	157	588	551	4.4	123	110	10	4	0.1	urease	Nitrogen metabolism
SAV2290	ureC	184	257	1269	1124	5.4	185	153	95	69	0.5	urease	Nitrogen metabolism
SAV2291	ureE	172	125	917	737	5.6	160	92	60	38	0.4	urease accessory protein	Nitrogen metabolism
SAV2292	ureF	202	256	745	878	3.5	139	150	90	88	0.6	urease accessory protein	Nitrogen metabolism
SAV2293	ureG	315	344	864	820	2.6	236	241	174	139	0.7	urease accessory protein	Nitrogen metabolism
SAV2294	ureD	173	104	447	505	3.4	124	125	71	68	0.6	urease accessory protein	Nitrogen metabolism
SAV2359		112	49	534	646	7.3	36	48	73	22	1.1	ABC transporter (ATP-	Transport and binding proteins
SAV2360		99	50	372	414	5.3	32	29	37	27	1	permease	Transport and binding proteins
SAV2389		109	98	237	311	2.7	38	43	53	54	1.3	conserved hypothetical	Conserved
SAV2419	hlgA	71	178	497	546	4.2	63	55	136	241	3.2	hlgA-like protein	Unclassified
SAV2420	hlgC	100	93	466	371	4.3	25	26	83	51	2.6	gamma-hemolysin	Toxin production and resistance
SAV2421	hlgB	205	242	625	607	2.8	83	69	151	109	1.7	gamma-hemolysin	Toxin production and resistance
SAV2424	bioF	273	329	743	802	2.6	275	300	304	407	1.2	8-amino-7-oxononanoate	Biosynthesis of cofactors, prosthetic
SAV2426	bioA	44	103	517	610	7.6	37	30	35	36	1.1	adenosylmethionine-8-	Biosynthesis of cofactors, prosthetic
SAV2427	bioD	46	112	265	307	3.6	4	14	6	26	1.8	dethiobiotin synthetase	Biosynthesis of cofactors, prosthetic
SAV2428		105	159	354	432	3.0	66	55	59	65	1	ABC transporter	Unclassified
SAV2429		119	74	430	584	5.3	49	45	34	57	1	ABC transporter	Unclassified
SAV2445	opuC	441	584	1901	2451	4.2	822	980	1354	1520	1.6	opuCD protein	Unclassified
SAV2446	opuCC	356	419	1361	1280	3.4	1114	1068	1266	1207	1.1	glycine	Amino acids, peptides and amines
SAV2447	opuCB	209	186	703	536	3.1	433	400	417	484	1.1	opuCB protein	Unclassified
SAV2448	opuCA	137	269	534	638	2.9	412	339	361	449	1.1	glycine	Amino acids, peptides and amines
SAV2450		407	381	1143	1202	3.0	127	136	173	71	0.9	amino acid transporter	Amino acids, peptides and amines
SAV2468		382	253	976	1048	3.2	101	105	77	55	0.6	conserved hypothetical	Conserved
SAV2469		229	175	523	520	2.6	97	133	98	59	0.7	conserved hypothetical	Conserved
SAV2502	fnbB	321	340	916	848	2.7	51	70	69	75	1.2	fibronectin-binding	Transport and binding proteins
SAV2503	fnb	95	121	424	489	4.2	13	21	41	4	1.3	Fibronectin-binding	Transport and binding proteins
SAV2505	gntP	270	382	806	1002	2.8	249	234	600	693	2.7	gluconate permease	Carbohydrates, organic alcohols, and
SAV2506	gntK	224	288	663	650	2.6	204	172	351	533	2.4	gluconate kinase	Sugars
SAV2512		6880	10034	3707	3839	0.4	5590	5608	4957	5395	0.9	glucarate transporter	Amino acids, peptides and amines
SAV2514		927	1046	394	354	0.4	1058	2612	1007	1257	0.6	ABC transporter protein	Amino acids, peptides and amines

SAV2515		600	644	149	257	0.3	663	1117	956	841	1	hydrophobic	Other
SAV2519		156	226	633	781	3.7	95	91	91	81	0.9	glyoxylase family protein	Unclassified
SAV2520		127	201	370	545	2.8	61	66	55	70	1	transcriptional regulator	Other
SAV2550	feoB	139	140	562	842	5.0	77	41	55	79	1.1	ferrous iron transport	Cations and iron carrying compounds
SAV2551		57	23	133	156	3.6	4	2	16	12	4.5	FeoA family protein	Unclassified
SAV2582		133	203	489	520	3.0	75	97	69	115	1.1	cobalamin synthesis	Heme, porphyrin, and cobalamin
SAV2583		97	127	632	601	5.5	47	44	48	46	1	ferrous iron transporter	Amino acids, peptides and amines
SAV2584		112	128	495	543	4.3	10	30	58	48	2.7	EF0074	Unclassified
SAV2586		280	307	936	665	2.7	288	258	164	213	0.7	conserved hypothetical	Conserved
SAV2594		201	232	791	836	3.8	156	87	72	80	0.6	acylase homolog lmo0493	Biosynthesis
SAV2595		136	270	592	443	2.6	90	93	68	62	0.7	LPXTG-motif cell wall	Other
SAV2596		20	16	243	246	13.6	20	3	30	19	2.1	glutamyl-endopeptidase	Unclassified
SAV2603		275	275	942	945	3.4	287	335	654	470	1.8	amino acid transporter	Amino acids, peptides and amines
SAV2604		214	201	616	774	3.3	89	96	181	76	1.4	aminotransferase	tRNA and rRNA base modification
SAV2630	clfB	8067	8266	2511	2588	0.3	2102	3047	1328	865	0.4	Clumping factor B	Pathogenesis
SAV2632	arcC	323	339	891	889	2.7	136	224	182	145	0.9	carbamate kinase	Energy metabolism
SAV2633	arcD	129	178	747	850	5.2	85	85	114	83	1.2	arginine/oirnithine	Energy metabolism
SAV2634	arcB	48	75	408	449	7.0	36	36	44	56	1.4	ornithine	Energy metabolism
SAV2635	arcA	97	144	527	492	4.2	54	35	58	33	1	arginine deiminase	Energy metabolism
SAV2638	isaB	1977	2476	817	832	0.4	4498	2512	1128	1123	0.3	immunodominant antigen	General
SAV2661		192	142	472	512	2.9	49	41	41	42	0.9	acetyltransferase	Other
SAV2662		9	25	363	418	22.9	59	71	72	46	0.9	capsular polysaccharide	Biosynthesis and degradation of
SAV2663		187	303	685	548	2.5	77	98	92	45	0.8	capsular polysaccharide	Biosynthesis and degradation of
SAV2664		40	69	138	183	2.9	7	24	17	6	0.7	Capsular polysaccharide	Biosynthesis and degradation of
SAV2666	icaA	61	155	281	445	3.3	18	5	7	8	0.7	intercellular adhesion	Pathogenesis
SAV2667		56	134	169	302	2.5	7	23	12	19	1		
SAV2668	icaB	47	104	308	287	3.9	34	36	60	19	1.1	intercellular adhesion	Pathogenesis
SAV2672	hisI	204	124	514	571	3.3	233	206	102	141	0.6	Histidine biosynthesis	Unclassified
SAV2674		266	229	629	729	2.7	232	343	145	100	0.4	phosphoribosylformimino-	Histidine family
SAV2676	hisB	146	216	444	521	2.7	92	143	72	53	0.5	Imidazoleglycerol-	Histidine family
SAV2677		170	203	475	498	2.6	121	171	92	76	0.6	aminotransferase	Other
SAV2678	hisD	140	216	519	457	2.7	137	193	75	83	0.5	histidinol dehydrogenase	Histidine family
SAV2679	hisG	126	182	599	543	3.7	64	102	58	60	0.7	ATP	Histidine family
SAV2680		116	133	425	468	3.6	82	77	60	31	0.6	ATP	Purines, pyrimidines, nucleosides, and
SAV2684		124	155	579	779	4.9	116	116	122	126	1.1	ABC transporter	Transport and binding proteins
SAV2701	vraD	2506	2192	758	1035	0.4	1142	1540	348	263	0.2	vraD protein	Unclassified
SAV2702	vraE	4724	4593	1681	2259	0.4	2526	3263	678	507	0.2	permease	Amino acids, peptides and amines

Table S3 Transcriptome: Mu50 low Spm. Ox. Spm+Ox (Assay I)

Spm (regulated by 1mM Spm, 2h)

For convenience, the processed and normalized signals from the array were subdivided into four categories according to their intensities
•100-500, •• 500-1500, ••• 1500-4500, •••• 4500-50000.

S: 1mM Spm; O: 16ng/µl Ox; SO: 1mM Spm+16ng/µl Ox; N: no treatment
S to N: ratio of signal intensity between S sample and N sample; O to N, SO to N by analogy

Spm 174
Ox 74
Spm+Ox 408 — Spm+Ox in common 172; Spm+Ox only 236

Locus tag	S to N	O to N	OS to N	signal intensity	Locus	Protein name	Functional categories
SAV1438	0.5	0.2	0.2	•	tdcB	threonine dehydratase	Amino acid metabolism, Aspartate family
SAV1439	0.6	0.1	0.3	••	ald1	alanine dehydrogenase	Amino acid metabolism, Branched chain amino aci
SAV0961	0.3	1.2	0.3	•	argG	argininosuccinate synthase	Amino acid metabolism, Urea and arginine metabc
SAV0147	2.8	0.8	3.6	•	-	transcriptional regulator	Amino acid transport and metabolism
SAV1048	0.3	0.8	0.4	••	sspA	serine protease	Amino acid transport and metabolism
SAV1099	4.5	1.6	6.3	•	potA	spermidine/putrescine ABC transporter	Amino acid transport and metabolism
SAV1608	4.9	1.2	4.8	•	-	hypothetical protein SAV1608	Amino acid transport and metabolism
SAV1716	4.7	1.1	3.3	•	-	iron-sulfur cofactor synthesis protein nifZ	Amino acid transport and metabolism
SAV1723	0.3	0.8	0.2	••	-	transaminase	Amino acid transport and metabolism
SAV1724	0.4	0.8	0.3	••	serA	D-3-phosphoglycerate dehydrogenase	Amino acid transport and metabolism
SAV2531	3.5	1.1	5.3	•	-	beta-subunit of L-serine dehydratase	Amino acid transport and metabolism
SAV2603	0.2	0.7	0.1	••	-	amino acid transporter	Amino acid transport and metabolism
SAV0318	4.4	2.0	5.3	•	-	N-acetylmannosamine-6-phosphate 2-epimerase	Carbohydrate transport and metabolism
SAV0331	3.8	2.1	2.9	•	-	hypothetical protein SAV0331	Carbohydrate transport and metabolism
SAV0699	0.5	0.3	0.2	•••	fruB	fructose 1-phosphate kinase	Carbohydrate transport and metabolism
SAV2462	3.4	1.0	1.7	•	-	antibiotic resistance protein	Carbohydrate transport and metabolism
SAV2506	2.6	1.0	3.0	•	gntK	gluconokinase	Carbohydrate transport and metabolism
SAV2532	3.1	1.5	5.0	•	-	regulatory protein pfoR	Carbohydrate transport and metabolism
SAV2642	4.2	1.7	3.6	•	pmi	mannose-6-phosphate isomerase	Carbohydrate transport and metabolism

SAV0287	0.4	0.5	0.1	•	-	DNA segregation ATPase and-like proteins	Cell cycle control, cell division, chromosome partiti
SAV0259	0.4	0.7	0.3	••	scdA	cell wall biosynthesis protein ScdA	Cell division
SAV0327	3.5	0.8	2.5	•	-	lipoate-protein ligase	Coenzyme transport and metabolism
SAV0516	2.2	0.9	3.7	•	folK	2-amino-4-hydroxy-6-hydroxymethyldihydropteridi	Coenzyme transport and metabolism
SAV2306	3.5	0.9	3.8	••	-	hypothetical protein SAV2306	Coenzyme transport and metabolism
SAV1662	3.3	0.6	2.8	•••	folC	folylpolyglutamate synthase	Cofactors, Folates and Pterines
SACOL0025	3.4	1.1	16.1	•	-	hypothetical protein SACOL0025	COG NA
SACOL1046	0.4	0.9	0.2	••••	-	hypothetical protein SACOL1046	COG NA
SACOL1165	0.3	1.1	1.7	•••	-	hypothetical protein SACOL1165	COG NA
SACOL2433	0.3	1.2	0.2	••••	-	hypothetical protein SACOL2433	COG NA
SACOL2568	2.8	1.5	4.3	•	-	hypothetical protein SACOL2568	COG NA
SAV0239	0.2	1.1	0.1	•	-	hypothetical protein SAV0239	COG NA
SAV0387	0.3	1.1	0.2	••••	-	hypothetical protein SAV0387	COG NA
SAV0447	2.3	0.3	3.0	•	-	hypothetical protein SAV0447	COG NA
SAV0682	0.5	0.3	0.2	•••	-	hypothetical protein SAV0682	COG NA
SAV0788	6.9	4.0	49.5	•	-	hypothetical protein SAV0788	COG NA
SAV0793	2.5	1.0	4.1	•	-	hypothetical protein SAV0793	COG NA
SAV0813	0.2	0.9	0.3	••	ssp	extracellular ECM and plasma binding protein	COG NA
SAV0854	0.1	1.1	0.1	••••	-	hypothetical protein SAV0854	COG NA
SAV0858	0.3	1.5	0.2	•••	-	hypothetical protein SAV0858	COG NA
SAV0867	0.3	1.4	0.3	••••	-	hypothetical protein SAV0867	COG NA
SAV1031	0.2	0.4	0.1	•	-	hypothetical protein SAV1031	COG NA
SAV1155	0.2	0.8	0.9	••••	-	hypothetical protein SAV1155	COG NA
SAV1156	0.3	0.5	0.5	•	-	formyl peptide receptor-like 1 inhibitory protein	COG NA
SAV1176	0.3	1.5	0.7	•••	-	hypothetical protein SAV1176	COG NA
SAV1287	0.1	1.3	0.2	••	-	hypothetical protein SAV1287	COG NA
SAV1624	0.3	0.8	0.5	••••	-	hypothetical protein SAV1624	COG NA
SAV1815	3.0	2.6	7.0	•	-	beta-lactamase	COG NA
SAV1939	3.4	4.1	19.0	•	-	hypothetical protein SAV1939	COG NA
SAV2009	2.9	2.1	9.1	•	sec3	enterotoxin typeC3	COG NA
SAV2085	0.3	1.3	0.6	••••	-	hypothetical protein SAV2085	COG NA
SAV2173	0.2	0.6	0.2	••••	-	hypothetical protein SAV2173	COG NA

SAV2252	0.4	1.6	0.3	•••	-	hypothetical protein SAV2252	COG NA
SAV2480	0.3	1.1	0.2	••••	-	hypothetical protein SAV2480	COG NA
SAV2492	0.3	1.2	0.1	•	-	hypothetical protein SAV2492	COG NA
SAV2626	2.8	1.0	3.6	••	-	hypothetical protein SAV2626	COG NA
SAV2638	0.1	0.5	0.3	••••	isaB	immunodominant antigen B	COG NA
SAV2639	0.1	0.6	0.6	••	-	hypothetical protein SAV2639	COG NA
SAV2359	3.1	1.3	9.9	•	-	ABC transporter ATP-binding protein	Defense mechanisms
SAV1297	3.0	0.4	1.2	•	mutL	DNA mismatch repair protein	DNA metabolism, Replication, recombination, and
SAV1895	3.2	1.6	8.0	••	dinB	DNA polymerase IV	DNA metabolism, Replication, recombination, and
SAV0605	0.3	0.5	0.1	••••	adh1	alcohol dehydrogenase	Energy metabolism, Fermentation
SAV2524	0.2	0.6	0.3	••••	ddh	D-lactate dehydrogenase	Energy metabolism, Fermentation
SAV2416	0.3	0.3	0.1	••••	gpmA	phosphoglyceromutase	Energy metabolism, Glycolysis/gluconeogenesis
SAV0021	3.2	0.7	2.1	••	-	hypothetical protein SAV0021	Function unknown
SAV0106	0.3	0.7	0.1	•••	-	myosin-cross-reactive antigen	Function unknown
SAV0181	0.2	0.7	0.1	•••	-	hypothetical protein SAV0181	Function unknown
SAV0282	0.1	0.9	0.2	••••	-	hypothetical protein SAV0282	Function unknown
SAV0370	0.1	1.0	0.3	•	-	hypothetical protein SAV0370	Function unknown
SAV0795	4.9	0.7	27.1	•	-	hypothetical protein SAV0795	Function unknown
SAV1106	0.3	1.0	0.3	•	-	hypothetical protein SAV1106	Function unknown
SAV1214	0.3	1.1	0.5	••••	-	hypothetical protein SAV1214	Function unknown
SAV1609	3.6	1.0	3.8	•	-	hypothetical protein SAV1609	Function unknown
SAV1845	0.2	0.7	0.2	••••	-	hypothetical protein SAV1845	Function unknown
SAV1877	3.2	1.1	3.5	•	-	hypothetical protein SAV1877	Function unknown
SAV1940	2.8	1.9	5.4	•	-	hypothetical protein SAV1940	Function unknown
SAV2021	3.5	0.9	18.9	•	-	hypothetical protein SAV2021	Function unknown
SAV2062	3.1	1.0	3.3	•	-	hypothetical protein SAV2062	Function unknown
SAV2374	3.6	1.7	4.6	•	-	hypothetical protein SAV2374	Function unknown
SAV2474	0.4	2.3	0.2	••	-	hypothetical protein SAV2474	Function unknown
SAV2510	0.3	0.5	0.2	••••	-	hypothetical protein SAV2510	Function unknown
SAV2533	0.1	5.9	0.9	••	-	hypothetical protein SAV2533	Function unknown
SAV2592	0.2	2.2	0.3	•••	-	hypothetical protein SAV2592	Function unknown
SAV2605	0.3	1.1	0.1	•	-	hypothetical protein SAV2605	Function unknown

SAV2687	0.3	1.3	0.2	•	-	hypothetical protein SAV2687	Function unknown
SAV2700	0.3	1.6	0.1	••	-	hypothetical protein SAV2700	Function unknown
SACOL0095	0.2	0.1	0.1	•	spa	immunoglobulin G binding protein A precursor	General function prediction only
SAV0111	0.2	0.1	0.0	••••	spa	immunoglobulin G binding protein A	General function prediction only
SAV0487	3.2	0.7	3.9	•	-	hypothetical protein SAV0487	General function prediction only
SAV0562	0.3	0.7	0.3	•	sdrD	Ser-Asp rich fibrinogen-binding, bone sialoprotein-b	General function prediction only
SAV0563	0.3	0.6	0.6	•	sdrE	Ser-Asp rich fibrinogen-binding, bone sialoprotein-b	General function prediction only
SAV0698	0.4	0.4	0.1	••	-	transcription repressor of fructose operon	General function prediction only
SAV0751	2.3	0.9	3.9	•	-	hypothetical protein SAV0751	General function prediction only
SAV0755	2.4	1.6	3.6	•	-	hypothetical protein SAV0755	General function prediction only
SAV0770	0.4	0.2	0.4	•••	-	hypothetical protein SAV0770	General function prediction only
SAV0779	2.5	0.9	4.1	••	-	carboxyesterase -like protein	General function prediction only
SAV1127	2.5	1.0	3.1	•••	-	hypothetical protein SAV1127	General function prediction only
SAV1307	2.4	1.0	3.1	••	-	GTP-binding proteinase modulator YnbA	General function prediction only
SAV1387	0.1	7.3	0.3	••	-	phosphate ABC transporter permease	General function prediction only
SAV1388	0.0	6.2	0.2	••	-	phosphate ABC transporter	General function prediction only
SAV1560	3.1	0.7	2.3	••	-	hypothetical protein SAV1560	General function prediction only
SAV2521	0.3	1.0	0.3	••	-	hypothetical protein SAV2521	General function prediction only
SAV2522	0.4	1.2	0.3	•	-	hypothetical protein SAV2522	General function prediction only
SAV2689	2.5	1.0	4.9	•	-	hypothetical protein SAV2689	General function prediction only
SAV2701	0.3	1.0	0.1	•••	vraD	ABC transporter ATP-binding protein	General function prediction only
SAV2548	0.3	1.0	0.1	••••	clpL	ATP-dependent Clp proteinase chain	Heat shock proteins, chaperones, and proteases
SAV0114	3.0	0.9	1.5	•	sirB	lipoprotein	Inorganic ion transport and metabolism
SAV0345	2.8	1.5	3.0	•	-	hypothetical protein SAV0345	Inorganic ion transport and metabolism
SAV0735	3.5	1.3	4.9	•	-	ferrichrome ABC transporter ATP-binding protein	Inorganic ion transport and metabolism
SAV1075	3.0	1.6	3.1	•	-	hypothetical protein SAV1075	Inorganic ion transport and metabolism
SAV1386	0.1	7.6	0.4	••	pstB	phosphate transporter ATP-binding protein	Inorganic ion transport and metabolism
SAV1389	0.0	2.5	0.3	•••	-	thioredoxine reductase	Inorganic ion transport and metabolism
SAV1774	2.5	1.5	5.6	•	-	aesenical pump membrane protein	Inorganic ion transport and metabolism
SAV2175	6.3	0.9	12.4	••	htsC	heme transport system permease	Inorganic ion transport and metabolism
SAV2176	5.1	0.9	11.6	•	htsB	heme transport system permease	Inorganic ion transport and metabolism
SAV2177	6.7	0.7	19.9	•	htsA	heme transport system lipoprotein	Inorganic ion transport and metabolism

SAV2347	2.4	1.4	4.4	••	-	divalent cation transport	Inorganic ion transport and metabolism
SAV2627	0.2	2.1	1.5	•	phoB	alkaline phosphatase III	Inorganic ion transport and metabolism
SAV1931	2.7	1.1	4.9	•	-	ABC transporter ATP-binding protein	Inorganic ion transport and metabolism, Cobalt
SAV1933	2.5	1.1	7.0	•	-	ABC transporter ATP-binding protein	Inorganic ion transport and metabolism, Cobalt
SAV0240	0.3	1.0	0.1	••	hmp	flavohemoprotein	Inorganic ion transport and metabolism, Iron
SAV0647	1.9	1.2	3.8	••	fhuA	ferrichrome transport ATP-binding protein	Inorganic ion transport and metabolism, Iron
SAV0648	2.7	1.4	4.2	••	fhuB	ferrichrome transport permease	Inorganic ion transport and metabolism, Iron
SAV0649	2.4	1.4	3.3	•	fhuG	ferrichrome transport permease	Inorganic ion transport and metabolism, Iron
SAV0733	2.1	2.7	4.2	•	-	ferrichrome ABC transporter permease	Inorganic ion transport and metabolism, Iron
SAV1484	3.4	1.5	9.0	••	fer	ferredoxin	Inorganic ion transport and metabolism, Iron
SAV1385	0.2	8.6	0.5	•	-	negative regulator PhoU	Inorganic ion transport and metabolism, Phosphat
SAV1260	2.0	1.1	3.2	••	uppS	UDP pyrophosphate synthase	Lipid transport and metabolism
SAV1606	3.2	1.0	2.9	••	-	acetyl-CoA carboxylase	Lipid transport and metabolism
SAV1607	4.2	0.7	4.1	•	-	acetyl-CoA carboxylase biotin carboxyl carrier prote	Lipid transport and metabolism
SAV2071	2.8	1.1	3.4	••	acpS	4\'-phosphopantetheinyl transferase	Lipid transport and metabolism
SAV2451	0.4	1.0	0.3	•••	-	para-nitrobenzyl esterase chain A	Lipid transport and metabolism
SAV0573	2.4	1.4	3.1	••	proP	proline/betaine transporter-like protein	Osmolarity
SAV2076	2.4	0.9	3.1	•	kdpB	potassium-transporting ATPase subunit B	Osmolarity
SAV2448	0.3	1.4	0.2	•	opuCA	glycine betaine/carnitine/choline ABC transporter	Osmolarity
SAV2613	3.5	1.6	8.9	•	gbsA	glycine betaine aldehyde dehydrogenase	Osmolarity
SAV2615	4.4	1.0	3.6	•	cudT	choline transporter	Osmolarity
SAV1713	0.4	1.2	0.3	•••	tpx	thiol peroxidase	Oxidative response
SAV0828	0.3	1.0	0.1	•••	-	general stress protein	Posttranslational modification, protein turnover, c
SAV1138	2.8	0.8	4.0	••	pheS	phenylalanyl-tRNA synthetase subunit alpha	Protein synthesis, tRNA aminoacylation
SAV1618	2.8	0.8	3.8	•••	alaS	alanyl-tRNA synthetase	Protein synthesis, tRNA aminoacylation
SAV0488	2.8	0.8	3.9	•	-	hypothetical protein SAV0488	Replication, recombination and repair
SAV1324	4.8	0.9	5.5	•	nuc	thermonuclease	Replication, recombination and repair
SAV1444	2.8	1.2	3.3	•	-	hypothetical protein SAV1444	Replication, recombination and repair
SAV1497	2.3	1.5	4.3	••	xerD	site-specific recombinase	Replication, recombination and repair
SAV1703	2.9	1.1	3.3	••	dnaE	DNA polymerase III subunit alpha	Replication, recombination and repair
SAV0657	0.3	2.0	0.8	••	-	hypothetical protein SAV0657	ribosomal structure and biogenesis
SAV0752	0.3	0.9	0.5	••••	-	ribosomal subunit interface protein	ribosomal structure and biogenesis

SAV1228	2.2	0.8	3.4	••	-	fatty acid biosynthesis transcriptional regulator	Secondary metabolites biosynthesis, transport and
SAV0840	0.3	0.9	0.2	••••	csbD	sigmaB-controlled protein	SigmaB operon
SAV2067	2.7	1.0	4.2	•	rsbU	sigmaB regulation protein	SigmaB operon
SAV2182	0.4	0.8	0.3	••••	asp23	alkaline shock protein 23	SigmaB operon
SAV1706	0.3	1.0	0.6	••••	-	hypothetical protein SAV1706	Signal transduction mechanisms
SAV1710	0.2	1.5	0.3	••••	-	universal stress protein family protein	Signal transduction mechanisms
SAV2068	2.2	1.0	3.3	••	-	PemK family protein	Signal transduction mechanisms
SAV0265	2.5	1.9	6.2	••	-	hypothetical protein SAV0265	Sugar metabolism and transport, Sugar specific PT
SAV2377	7.6	1.2	27.5	•	scrA	PTS system, sucrose-specific IIBC component	Sugar metabolism and transport, Sugar specific PT
SAV2641	4.5	2.1	3.6	•	-	fructose phosphotransferase system enzyme fruA-li	Sugar metabolism and transport, Sugar specific PT
SAV0332	3.4	1.8	2.7	•	-	hypothetical protein SAV0332	Transcription
SAV0395	0.4	3.1	0.5	•	-	hypothetical protein SAV0395	Transcription
SAV0533	3.1	0.5	1.3	•	-	hypothetical protein SAV0533	Transcription
SAV0780	2.2	0.7	3.3	••••	-	ribonuclease R	Transcription
SAV1026	0.2	1.3	0.4	•	-	competence transcription factor	Transcription
SAV1098	5.4	1.0	8.3	•	potR	Cro/CI family transcriptional regulator protein	Transcription
SAV1455	3.3	1.2	2.0	•	dinG	ATP-dependent DNA helicase	Transcription
SAV2063	3.3	0.7	2.8	••	-	transcription accessory protein	Transcription
SAV0398	19.5	0.9	19.4	••	tetM	tetracycline resistance protein	Translation, ribosomal structure and biogenesis
SAV2219	2.6	1.8	3.1	••	truA	tRNA pseudouridine synthase A	Translation, ribosomal structure and biogenesis
SAV2463	5.1	1.0	2.1	•	opp-1F	oligopeptide transporter ATPase subunit	Transporters and efflux pumps, ATP-binding casset
SAV2464	4.0	1.1	1.5	•	opp-1D	oligopeptide transporter ATPase subunit	Transporters and efflux pumps, ATP-binding casset
SAV2465	3.0	1.3	1.6	•	opp-1C	oligopeptide transporter permease	Transporters and efflux pumps, ATP-binding casset
SAV0137	2.1	1.1	6.1	•	tet38	transmembrane protein	Transporters and efflux pumps, Secondary transpc
SAV0334	2.5	1.4	4.6	•	mepA	hypothetical protein SAV0334	Transporters and efflux pumps, Secondary transpc
SAV2625	2.7	1.1	3.4	•	-	two-component response regulator	Two component Systems
SAV2502	0.5	0.3	0.5	•	fnbB	fibronectin-binding protein	Virulence factor

Ox (regulated by 16ng/µl Ox, 2h)

For convenience, the processed and normalized signals from the array were subdivided into four categories according to their intensities
•100-500, •• 500-1500, ••• 1500-4500, •••• 4500-50000.

S: 1mM Spm; O: 16ng/µl Ox; SO: 1mM Spm+16ng/µl Ox; N: no treatment
S to N: ratio of signal intensity between S sample and N sample; O to N, SO to N by analogy

Spm 174
Ox 74
Spm+Ox 408 [Spm+Ox in c
Spm+Ox onl

Locus tag	S to N	O to N	OS to N	signal intensity	Locus	Protein name	Functional categories
SAV1438	0.5	0.2	0.2	•	tdcB	threonine dehydratase	Amino acid metabolism, Aspartate family
SAV1439	0.6	0.1	0.3	••	ald1	alanine dehydrogenase	Amino acid metabolism, Branched chain amino aci
SAV0263	0.8	4.9	1.8	••	lrgB	antiholin-like protein LrgB	Autolysis
SAV0262	0.7	6.0	2.7	•	lrgA	murein hydrolase regulator LrgA	Autolysis
SAV0699	0.5	0.3	0.2	•••	fruB	fructose 1-phosphate kinase	Carbohydrate transport and metabolism
SAV0222	0.7	3.3	0.2	••	uhpT	hexose phosphate transport protein	Carbohydrate transport and metabolism
SAV1741	1.6	0.3	0.5	•••	-	DNA translocase stage III sporulation prot-like prote	Cell cycle control, cell division, chromosome partiti
SAV0507	2.1	0.3	1.6	••	-	cell-division initiation protein	Cell cycle control, cell division, chromosome partiti
SAV0287	0.4	0.5	0.1	•	-	DNA segregation ATPase and-like proteins	Cell cycle control, cell division, chromosome partiti
SAV0259	0.4	0.7	0.3	••	scdA	cell wall biosynthesis protein ScdA	Cell division
SAV0798	1.0	0.3	4.0	•	-	hypothetical protein SAV0798	Cell wall/membrane/envelope biogenesis
SAV0292	0.6	0.2	0.1	•	-	hypothetical protein SAV0292	COG NA
SAV0289	0.6	0.3	0.1	•	-	hypothetical protein SAV0289	COG NA
SAV0290	0.7	0.3	0.2	•	-	hypothetical protein SAV0290	COG NA
SAV0291	0.5	0.3	0.2	•	-	hypothetical protein SAV0291	COG NA
SAV0280	0.7	0.3	0.3	•	-	hypothetical protein SAV0280	COG NA
SAV1821	1.9	2.5	4.8	•	-	hypothetical protein SAV1821	COG NA
SAV1108	1.8	2.8	3.4	••	-	hypothetical protein SAV1108	COG NA

SACOL0850	0.7	0.3	1.5	•	-	hypothetical protein SACOL0850	COG NA
SAV0433	1.0	0.3	1.4	•	set15	superantigen-like protein	COG NA
SAV2418	0.5	0.3	1.2	•••	sbi	IgG-binding protein	COG NA
SAV0447	2.3	0.3	3.0	•	-	hypothetical protein SAV0447	COG NA
SAV1031	0.2	0.4	0.1	•	-	hypothetical protein SAV1031	COG NA
SAV0682	0.5	0.3	0.2	•••	-	hypothetical protein SAV0682	COG NA
SAV2009	2.9	2.1	9.1	•	sec3	enterotoxin typeC3	COG NA
SAV1815	3.0	2.6	7.0	•	-	beta-lactamase	COG NA
SAV0788	6.9	4.0	49.5	•	-	hypothetical protein SAV0788	COG NA
SAV1939	3.4	4.1	19.0	•	-	hypothetical protein SAV1939	COG NA
SAV0797	0.7	0.3	3.0	••	-	hypothetical protein SAV0797	COG NA
SAV0148	0.7	0.3	0.3	••	adhE	bifunctional acetaldehyde-CoA/alcohol dehydrogen	Energy metabolism, Fermentation
SAV2416	0.3	0.3	0.1	••••	gpmA	phosphoglyceromutase	Energy metabolism, Glycolysis/gluconeogenesis
SAV0307	0.8	0.2	0.2	•	-	outer membrane protein	Function unknown
SAV0372	0.6	0.3	0.2	••••	-	hypothetical protein SAV0372	Function unknown
SAV0826	1.7	3.0	4.1	•	-	hypothetical protein SAV0826	Function unknown
SAV2608	0.7	3.9	3.8	•	-	hypothetical protein SAV2608	Function unknown
SAV2496	0.9	0.2	0.7	•	-	hypothetical protein SAV2496	Function unknown
SAV1625	0.5	0.3	0.7	••	csbD	sigmaB-controlled gene product	Function unknown
SAV0144	1.2	3.3	1.2	•	-	hypothetical protein SAV0144	Function unknown
SAV2533	0.1	5.9	0.9	••	-	hypothetical protein SAV2533	Function unknown
SAV0320	0.9	0.3	0.8	•••	geh	glycerol ester hydrolase	General function prediction only
SAV0770	0.4	0.2	0.4	•••	-	hypothetical protein SAV0770	General function prediction only
SAV1388	0.0	6.2	0.2	••	-	phosphate ABC transporter	General function prediction only
SAV1387	0.1	7.3	0.3	••	-	phosphate ABC transporter permease	General function prediction only
SAV0698	0.4	0.4	0.1	••	-	transcription repressor of fructose operon	General function prediction only
SAV0111	0.2	0.1	0.0	••••	spa	immunoglobulin G binding protein A	General function prediction only
SACOL0095	0.2	0.1	0.1	•	spa	immunoglobulin G binding protein A precursor	General function prediction only
SAV0522	1.2	3.9	9.0	•	ctsR	transcription repressor of class III stress genes-like p	Heat shock proteins, chaperones, and proteases
SAV1386	0.1	7.6	0.4	••	pstB	phosphate transporter ATP-binding protein	Inorganic ion transport and metabolism
SAV0631	0.5	0.3	0.4	••••	mntC	lipoprotein	Inorganic ion transport and metabolism, Mangane
SAV1105	1.0	3.3	2.0	•	mntH	manganese transport protein MntH	Inorganic ion transport and metabolism, Mangane

SAV1385	0.2	8.6	0.5	•	-	negative regulator PhoU	Inorganic ion transport and metabolism, Phosphat
SAV2240	0.9	0.2	0.6	••••	rplN	50S ribosomal protein L14	Protein synthesis, Ribosomal units
SAV2242	1.1	0.2	0.7	••••	rpmC	50S ribosomal protein L29	Protein synthesis, Ribosomal units
SAV2239	0.7	0.2	0.5	••••	rplX	50S ribosomal protein L24	Protein synthesis, Ribosomal units
SAV2236	0.9	0.2	0.6	••••	rpsH	30S ribosomal protein S8	Protein synthesis, Ribosomal units
SAV2243	1.0	0.3	0.7	••••	rplP	50S ribosomal protein L16	Protein synthesis, Ribosomal units
SAV2238	0.8	0.3	0.6	••••	rplE	50S ribosomal protein L5	Protein synthesis, Ribosomal units
SAV2237	0.9	0.3	0.6	••••	rpsN	30S ribosomal protein S14	Protein synthesis, Ribosomal units
SAV2235	1.3	0.3	0.8	••••	rplF	50S ribosomal protein L6	Protein synthesis, Ribosomal units
SAV2244	1.0	0.3	0.6	••••	rpsC	30S ribosomal protein S3	Protein synthesis, Ribosomal units
SAV2247	0.8	0.3	0.5	••••	rplB	50S ribosomal protein L2	Protein synthesis, Ribosomal units
SAV2232	0.6	0.3	0.4	••••	rpmD	50S ribosomal protein L30	Protein synthesis, Ribosomal units
SAV2249	1.3	0.3	0.7	••••	rplD	50S ribosomal protein L4	Protein synthesis, Ribosomal units
SAV2245	1.0	0.3	0.6	••••	rplV	50S ribosomal protein L22	Protein synthesis, Ribosomal units
SAV2246	0.9	0.3	0.5	••••	rpsS	30S ribosomal protein S19	Protein synthesis, Ribosomal units
SAV2234	0.8	0.3	0.6	••••	rplR	50S ribosomal protein L18	Protein synthesis, Ribosomal units
SAV0815	1.3	0.3	0.7	•	nuc	nuclease	Replication, recombination and repair
SAV1268	0.8	0.2	0.4	••	-	ribosomal protein L7AE family protein	ribosomal structure and biogenesis
SAV0506	1.9	0.3	1.2	••	-	ribosome-associated heat shock protein	ribosomal structure and biogenesis
SA0214	0.7	3.2	0.2	•••	uhpT	sugar phosphate antiporter	Sugar metabolism and transport
SAV0395	0.4	3.1	0.5	•	-	hypothetical protein SAV0395	Transcription
SAV2241	1.1	0.2	0.9	••••	rpsQ	30S ribosomal protein S17	Translation, ribosomal structure and biogenesis
SAV2248	1.4	0.3	0.8	••••	rplW	50S ribosomal protein L23	Translation, ribosomal structure and biogenesis
SAV2502	0.5	0.3	0.5	•	fnbB	fibronectin-binding protein	Virulence factor

Spm Ox in common (regulated by 1mM Spm and 16ng/µl Ox combo treatment, which also can be regulated by Spm or Ox mono-treatment

For convenience, the processed and normalized signals from the array were subdivided into four categories according to their intensities

•100-500, •• 500-1500, ••• 1500-4500, •••• 4500-50000.

S: 1mM Spm; O: 16ng/µl Ox; SO: 1mM Spm+16ng/µl Ox; N: no treatment

S to N: ratio of signal intensity between S sample and N sample; O to N, SO to N by analogy

Spm 174

Ox 74

Spm+Ox 408 — Spm+Ox in c / Spm+Ox onl

Locus tag	S to N	O to N	OS to N	signal intensi	Locus	Protein name	Functional cate
SAV1438	0.5	0.2	0.2	•	tdcB	threonine dehydratase	Amino acid metabolism, Aspartate family
SAV1439	0.6	0.1	0.3	••	ald1	alanine dehydrogenase	Amino acid metabolism, Branched chain amino aci
SAV0961	0.3	1.2	0.3	•	argG	argininosuccinate synthase	Amino acid metabolism, Urea and arginine metabc
SAV1048	0.3	0.8	0.4	••	sspA	serine protease	Amino acid transport and metabolism
SAV2603	0.2	0.7	0.1	••	-	amino acid transporter	Amino acid transport and metabolism
SAV1723	0.3	0.8	0.2	••	-	transaminase	Amino acid transport and metabolism
SAV1716	4.7	1.1	3.3	•	-	iron-sulfur cofactor synthesis protein nifZ	Amino acid transport and metabolism
SAV1608	4.9	1.2	4.8	•	-	hypothetical protein SAV1608	Amino acid transport and metabolism
SAV2531	3.5	1.1	5.3	•	-	beta-subunit of L-serine dehydratase	Amino acid transport and metabolism
SAV1099	4.5	1.6	6.3	•	potA	spermidine/putrescine ABC transporter	Amino acid transport and metabolism
SAV1724	0.4	0.8	0.3	••	serA	D-3-phosphoglycerate dehydrogenase	Amino acid transport and metabolism
SAV0147	2.8	0.8	3.6	•	-	transcriptional regulator	Amino acid transport and metabolism
SAV0263	0.8	4.9	1.8	••	lrgB	antiholin-like protein LrgB	Autolysis
SAV0262	0.7	6.0	2.7	•	lrgA	murein hydrolase regulator LrgA	Autolysis
SAV0331	3.8	2.1	2.9	•	-	hypothetical protein SAV0331	Carbohydrate transport and metabolism
SAV2642	4.2	1.7	3.6	•	pmi	mannose-6-phosphate isomerase	Carbohydrate transport and metabolism
SAV2532	3.1	1.5	5.0	•	-	regulatory protein pfoR	Carbohydrate transport and metabolism
SAV0318	4.4	2.0	5.3	•	-	N-acetylmannosamine-6-phosphate 2-epimerase	Carbohydrate transport and metabolism
SAV2506	2.6	1.0	3.0	•	gntK	gluconokinase	Carbohydrate transport and metabolism
SAV0699	0.5	0.3	0.2	•••	fruB	fructose 1-phosphate kinase	Carbohydrate transport and metabolism
SAV0222	0.7	3.3	0.2	••	uhpT	hexose phosphate transport protein	Carbohydrate transport and metabolism
SAV0287	0.4	0.5	0.1	•	-	DNA segregation ATPase and-like proteins	Cell cycle control, cell division, chromosome partiti

SAV0259	0.4	0.7	0.3	••	scdA	cell wall biosynthesis protein ScdA	Cell division
SAV0798	1.0	0.3	4.0	•	-	hypothetical protein SAV0798	Cell wall/membrane/envelope biogenesis
SAV0327	3.5	0.8	2.5	•	-	lipoate-protein ligase	Coenzyme transport and metabolism
SAV2306	3.5	0.9	3.8	••	-	hypothetical protein SAV2306	Coenzyme transport and metabolism
SAV0516	2.2	0.9	3.7	•	folK	2-amino-4-hydroxy-6-hydroxymethyldihydropteridi	Coenzyme transport and metabolism
SAV1662	3.3	0.6	2.8	•••	folC	folylpolyglutamate synthase	Cofactors, Folates and Pterines
SAV0239	0.2	1.1	0.1	•	-	hypothetical protein SAV0239	COG NA
SAV0854	0.1	1.1	0.1	••••	-	hypothetical protein SAV0854	COG NA
SAV2492	0.3	1.2	0.1	•	-	hypothetical protein SAV2492	COG NA
SAV2173	0.2	0.6	0.2	••••	-	hypothetical protein SAV2173	COG NA
SAV1287	0.1	1.3	0.2	••	-	hypothetical protein SAV1287	COG NA
SAV2480	0.3	1.1	0.2	••••	-	hypothetical protein SAV2480	COG NA
SAV0858	0.3	1.5	0.2	•••	-	hypothetical protein SAV0858	COG NA
SAV0813	0.2	0.9	0.3	••	ssp	extracellular ECM and plasma binding protein	COG NA
SAV0867	0.3	1.4	0.3	••••	-	hypothetical protein SAV0867	COG NA
SAV2638	0.1	0.5	0.3	••••	isaB	immunodominant antigen B	COG NA
SACOL0025	3.4	1.1	16.1	•	-	hypothetical protein SACOL0025	COG NA
SACOL1046	0.4	0.9	0.2	••••	-	hypothetical protein SACOL1046	COG NA
SAV0387	0.3	1.1	0.2	••••	-	hypothetical protein SAV0387	COG NA
SACOL2433	0.3	1.2	0.2	••••	-	hypothetical protein SACOL2433	COG NA
SAV2252	0.4	1.6	0.3	•••	-	hypothetical protein SAV2252	COG NA
SAV2626	2.8	1.0	3.6	••	-	hypothetical protein SAV2626	COG NA
SAV0793	2.5	1.0	4.1	•	-	hypothetical protein SAV0793	COG NA
SACOL2568	2.8	1.5	4.3	•	-	hypothetical protein SACOL2568	COG NA
SAV0292	0.6	0.2	0.1	•	-	hypothetical protein SAV0292	COG NA
SAV0289	0.6	0.3	0.1	•	-	hypothetical protein SAV0289	COG NA
SAV0290	0.7	0.3	0.2	•	-	hypothetical protein SAV0290	COG NA
SAV0291	0.5	0.3	0.2	•	-	hypothetical protein SAV0291	COG NA
SAV0280	0.7	0.3	0.3	•	-	hypothetical protein SAV0280	COG NA
SAV1108	1.8	2.8	3.4	••	-	hypothetical protein SAV1108	COG NA
SAV1821	1.9	2.5	4.8	•	-	hypothetical protein SAV1821	COG NA
SAV0447	2.3	0.3	3.0	•	-	hypothetical protein SAV0447	COG NA

SAV1031	0.2	0.4	0.1	•	-	hypothetical protein SAV1031	COG NA
SAV0682	0.5	0.3	0.2	•••	-	hypothetical protein SAV0682	COG NA
SAV1939	3.4	4.1	19.0	•	-	hypothetical protein SAV1939	COG NA
SAV0788	6.9	4.0	49.5	•	-	hypothetical protein SAV0788	COG NA
SAV1815	3.0	2.6	7.0	•	-	beta-lactamase	COG NA
SAV2009	2.9	2.1	9.1	•	sec3	enterotoxin typeC3	COG NA
SAV0797	0.7	0.3	3.0	••	-	hypothetical protein SAV0797	COG NA
SAV2359	3.1	1.3	9.9	•	-	ABC transporter ATP-binding protein	Defense mechanisms
SAV1895	3.2	1.6	8.0	••	dinB	DNA polymerase IV	DNA metabolism, Replication, recombination, and
SAV2524	0.2	0.6	0.3	••••	ddh	D-lactate dehydrogenase	Energy metabolism, Fermentation
SAV0605	0.3	0.5	0.1	••••	adh1	alcohol dehydrogenase	Energy metabolism, Fermentation
SAV0148	0.7	0.3	0.3	••	adhE	bifunctional acetaldehyde-CoA/alcohol dehydrogen	Energy metabolism, Fermentation
SAV2416	0.3	0.3	0.1	••••	gpmA	phosphoglyceromutase	Energy metabolism, Glycolysis/gluconeogenesis
SAV0021	3.2	0.7	2.1	••	-	hypothetical protein SAV0021	Function unknown
SAV0106	0.3	0.7	0.1	•••	-	myosin-cross-reactive antigen	Function unknown
SAV0181	0.2	0.7	0.1	•••	-	hypothetical protein SAV0181	Function unknown
SAV2700	0.3	1.6	0.1	••	-	hypothetical protein SAV2700	Function unknown
SAV2510	0.3	0.5	0.2	••••	-	hypothetical protein SAV2510	Function unknown
SAV0282	0.1	0.9	0.2	••••	-	hypothetical protein SAV0282	Function unknown
SAV2687	0.3	1.3	0.2	•	-	hypothetical protein SAV2687	Function unknown
SAV1845	0.2	0.7	0.2	••••	-	hypothetical protein SAV1845	Function unknown
SAV1106	0.3	1.0	0.3	•	-	hypothetical protein SAV1106	Function unknown
SAV2592	0.2	2.2	0.3	•••	-	hypothetical protein SAV2592	Function unknown
SAV2605	0.3	1.1	0.1	•	-	hypothetical protein SAV2605	Function unknown
SAV0370	0.1	1.0	0.3	•	-	hypothetical protein SAV0370	Function unknown
SAV2062	3.1	1.0	3.3	•	-	hypothetical protein SAV2062	Function unknown
SAV1877	3.2	1.1	3.5	•	-	hypothetical protein SAV1877	Function unknown
SAV1609	3.6	1.0	3.8	•	-	hypothetical protein SAV1609	Function unknown
SAV2374	3.6	1.7	4.6	•	-	hypothetical protein SAV2374	Function unknown
SAV2021	3.5	0.9	18.9	•	-	hypothetical protein SAV2021	Function unknown
SAV0795	4.9	0.7	27.1	•	-	hypothetical protein SAV0795	Function unknown
SAV2474	0.4	2.3	0.2	••	-	hypothetical protein SAV2474	Function unknown

SAV1940	2.8	1.9	5.4	•	-	hypothetical protein SAV1940	Function unknown
SAV0307	0.8	0.2	0.2	•	-	outer membrane protein	Function unknown
SAV0372	0.6	0.3	0.2	••••	-	hypothetical protein SAV0372	Function unknown
SAV2608	0.7	3.9	3.8	•	-	hypothetical protein SAV2608	Function unknown
SAV0826	1.7	3.0	4.1	•	-	hypothetical protein SAV0826	Function unknown
SAV1560	3.1	0.7	2.3	••	-	hypothetical protein SAV1560	General function prediction only
SAV0562	0.3	0.7	0.3	•	sdrD	Ser-Asp rich fibrinogen-binding, bone sialoprotein-b	General function prediction only
SAV2701	0.3	1.0	0.1	•••	vraD	ABC transporter ATP-binding protein	General function prediction only
SAV0487	3.2	0.7	3.9	•	-	hypothetical protein SAV0487	General function prediction only
SAV2522	0.4	1.2	0.3	•	-	hypothetical protein SAV2522	General function prediction only
SAV2521	0.3	1.0	0.3	••	-	hypothetical protein SAV2521	General function prediction only
SAV1127	2.5	1.0	3.1	•••	-	hypothetical protein SAV1127	General function prediction only
SAV1307	2.4	1.0	3.1	••	-	GTP-binding proteinase modulator YnbA	General function prediction only
SAV0755	2.4	1.6	3.6	•	-	hypothetical protein SAV0755	General function prediction only
SAV0751	2.3	0.9	3.9	•	-	hypothetical protein SAV0751	General function prediction only
SAV0779	2.5	0.9	4.1	••	-	carboxyesterase -like protein	General function prediction only
SAV2689	2.5	1.0	4.9	•	-	hypothetical protein SAV2689	General function prediction only
SAV0770	0.4	0.2	0.4	•••	-	hypothetical protein SAV0770	General function prediction only
SAV1388	0.0	6.2	0.2	••	-	phosphate ABC transporter	General function prediction only
SAV1387	0.1	7.3	0.3	••	-	phosphate ABC transporter permease	General function prediction only
SAV0111	0.2	0.1	0.0	••••	spa	immunoglobulin G binding protein A	General function prediction only
SACOL0095	0.2	0.1	0.1	•	spa	immunoglobulin G binding protein A precursor	General function prediction only
SAV0698	0.4	0.4	0.1	••	-	transcription repressor of fructose operon	General function prediction only
SAV2548	0.3	1.0	0.1	••••	clpL	ATP-dependent Clp proteinase chain	Heat shock proteins, chaperones, and proteases
SAV0522	1.2	3.9	9.0	•	ctsR	transcription repressor of class III stress genes-like p	Heat shock proteins, chaperones, and proteases
SAV1389	0.0	2.5	0.3	•••	-	thioredoxine reductase	Inorganic ion transport and metabolism
SAV1075	3.0	1.6	3.1	•	-	hypothetical protein SAV1075	Inorganic ion transport and metabolism
SAV0735	3.5	1.3	4.9	•	-	ferrichrome ABC transporter ATP-binding protein	Inorganic ion transport and metabolism
SAV2176	5.1	0.9	11.6	•	htsB	heme transport system permease	Inorganic ion transport and metabolism
SAV2175	6.3	0.9	12.4	••	htsC	heme transport system permease	Inorganic ion transport and metabolism
SAV2177	6.7	0.7	19.9	•	htsA	heme transport system lipoprotein	Inorganic ion transport and metabolism
SAV0345	2.8	1.5	3.0	•	-	hypothetical protein SAV0345	Inorganic ion transport and metabolism

SAV2347	2.4	1.4	4.4	••	-	divalent cation transport	Inorganic ion transport and metabolism
SAV1774	2.5	1.5	5.6	•	-	aesenical pump membrane protein	Inorganic ion transport and metabolism
SAV1386	0.1	7.6	0.4	••	pstB	phosphate transporter ATP-binding protein	Inorganic ion transport and metabolism
SAV1931	2.7	1.1	4.9	•	-	ABC transporter ATP-binding protein	Inorganic ion transport and metabolism, Cobalt
SAV1933	2.5	1.1	7.0	•	-	ABC transporter ATP-binding protein	Inorganic ion transport and metabolism, Cobalt
SAV0240	0.3	1.0	0.1	••	hmp	flavohemoprotein	Inorganic ion transport and metabolism, Iron
SAV1484	3.4	1.5	9.0	••	fer	ferredoxin	Inorganic ion transport and metabolism, Iron
SAV0649	2.4	1.4	3.3	•	fhuG	ferrichrome transport permease	Inorganic ion transport and metabolism, Iron
SAV0647	1.9	1.2	3.8	••	fhuA	ferrichrome transport ATP-binding protein	Inorganic ion transport and metabolism, Iron
SAV0733	2.1	2.7	4.2	•	-	ferrichrome ABC transporter permease	Inorganic ion transport and metabolism, Iron
SAV0648	2.7	1.4	4.2	••	fhuB	ferrichrome transport permease	Inorganic ion transport and metabolism, Iron
SAV0631	0.5	0.3	0.4	••••	mntC	lipoprotein	Inorganic ion transport and metabolism, Mangane
SAV1105	1.0	3.3	2.0	•	mntH	manganese transport protein MntH	Inorganic ion transport and metabolism, Mangane
SAV1385	0.2	8.6	0.5	•	-	negative regulator PhoU	Inorganic ion transport and metabolism, Phosphat
SAV1606	3.2	1.0	2.9	••	-	acetyl-CoA carboxylase	Lipid transport and metabolism
SAV1607	4.2	0.7	4.1	•	-	acetyl-CoA carboxylase biotin carboxyl carrier prote	Lipid transport and metabolism
SAV2451	0.4	1.0	0.3	•••	-	para-nitrobenzyl esterase chain A	Lipid transport and metabolism
SAV1260	2.0	1.1	3.2	••	uppS	UDP pyrophosphate synthase	Lipid transport and metabolism
SAV2071	2.8	1.1	3.4	••	acpS	4\'-phosphopantetheinyl transferase	Lipid transport and metabolism
SAV2448	0.3	1.4	0.2	•	opuCA	glycine betaine/carnitine/choline ABC transporter	Osmolarity
SAV2615	4.4	1.0	3.6	•	cudT	choline transporter	Osmolarity
SAV2613	3.5	1.6	8.9	•	gbsA	glycine betaine aldehyde dehydrogenase	Osmolarity
SAV0573	2.4	1.4	3.1	••	proP	proline/betaine transporter-like protein	Osmolarity
SAV2076	2.4	0.9	3.1	•	kdpB	potassium-transporting ATPase subunit B	Osmolarity
SAV1713	0.4	1.2	0.3	•••	tpx	thiol peroxidase	Oxidative response
SAV0828	0.3	1.0	0.1	•••	-	general stress protein	Posttranslational modification, protein turnover, c
SAV1618	2.8	0.8	3.8	•••	alaS	alanyl-tRNA synthetase	Protein synthesis, tRNA aminoacylation
SAV1138	2.8	0.8	4.0	••	pheS	phenylalanyl-tRNA synthetase subunit alpha	Protein synthesis, tRNA aminoacylation
SAV1324	4.8	0.9	5.5	•	nuc	thermonuclease	Replication, recombination and repair
SAV1444	2.8	1.2	3.3	•	-	hypothetical protein SAV1444	Replication, recombination and repair
SAV1703	2.9	1.1	3.3	••	dnaE	DNA polymerase III subunit alpha	Replication, recombination and repair
SAV0488	2.8	0.8	3.9	•	-	hypothetical protein SAV0488	Replication, recombination and repair

SAV1497	2.3	1.5	4.3	••	xerD	site-specific recombinase	Replication, recombination and repair
SAV1228	2.2	0.8	3.4	••	-	fatty acid biosynthesis transcriptional regulator	Secondary metabolites biosynthesis, transport and
SAV0840	0.3	0.9	0.2	••••	csbD	sigmaB-controlled protein	SigmaB operon
SAV2182	0.4	0.8	0.3	••••	asp23	alkaline shock protein 23	SigmaB operon
SAV2067	2.7	1.0	4.2	•	rsbU	sigmaB regulation protein	SigmaB operon
SAV1710	0.2	1.5	0.3	••••	-	universal stress protein family protein	Signal transduction mechanisms
SAV2068	2.2	1.0	3.3	••	-	PemK family protein	Signal transduction mechanisms
SA0214	0.7	3.2	0.2	•••	uhpT	sugar phosphate antiporter	Sugar metabolism and transport
SAV2641	4.5	2.1	3.6	•	-	fructose phosphotransferase system enzyme fruA-li	Sugar metabolism and transport, Sugar specific PT
SAV2377	7.6	1.2	27.5	•	scrA	PTS system, sucrose-specific IIBC component	Sugar metabolism and transport, Sugar specific PT
SAV0265	2.5	1.9	6.2	••	-	hypothetical protein SAV0265	Sugar metabolism and transport, Sugar specific PT
SAV0332	3.4	1.8	2.7	•	-	hypothetical protein SAV0332	Transcription
SAV2063	3.3	0.7	2.8	••	-	transcription accessory protein	Transcription
SAV1098	5.4	1.0	8.3	•	potR	Cro/CI family transcriptional regulator protein	Transcription
SAV0780	2.2	0.7	3.3	••••	-	ribonuclease R	Transcription
SAV0395	0.4	3.1	0.5	•	-	hypothetical protein SAV0395	Transcription
SAV0398	19.5	0.9	19.4	••	tetM	tetracycline resistance protein	Translation, ribosomal structure and biogenesis
SAV2219	2.6	1.8	3.1	••	truA	tRNA pseudouridine synthase A	Translation, ribosomal structure and biogenesis
SAV0334	2.5	1.4	4.6	•	mepA	hypothetical protein SAV0334	Transporters and efflux pumps, Secondary transpc
SAV0137	2.1	1.1	6.1	•	tet38	transmembrane protein	Transporters and efflux pumps, Secondary transpc
SAV2625	2.7	1.1	3.4	•	-	two-component response regulator	Two component Systems
SAV2502	0.5	0.3	0.5	•	fnbB	fibronectin-binding protein	Virulence factor

Spm Ox only (regulated only by 1mM Spm and 16ng/µl Ox combo treatment, but not by Spm or Ox mono-treatment)

For convenience, the processed and normalized signals from the array were subdivided into four categories according to their intensities

•100-500, •• 500-1500, ••• 1500-4500, •••• 4500-50000.

S: 1mM Spm; O: 16ng/µl Ox; SO: 1mM Spm+16ng/µl Ox; N: no treatment

S to N: ratio of signal intensity between S sample and N sample; O to N, SO to N by analogy

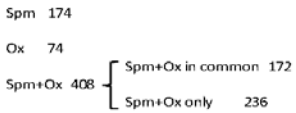

Locus tag	S to N	O to N	OS to N	signal intens	Locus	Protein name	Functional cat
SAV1394	0.6	1.2	0.3	••	asd	aspartate semialdehyde dehydrogenase	Amino acid metabolism, Aspartate family
SAV1393	0.6	1.5	0.3	•	lysC	aspartate kinase	Amino acid metabolism, Aspartate family
SAV1397	0.6	1.6	0.3	••	dapD	tetrahydrodipicolinate acetyltransferase	Amino acid metabolism, Aspartate family
SAV1681	0.8	1.1	0.3	•	lysP	amino-acid permease	Amino acid metabolism, Aspartate family
SAV1396	0.6	1.4	0.3	••	dapB	dihydrodipicolinate reductase	Amino acid metabolism, Aspartate family
SAV1395	0.6	1.5	0.3	••	dapA	dihydrodipicolinate synthase	Amino acid metabolism, Aspartate family
SAV2058	0.5	0.6	0.1	•	leuB	3-isopropylmalate dehydrogenase	Amino acid metabolism, Branched chain amino aci
SAV2057	0.5	0.8	0.1	••	leuA	2-isopropylmalate synthase	Amino acid metabolism, Branched chain amino aci
SAV2059	0.6	0.8	0.1	•	leuC	isopropylmalate isomerase large subunit	Amino acid metabolism, Branched chain amino aci
SAV1310	0.5	1.1	0.2	••••	glnA	glutamine-ammonia ligase	Amino acid metabolism, Glutamate family
SAV2055	0.5	0.6	0.0	•	-	acetolactate synthase 1 regulatory subunit	Amino acid transport and metabolism
SAV2053	0.5	0.4	0.1	•••	ilvD	dihydroxy-acid dehydratase	Amino acid transport and metabolism
SAV2054	0.5	0.6	0.1	••	ilvB	acetolactate synthase large subunit	Amino acid transport and metabolism
SAV2056	0.6	1.0	0.1	••	ilvC	ketol-acid reductoisomerase	Amino acid transport and metabolism
SAV2604	0.4	0.7	0.2	•	-	4-aminobutyrate aminotransferase	Amino acid transport and metabolism
SAV1013	0.4	1.2	0.2	••	-	sodium/proton-dependent alanine carrier protein	Amino acid transport and metabolism
SAV2679	0.5	0.8	0.2	•	hisG	ATP phosphoribosyltransferase catalytic subunit	Amino acid transport and metabolism
SAV0306	0.4	1.0	0.2	•••	-	branched chain amino acid ABC transporter	Amino acid transport and metabolism
SAV2061	0.6	1.2	0.3	•	ilvA	threonine dehydratase	Amino acid transport and metabolism
SAV2680	0.5	0.7	0.3	•	hisZ	ATP phosphoribosyltransferase regulatory subunit	Amino acid transport and metabolism
SAV0186	0.8	1.1	0.3	••	-	branched chain amino acid ABC transporter carrier	Amino acid transport and metabolism
SAV1000	0.6	1.2	0.3	•••	-	thimet oligopeptidase-like protein	Amino acid transport and metabolism

SAV1536	0.8	1.0	0.3	•••	-	glycine dehydrogenase subunit 1	Amino acid transport and metabolism
SAV0829	1.7	1.3	3.0	•	-	3-dehydroquinate dehydratase	Amino acid transport and metabolism
SAV2519	2.3	2.2	10.9	•	-	glyoxylase	Amino acid transport and metabolism
SAV2323	0.7	0.6	0.3	••	glvC	PTS system arbutin-like transporter subunit IIBC	Carbohydrate transport and metabolism
SAV2688	0.6	0.7	0.3	•••	drp35	hypothetical protein SAV2688	Carbohydrate transport and metabolism
SAV2159	0.9	1.3	0.3	••	mtlD	mannitol-1-phosphate 5-dehydrogenase	Carbohydrate transport and metabolism
SAV1507	2.0	1.6	3.4	••	malA	alpha-D-1,4-glucosidase	Carbohydrate transport and metabolism
SAV0824	1.8	0.9	4.0	••	-	phosphoglycerate mutase	Carbohydrate transport and metabolism
SAV1362	2.1	1.4	3.9	••	msrR	peptide methionine sulfoxide reductase regulator	Cell wall stress stimulon
SAV0150	1.3	0.8	0.3	••	capB	capsular polysaccharide synthesis enzyme Cap5B	Cell wall/membrane/envelope biogenesis
SAV0151	1.4	0.8	0.3	••	capC	capsular polysaccharide synthesis enzyme Cap8C	Cell wall/membrane/envelope biogenesis
SAV2185	0.6	1.3	0.2	••••	-	glycine betaine transporter opuD-like protein	Cell wall/membrane/envelope biogenesis
SAV2144	0.8	1.2	0.2	•••	-	hypothetical protein SAV2144	Cell wall/membrane/envelope biogenesis
SAV0149	1.1	1.0	0.2	••	capA	capsular polysaccharide synthesis enzyme Cap5A	Cell wall/membrane/envelope biogenesis
SAV1892	2.0	1.0	3.2	•••	-	UDP-N-acetylmuramyl tripeptide synthetase-like	Cell wall/membrane/envelope biogenesis
SAV2070	2.5	1.2	3.4	••	alr	alanine racemase	Cell wall/membrane/envelope biogenesis
SAV1648	2.0	1.2	3.6	•	-	cell shape determinant mreD	Cell wall/membrane/envelope biogenesis
SAV1649	1.8	1.4	4.3	••	-	rod shape-determining protein MreC	Cell wall/membrane/envelope biogenesis
SAV2360	2.6	1.9	6.6	•	-	ABC transporter permease	Cell wall/membrane/envelope biogenesis
SAV0678	0.5	0.8	0.2	•••	-	hypothetical protein SAV0678	COG NA
SAV0109	0.7	1.2	0.2	••	-	hypothetical protein SAV0109	COG NA
SAV1734	0.5	1.4	0.2	•	acuA	acetoin dehydrogenase-like protein	COG NA
SAV0200	0.9	0.5	0.3	••	-	hypothetical protein SAV0200	COG NA
SAV0823	0.6	0.9	0.3	••••	-	hypothetical protein SAV0823	COG NA
SAV2707	0.6	0.8	0.3	••	-	hypothetical protein SAV2707	COG NA
SAV1752	0.5	0.6	0.3	••••	-	hypothetical protein SAV1752	COG NA
SAV2364	1.0	1.8	0.3	••	-	hypothetical protein SAV2364	COG NA
SAV2184	0.7	1.0	0.3	••••	-	hypothetical protein SAV2184	COG NA
SACOL2002	0.8	0.7	3.0	•	map	map protein, programmed frameshift	COG NA
SAV1938	0.9	0.5	3.0	••	-	hypothetical protein SAV1938	COG NA
SAV0850	0.9	1.1	3.0	•	-	hypothetical protein SAV0850	COG NA
SAV1999	1.3	0.7	3.1	•	-	hypothetical protein SAV1999	COG NA

SAV0799	0.9	0.6	3.2	•	-	hypothetical protein SAV0799	COG NA
SAV0656	1.3	1.3	3.2	•	-	hypothetical protein SAV0656	COG NA
SAV2210	1.9	0.9	3.4	•	-	hypothetical protein SAV2210	COG NA
SAV1206	2.1	0.9	3.8	•	-	hypothetical protein SAV1206	COG NA
SAV1430	2.2	1.2	3.9	••	-	hypothetical protein SAV1430	COG NA
SAV0794	1.6	1.0	3.9	•	-	hypothetical protein SAV0794	COG NA
SAV1158	1.3	0.6	3.9	•••	-	fibrinogen-binding protein	COG NA
SACOL1556	1.9	1.5	4.3	•	-	hypothetical protein SACOL1556	COG NA
SAV2020	1.4	1.5	4.3	•	-	hypothetical protein SAV2020	COG NA
SAV0229	1.6	1.2	4.4	•	-	hypothetical protein SAV0229	COG NA
SAV1157	1.1	0.7	4.4	•	-	hypothetical protein SAV1157	COG NA
SAV1163	1.3	0.5	4.5	••	-	alpha-hemolysin	COG NA
SAV1172	1.5	0.8	4.5	••	-	hypothetical protein SAV1172	COG NA
SACOL1170	1.5	0.6	4.6	•	-	hypothetical protein SACOL1170	COG NA
SAV2151	1.7	1.1	4.7	•	-	hypothetical protein SAV2151	COG NA
SAV1159	1.3	0.4	4.8	•	-	fibrinogen-binding protein	COG NA
SAV2010	0.8	0.4	5.1	•	-	hypothetical protein SAV2010	COG NA
SAV2025	1.2	1.3	6.1	•	-	hypothetical protein SAV2025	COG NA
SAV1805	1.0	1.3	6.2	•	-	transposase	COG NA
SAV1952	1.6	1.1	6.6	•	-	hypothetical protein SAV1952	COG NA
SAV2420	1.9	1.9	7.2	•	hlgC	gamma-hemolysin component C	COG NA
SAV1922	2.1	1.2	7.9	•	-	hypothetical protein SAV1922	COG NA
SAV2421	2.2	2.5	8.5	•	hlgB	gamma-hemolysin component B	COG NA
SACOL0911	2.6	1.2	8.7	•••	-	hypothetical protein SACOL0911	COG NA
SAV0796	1.9	0.4	10.2	•	-	hypothetical protein SAV0796	COG NA
SACOL1372	2.1	1.0	13.0	•	-	hypothetical protein SACOL1372	COG NA
SAV0914	2.7	0.8	13.9	••	-	hypothetical protein SAV0914	COG NA
SAV2514	0.7	0.5	0.2	•••	-	transporter	Defense mechanisms
SAV0309	0.6	1.2	0.3	••	-	ABC transporter ATP-binding protein	Defense mechanisms
SAV1473	0.4	1.1	0.3	••••	hu	DNA-binding protein II	DNA metabolism, Replication, recombination, and
SAV1449	2.0	1.5	3.7	•••	recU	Holliday junction-specific endonuclease	DNA metabolism, Replication, recombination, and
SAV2602	0.4	0.6	0.1	••••	ldhB	L-lactate dehydrogenase	Energy metabolism, Fermentation

SAV0226	0.5	1.1	0.2	••••	pflB	formate acetyltransferase	Energy metabolism, Fermentation
SAV0241	0.6	0.6	0.3	••••	lctE	L-lactate dehydrogenase	Energy metabolism, Fermentation
SAV0227	0.5	1.2	0.3	••••	pflA	formate acetyltransferase activating enzyme	Energy metabolism, Fermentation
SAV0774	0.6	0.9	0.2	••••	tpiA	triosephosphate isomerase	Energy metabolism, Glycolysis/gluconeogenesis
SAV0773	0.7	0.9	0.2	••••	pgk	phosphoglycerate kinase	Energy metabolism, Glycolysis/gluconeogenesis
SAV0772	0.4	1.1	0.3	••••	gap	glyceraldehyde-3-phosphate dehydrogenase	Energy metabolism, Glycolysis/gluconeogenesis
SAV0775	0.7	1.0	0.3	••••	pgm	phosphoglyceromutase	Energy metabolism, Glycolysis/gluconeogenesis
SAV0776	0.5	1.4	0.3	••••	eno	phosphopyruvate hydratase	Energy metabolism, Glycolysis/gluconeogenesis
SAV2606	0.5	0.5	0.3	••••	fda	fructose-1,6-bisphosphate aldolase	Energy metabolism, Glycolysis/gluconeogenesis
SAV1087	0.4	0.6	0.3	•••	cydB	cytochrome D ubiquinol oxidase subunit II-like prot	Energy metabolism, TCA cycle
SAV1086	0.6	0.8	0.3	•••	cydA	cytochrome D ubiquinol oxidase subunit 1-like prot	Energy metabolism, TCA cycle
SAV0305	0.5	0.7	0.1	••	-	formate-nitrite transporter	Energy metabolism,Nitrate/nitrite reduction
SAV2388	0.6	1.1	0.3	••••	narK	nitrite extrusion protein	Energy metabolism,Nitrate/nitrite reduction
SAV2366	0.4	0.5	0.1	••••	-	L-lactate permease lctP-like protein	Energy production and conversion
SAV1058	0.5	1.0	0.3	••••	-	quinol oxidase polypeptide IV QoxD	Energy production and conversion
SAV1059	0.5	1.3	0.3	••••	qoxC	quinol oxidase polypeptide III	Energy production and conversion
SAV0830	2.1	1.1	7.4	•	-	hypothetical protein SAV0830	Energy production and conversion
SAV2562	1.8	1.1	0.3	••	crtM	squalene desaturase	Fatty acid and phospholipid metabolism
SAV2563	1.7	1.0	0.3	••	crtQ	hypothetical protein SAV2563	Fatty acid and phospholipid metabolism
SAV2564	1.7	0.9	0.3	••	crtP	phytoene dehydrogenase	Fatty acid and phospholipid metabolism
SAV2565	1.2	0.7	0.2	•	crtO	hypothetical protein SAV2565	Fatty acid and phospholipid metabolism
SAV2588	0.5	0.9	0.2	••	-	hypothetical protein SAV2588	Function unknown
SAV0310	0.5	1.0	0.3	••	-	regulatory protein PfoR	Function unknown
SAV2453	0.8	1.0	0.3	•••	-	hypothetical protein SAV2453	Function unknown
SAV0374	0.4	1.0	0.2	••••	-	hypothetical protein SAV0374	Function unknown
SAV2515	0.6	0.6	0.2	•••	-	transmembrane protein smpB	Function unknown
SAV2183	0.5	0.7	0.2	••••	-	hypothetical protein SAV2183	Function unknown
SAV1883	1.0	0.7	0.2	•••	-	transporter	Function unknown
SAV2303	0.5	1.4	0.3	••	-	hypothetical protein SAV2303	Function unknown
SAV2140	1.0	0.5	0.3	••	-	hypothetical protein SAV2140	Function unknown
SAV2686	0.5	0.8	0.3	•	-	hypothetical protein SAV2686	Function unknown
SAV2436	0.6	1.2	0.3	••	-	hypothetical protein SAV2436	Function unknown

SAV2658	0.6	1.4	0.2	•••	-	hypothetical protein SAV2658	Function unknown
SAV2590	0.5	0.8	0.2	••	-	hypothetical protein SAV2590	Function unknown
SAV2404	0.8	0.7	0.3	•	-	hypothetical protein SAV2404	Function unknown
SAV0335	1.3	1.2	3.1	•	-	hypothetical protein SAV0335	Function unknown
SAV2691	1.4	1.1	3.2	•	-	hypothetical protein SAV2691	Function unknown
SAV2267	1.2	0.6	3.4	•	-	hypothetical protein SAV2267	Function unknown
SAV0671	1.7	1.1	3.4	•	-	hypothetical protein SAV0671	Function unknown
SAV0654	2.2	1.2	3.4	•••	-	hypothetical protein SAV0654	Function unknown
SAV0454	0.8	1.8	3.4	•	-	hypothetical protein SAV0454	Function unknown
SAV1778	1.3	0.9	3.6	•	-	hypothetical protein SAV1778	Function unknown
SAV1603	2.0	1.9	3.6	•	-	hypothetical protein SAV1603	Function unknown
SAV0593	1.8	0.6	4.0	•	-	hypothetical protein SAV0593	Function unknown
SAV0176	1.2	1.7	4.1	•	-	hypothetical protein SAV0176	Function unknown
SAV0210	1.5	1.2	4.6	•	-	hypothetical protein SAV0210	Function unknown
SAV1932	2.0	1.0	4.7	•	-	hypothetical protein SAV1932	Function unknown
SAV1177	1.8	1.1	4.8	•	-	hypothetical protein SAV1177	Function unknown
SAV0350	2.0	1.1	4.9	•	-	hypothetical protein SAV0350	Function unknown
SAV2449	1.1	1.3	5.9	•	-	hypothetical protein SAV2449	Function unknown
SAV2034	1.8	2.1	6.5	•	-	hypothetical protein SAV2034	Function unknown
SAV1340	2.3	1.3	10.2	•	-	hypothetical protein SAV1340	Function unknown
SAV2026	2.4	0.9	11.8	•	-	hypothetical protein SAV2026	Function unknown
SAV0167	0.5	1.1	0.3	••	aldA	aldehyde dehydrogenase-like protein	General function prediction only
SAV0215	0.7	0.9	0.3	••	-	maltose/maltodextrin transport permease-like prot	General function prediction only
SAV2684	0.4	0.7	0.3	•	-	ABC transporter ATP-binding protein	General function prediction only
SAV2702	0.4	0.9	0.1	•••	vraE	vraE protein	General function prediction only
SAV2581	0.5	1.2	0.1	•••	-	hypothetical protein SAV2581	General function prediction only
SAV2471	0.6	1.2	0.2	•••	-	hypothetical protein SAV2471	General function prediction only
SAV0348	0.4	1.1	0.2	•	-	hypothetical protein SAV0348	General function prediction only
SAV2580	0.8	1.0	0.2	••	-	hypothetical protein SAV2580	General function prediction only
SAV0551	0.8	1.1	0.2	•••	-	chaperone protein HchA	General function prediction only
SAV0703	1.0	0.9	0.2	••	-	oxidoreductase	General function prediction only
SAV2570	0.4	0.6	0.3	••	-	hypothetical protein SAV2570	General function prediction only

SAV2659	0.9	1.0	0.3	••	-	hypothetical protein SAV2659	General function prediction only
SAV1739	0.5	0.8	0.3	••••	-	hypothetical protein SAV1739	General function prediction only
SAV1839	0.6	0.9	0.3	••••	-	hypothetical protein SAV1839	General function prediction only
SAV1755	1.7	1.1	3.0	••	-	NAD(FAD)-utilizing dehydrogenase	General function prediction only
SAV0468	1.4	1.3	3.2	•	-	hypothetical protein SAV0468	General function prediction only
SAV0351	1.8	0.9	3.2	•	-	ABC transporter ATP-binding protein	General function prediction only
SAV1780	1.3	1.2	3.7	•	-	hypothetical protein SAV1780	General function prediction only
SAV1777	1.5	1.9	3.8	•	-	hypothetical protein SAV1777	General function prediction only
SAV0349	1.7	1.3	4.1	•	-	transcriptional regulator	General function prediction only
SAV0595	1.6	1.1	4.2	•	-	hypothetical protein SAV0595	General function prediction only
SAV0086	1.1	1.5	4.4	•	-	hypothetical protein SAV0086	General function prediction only
SAV1051	1.3	1.0	5.1	•	-	ATL autolysin transcription regulator	General function prediction only
SAV2692	1.4	1.3	5.4	•	-	hypothetical protein SAV2692	General function prediction only
SAV0063	1.8	1.9	5.7	•	abcA	hypothetical protein SAV0063	General function prediction only
SAV0450	1.8	1.8	6.0	•	-	cobalamin synthesis protein	General function prediction only
SAV0087	2.6	1.3	6.5	•	-	hypothetical protein SAV0087	General function prediction only
SAV1934	2.3	1.4	8.0	•	-	GntR family transcriptional regulator	General function prediction only
SAV0049	1.7	1.5	9.5	•	-	hypothetical protein SAV0049	General function prediction only
SAV2022	2.0	0.5	11.9	•	-	hypothetical protein SAV2022	General function prediction only
SAV2520	2.2	2.0	21.4	•	-	MarR family transcriptional regulator	General function prediction only
SAV2030	0.8	0.6	3.4	•••	groES	co-chaperonin GroES	Heat shock proteins, chaperones, and proteases
SAV1580	2.2	0.6	4.3	•••	dnaK	molecular chaperone DnaK	Heat shock proteins, chaperones, and proteases
SAV0525	1.5	1.4	4.5	••	clpC	endopeptidase	Heat shock proteins, chaperones, and proteases
SAV1582	1.7	1.0	5.4	••	hrcA	heat-inducible transcriptional repressor	Heat shock proteins, chaperones, and proteases
SAV0524	1.5	2.1	5.7	••	mcsB	ATP:guanido phosphotransferase	Heat shock proteins, chaperones, and proteases
SAV1581	2.5	0.5	6.5	••	grpE	heat shock protein GrpE	Heat shock proteins, chaperones, and proteases
SAV0523	1.4	2.7	7.1	••	mcsA	hypothetical protein SAV0523	Heat shock proteins, chaperones, and proteases
SAV0975	1.8	2.2	8.3	••	clpB	ClpB chaperone-like protein	Heat shock proteins, chaperones, and proteases
SAV2139	1.5	0.7	4.1	•••	dps	general stress protein 20U	Inorganic ion transport and metabolism
SAV2557	1.5	1.8	4.1	•	copA	copper-transporting ATPase	Inorganic ion transport and metabolism, Copper
SAV1038	1.3	0.7	3.3	•	-	ferrichrome ABC transporter	Inorganic ion transport and metabolism, Iron
SAV1498	1.6	1.6	3.5	•••	fur	ferric uptake regulator-like protein	Inorganic ion transport and metabolism, Iron

SAV1861	1.6	1.6	3.6	•••	perR	FUR family transcriptional regulator	Inorganic ion transport and metabolism, Iron
SAV0634	1.3	0.6	3.6	••	mntR	iron dependent repressor	Inorganic ion transport and metabolism, Mangane
SAV2146	1.6	0.9	4.8	•••	czrB	cation-efflux system membrane protein	Inorganic ion transport and metabolism, Zinc
SAV2145	1.7	1.1	5.3	•••	czrA	repressor protein	Inorganic ion transport and metabolism, Zinc
SAV0851	0.7	1.3	4.2	•	-	hypothetical protein SAV0851	Intracellular trafficking, secretion, and vesicular tra
SAV2328	0.4	1.3	0.1	•••	-	dehydrogenase	Lipid transport and metabolism
SAV2472	0.6	1.2	0.2	•••	-	short chain dehydrogenase	Lipid transport and metabolism
SAV0235	0.3	1.1	0.2	•	-	acetyl-CoA/acetoacetyl-CoA transferase	Lipid transport and metabolism
SAV0726	0.7	1.2	0.3	•••	-	multidrug resistance protein	Lipid transport and metabolism
SAV0038	0.9	1.3	3.4	•	-	HMG-CoA synthase	Lipid transport and metabolism
SAV1202	1.0	0.6	0.2	••	pyrAA	carbamoyl phosphate synthase small subunit	Nucleotide transport and metabolism
SAV1203	1.8	0.7	0.3	••	carB	carbamoyl phosphate synthase large subunit	Nucleotide transport and metabolism
SAV1199	0.6	0.7	0.1	••	pyrP	uracil permease	Nucleotide transport and metabolism
SAV1200	0.7	0.7	0.1	••	pyrB	aspartate carbamoyltransferase catalytic subunit	Nucleotide transport and metabolism
SAV1201	0.9	0.7	0.1	•••	pyrC	dihydroorotase	Nucleotide transport and metabolism
SAV2617	0.5	0.4	0.1	•••	nrdD	anaerobic ribonucleoside triphosphate reductase	Nucleotide transport and metabolism
SAV2589	0.5	0.8	0.2	•••	pyrD	dihydroorotate dehydrogenase 2	Nucleotide transport and metabolism
SAV0017	0.5	0.6	0.2	•••	purA	adenylosuccinate synthetase	Nucleotide transport and metabolism
SAV0388	1.1	1.0	0.2	••	xprT	xanthine phosphoribosyltransferase	Nucleotide transport and metabolism
SAV2138	0.4	1.2	0.2	••••	deoD	purine nucleoside phosphorylase	Nucleotide transport and metabolism
SAV0391	0.6	0.7	0.2	••••	guaA	GMP synthase	Nucleotide transport and metabolism
SAV0389	1.2	0.9	0.2	••	pbuX	xanthine permease	Nucleotide transport and metabolism
SAV1068	0.5	0.9	0.3	•	purQ	phosphoribosylformylglycinamidine synthase I	Nucleotide transport and metabolism
SAV1067	0.4	0.7	0.3	•	purS	hypothetical protein SAV1067	Nucleotide transport and metabolism
SAV0732	0.8	1.2	0.3	•••	nrdF	ribonucleotide-diphosphate reductase subunit beta	Nucleotide transport and metabolism
SAV0731	0.9	1.2	0.3	•••	nrdE	ribonucleotide-diphosphate reductase subunit alph	Nucleotide transport and metabolism
SAV0730	0.8	1.0	0.3	•••	nrdI	ribonucleotide reductase stimulatory protein	Nucleotide transport and metabolism
SAV1204	2.6	0.5	0.3	•	pyrF	orotidine 5\'-phosphate decarboxylase	Nucleotide transport and metabolism
SAV1066	0.5	0.5	0.3	•	purC	phosphoribosylaminoimidazole-succinocarboxamid	Nucleotide transport and metabolism
SAV2616	0.6	0.4	0.2	••	nrdG	anaerobic (class III) ribonucleotide reductase small :	Nucleotide transport and metabolism
SAV0136	1.3	1.0	5.3	•	pnp	purine nucleoside phosphorylase	Nucleotide transport and metabolism
SAV2150	1.3	0.9	3.1	•	-	hypothetical protein SAV2150	Replication, recombination and repair

SAV0800	1.0	0.4	3.3	••	-	bacteriophage terminase small subunit	Replication, recombination and repair
SAV1804	1.1	0.5	5.0	•	-	transposase	Replication, recombination and repair
SAV2181	1.9	1.4	3.5	•	-	hypothetical protein SAV2181	Secondary metabolites biosynthesis, transport and
SAV0213	0.7	1.2	0.3	•	msmX	multiple sugar-binding transport ATP-binding prote	Sugar metabolism and transport
SAV2189	1.4	1.0	3.1	•	lacG	6-phospho-beta-galactosidase	Sugar metabolism and transport, Operon lactose
SAV1508	1.6	1.9	3.2	•	malR	maltose operon transcriptional repressor	Sugar metabolism and transport, Operon maltose
SAV0700	0.6	0.7	0.2	••	fruA	fructose specific permease	Sugar metabolism and transport, Sugar specific PT
SAV0189	0.9	0.7	0.3	••••	glcA	PTS enzyme II	Sugar metabolism and transport, Sugar specific PT
SAV1998	1.3	0.7	3.7	•••	-	repressor-like protein	Transcription
SAV0333	1.5	1.6	4.1	•	-	hypothetical protein SAV0333	Transcription
SAV0786	1.4	0.6	6.6	•	-	hypothetical protein SAV0786	Transcription
SAV0342	0.6	1.1	0.3	••	-	ribosomal-protein-serine N-acetyltransferase	Translation, ribosomal structure and biogenesis
SAV2129	1.6	1.2	3.3	••	-	spermine/spermidine acetyltransferase blt	Translation, ribosomal structure and biogenesis
SAV1867	1.8	1.1	4.3	••	-	hypothetical protein SAV1867	Translation, ribosomal structure and biogenesis
SAV0987	0.6	1.1	0.3	•••	-	oligopeptide transport system permease OppC	Transporters and efflux pumps, ATP-binding casset
SAV0986	0.5	1.1	0.3	••	oppB	oligopeptide transport system permease	Transporters and efflux pumps, ATP-binding casset
SAV1321	1.8	1.2	3.2	•	-	two-component sensor histidine kinase	Two component Systems
SAV2457	0.7	0.9	5.0	•	-	hypothetical protein SAV2457	Virulence factor
SAV2456	0.9	1.0	6.0	••	-	hypothetical protein SAV2456	Virulence factor
SAV0425	2.0	1.2	7.0	•	set10	superantigen-like protein 5	Virulence factor
SAV2408	1.4	1.2	7.6	•	-	hypothetical protein SAV2408	Virulence factor
SAV2407	1.9	1.3	9.2	•	-	hypothetical protein SAV2407	Virulence factor

Table S4 Transcriptome: Mu50 high Spm (Assay II)

regulated by 10mM Spm (15min,60min), belong to σB regulon

if in σB regulon, negatively(-) or positively(+) controlled by σB	changing trend by high Spm (yellow-up, green-down)	Locus tag	15' Spm to N	60' Spm to N	sigmal intensity	Locus	Protein name	For convenience, the processed and normalized signals from the array were subdivided into four categories according to their intensities •100-500, •• 500-1500, ••• 1500-4500, •••• 4500-50000. 15'Spm: 10mM Spm for 15min; 60'Spm: 10mM Spm for 15min; N: no treatment 15'Spm to N: ratio of signal intensity between 15'Spm sample and N sample; 60'Spm, by analogy	Function
σB -		SAV1048	0.7	2.9	•	sspA	serine protease		Amino acid transport and metabolism
σB -		SAV0268	0.4	0.7	••	rbsK	ribokinase		Carbohydrate transport and metabolism
σB -		SAV0824	5.9	10.0	•	-	phosphoglycerate mutase		Carbohydrate transport and metabolism
σB -		SAV1046	1.4	3.3	•	sspC	cysteine protease		COG NA
σB -		SAV1163	4.9	8.9	•	hla	alpha-hemolysin		vitulece factor
σB -		SAV2421	1.8	3.2	•	hlgB	gamma-hemolysin component B		vitulece factor
σB -		SAV1114	0.7	0.4	•••	pycA	pyruvate carboxylase		Energy metabolism, Glycolysis/gluconeogenesis
σB -		SAV2618	3.0	2.7	•	citM	magnesium citrate secondary		Energy production and conversion
σB -		SAV0307	0.4	0.2	•	-	outer membrane protein		Function unknown
σB -		SAV1911	2.0	2.6	••	-	hypothetical protein SAV1911		Function unknown
σB -		SAV0383	1.5	3.1	••	-	proton/sodium-glutamate symport		General function prediction only
σB -		SAV0710	3.1	3.4	••	-	coenzyme PQQ synthesis-like protein		General function prediction only
σB -		SAV0712	2.1	2.8	••	-	aluminum resistance protein		General function prediction only
σB +		SAV2334	0.4	0.3	•••	hutG	formimidoylglutamase		Amino acid transport and metabolism
σB +		SAV2539	0.4	0.3	•••	cidC	pyruvate oxidase		Autolysis
σB +		SAV2540	0.3	0.3	•••	cidB	hypothetical protein SAV2540		Autolysis
σB +		SAV1854	0.4	0.4	•••	-	hypothetical protein SAV1854		Carbohydrate transport and metabolism
σB +		SAV2159	0.2	0.4	••	mtlD	mannitol-1-phosphate 5-		Carbohydrate transport and metabolism
σB +		SAV2688	0.3	0.1	•••	drp35	hypothetical protein SAV2688		Carbohydrate transport and metabolism
σB +		SAV0149	0.4	0.3	••	capA	capsular polysaccharide synthesis		Cell wall/membrane/envelope biogenesis
σB +		SAV0150	0.5	0.4	••	capB	capsular polysaccharide synthesis		Cell wall/membrane/envelope biogenesis
σB +		SAV0151	0.5	0.4	••	capC	capsular polysaccharide synthesis		Cell wall/membrane/envelope biogenesis
σB +		SAV0152	0.5	0.4	••	capD	capsular polysaccharide synthesis		Cell wall/membrane/envelope biogenesis
σB +		SAV0153	0.3	0.3	••	capE	capsular polysaccharide synthesis		Cell wall/membrane/envelope biogenesis
σB +		SAV0154	0.4	0.4	••	capF	capsular polysaccharide synthesis		Cell wall/membrane/envelope biogenesis
σB +		SAV0155	0.3	0.4	•	capG	capsular polysaccharide synthesis		Cell wall/membrane/envelope biogenesis
σB +		SAV0156	0.3	0.4	•	capH	capsular polysaccharide synthesis		Cell wall/membrane/envelope biogenesis
σB +		SAV0157	0.4	0.5	•	capI	capsular polysaccharide synthesis		Cell wall/membrane/envelope biogenesis
σB +		SAV0704	0.2	0.2	••	-	CsbB stress response protein		Cell wall/membrane/envelope biogenesis
σB +		SAV2144	0.3	0.2	••	-	hypothetical protein SAV2144		Cell wall/membrane/envelope biogenesis
σB +		SAV2185	0.2	0.1	•••	opuD	glycine betaine transporter opuD-like		Cell wall/membrane/envelope biogenesis
σB +		SAV0678	0.3	0.2	•••	-	hypothetical protein SAV0678		COG NA

σB +		SAV0682	0.3	0.2 ••••	-	hypothetical protein SAV0682	COG NA
σB +		SAV0823	0.2	0.1 •••	-	hypothetical protein SAV0823	COG NA
σB +		SAV1082	0.3	0.2 •••	-	hypothetical protein SAV1082	COG NA
σB +		SAV1624	0.3	0.2 ••••	-	hypothetical protein SAV1624	COG NA
σB +		SAV1752	0.5	0.4 ••••	-	hypothetical protein SAV1752	COG NA
σB +		SAV1816	2.7	5.3 •	-	hypothetical protein SAV1816	COG NA
σB +		SAV2184	0.3	0.1 ••••	-	hypothetical protein SAV2184	COG NA
σB +		SAV2480	0.6	0.2 ••••	-	hypothetical protein SAV2480	COG NA
σB +		SAV2606	0.3	0.4 •••	fda	fructose-1	Energy metabolism, Glycolysis/gluconeogenesis
σB +		SAV2554	0.3	0.2 •••	rocA	1-pyrroline-5-carboxylate	Energy production and conversion
σB +		SAV2561	0.4	0.2 •••	crtN	squalene synthase	Fatty acid and phospholipid metabolism
σB +		SAV2562	0.3	0.2 ••	crtM	squalene desaturase	Fatty acid and phospholipid metabolism
σB +		SAV2563	0.3	0.1 •••	crtQ	hypothetical protein SAV2563	Fatty acid and phospholipid metabolism
σB +		SAV2564	0.3	0.1 •••	crtP	phytoene dehydrogenase	Fatty acid and phospholipid metabolism
σB +		SAV2565	0.4	0.1 ••	crtO	hypothetical protein SAV2565	Fatty acid and phospholipid metabolism
σB +		SAV0681	0.5	0.4 •••	-	hypothetical protein SAV0681	Function unknown
σB +		SAV1214	0.5	0.4 •••	-	hypothetical protein SAV1214	Function unknown
σB +		SAV1625	0.3	0.2 •••	csbD	sigmaB-controlled gene product	Function unknown
σB +		SAV1883	0.2	0.2 •••	-	transporter	Function unknown
σB +		SAV2183	0.3	0.1 ••••	-	hypothetical protein SAV2183	Function unknown
σB +		SAV2453	0.4	0.3 •••	-	hypothetical protein SAV2453	Function unknown
σB +		SAV2474	0.3	0.2 •	-	hypothetical protein SAV2474	Function unknown
σB +		SAV2588	0.3	0.3 ••	-	hypothetical protein SAV2588	Function unknown
σB +		SAV2658	0.3	0.2 ••	-	hypothetical protein SAV2658	Function unknown
σB +		SAV2700	0.5	0.3 •	-	hypothetical protein SAV2700	Function unknown
σB +		SAV0615	0.2	0.1 •••	-	esterase/lipase	General function prediction only
σB +		SAV0621	0.4	0.4 •	-	monovalent cation/H+ antiporter	General function prediction only
σB +		SAV0625	0.4	0.4 ••	-	monovalent cation/H+ antiporter	General function prediction only
σB +		SAV0703	0.1	0.1 ••	-	oxidoreductase	General function prediction only
σB +		SAV0769	0.3	0.2 •••	-	hypothetical protein SAV0769	General function prediction only
σB +		SAV0810	1.5	2.5 ••	-	hypothetical protein SAV0810	General function prediction only
σB +		SAV0920	0.3	0.5 ••••	-	2-nitropropane dioxygenase	General function prediction only
σB +		SAV1739	0.5	0.4 ••••	-	hypothetical protein SAV1739	General function prediction only
σB +		SAV1839	0.4	0.3 •••	-	hypothetical protein SAV1839	General function prediction only
σB +		SAV2207	1.7	3.1 •	alsS	acetolactate synthase	General function prediction only
σB +		SAV2309	0.6	0.4 •••	-	formate dehydrogenase-like protein	General function prediction only
σB +		SAV2478	1.1	0.3 ••	-	oxidoreductase	General function prediction only
σB +		SAV2509	0.4	0.2 ••	-	hypothetical protein SAV2509	General function prediction only
σB +		SAV2521	0.3	0.2 ••	-	hypothetical protein SAV2521	General function prediction only
σB +		SAV2580	0.3	0.3 ••	-	hypothetical protein SAV2580	General function prediction only
σB +		SAV2581	0.2	0.2 •••	-	hypothetical protein SAV2581	General function prediction only
σB +		SAV2659	0.4	0.3 •	-	hypothetical protein SAV2659	General function prediction only
σB +		SAV2689	4.0	6.6 •	-	hypothetical protein SAV2689	General function prediction only

σB +		SAV2548	0.2	0.1 ●●●	clpL	ATP-dependent Clp proteinase chain	Heat shock proteins, chaperones, and proteases
σB +		SAV0919	0.4	0.5 ●●●	-	hypothetical protein SAV0919	Inorganic ion transport and metabolism
σB +		SAV2694	0.6	0.4 ●●	-	2-oxoglutarate/malate translocator	Inorganic ion transport and metabolism
σB +		SAV0726	0.4	0.2 ●●●	-	multidrug resistance protein	Lipid transport and metabolism
σB +		SAV2328	0.2	0.2 ●●●	-	dehydrogenase	Lipid transport and metabolism
σB +		SAV2451	0.4	0.4 ●●	-	para-nitrobenzyl esterase chain A	Lipid transport and metabolism
σB +		SAV2472	0.2	0.1 ●●●	-	short chain dehydrogenase	Lipid transport and metabolism
σB +		SAV1203	2.5	6.5 ●●	carB	carbamoyl phosphate synthase large	Nucleotide transport and metabolism
σB +		SAV0828	0.4	0.4 ●●	-	general stress protein	Posttranslational modification, protein turnover, chaperones
σB +		SAV0112	0.5	0.3 ●●●	sarH1	accessory regulator A-like protein	Regulators
σB +		SAV2212	2.0	2.9 ●	-	hypothetical protein SAV2212	Replication, recombination and repair
σB +		SAV0840	0.4	0.2 ●●●●	csbD-like	sigmaB-controlled protein	SigmaB operon
σB +		SAV2182	0.4	0.2 ●●●●	asp23	alkaline shock protein 23	SigmaB operon
σB +		SAV1881	0.4	0.2 ●●●	-	protein-tyrosine phosphatase	Signal transduction mechanisms
σB +		SAV2158	0.2	0.2 ●●	mtlA	PTS system mannitol specific	Sugar metabolism and transport, Sugar specific PTS
σB +		SAV2157	0.2	0.3 ●●●	-	hypothetical protein SAV2157	Transcription
σB +		SAV0679	0.6	0.4 ●●	-	hypothetical protein SAV0679	Translation, ribosomal structure and biogenesis

up-regulated by 10mM Spm (15min, 60min), excluding those σB regulon genes

changing trend by high Spm (yellow-up)	Locus tag	15' Spm to N	60' Spm to N	sigmal intensity	Locus	Protein name	Function
	SAV1330	1.7	2.8	•	thrB	homoserine kinase	Amino acid metabolism, threonine
	SAV0012	4.3	5.3	•	-	homoserine-o-acetyltransferase	Amino acid metabolism, Aspartate family
	SAV0459	1.2	3.3	••	cysM	cysteine synthase-like protein	Amino acid metabolism, Cysteine and methionine metabolism
	SAV0460	1.5	3.0	••	yrhB	cystathionine gamma-synthase	Amino acid metabolism, Cysteine and methionine metabolism
	SAV2530	2.8	6.0	••	-	L-serine dehydratase	Amino acid metabolism, Cysteine and methionine metabolism
	SAV0472	3.2	5.1	•	gltB	glutamate synthase large subunit	Amino acid metabolism, Glutamate family
	SAV0473	3.4	5.4	•	gltD	glutamate synthase subunit beta	Amino acid metabolism, Glutamate family
	SAV0184	1.8	4.3	•	argC	N-acetyl-gamma-glutamyl-phosphate	Amino acid metabolism, Urea and arginine metabolism
	SAV0183	2.1	4.9	•	argJ	bifunctional ornithine	Amino acid metabolism, Urea and arginine metabolism
	SAV0185	2.0	6.7	•	rocD1	ornithine aminotransferase	Amino acid metabolism, Urea and arginine metabolism
	SAV1170	2.3	2.8	•	arcC1	carbamate kinase	Amino acid metabolism, Urea and arginine metabolism
	SAV2632	2.1	3.7	•	arcC2	carbamate kinase	Amino acid metabolism, Urea and arginine metabolism
	SAV0182	3.1	5.7	•	argB	hypothetical protein SAV0182	Amino acid metabolism, Urea and arginine metabolism
	SAV2290	1.6	3.3	•	ureC	urease subunit alpha	Amino acid metabolism, Urea and arginine metabolism
	SAV0960	1.0	2.8	•	argH	argininosuccinate lyase	Amino acid metabolism, Urea and arginine metabolism
	SAV2293	1.5	2.6	•	ureG	urease accessory protein UreG	Amino acid metabolism, Urea and arginine metabolism
	SAV2294	1.4	3.1	•	ureD	urease accessory protein UreD	Amino acid metabolism, Urea and arginine metabolism
	SAV1373	1.9	3.4	•	trpA	tryptophan synthase subunit alpha	Amino acid metabolism,tryptophan
	SAV2345	2.6	2.4	••	-	sodium/glutamate symporter	Amino acid transport
	SAV1099	4.7	6.1	••	potA	spermidine/putrescine ABC transporter	Amino acid transport
	SAV1100	5.5	6.5	•	potB	spermidine/putrescine ABC transporter	Amino acid transport
	SAV1101	4.9	6.2	•	potC	spermidine/putrescine ABC transporter	Amino acid transport
	SAV1102	2.9	2.9	•••	potD	spermidine/putrescine-binding protein -	Amino acid transport
	SAV1379	2.0	3.4	•	-	oligopeptide transporter ATPase	Amino acid transport
	SAV1380	4.6	12.7	•	-	oligopeptide transport ATPase	Amino acid transport
	SAV1381	2.7	7.5	•	-	oligopeptide transporter permease	Amino acid transport
	SAV1382	5.2	12.1	•	-	oligopeptide transporter permease	Amino acid transport
	SAV0147	1.5	2.7	•	-	transcriptional regulator	Amino acid transport and metabolism
	SAV2440	3.3	3.0	•	-	hypothetical protein SAV2440	Amino acid transport and metabolism
	SAV2531	3.9	8.4	•	-	beta-subunit of L-serine dehydratase	Amino acid transport and metabolism
	SAV1857	1.4	2.8	•	-	glutamate ABC transporter ATP-binding	Amino acid transport and metabolism
	SAV1858	1.6	3.1	•	-	glutamine-binding periplasmic protein	Amino acid transport and metabolism
	SAV2450	4.6	11.9	•	-	amino acid transporter	Amino acid transport and metabolism
	SAV1247	1.6	3.1	•	lytN	LytN protein	Cell wall/membrane biogenesis

	SAV0742	2.0	3.0 ••	-	glycerate kinase	Carbohydrate transport and metabolism
	SAV0122	1.5	2.7 •	-	hypothetical protein SAV0122	Carbohydrate transport and metabolism
	SAV0274	1.7	2.5 •	-	transmembrane efflux pump protein	Carbohydrate transport and metabolism
	SAV1050	3.8	7.2 •	-	hypothetical protein SAV1050	Carbohydrate transport and metabolism
	SAV2166	2.2	3.6 ••	-	multidrug resistance protein	Carbohydrate transport and metabolism
	SAV2532	3.8	10.0 •	-	regulatory protein pfoR	Carbohydrate transport and metabolism
	SAV0007	3.0	5.9 •	-	hypothetical protein SAV0007	Carbohydrate transport and metabolism
	SAV1761	1.9	2.8 ••	-	multidrug resistance protein	Carbohydrate transport and metabolism
	SAV2711	2.5	2.3 •••	gidA	tRNA uridine 5-	Cell cycle control, cell division, chromosome partitioning
	SAV0747	2.0	2.9 •	tagO	lipophilic protein affecting lysis rate and	Cell wall/membrane biogenesis
	SAV1248	2.1	4.5 •	fmhC	FmhC protein	Cell wall/membrane biogenesis
	SAV2411	2.1	4.2 •	fmhA	fmhA protein	Cell wall/membrane biogenesis
	SAV0642	2.7	3.6 ••	pbp4	penicillin binding protein 4	Cell wall/membrane biogenesis
	SAV0658	2.0	2.8 ••	-	hypothetical protein SAV0658	Cell wall/membrane/envelope biogenesis
	SAV0798	1.3	2.5 •	-	hypothetical protein SAV0798	Cell wall/membrane/envelope biogenesis
	SAV2032	2.5	1.8 •••	-	hypothetical protein SAV2032	Cell wall/membrane/envelope biogenesis
	SAV2423	2.6	2.6 •	-	6-carboxyhexanoate--CoA ligase	Coenzyme transport and metabolism
	SAV0516	2.9	3.2 ••	folK	2-amino-4-hydroxy-6-	Coenzyme transport and metabolism
	SAV2599	1.8	2.9 •••	panB	3-methyl-2-oxobutanoate	Cofactors and Vitamins, Pantothenate and CoA
	SAV1125	2.2	2.8 •	coaD	phosphopantetheine	Cofactors and Vitamins, Pantothenate and CoA
	SAV2071	1.9	2.6 ••	acpS	4\'-phosphopantetheinyl transferase	Cofactors and Vitamins, Pantothenate and CoA
	SAV2597	2.1	2.7 ••	panD	aspartate alpha-decarboxylase	Cofactors and Vitamins, Pantothenate and CoA
	SAV1716	1.8	2.9 ••	-	iron-sulfur cofactor synthesis protein	Cofactors and Vitamins, Thiamine
	SAV1770	1.8	3.8 ••	ribB	riboflavin synthase subunit alpha	Cofactors, Riboflavin, FMN, and FAD
	SAV1767	1.9	3.6 •	ribH	6	Cofactors, Riboflavin, FMN, and FAD
	SAV1769	1.7	2.6 ••	ribA	riboflavin biosynthesis protein	Cofactors, Riboflavin, FMN, and FAD
	SACOL0025	10.3	24.5 •	-	hypothetical protein SACOL0025	COG NA
	SACOL0919	2.5	4.8 •	-	hypothetical protein SACOL0919	COG NA
	SACOL1165	3.3	3.1 ••	-	hypothetical protein SACOL1165	COG NA
	SACOL1186	2.3	3.4 •	-	anti protein (phenol soluble modulin)	COG NA
	SACOL1187	2.2	3.6 •	-	anti protein (phenol soluble modulin)	COG NA
	SACOL1379	2.2	3.1 •	-	hypothetical protein SACOL1379	COG NA
	SACOL1953	3.6	3.2 •	-	hypothetical protein SACOL1953	COG NA
	SACOL1972	1.8	2.8 ••	-	hypothetical protein SACOL1972	COG NA
	SACOL2002	3.0	3.5 •	map	map protein	COG NA
	SACOL2331	2.5	2.0 •	-	hypothetical protein SACOL2331	COG NA
	SACOL2492	2.6	3.8 •	-	hypothetical protein SACOL2492	COG NA
	SAV0146	3.0	5.0 •	-	hypothetical protein SAV0146	COG NA
	SAV0273	3.0	8.1 •	-	hypothetical protein SAV0273	COG NA
	SAV0373	2.3	2.6 •	-	hypothetical protein SAV0373	COG NA
	SAV0377	2.5	3.3 •	-	hypothetical protein SAV0377	COG NA
	SAV0429	2.2	4.3 •	set14	superantigen-like protein	virurence factor
	SAV0656	3.0	4.4 •	-	hypothetical protein SAV0656	COG NA

	SAV0692	2.1	4.2 •	-	hypothetical protein SAV0692	COG NA
	SAV0709	3.5	4.1 •	-	hypothetical protein SAV0709	COG NA
	SAV0739	2.8	5.3 •	-	hypothetical protein SAV0739	COG NA
	SAV0788	1.9	5.6 •	-	hypothetical protein SAV0788	COG NA
	SAV0793	1.5	4.5 •	-	hypothetical protein SAV0793	COG NA
	SAV0794	2.2	4.2 •	-	hypothetical protein SAV0794	COG NA
	SAV0799	2.0	3.0 •	-	hypothetical protein SAV0799	COG NA
	SAV0927	1.8	2.8 •	-	hypothetical protein SAV0927	COG NA
	SAV1157	4.0	4.5 •	-	hypothetical protein SAV1157	COG NA
	SAV1172	2.6	4.3 •	-	hypothetical protein SAV1172	COG NA
	SAV1206	3.7	6.2 •	-	hypothetical protein SAV1206	COG NA
	SAV1448	1.5	2.6 •	-	hypothetical protein SAV1448	COG NA
	SAV1501	1.8	2.7 •	-	hypothetical protein SAV1501	COG NA
	SAV1691	2.2	3.6 •	-	hypothetical protein SAV1691	COG NA
	SAV1776	2.0	3.3 •	-	hypothetical protein SAV1776	COG NA
	SAV1815	5.6	9.5 •	-	beta-lactamase	COG NA
	SAV1840	2.2	4.3 •	-	hypothetical protein SAV1840	COG NA
	SAV1896	2.6	1.7 ••	-	hypothetical protein SAV1896	COG NA
	SAV1939	5.7	3.8 •	-	hypothetical protein SAV1939	COG NA
	SAV1952	2.0	4.4 •	-	hypothetical protein SAV1952	COG NA
	SAV1992	3.0	7.8 •	-	hypothetical protein SAV1992	COG NA
	SAV2020	3.0	4.9 •	-	hypothetical protein SAV2020	COG NA
	SAV2086	1.8	2.6 ••	-	hypothetical protein SAV2086	COG NA
	SAV2095	2.1	4.0 ••	-	SceD	COG NA
	SAV2131	1.9	2.6 ••	-	hypothetical protein SAV2131	COG NA
	SAV2167	2.1	2.9 •	-	hypothetical protein SAV2167	COG NA
	SAV2168	2.3	2.5 •	-	multidrug transporter	COG NA
	SAV2430	1.5	4.6 •	-	hypothetical protein SAV2430	COG NA
	SAV2572	1.3	2.8 •	-	hypothetical protein SAV2572	COG NA
	SAV2639	1.0	3.3 •	-	hypothetical protein SAV2639	COG NA
	SACOL0066	2.5	2.5 •	-	hypothetical protein SACOL0066	COG NA
	SACOL0911	3.1	4.1 ••	-	hypothetical protein SACOL0911	COG NA
	SAV0393	4.3	7.7 •	-	hypothetical protein SAV0393	COG NA
	SAV0416	1.2	3.9 •	-	hypothetical protein SAV0416	COG NA
	SAV0741	1.9	2.8 ••	-	hypothetical protein SAV0741	COG NA
	SAV0796	1.3	2.9 ••	-	hypothetical protein SAV0796	COG NA
	SAV0914	1.3	8.7 ••	-	hypothetical protein SAV0914	COG NA
	SAV1805	4.0	14.5 •	-	transposase	COG NA
	SAV1922	3.1	6.3 •	-	hypothetical protein SAV1922	COG NA
	SAV2151	2.2	3.3 •	-	hypothetical protein SAV2151	COG NA
	SAV2359	3.7	5.8 •	-	ABC transporter ATP-binding protein	Defense mechanisms
	SAV1146	1.5	2.5 ••	uvrC	excinuclease ABC subunit C	DNA metabolism, Replication, recombination, and repair
	SAV1249	2.5	3.4 •	-	DNA processing Smf protein	DNA metabolism, Replication, recombination, and repair

	SAV1324	3.1	5.2	•	nuc	thermonuclease	DNA metabolism, Replication, recombination, and repair
	SAV1354	2.0	2.5	•••	parE	DNA topoisomerase IV subunit B	DNA metabolism, Replication, recombination, and repair
	SAV1444	1.5	2.7	••	-	hypothetical protein SAV1444	DNA metabolism, Replication, recombination, and repair
	SAV1497	4.6	6.8	••	xerD	site-specific recombinase	DNA metabolism, Replication, recombination, and repair
	SAV1587	2.8	3.5	•	holA	DNA polymerase III subunit delta	DNA metabolism, Replication, recombination, and repair
	SAV1590	2.4	2.8	•	-	competence protein ComEA	DNA metabolism, Replication, recombination, and repair
	SAV1868	2.2	2.9	•	-	A/G-specific adenine glycosylase	DNA metabolism, Replication, recombination, and repair
	SAV1895	4.3	2.9	••	dinB	DNA polymerase IV	DNA metabolism, Replication, recombination, and repair
	SAV0323	2.2	2.8	••	-	luciferase family protein	Energy metabolism
	SAV0177	2.2	4.5	•	fdh	formate dehydrogenase	Energy metabolism,Nitrate/nitrite reduction
	SAV0684	2.5	2.0	••	-	hypothetical protein SAV0684	Energy production and conversion
	SAV1721	3.1	5.5	•	-	glycerophosphoryl diester	Energy production and conversion
	SAV0830	1.7	3.0	••	-	hypothetical protein SAV0830	Energy production and conversion
	SAV1623	1.1	3.6	•	-	flavin dependent oxidoreductase	Energy production and conversion
	SACOL1707	1.4	3.9	•	radC	DNA repair protein RadC	DNA metabolism, Replication, recombination, and repair
	SAV0069	4.6	12.1	•	-	hypothetical protein SAV0069	Function unknown
	SAV0084	3.3	6.3	•	-	hypothetical protein SAV0084	Function unknown
	SAV0085	1.9	4.8	•	-	hypothetical protein SAV0085	Function unknown
	SAV0166	2.3	2.8	•	-	hypothetical protein SAV0166	Function unknown
	SAV0171	1.1	2.9	••	-	hypothetical protein SAV0171	Function unknown
	SAV0176	2.9	4.6	•	-	hypothetical protein SAV0176	Function unknown
	SAV0210	2.5	3.3	•	-	hypothetical protein SAV0210	Function unknown
	SAV0335	4.8	8.9	•	-	hypothetical protein SAV0335	Function unknown
	SAV0350	5.0	5.2	•	-	hypothetical protein SAV0350	Function unknown
	SAV0352	2.6	1.9	•	-	hypothetical protein SAV0352	Function unknown
	SAV0353	2.0	3.1	•	-	hypothetical protein SAV0353	Function unknown
	SAV0617	1.3	2.8	•	-	hypothetical protein SAV0617	Function unknown
	SAV0646	3.0	4.3	••	-	hypothetical protein SAV0646	Function unknown
	SAV0654	3.7	3.6	•••	-	hypothetical protein SAV0654	Function unknown
	SAV0675	1.8	2.7	•	-	hypothetical protein SAV0675	Function unknown
	SAV0693	2.0	3.6	•	-	hypothetical protein SAV0693	Function unknown
	SAV0795	2.1	8.2	•	-	hypothetical protein SAV0795	Function unknown
	SAV0841	2.0	3.6	•	-	hypothetical protein SAV0841	Function unknown
	SAV0918	3.4	4.1	•	-	hypothetical protein SAV0918	Function unknown
	SAV0940	2.4	2.6	•	-	hypothetical protein SAV0940	Function unknown
	SAV0963	2.9	2.2	••	-	hypothetical protein SAV0963	Function unknown
	SAV1161	2.6	1.9	•	-	hypothetical protein SAV1161	Function unknown
	SAV1177	1.9	4.6	•	-	hypothetical protein SAV1177	Function unknown
	SAV1190	2.2	2.5	••	-	hypothetical protein SAV1190	Function unknown
	SAV1338	2.6	2.6	••	-	hypothetical protein SAV1338	Function unknown
	SAV1340	3.0	12.0	•	-	hypothetical protein SAV1340	Function unknown
	SAV1432	3.6	7.3	•	-	hypothetical protein SAV1432	Function unknown
	SAV1778	7.0	10.8	•	-	hypothetical protein SAV1778	Function unknown

	SAV1798	2.9	4.4 ●	-	hypothetical protein SAV1798	Function unknown
	SAV1877	2.2	2.7 ●●	-	hypothetical protein SAV1877	Function unknown
	SAV1932	1.8	2.6 ●	-	hypothetical protein SAV1932	Function unknown
	SAV1940	1.8	2.8 ●	-	hypothetical protein SAV1940	Function unknown
	SAV1991	2.0	3.0 ●	-	hypothetical protein SAV1991	Function unknown
	SAV2000	2.3	2.5 ●●	-	hypothetical protein SAV2000	Function unknown
	SAV2034	2.0	5.1 ●	-	hypothetical protein SAV2034	Function unknown
	SAV2073	2.0	2.8 ●●	-	hypothetical protein SAV2073	Function unknown
	SAV2074	2.0	3.0 ●	-	hypothetical protein SAV2074	Function unknown
	SAV2087	3.2	5.2 ●	-	hypothetical protein SAV2087	Function unknown
	SAV2358	1.5	2.5 ●	-	hypothetical protein SAV2358	Function unknown
	SAV2556	3.6	2.2 ●●	-	hypothetical protein SAV2556	Function unknown
	SAV2608	1.7	2.6 ●	-	hypothetical protein SAV2608	Function unknown
	SAV2691	2.0	3.1 ●	-	hypothetical protein SAV2691	Function unknown
	SAV2712	3.6	3.9 ●●●	trmE	tRNA modification GTPase TrmE	Function unknown
	SAV0075	1.6	3.4 ●	-	hypothetical protein SAV0075	Function unknown
	SAV1288	2.2	2.5 ●●●	-	hypothetical protein SAV1288	Function unknown
	SAV2021	3.4	10.0 ●	-	hypothetical protein SAV2021	Function unknown
	SAV2374	3.6	5.4 ●	-	hypothetical protein SAV2374	Function unknown
	SAV2496	3.0	4.6 ●	-	hypothetical protein SAV2496	Function unknown
	SAV2206	2.4	4.9 ●	-	alpha-acetolactate decarboxylase	General function prediction only
	SAV2003	2.2	3.1 ●●	truncate	hypothetical protein SAV2003	General function prediction only
	SA1577	2.9	6.0 ●	-	hypothetical protein SA1577	General function prediction only
	SAV0049	2.0	3.4 ●	-	hypothetical protein SAV0049	General function prediction only
	SAV0086	3.4	12.6 ●	-	hypothetical protein SAV0086	General function prediction only
	SAV0087	2.5	8.7 ●	-	hypothetical protein SAV0087	General function prediction only
	SAV0205	1.7	3.0 ●	oppF	oligopeptide transport ATP-binding	General function prediction only
	SAV0275	2.2	5.5 ●	-	penicillin amidase V	General function prediction only
	SAV0349	3.4	3.9 ●	-	transcriptional regulator	General function prediction only
	SAV0351	2.9	2.7 ●	-	ABC transporter ATP-binding protein	General function prediction only
	SAV0450	2.4	5.5 ●	-	cobalamin synthesis protein	General function prediction only
	SAV0477	1.8	2.7 ●	-	hypothetical protein SAV0477	General function prediction only
	SAV0594	2.1	3.3 ●	-	mercuric reductase-like protein	General function prediction only
	SAV0595	3.7	6.5 ●	-	hypothetical protein SAV0595	General function prediction only
	SAV0627	1.8	3.3 ●	-	monovalent cation/H+ antiporter	General function prediction only
	SAV0666	1.8	3.2 ●	-	hypothetical protein SAV0666	General function prediction only
	SAV0750	3.3	5.4 ●	-	comF operon protein 1	General function prediction only
	SAV0751	2.7	3.9 ●	-	hypothetical protein SAV0751	General function prediction only
	SAV0755	2.2	3.5 ●	-	hypothetical protein SAV0755	General function prediction only
	SAV0825	1.8	2.6 ●	-	amino acid transporter LysE	General function prediction only
	SAV1051	3.0	7.7 ●	-	ATL autolysin transcription regulator	General function prediction only
	SAV1307	2.2	4.0 ●●	-	GTP-binding proteinase modulator	General function prediction only
	SAV1544	2.8	4.3 ●	-	late competence protein comGA	General function prediction only

	SAV1747	1.8	2.6 •	-	metal-dependent hydrolase	General function prediction only
	SAV1756	2.7	2.8 •	-	hypothetical protein SAV1756	General function prediction only
	SAV1777	3.8	6.6 •	-	hypothetical protein SAV1777	General function prediction only
	SAV1780	5.8	7.5 •	-	hypothetical protein SAV1780	General function prediction only
	SAV1934	1.9	3.9 •	-	GntR family transcriptional regulator	General function prediction only
	SAV2022	5.2	16.1 •	-	hypothetical protein SAV2022	General function prediction only
	SAV2033	2.1	4.7 •	-	hypothetical protein SAV2033	General function prediction only
	SAV2045	1.3	2.9 •	-	hypothetical protein SAV2045	General function prediction only
	SAV2180	2.1	5.1 •	-	transporter	General function prediction only
	SAV2258	3.4	4.9 •	-	hypothetical protein SAV2258	General function prediction only
	SAV2266	3.9	8.5 •	-	transporter ybfD	General function prediction only
	SAV2280	1.9	3.1 •	narQ	formate dehydrogenase accessory	General function prediction only
	SAV2329	1.7	2.9 •	-	amino acid amidohydrolase	General function prediction only
	SAV2376	1.7	2.5 ••	-	cationic transporter	General function prediction only
	SAV2417	2.3	3.0 •	-	cation efflux family protein	General function prediction only
	SAV2566	2.7	2.8 ••	-	secretory antigen precursor SsaA	General function prediction only
	SAV2692	2.6	3.4 •	-	hypothetical protein SAV2692	General function prediction only
	SAV0063	4.3	8.2 •	abcA	hypothetical protein SAV0063	General function prediction only
	SAV0458	1.3	3.7 •	-	sodium-dependent transporter	General function prediction only
	SAV0943	1.3	2.8 ••	-	transporter	General function prediction only
	SAV1758	2.0	3.5 •	mrp	Mrp protein	General function prediction only
	SAV2631	3.9	6.5 •	-	transcriptional regulator	General function prediction only
	SAV1075	2.7	3.4 •	-	hypothetical protein SAV1075	Inorganic ion transport and metabolism
	SAV0647	2.2	3.2 ••	fhuA	ferrichrome transport ATP-binding	Inorganic ion transport and metabolism
	SAV0735	1.9	2.7 •	-	ferrichrome ABC transporter ATP-	Inorganic ion transport and metabolism
	SAV0648	2.1	3.1 ••	fhuB	ferrichrome transport permease	Inorganic ion transport and metabolism
	SAV0649	2.6	3.5 ••	fhuG	ferrichrome transport permease	Inorganic ion transport and metabolism
	SAV2175	1.9	3.6 ••	htsC	heme transport system permease	Inorganic ion transport and metabolism
	SAV2176	2.5	3.4 ••	htsB	heme transport system permease	Inorganic ion transport and metabolism
	SAV1038	1.5	2.5 •	-	ferrichrome ABC transporter	Inorganic ion transport and metabolism
	SAV0464	1.6	3.2 •	-	lipoprotein	Inorganic ion transport and metabolism
	SAV1774	4.4	8.9 •	-	aesenical pump membrane protein	Inorganic ion transport and metabolism
	SAV2139	2.9	4.7 ••	dps	general stress protein 20U	Inorganic ion transport and metabolism
	SAV2439	2.3	3.1 •	-	Na_ antiporter-like protein	Inorganic ion transport and metabolism
	SAV1933	1.5	2.5 •	-	ABC transporter ATP-binding protein	Inorganic ion transport and metabolism, Cobalt
	SAV2557	2.6	2.6 •	copA	copper-transporting ATPase	Inorganic ion transport and metabolism, Copper
	SAV1134	2.0	3.4 •	isdF	iron transport permease SirG	Inorganic ion transport and metabolism, Iron
	SAV1484	3.8	6.2 ••	fer	ferredoxin	Inorganic ion transport and metabolism, Iron
	SAV1498	2.6	4.1 ••	fur	ferric uptake regulator-like protein	Inorganic ion transport and metabolism, Iron
	SAV1861	2.7	2.3 •••	perR	FUR family transcriptional regulator	Inorganic ion transport and metabolism, Iron
	SAV1105	2.9	5.3 •	mntH	manganese transport protein MntH	Inorganic ion transport and metabolism, Manganese
	SAV1554	2.5	2.7 •	zur	ferric uptake regulator-like protein	Inorganic ion transport and metabolism, Zinc
	SAV2145	9.6	14.6 •	czrA	repressor protein	Inorganic ion transport and metabolism, Zinc

	SAV2146	7.2	12.0 ●	czrB	cation-efflux system membrane protein	Inorganic ion transport and metabolism, Zinc
	SAV0851	1.6	3.6 ●	-	hypothetical protein SAV0851	Intracellular trafficking, secretion, and vesicular transport
	SAV0038	2.1	3.9 ●	-	HMG-CoA synthase	Lipid transport and metabolism
	SAV0655	3.3	4.9 ●●	lipA	lipase LipA	Lipid transport and metabolism
	SAV1337	2.3	2.6 ●●	guaC	guanosine 5\'-monophosphate	Nucleotide transport and metabolism
	SAV1074	1.6	2.6 ●	purD	phosphoribosylamine--glycine ligase	Nucleotide transport and metabolism
	SAV1205	3.3	5.6 ●●	pyrE	orotate phosphoribosyltransferase	Nucleotide transport and metabolism
	SAV1198	5.3	8.8 ●●	pyrR	bifunctional pyrimidine regulatory	Nucleotide transport and metabolism
	SAV2445	1.9	2.8 ●	opuCD	glycine betaine/carnitine/choline ABC	Osmolarity
	SAV2612	2.1	3.3 ●	betA	choline dehydrogenase	Osmolarity
	SAV2613	1.7	4.7 ●	gbsA	glycine betaine aldehyde	Osmolarity
	SAV0072	5.5	10.8 ●	kdpA	potassium-transporting ATPase subunit	osmolarity
	SAV0073	3.4	7.2 ●	kdpB	potassium-transporting ATPase subunit	osmolarity
	SAV0074	5.8	14.0 ●	kdpC	potassium-transporting ATPase subunit	osmolarity
	SAV2075	4.2	8.6 ●	kdpC	potassium-transporting ATPase subunit	Osmolarity
	SAV2078	2.5	5.3 ●	kdpD	sensor protein	Osmolarity
	SAV2079	1.1	2.5 ●	kdpE	KDP operon transcriptional regulatory	Osmolarity
	SAV0573	1.6	3.6 ●●	proP	proline/betaine transporter-like protein	Osmolarity
	SAV2615	3.7	6.3 ●	cudT	choline transporter	Osmolarity
	SAV2076	3.7	7.1 ●	kdpB	potassium-transporting ATPase subunit	Osmolarity
	SAV2077	6.8	12.9 ●	kdpA	potassium-transporting ATPase subunit	Osmolarity
	SAV0345	2.5	3.7 ●	-	hypothetical protein SAV0345	osmolarity
	SAV1085	2.2	3.8 ●	-	NrdH-redoxin	Posttranslational modification, protein turnover, chaperones
	SAV1344	1.6	2.5 ●●	-	hypothetical protein SAV1344	Posttranslational modification, protein turnover, chaperones
	SAV2044	1.2	2.5 ●	-	hypothetical protein SAV2044	Posttranslational modification, protein turnover, chaperones
	SAV2389	1.9	2.9 ●	-	hypothetical protein SAV2389	Posttranslational modification, protein turnover, chaperones
	SAV2690	2.1	2.9 ●	pcp	pyrrolidone-carboxylate peptidase	Posttranslational modification, protein turnover, chaperones
	SAV2035	2.6	3.0 ●	hld	delta-hemolysin	Regulators
	SAV2386	1.4	2.7 ●●	sarZ	transcriptional regulator	Regulators
	SAV2357	2.4	2.7 ●●	tcaR	TcaR transcription regulator	Regulators
	SAV2344	1.4	2.6 ●	-	3-methyladenine DNA glycosylate	DNA metabolism, Replication, recombination, and repair
	SAV0061	4.5	6.0 ●	ccrB	cassette chromosome recombinase B	DNA metabolism, Replication, recombination, and repair
	SAV0062	2.8	4.9 ●	ccrA	cassette chromosome recombinase A	DNA metabolism, Replication, recombination, and repair
	SAV0076	1.6	2.8 ●	-	hypothetical protein SAV0076	DNA metabolism, Replication, recombination, and repair
	SAV0369	2.1	3.6 ●	-	hypothetical protein SAV0369	DNA metabolism, Replication, recombination, and repair
	SAV0800	1.3	2.5 ●●	-	bacteriophage terminase small subunit	DNA metabolism, Replication, recombination, and repair
	SAV1804	4.3	14.6 ●	-	transposase	DNA metabolism, Replication, recombination, and repair
	SAV2150	2.5	3.9 ●	-	hypothetical protein SAV2150	DNA metabolism, Replication, recombination, and repair
	SAV0944	1.7	2.7 ●	-	hypothetical protein SAV0944	Secondary metabolites biosynthesis, transport and
	SAV2181	1.9	3.7 ●	-	hypothetical protein SAV2181	Secondary metabolites biosynthesis, transport and
	SAV0746	2.2	3.7 ●●	-	hypothetical protein SAV0746	Signal transduction mechanisms
	SAV1233	2.5	2.6 ●●	rnc	ribonuclease III	Transcription
	SAV0124	1.7	2.8 ●	-	hypothetical protein SAV0124	Transcription

	SAV0333	6.7	11.2 •	-	hypothetical protein SAV0333	Transcription
	SAV0397	1.9	3.4 •	-	transcriptional regulator	Transcription
	SAV0667	1.6	3.0 •	-	AraC/XylS family transcriptional	Transcription
	SAV0786	1.5	7.9 •	-	hypothetical protein SAV0786	Transcription
	SAV1026	2.0	11.3 •	-	competence transcription factor	Transcription
	SAV2265	4.6	9.1 •	-	MarR family transcriptional regulator	Transcription
	SAV2381	1.9	2.7 ••	-	transcription regulatory protein	Transcription
	SAV2553	2.1	3.2 •	-	hypothetical protein SAV2553	Transcription
	SAV2571	1.9	3.5 •	-	hypothetical protein SAV2571	Transcription
	SAV2713	7.2	8.2 •	rnpA	ribonuclease P	Transcription
	SAV1098	5.2	7.5 ••	-	Cro/CI family transcriptional regulator	Transcription
	SAV2297	1.6	3.4 •	-	hypothetical protein SAV2297	Transcription
	SAV0398	3.1	1.9 •••	tetM	tetracycline resistance protein	Translation, ribosomal structure and biogenesis
	SAV0541	2.7	2.0 •••	-	hypothetical protein SAV0541	Translation, ribosomal structure and biogenesis
	SAV0462	1.1	3.2 •	metN1	ABC transporter ATP-binding protein	Transporters and efflux pumps, ATP-binding cassette super
	SAV0334	4.7	7.3 •	mepA	hypothetical protein SAV0334	Transporters and efflux pumps, Secondary transporter
	SAV0695	2.2	2.7 ••	norA	quinolone resistance protein	Transporters and efflux pumps, Secondary transporter
	SAV2038	2.2	2.5 ••	agrC	accessory gene regulator C	Two component Systems
	SAV2039	3.0	3.6 ••	agrA	accessory gene regulator A	Two component Systems
	SAV1321	2.3	3.8 •	desK	two-component sensor histidine kinase	Two component Systems
	SAV2036	2.4	2.6 •	agrB	accessory gene regulator B	Two component Systems
	SAV0660	2.1	2.9 •	bceS	two-component sensor histidine kinase	Two component Systems
	SAV0659	1.9	2.9 •	bceR	two-component response regulator	Two component Systems
	SAV1322	2.3	3.6 •	-	two-component response regulator	Two component Systems
	SAV2009	4.2	6.7 •	sec3	enterotoxin typeC3	Virulence factor
	SAV2497	3.2	3.7 •	-	accumulation-associated protein	Virulence factor
	SAV0229	6.1	6.5 •	-	hypothetical protein SAV0229	Virulence factor
	SAV1938	2.5	3.4 ••	-	hypothetical protein SAV1938	Virulence factor
	SAV0424	1.2	3.2 •	set8	superantigen-like protein	Virulence factor
	SAV0425	3.0	5.5 •	set10	superantigen-like protein 5	Virulence factor
	SAV1434	2.8	6.6 •	ebhA	hypothetical protein SAV1434	Virulence factor
	SAV2407	2.2	3.4 •	-	hypothetical protein SAV2407	Virulence factor
	SAV2299	3.2	2.4 •••	ssaA	secretory antigen SsaA-like protein	Virulence factor

down-regulated by 10mM Spm (15min, 60min), excluding those σB regulon genes

changing trend by high Spm (green-down)	Locus tag	15' Spm to N	60' Spm to N	sigmal intensity	Locus	Protein name	Function
	SAV2053	0.3	0.3	•	ilvD	dihydroxy-acid dehydratase	Amino acid metabolism,BCAA
	SAV1535	0.3	0.4	•••	gcvPB	glycine dehydrogenase subunit 2	Amino Acid Metabolism,
	SAV0957	0.4	0.3	•••	rocD	ornithine--oxo-acid transaminase	Amino acid metabolism, Arginine
	SAV1394	0.4	0.6	•	asd	aspartate semialdehyde dehydrogenase	Amino acid metabolism, Aspartate family
	SAV0554	0.4	0.5	•••	ilvE	branched-chain amino acid	Amino acid metabolism, BCAA
	SAV1439	0.7	0.3	•	ald1	alanine dehydrogenase	Amino acid metabolism, Branched chain amino acids family
	SAV1709	0.4	0.4	••	ald	alanine dehydrogenase	Amino acid metabolism, Branched chain amino acids family
	SAV2113	0.6	0.4	••••	glyA	serine hydroxymethyltransferase	Amino acid metabolism, Serine family
	SAV0722	0.4	0.3	•••	-	choline transport ATP-binding protein	Amino acid transport
	SAV0186	0.5	0.4	•	-	branched chain amino acid ABC	Amino acid transport
	SAV0727	0.6	0.4	•••	-	di-tripeptide ABC transporter	Amino acid transport
	SAV0315	0.5	0.2	••	nanA	N-acetylneuraminate lyase	Amino acid transport and metabolism
	SAV0314	0.6	0.3	•	-	sodium/glucose cotransporter	Amino acid transport and metabolism
	SAV1000	0.2	0.2	•••	-	thimet oligopeptidase-like protein	Amino acid transport and metabolism
	SAV1384	0.4	0.6	••	-	oligoendopeptidase	Amino acid transport and metabolism
	SAV2560	0.5	0.4	••	-	N-succinyldiaminopimelate	Amino acid transport and metabolism
	SAV1536	0.3	0.5	•••	gcvPA	glycine dehydrogenase subunit 1	Amino acid transport and metabolism
	SAV1537	0.2	0.4	•••	gcvT	glycine cleavage system	Amino acid transport and metabolism
	SAV0555	0.5	0.3	••	-	phosphoglycolate phosphatase	Carbohydrate Metabolism
	SAV0215	0.3	0.2	••	-	maltose/maltodextrin transport	Carbohydrate transport and metabolism
	SAV0216	0.4	0.3	•	-	maltose/maltodextrin transport	Carbohydrate transport and metabolism
	SAV1084	0.5	0.4	••••	ptsI	phosphoenolpyruvate-protein	Carbohydrate transport and metabolism
	SAV0376	0.4	0.3	••	-	phosphoglycerate mutase Gpm3p	Carbohydrate transport and metabolism
	SAV0929	0.5	0.3	•••	-	N-acetyl-glucosamine catabolism-like	Carbohydrate transport and metabolism
	SAV1083	0.5	0.4	••••	ptsH	phosphocarrier protein HPr	Carbohydrate transport and metabolism
	SAV0650	0.3	0.5	••	dhaK	dihydroxyacetone kinase subunit DhaK	Carbohydrate transport and metabolism
	SAV0188	0.4	0.6	••	-	indole-3-pyruvate decarboxylase	Carbohydrate transport and metabolism
	SAV0570	0.3	0.4	••••	-	hexulose-6-phosphate synthase	Carbohydrate transport and metabolism
	SAV1374	0.4	0.4	•••	femA	factor essential for expression of	Cell wall/membrane biogenesis
	SAV2111	0.6	0.4	••••	mnaA	UDP-GlcNAc 2-epimerase	Cell wall/membrane/envelope biogenesis
	SAV0571	0.3	0.4	•••	-	hypothetical protein SAV0571	Cell wall/membrane/envelope biogenesis
	SAV1028	0.4	0.8	••	-	lipoate-protein ligase-like protein	Coenzyme transport and metabolism
	SAV0519	0.5	0.4	••••	-	pyridoxal biosynthesis lyase PdxS	Cofactors and Vitamins, VitaminB6
	SAV1913	0.4	0.4	•••	-	nicotinate phosphoribosyltransferase	Cofactors, Pyridine nucleotides
	SACOL1046	0.4	0.3	••••	-	hypothetical protein SACOL1046	COG NA

	SAV0054	0.4	0.5	••	tnpC	transposase C	COG NA
	SAV0109	0.3	0.1	••	-	hypothetical protein SAV0109	COG NA
	SAV0200	0.6	0.3	••	-	hypothetical protein SAV0200	COG NA
	SAV0280	0.6	0.3	•	-	hypothetical protein SAV0280	COG NA
	SAV0387	0.4	0.3	•••	-	hypothetical protein SAV0387	COG NA
	SAV0867	0.6	0.4	••	-	hypothetical protein SAV0867	COG NA
	SAV1800	0.4	0.8	•	-	hypothetical protein SAV1800	COG NA
	SAV2252	0.4	0.2	••	-	hypothetical protein SAV2252	COG NA
	SAV2543	0.6	0.4	••••	-	hypothetical protein SAV2543	COG NA
	SAV2638	0.4	0.5	•••	isaB	immunodominant antigen B	COG NA
	SAV2173	0.5	0.3	•••	-	hypothetical protein SAV2173	COG NA
	SAV0431	0.5	0.3	••	hsdM	type I site-specific deoxyribonuclease	Defense mechanisms
	SAV0339	0.4	0.6	•	-	luciferase family protein	Energy metabolism
	SAV2103	0.6	0.4	••••	atpD	F0F1 ATP synthase subunit beta	Energy metabolism, ATP-proton motive force interconversion
	SAV2108	0.6	0.4	••••	atpE	F0F1 ATP synthase subunit C	Energy metabolism, ATP-proton motive force interconversion
	SAV0126	0.5	0.4	•	butA	acetoin reductase	Energy metabolism, Fermentation
	SAV0241	0.6	0.3	••••	lctE	L-lactate dehydrogenase	Energy metabolism, Fermentation
	SAV0605	0.4	0.2	•••	adh1	alcohol dehydrogenase	Energy metabolism, Fermentation
	SAV2602	0.3	0.5	•••	ldhB	L-lactate dehydrogenase	Energy metabolism, Fermentation
	SAV0772	0.4	0.3	••••	gap	glyceraldehyde-3-phosphate	Energy metabolism, Glycolysis/gluconeogenesis
	SAV0773	0.4	0.2	••••	pgk	phosphoglycerate kinase	Energy metabolism, Glycolysis/gluconeogenesis
	SAV0774	0.3	0.2	••••	tpiA	triosephosphate isomerase	Energy metabolism, Glycolysis/gluconeogenesis
	SAV0775	0.4	0.2	••••	pgm	phosphoglyceromutase	Energy metabolism, Glycolysis/gluconeogenesis
	SAV0776	0.3	0.2	••••	eno	phosphopyruvate hydratase	Energy metabolism, Glycolysis/gluconeogenesis
	SAV1791	0.4	0.6	••	pckA	phosphoenolpyruvate carboxykinase	Energy metabolism, Glycolysis/gluconeogenesis
	SAV2125	0.4	0.4	••••	fbaA	fructose-bisphosphate aldolase	Energy metabolism, Glycolysis/gluconeogenesis
	SAV2491	0.5	0.4	•	-	phosphomannomutase	Energy metabolism, Glycolysis/gluconeogenesis
	SAV2516	0.3	0.4	••	fbp	fructose-bisphosphatase	Energy metabolism, Glycolysis/gluconeogenesis
	SAV0962	0.4	0.3	•••	pgi	glucose-6-phosphate isomerase	Energy metabolism, Glycolysis/gluconeogenesis
	SAV2416	0.4	0.3	••	gpmA	phosphoglyceromutase	Energy metabolism, Glycolysis/gluconeogenesis
	SAV2399	0.7	0.3	••	nasE	assimilatory nitrite reductase	Energy Metabolism, nitrogen
	SAV0452	0.3	0.2	••	ndhF	NADH dehydrogenase subunit 5	Energy metabolism, Oxidative phosphorylatio
	SAV1060	0.7	0.4	••••	qoxB	quinol oxidase polypeptide I	Energy metabolism, Oxidative phosphorylatio
	SAV0552	0.4	0.5	••	araB	ribulokinase	Energy metabolism, Pentose phosphate cycle
	SAV0138	0.4	0.5	••••	dra	deoxyribose-phosphate aldolase	Energy metabolism, Pentose phosphate cycle
	SAV1342	0.4	0.4	••••	tkt	transketolase	Energy metabolism, Pentose phosphate cycle
	SAV1511	0.4	0.4	••••	gnd	6-phosphogluconate dehydrogenase	Energy metabolism, Pentose phosphate cycle
	SAV1781	0.4	0.4	•••	-	translaldolase	Energy metabolism, Pentose phosphate cycle
	SAV1093	0.5	0.4	••••	pdhA	pyruvate dehydrogenase E1 component	Energy metabolism, Pyruvate
	SAV1094	0.7	0.4	••••	phdB	pyruvate dehydrogenase E1 component	Energy metabolism, Pyruvate
	SAV1095	0.6	0.4	••••	pdhC	branched-chain alpha-keto acid	Energy metabolism, Pyruvate
	SAV2365	0.5	0.4	••	mqo1	malate:quinone oxidoreductase	Energy metabolism, TCA cycle
	SAV1412	0.4	0.6	••••	sucA	dihydrolipoamide succinyltransferase	Energy metabolism, TCA cycle

	SAV1413	0.4	0.3	●●●●	sucA	2-oxoglutarate dehydrogenase E1	Energy metabolism, TCA cycle
	SAV2559	0.5	0.4	●●	-	D-lactate dehydrogenase	Energy production and conversion
	SAV0930	0.6	0.4	●●●	-	glycerate dehydrogenase	Energy production and conversion
	SAV2302	0.5	0.4	●●●●	-	D-octopine dehydrogenase	Energy production and conversion
	SAV0025	0.4	0.3	●●	-	hypothetical protein SAV0025	Function unknown
	SAV0106	0.2	0.1	●●	-	myosin-cross-reactive antigen	Function unknown
	SAV0217	0.3	0.3	●●	-	NADH-dependent dehydrogenase	Function unknown
	SAV0282	0.5	0.3	●●●	-	hypothetical protein SAV0282	Function unknown
	SAV0308	0.4	0.2	●●●	-	ABC transporter permease	Function unknown
	SAV0372	0.4	0.2	●●●	-	hypothetical protein SAV0372	Function unknown
	SAV0374	0.4	0.1	●●●●	-	hypothetical protein SAV0374	Function unknown
	SAV0453	0.4	0.4	●●●	-	hypothetical protein SAV0453	Function unknown
	SAV0928	0.8	0.4	●●	-	hypothetical protein SAV0928	Function unknown
	SAV1004	0.3	0.3	●	-	hypothetical protein SAV1004	Function unknown
	SAV1106	0.3	0.2	●	-	hypothetical protein SAV1106	Function unknown
	SAV1425	0.5	0.4	●●●	-	hypothetical protein SAV1425	Function unknown
	SAV1573	0.6	0.4	●●●●	-	hypothetical protein SAV1573	Function unknown
	SAV2401	1.5	0.3	●●	-	NirR protein	Function unknown
	SAV2436	0.3	0.4	●●	-	hypothetical protein SAV2436	Function unknown
	SAV0551	0.1	0.1	●●●●	-	chaperone protein HchA	General function prediction only
	SAV0601	0.4	0.5	●●	-	hypothetical protein SAV0601	General function prediction only
	SAV0970	0.3	0.3	●●●	cdr	coenzyme A disulfide reductase	General function prediction only
	SAV1279	0.5	0.4	●●●	-	processing proteinase	General function prediction only
	SAV1481	0.3	0.4	●●●●	ebpS	elastin binding protein	General function prediction only
	SAV1799	0.4	0.5	●●	-	hypothetical protein SAV1799	General function prediction only
	SAV2188	0.4	0.5	●●	-	hypothetical protein SAV2188	General function prediction only
	SAV2471	0.2	0.1	●●	-	hypothetical protein SAV2471	General function prediction only
	SAV2701	0.2	0.1	●●●	vraD	ABC transporter ATP-binding protein	General function prediction only
	SAV2702	0.2	0.1	●●●●	vraE	vraE protein	General function prediction only
	SAV1363	0.3	0.3	●●●	-	4-oxalocrotonate tautomerase	General function prediction only
	SAV0111	0.3	0.4	●●	spa	immunoglobulin G binding protein A	General function prediction only
	SAV0167	0.4	0.6	●	aldA	aldehyde dehydrogenase-like protein	General function prediction only
	SAV1707	0.4	0.5	●●●	-	metal-dependent hydrolase	General function prediction only
	SAV0832	0.4	0.2	●●●	-	hypothetical protein SAV0832	Inorganic ion transport and metabolism
	SAV0951	0.8	0.4	●●●	mnhB	monovalent cation/H+ antiporter	Inorganic ion transport and metabolism
	SAV0952	0.6	0.4	●●●●	mnhA	monovalent cation/H+ antiporter	Inorganic ion transport and metabolism
	SAV0240	0.3	0.2	●●	hmp	flavohemoprotein	Inorganic ion transport and metabolism, Iron
	SAV0039	0.3	0.4	●●	-	glycerophosphoryl diester	Lipid Metabolism
	SAV0040	0.4	0.3	●	-	hypothetical protein SAV0040	Lipid transport and metabolism
	SAV0456	0.4	0.4	●●●	-	hypothetical protein SAV0456	Lipid transport and metabolism
	SAV1908	0.5	0.3	●●●	purB	adenylosuccinate lyase	Nucleotide transport and metabolism
	SAV1427	0.5	0.4	●●●	thyA	thymidylate synthase	Nucleotide transport and metabolism
	SAV2112	0.6	0.4	●●●●	upp	uracil phosphoribosyltransferase	Nucleotide transport and metabolism

	SAV2617	0.6	0.3	••	nrdD	anaerobic ribonucleoside triphosphate	Nucleotide transport and metabolism
	SAV0730	0.7	0.4	•••	nrdI	ribonucleotide reductase stimulatory	Nucleotide transport and metabolism
	SAV0731	0.6	0.3	••••	nrdE	ribonucleotide-diphosphate reductase	Nucleotide transport and metabolism
	SAV0732	0.7	0.3	•••	nrdF	ribonucleotide-diphosphate reductase	Nucleotide transport and metabolism
	SAV1732	0.4	0.5	••	fhs	formate--tetrahydrofolate ligase	Nucleotide transport and metabolism
	SAV2138	0.3	0.2	•••	deoD	purine nucleoside phosphorylase	Nucleotide transport and metabolism
	SAV2136	0.4	0.6	•••	pdp	pyrimidine-nucleoside phosphorylase	Nucleotide transport and metabolism
	SAV0723	0.6	0.4	•••	opuBB	choline transporter	Osmolarity
	SAV0071	0.4	0.4	••	kdpD	sensor protein KdpD	osmolarity
	SAV1306	0.4	0.6	••	bsaA	glutathione peroxidase	Oxidative response
	SAV1553	0.3	0.5	••••	sodA	superoxide dismutase	Oxidative response
	SAV1574	0.6	0.4	••••	-	hypothetical protein SAV1574	Posttranslational modification, protein turnover, chaperones
	SAV1728	0.3	0.1	••••	-	serine proteinase Do	Posttranslational modification, protein turnover, chaperones
	SAV1744	0.4	0.5	••	-	thioredoxin-like protein	Posttranslational modification, protein turnover, chaperones
	SAV0831	0.3	0.3	••	-	thioredoxin	Posttranslational modification, protein turnover, chaperones
	SAV1929	0.2	0.3	•••	-	hypothetical protein SAV1929	Posttranslational modification, protein turnover, chaperones
	SAV0548	0.7	0.4	••••	tuf	elongation factor Tu	Protein synthesis, Translation factors
	SAV0547	0.7	0.4	••••	fus	elongation factor G	Protein synthesis, Translation factors
	SAV0009	0.6	0.4	•••	serS	seryl-tRNA synthetase	Protein synthesis, tRNA aminoacylation
	SAV0491	0.7	0.4	••••	-	deoxyribonuclease	Replication, recombination and repair
	SAV1001	0.4	0.7	••	yjbM	hypothetical protein SAV1001	Secondary metabolites biosynthesis, transport and
	SAV0309	0.6	0.4	••	-	ABC transporter ATP-binding protein	Signal transduction mechanisms
	SAV1710	0.3	0.1	••••	-	universal stress protein family protein	Signal transduction mechanisms
	SAV0553	0.5	0.3	•••	-	UDP-glucose 4-epimerase-like protein	Sugar metabolism and transport
	SAV2195	0.2	0.1	•••	lacA	galactose-6-phosphate isomerase	Sugar metabolism and transport, Operon lactose
	SAV2500	0.7	0.4	•••	gtaB	UTP-glucose-1-phosphate	Sugar metabolism and transport, Operon lactose
	SAV2189	0.4	0.8	••	lacG	6-phospho-beta-galactosidase	Sugar metabolism and transport, Operon lactose
	SAV2190	0.2	0.2	•••	lacE	PTS system lactose-specific transporter	Sugar metabolism and transport, Operon lactose
	SAV2191	0.3	0.2	•	lacF	PTS system lactose-specific transporter	Sugar metabolism and transport, Operon lactose
	SAV2192	0.2	0.2	•••	lacD	tagatose 1	Sugar metabolism and transport, Operon lactose
	SAV2193	0.2	0.2	•••	lacC	tagatose-6-phosphate kinase	Sugar metabolism and transport, Operon lactose
	SAV2194	0.3	0.2	••	lacB	galactose-6-phosphate isomerase	Sugar metabolism and transport, Operon lactose
	SAV2332	0.4	0.3	••	-	hypothetical protein SAV2332	Transcription
	SAV2508	0.4	0.2	•••	-	MerR family transcriptional regulator	Transcription
	SAV2665	0.4	0.4	•	icaR	ica operon transcriptional regulator	Regulators
	SAV1899	0.6	0.4	••••	gatB	aspartyl/glutamyl-tRNA	Translation, ribosomal structure and biogenesis
	SAV1900	0.5	0.4	••••	gatA	aspartyl/glutamyl-tRNA	Translation, ribosomal structure and biogenesis
	SAV0752	0.3	0.2	••••	-	ribosomal subunit interface protein	Translation, ribosomal structure and biogenesis
	SAV1888	0.5	0.3	•••	map	methionine aminopeptidase	Translation, ribosomal structure and biogenesis
	SAV1476	0.4	0.6	•••	rpsA	30S ribosomal protein S1	Translation, ribosomal structure and biogenesis
	SAV1696	0.5	0.4	••••	aapA	D-serine/D-alanine/glycine transporter	Transporters and efflux pumps, ATP-binding cassette super
	SAV2467	0.4	0.6	•	opp-1A	oligopeptide transporter substrate	Transporters and efflux pumps, ATP-binding cassette super
	SAV1492	0.5	0.4	••••	srrA	respiratory response protein	Two component Systems

Table S5 Transcriptome: RN4220 vs its Spm^R mutants (no Spm)

RNM2 vs RN4220

signal intensity over 200, fold change over 2.5;

data from two independent biological experiments (average)

	RNM2 to RN4220	RNM4 to RN4220	RNM6 to RN4220	RN4220 signal intensity	RNM2 signal intensity	gene symbol	Locus ID	Protein name
RNM2 up	4.0	1.4	0.6	749	3005	sarH1	SAV0112	accessory regulator A-like protein
RNM2 up	3.2	1.5	1.1	149	477	sirA	SAV0115	lipoprotein
RNM2 up	3.0	1.3	2.4	136	413	-	SAV0214	maltose/maltodextrin transport system
RNM2 up	2.7	0.7	1.2	493	1333	-	SAV0278	hypothetical protein SAV0278
RNM2 up	2.6	1.4	1.1	771	2042	glpT	SAV0337	glycerol-3-phosphate transporter
RNM2 up	4.9	1.3	2.1	2961	14492	sdrD	SAV0562	Ser-Asp rich fibrinogen-binding, bone
RNM2 up	3.0	1.7	2.7	81	247	-	SAV0656	hypothetical protein SAV0656
RNM2 up	2.5	1.7	0.1	2584	6411	-	SAV0736	lipoprotein
RNM2 up	3.6	1.0	0.9	164	586	-	SAV1036	hypothetical protein SAV1036
RNM2 up	3.2	1.1	3.7	137	440	-	SAV1051	ATL autolysin transcription regulator
RNM2 up	3.1	1.4	0.6	339	1057	potA	SAV1099	spermidine/putrescine ABC transporter
RNM2 up	3.0	1.4	0.4	216	655	potB	SAV1100	spermidine/putrescine ABC transporter
RNM2 up	2.5	1.2	0.3	414	1032	potC	SAV1101	spermidine/putrescine ABC transporter
RNM2 up	2.5	1.6	0.3	1206	3066	potD	SAV1102	spermidine/putrescine-binding protein
RNM2 up	2.6	0.8	0.9	2044	5251	pyrR	SAV1198	bifunctional pyrimidine regulatory protein PyrR
RNM2 up	2.8	0.8	0.3	732	2026	pyrP	SAV1199	uracil permease
RNM2 up	2.9	1.0	0.3	1459	4213	pyrB	SAV1200	aspartate carbamoyltransferase catalytic subunit
RNM2 up	2.9	1.1	0.3	3380	9956	pyrC	SAV1201	dihydroorotase
RNM2 up	3.1	1.2	0.4	2056	6395	pyrAA	SAV1202	carbamoyl phosphate synthase small subunit
RNM2 up	3.1	1.3	0.4	3468	10635	carB	SAV1203	carbamoyl phosphate synthase large subunit
RNM2 up	2.8	1.4	0.3	2409	6809	pyrF	SAV1204	orotidine 5'-phosphate decarboxylase
RNM2 up	2.6	1.6	0.3	2220	5824	pyrE	SAV1205	orotate phosphoribosyltransferase
RNM2 up	2.6	1.8	0.6	948	2484	-	SAV1206	hypothetical protein SAV1206
RNM2 up	2.5	0.9	1.5	605	1505	-	SAV1384	oligoendopeptidase
RNM2 up	3.0	1.5	1.0	150	447	-	SAV1432	hypothetical protein SAV1432
RNM2 up	2.5	1.2	1.7	798	1981	-	SAV1608	hypothetical protein SAV1608
RNM2 up	2.6	1.1	1.4	301	775	-	SAV1774	aesenical pump membrane protein
RNM2 up	4.3	0.8	2.0	182	790	-	SAV1801	hypothetical protein SAV1801
RNM2 up	2.9	1.3	2.2	629	1806	czrA	SAV2145	repressor protein
RNM2 up	2.5	1.6	1.4	962	2437	czrB	SAV2146	cation-efflux system membrane protein
RNM2 up	2.8	0.8	1.2	1243	3426	ssaA	SAV2299	secretory antigen precursor SsaA-like protein
RNM2 up	3.0	0.9	0.6	923	2726	-	SAV2345	sodium/glutamate symporter
RNM2 up	2.8	1.2	0.7	252	716	-	SAV2463	oligopeptide transporter ATPase subunit
RNM2 up	3.2	1.1	0.8	152	484	-	SAV2465	oligopeptide transporter permease
RNM2 up	3.1	1.1	0.7	138	424	-	SAV2466	oligopeptide transporter permease
RNM2 up	3.8	1.4	0.4	2934	11076	ddh	SAV2524	D-lactate dehydrogenase
RNM2 up	3.4	0.6	0.9	755	2601	betA	SAV2612	choline dehydrogenase
RNM2 up	3.5	0.7	0.8	1243	4320	cudT	SAV2615	choline transporter
RNM2 down	0.4	0.6	1.1	1353	591	hutH	SAV0008	histidine ammonia-lyase
RNM2 down	0.4	1.0	1.4	215	85	-	SAV0102	aminoacylase

RNM2 down	0.4	0.5	1.7	3593	1299	butA	SAV0126	acetoin reductase
RNM2 down	0.2	0.6	0.6	20598	5038	-	SAV0134	hypothetical protein SAV0134
RNM2 down	0.1	0.7	0.9	5848	718	adhE	SAV0148	bifunctional acetaldehyde-CoA/alcohol
RNM2 down	0.4	0.7	7.6	206	87	capC	SAV0151	capsular polysaccharide synthesis enzyme Cap8C
RNM2 down	0.4	1.0	0.9	3408	1415	-	SAV0181	hypothetical protein SAV0181
RNM2 down	0.4	0.7	1.2	2612	1069	-	SAV0240	putative flavohemoprotein
RNM2 down	0.3	0.5	21.7	443	153	lrgA	SAV0262	murein hydrolase regulator LrgA
RNM2 down	0.2	0.4	16.9	1503	277	lrgB	SAV0263	antiholin-like protein LrgB
RNM2 down	0.4	0.5	1.2	313	122	-	SAV0297	hypothetical protein SAV0297
RNM2 down	0.4	0.8	0.7	1978	765	-	SAV0304	hypothetical protein SAV0304
RNM2 down	0.4	0.4	2.7	1854	739	-	SAV0435	hypothetical protein SAV0435
RNM2 down	0.3	0.5	1.0	574	173	proP	SAV0573	proline/betaine transporter-like protein
RNM2 down	0.4	0.6	1.2	775	339	-	SAV0596	hypothetical protein SAV0596
RNM2 down	0.2	0.8	0.7	25811	4128	adh1	SAV0605	alcohol dehydrogenase
RNM2 down	0.2	1.0	0.6	364	90	-	SAV0668	hypothetical protein SAV0668
RNM2 down	0.4	1.0	0.2	10034	4183	fruB	SAV0699	fructose 1-phosphate kinase
RNM2 down	0.3	0.8	1.7	2019	675	-	SAV0708	hypothetical protein SAV0708
RNM2 down	0.4	1.0	0.7	1554	577	-	SAV0808	hypothetical protein SAV0808
RNM2 down	0.4	0.3	3.7	868	365	nuc	SAV0815	staphylococcal nuclease
RNM2 down	0.4	0.8	1.3	203	88	-	SAV0821	hypothetical protein SAV0821
RNM2 down	0.4	0.8	0.6	1345	561	-	SAV0981	hypothetical protein SAV0981
RNM2 down	0.4	0.6	1.3	641	276	sspC	SAV1046	cysteine protease
RNM2 down	0.4	0.5	1.6	1093	394	sspB	SAV1047	cysteine protease precursor
RNM2 down	0.3	0.4	1.4	1711	492	sspA	SAV1048	serine protease
RNM2 down	0.4	0.5	3.3	5326	1869	-	SAV1163	alpha-hemolysin precursor
RNM2 down	0.4	0.4	1.9	400	149	-	SAV1389	thioredoxine reductase
RNM2 down	0.4	0.9	0.9	4771	1701	-	SAV1437	amino acid permease family protein
RNM2 down	0.3	0.9	0.8	20124	6610	-	SAV1439	alanine dehydrogenase
RNM2 down	0.4	0.9	1.0	659	293	-	SAV1624	hypothetical protein SAV1624
RNM2 down	0.2	0.6	2.8	656	123	-	SAV1940	hypothetical protein SAV1940
RNM2 down	0.1	0.7	2.3	1028	135	truncat	SAV2003	truncated beta-hemolysin
RNM2 down	0.2	0.7	3.0	1231	249	-	SAV2004	hypothetical protein SAV2004
RNM2 down	0.1	0.6	4.0	1877	258	-	SAV2005	hypothetical protein SAV2005
RNM2 down	0.0	0.1	2.3	19605	624	hld	SAV2035	delta-hemolysin
RNM2 down	0.2	0.3	1.5	1475	266	agrA	SAV2039	accessory gene regulator A
RNM2 down	0.4	0.8	14.6	218	85	kdpD	SAV2078	sensor protein
RNM2 down	0.4	0.5	0.9	210	92	-	SAV2144	hypothetical protein SAV2144
RNM2 down	0.4	1.0	0.8	1084	460	-	SAV2147	lytic regulatory protein truncated with Tn554
RNM2 down	0.4	1.1	1.2	932	334	-	SAV2148	hypothetical protein SAV2148
RNM2 down	0.4	1.0	0.8	2554	952	asp23	SAV2182	alkaline shock protein 23
RNM2 down	0.4	1.0	1.0	616	262	-	SAV2183	hypothetical protein SAV2183
RNM2 down	0.4	1.1	1.4	1194	481	-	SAV2184	hypothetical protein SAV2184
RNM2 down	0.4	0.8	0.4	252	106	lacG	SAV2189	6-phospho-beta-galactosidase
RNM2 down	0.4	0.7	1.6	560	220	-	SAV2199	hypothetical protein SAV2199
RNM2 down	0.3	0.9	1.0	1293	439	-	SAV2310	transcription antiterminator LytR
RNM2 down	0.1	0.2	1.4	1748	213	hutI	SAV2330	imidazolonepropionase

RNM2 down	0.1	0.2	1.3	2756	157	hutU	SAV2331	urocanate hydratase
RNM2 down	0.4	1.3	0.7	413	154	-	SAV2353	hypothetical protein SAV2353
RNM2 down	0.1	0.8	1.2	2557	368	narK	SAV2388	nitrite extrusion protein
RNM2 down	0.4	1.1	0.7	1301	526	-	SAV2391	response regulators of two-component
RNM2 down	0.2	1.1	0.3	951	231	-	SAV2395	nitrate reductase delta chain
RNM2 down	0.2	1.0	0.4	1634	385	narH	SAV2396	nitrate reductase beta chain
RNM2 down	0.2	0.8	1.0	2955	489	narG	SAV2397	respiratory nitrate reductase alpha chain
RNM2 down	0.4	1.0	0.6	740	302	nasF	SAV2398	uroporphyrin-III C-methyl transferase
RNM2 down	0.4	0.9	0.7	718	285	nasE	SAV2399	assimilatory nitrite reductase
RNM2 down	0.2	0.8	0.8	3359	724	nasD	SAV2400	nitrite reductase
RNM2 down	0.1	0.6	1.6	3937	462	-	SAV2401	NirR protein
RNM2 down	0.4	0.9	0.6	4238	1584	-	SAV2451	para-nitrobenzyl esterase chain A
RNM2 down	0.3	0.8	0.3	7129	2060	ptsG	SAV2538	PTS system, glucose-specific II ABC component
RNM2 down	0.4	1.3	2.6	332	130	-	SAV2616	anaerobic (class III) ribonucleotide reductase
RNM2 down	0.3	1.5	3.0	1017	301	nrdD	SAV2617	anaerobic ribonucleoside triphosphate
RNM2 down	0.4	0.6	1.1	270	112	-	SAV2623	ABC transporter ATP-binding protein
RNM2 down	0.3	0.3	8.4	750	228	arcD	SAV2633	arginine/oirnithine antiporter
RNM2 down	0.2	0.2	9.4	638	121	arcB	SAV2634	ornithine carbamoyltransferase
RNM2 down	0.1	0.2	8.2	1186	118	arcA	SAV2635	arginine deiminase
RNM2 down	0.1	0.1	0.5	3243	311	aur	SAV2637	zinc metalloproteinase aureolysin
RNM2 down	0.4	0.7	2.2	370	156	-	SAV2655	hypothetical protein SAV2655
RNM2 down	0.4	1.0	1.7	717	312	-	SAV2707	hypothetical protein SAV2707

RNM4 vs RN4220

signal intensity over 200, fold change over 2.5;

data from two independent biological experiments (average)

	RNM2 to RN4220	**RNM4 to RN4220**	RNM6 to RN4220	**RN4220 signal intensity**	**RNM4 signal intensity**	gene symbol	locus ID	Protein name
RNM4 down	1.0	0.4	1.4	2875	1263	-	SAV0104	transport protein
RNM4 down	0.7	0.3	2.5	870	280	-	SAV0190	hypothetical protein SAV0190
RNM4 down	0.6	0.4	2.2	862	317	murQ	SAV0191	N-acetylmuramic acid-6-phosphate etherase
RNM4 down	1.3	0.4	1.9	1090	446	-	SAV0234	putative acyl-CoA synthetase FadE
RNM4 down	0.2	0.4	16.9	1503	599	lrgB	SAV0263	antiholin-like protein LrgB
RNM4 down	1.5	0.4	2.9	203	91	-	SAV0264	hypothetical protein SAV0264
RNM4 down	0.4	0.4	2.7	1854	832	-	SAV0435	hypothetical protein SAV0435
RNM4 down	0.4	0.3	3.7	868	276	nuc	SAV0815	staphylococcal nuclease
RNM4 down	0.3	0.4	1.4	1711	731	sspA	SAV1048	serine protease
RNM4 down	0.4	0.4	1.9	400	161	-	SAV1389	thioredoxine reductase
RNM4 down	0.7	0.4	1.2	981	413	ribD	SAV1771	riboflavin specific deaminase
RNM4 down	0.0	0.1	2.3	19605	1830	hld	SAV2035	delta-hemolysin
RNM4 down	0.2	0.3	1.5	1475	507	agrA	SAV2039	accessory gene regulator A
RNM4 down	0.1	0.2	1.4	1748	409	hutI	SAV2330	imidazolonepropionase
RNM4 down	0.1	0.2	1.3	2756	452	hutU	SAV2331	urocanate hydratase
RNM4 down	0.8	0.4	1.7	418	188	gntK	SAV2506	gluconokinase
RNM4 down	0.5	0.3	1.4	3680	1230	-	SAV2533	hypothetical protein SAV2533
RNM4 down	0.3	0.3	8.4	750	252	arcD	SAV2633	arginine/oirnithine antiporter
RNM4 down	0.2	0.2	9.4	638	134	arcB	SAV2634	ornithine carbamoyltransferase
RNM4 down	0.1	0.2	8.2	1186	227	arcA	SAV2635	arginine deiminase
RNM4 down	0.1	0.1	0.5	3243	447	aur	SAV2637	zinc metalloproteinase aureolysin

RNM6 vs RN4220

signal intensity over 200, fold change over 2.5;

data from two independent biological experiments (average)

	RNM2 to RN4220	RNM4 to RN4220	RNM6 to RN4220	RN4220 signal intensity	RN+F127M6 signal intensity	gene symbol	Locus ID	Protein name
RNM6 up	0.7	0.8	2.6	126	325	plc	SAV0095	1-phosphatidylinositol phosphodiesterase
RNM6 up	0.3	0.4	8.9	129	1148	capA	SAV0149	capsular polysaccharide synthesis enzyme
RNM6 up	0.1	0.4	10.9	162	1772	capB	SAV0150	capsular polysaccharide synthesis enzyme Cap5B
RNM6 up	0.4	0.7	7.6	206	1567	capC	SAV0151	capsular polysaccharide synthesis enzyme Cap8C
RNM6 up	0.6	0.5	4.3	276	1195	capD	SAV0152	capsular polysaccharide synthesis enzyme
RNM6 up	0.4	0.8	4.3	185	795	capE	SAV0153	capsular polysaccharide synthesis enzyme Cap8E
RNM6 up	0.3	0.7	3.1	149	469	capF	SAV0154	capsular polysaccharide synthesis enzyme Cap5F
RNM6 up	0.2	0.8	2.9	135	395	capG	SAV0155	capsular polysaccharide synthesis enzyme
RNM6 up	0.9	0.8	3.8	141	540	-	SAV0185	ornithine aminotransferase
RNM6 up	0.7	0.3	2.5	870	2210	-	SAV0190	hypothetical protein SAV0190
RNM6 up	1.5	0.5	3.7	868	3220	-	SAV0235	putative acetyl-CoA/acetoacetyl-CoA transferase
RNM6 up	0.3	0.5	21.7	443	9597	lrgA	SAV0262	murein hydrolase regulator LrgA
RNM6 up	0.2	0.4	16.9	1503	25327	lrgB	SAV0263	antiholin-like protein LrgB
RNM6 up	1.5	0.4	2.9	203	581	-	SAV0264	hypothetical protein SAV0264
RNM6 up	0.5	0.6	2.7	317	842	-	SAV0281	hypothetical protein SAV0281
RNM6 up	1.5	0.9	2.8	83	235	-	SAV0285	hypothetical protein SAV0285
RNM6 up	0.5	0.7	2.8	586	1661	-	SAV0308	ABC transporter permease
RNM6 up	1.5	1.1	2.9	149	435	nanA	SAV0315	N-acetylneuraminate lyase
RNM6 up	0.7	0.7	4.2	122	520	-	SAV0319	hypothetical protein SAV0319
RNM6 up	1.3	1.8	2.6	237	624	-	SAV0342	ribosomal-protein-serine N-acetyltransferase
RNM6 up	1.0	1.4	2.8	211	592	-	SAV0348	hypothetical protein SAV0348
RNM6 up	0.4	0.4	2.7	1854	5020	-	SAV0435	hypothetical protein SAV0435
RNM6 up	0.6	0.6	2.6	188	499	-	SAV0462	ABC transporter ATP-binding protein
RNM6 up	0.9	0.9	3.9	159	616	-	SAV0463	ABC transporter permease protein
RNM6 up	0.9	0.9	2.6	540	1378	-	SAV0555	putative phosphoglycolate phosphatase
RNM6 up	0.8	0.9	3.4	809	2729	-	SAV0564	poly (glycerol-phosphate) alpha-
RNM6 up	1.3	1.6	2.5	281	696	-	SAV0602	hypothetical protein SAV0602
RNM6 up	3.0	1.7	2.7	81	220	-	SAV0656	hypothetical protein SAV0656
RNM6 up	1.2	1.0	3.4	105	359	-	SAV0675	hypothetical protein SAV0675
RNM6 up	1.8	0.9	3.7	181	678	-	SAV0696	hypothetical protein SAV0696
RNM6 up	0.6	1.3	2.9	4140	11846	nrdI	SAV0730	ribonucleotide reductase stimulatory protein
RNM6 up	1.1	1.1	3.0	140	421	-	SAV0756	HD superfamily hydrolase
RNM6 up	0.4	0.3	3.7	868	3202	nuc	SAV0815	staphylococcal nuclease
RNM6 up	1.1	1.2	4.6	47	216	-	SAV0826	hypothetical protein SAV0826
RNM6 up	0.7	0.8	4.5	621	2809	-	SAV0834	hypothetical protein SAV0834
RNM6 up	1.1	0.9	4.7	183	855	-	SAV0835	hypothetical protein SAV0835
RNM6 up	0.4	1.0	3.7	64	240	-	SAV0836	hypothetical protein SAV0836
RNM6 up	1.4	1.1	2.5	127	322	-	SAV0927	hypothetical protein SAV0927
RNM6 up	0.7	0.5	2.5	1455	3691	-	SAV0955	polyribonucleotide nucleotidyltransferase
RNM6 up	0.8	0.5	3.4	347	1178	oppB	SAV0986	oligopeptide transport system permease protein

RNM6 up	0.7	0.6	3.0	707	2126	-	SAV0987	oligopeptide transport system permease protein
RNM6 up	1.2	0.5	4.8	128	611	-	SAV1026	competence transcription factor
RNM6 up	3.2	1.1	3.7	137	507	-	SAV1051	ATL autolysin transcription regulator
RNM6 up	1.8	1.3	4.6	94	434	-	SAV1105	manganese transport protein MntH
RNM6 up	0.8	0.8	2.9	1234	3554	-	SAV1152	hypothetical protein SAV1152
RNM6 up	0.9	1.0	2.5	685	1729	-	SAV1153	hypothetical protein SAV1153
RNM6 up	1.3	0.9	2.5	905	2219	-	SAV1156	formyl peptide receptor-like 1 inhibitory protein
RNM6 up	0.4	0.5	3.3	5326	17566	-	SAV1163	alpha-hemolysin precursor
RNM6 up	2.3	1.0	3.2	907	2895	-	SAV1171	hypothetical protein SAV1171
RNM6 up	1.0	0.7	2.9	1010	2976	glpF	SAV1300	glycerol uptake facilitator
RNM6 up	1.0	0.9	3.7	237	880	-	SAV1303	lysophospholipase
RNM6 up	1.0	1.0	2.5	606	1497	miaA	SAV1304	tRNA delta(2)-isopentenylpyrophosphate
RNM6 up	2.4	1.1	2.5	84	209	-	SAV1314	hypothetical protein SAV1314
RNM6 up	1.5	1.0	2.5	501	1267	-	SAV1377	hypothetical protein SAV1377
RNM6 up	0.8	0.8	3.8	225	852	-	SAV1403	hypothetical protein SAV1403
RNM6 up	1.4	1.1	3.2	765	2486	-	SAV1431	hypothetical protein SAV1431
RNM6 up	1.2	1.2	2.9	95	276	-	SAV1496	hypothetical protein SAV1496
RNM6 up	1.3	1.1	2.5	684	1695	-	SAV1503	putative pyrroline-5-carboxylate reductase
RNM6 up	0.9	0.8	2.8	332	946	-	SAV1538	shikimate kinase
RNM6 up	0.9	1.1	3.5	659	2307	tag	SAV1664	DNA-3-methyladenine glycosidase
RNM6 up	0.5	0.5	2.5	1492	3746	phoP	SAV1693	alkaline phosphatase synthesis transcriptional
RNM6 up	1.2	1.0	4.0	373	1489	-	SAV1723	transaminase
RNM6 up	1.3	0.9	3.6	635	2279	serA	SAV1724	D-3-phosphoglycerate dehydrogenase
RNM6 up	0.8	1.1	4.9	106	522	acuA	SAV1734	acetoin dehydrogenase-like protein
RNM6 up	1.1	0.8	3.8	265	996	acuC	SAV1735	acetoin utilization protein
RNM6 up	1.1	0.9	2.6	1009	2652	-	SAV1775	glucosaminidase
RNM6 up	0.8	0.8	2.7	312	829	-	SAV1776	hypothetical protein SAV1776
RNM6 up	0.9	0.7	3.3	73	242	splB	SAV1812	serine protease
RNM6 up	0.6	0.8	2.5	412	1036	-	SAV1938	truncated map-w protein
RNM6 up	0.2	0.6	2.8	656	1838	-	SAV1940	hypothetical protein SAV1940
RNM6 up	0.2	0.7	3.0	1231	3690	-	SAV2004	hypothetical protein SAV2004
RNM6 up	0.1	0.6	4.0	1877	7578	-	SAV2005	hypothetical protein SAV2005
RNM6 up	1.3	0.9	2.5	379	939	-	SAV2033	hypothetical protein SAV2033
RNM6 up	0.9	1.1	2.8	330	924	ilvB	SAV2054	acetolactate synthase large subunit
RNM6 up	0.7	1.2	2.7	248	664	-	SAV2055	acetolactate synthase 1 regulatory subunit
RNM6 up	0.9	0.5	4.0	223	883	kdpC	SAV2075	potassium-transporting ATPase subunit C
RNM6 up	0.8	0.8	7.2	220	1574	kdpB	SAV2076	potassium-transporting ATPase subunit B
RNM6 up	0.8	0.7	17.2	117	2021	kdpA	SAV2077	potassium-transporting ATPase subunit A
RNM6 up	0.4	0.8	14.6	218	3190	kdpD	SAV2078	sensor protein
RNM6 up	0.3	1.0	15.7	150	2340	kdpE	SAV2079	KDP operon transcriptional regulatory protein
RNM6 up	1.3	0.8	3.0	127	384	-	SAV2321	sodium-dependent transporter
RNM6 up	0.9	0.7	3.0	174	531	-	SAV2354	transcriptional regulator
RNM6 up	1.1	1.2	2.8	224	623	-	SAV2369	transcription repressor of sporulation, septation
RNM6 up	1.5	1.0	2.9	163	480	-	SAV2405	hypothetical protein SAV2405
RNM6 up	0.5	0.7	2.7	1878	5014	-	SAV2415	multidrug resistance protein YcnB
RNM6 up	0.5	0.8	3.0	1027	3126	-	SAV2440	hypothetical protein SAV2440

RNM6 up	1.1	0.8	2.7	332	898	opuCA	SAV2448	glycine betaine/carnitine/choline ABC
RNM6 up	1.0	0.8	2.6	191	489	-	SAV2492	hypothetical protein SAV2492
RNM6 up	0.7	0.8	4.2	331	1390	-	SAV2508	MerR family transcription regulator
RNM6 up	0.8	0.9	3.0	264	782	-	SAV2513	alkaline phosphatase
RNM6 up	1.3	1.1	3.3	121	403	-	SAV2518	phospholipase/carboxylesterase family protein
RNM6 up	0.7	0.7	3.8	199	758	-	SAV2519	glyoxylase family protein
RNM6 up	1.5	0.8	3.0	172	522	-	SAV2520	MarR family transcription regulator
RNM6 up	0.9	1.2	3.2	143	454	-	SAV2537	hypothetical protein SAV2537
RNM6 up	1.3	0.9	3.4	281	950	-	SAV2544	secretory antigen precursor SsaA
RNM6 up	0.7	0.8	2.7	393	1065	-	SAV2603	amino acid transporter
RNM6 up	0.5	0.7	3.9	143	552	-	SAV2604	4-aminobutyrate aminotransferase
RNM6 up	0.4	1.3	2.6	332	866	-	SAV2616	anaerobic (class III) ribonucleotide reductase
RNM6 up	0.3	1.5	3.0	1017	3045	nrdD	SAV2617	anaerobic ribonucleoside triphosphate
RNM6 up	0.9	0.6	7.9	235	1863	-	SAV2631	transcriptional regulator
RNM6 up	0.6	0.5	8.3	932	7734	arcC	SAV2632	carbamate kinase
RNM6 up	0.3	0.3	8.4	750	6325	arcD	SAV2633	arginine/oirnithine antiporter
RNM6 up	0.2	0.2	9.4	638	6005	arcB	SAV2634	ornithine carbamoyltransferase
RNM6 up	0.1	0.2	8.2	1186	9694	arcA	SAV2635	arginine deiminase
RNM6 up	1.6	1.2	2.9	91	264	-	SAV2682	hypothetical protein SAV2682
RNM6 up	1.2	0.9	2.7	164	436	-	SAV2683	cobalt ABC transporter
RNM6 down	0.9	1.0	0.4	6005	2584	gyrB	SAV0005	DNA gyrase subunit B
RNM6 down	0.5	1.1	0.4	362	131	-	SAV0122	hypothetical protein SAV0122
RNM6 down	0.7	0.9	0.4	11370	5073	glcA	SAV0189	PTS enzyme II
RNM6 down	1.9	1.8	0.2	1877	417	xprT	SAV0388	xanthine phosphoribosyltransferase
RNM6 down	1.9	1.8	0.1	3554	425	pbuX	SAV0389	xanthine permease
RNM6 down	1.5	1.8	0.4	12104	4349	guaB	SAV0390	inositol-monophosphate dehydrogenase
RNM6 down	1.3	1.6	0.3	8717	2610	guaA	SAV0391	GMP synthase
RNM6 down	1.0	1.3	0.4	6726	2773	-	SAV0519	pyridoxal biosynthesis lyase PdxS
RNM6 down	1.1	1.0	0.4	14816	5789	rplA	SAV0538	50S ribosomal protein L1
RNM6 down	1.1	1.0	0.4	7158	2829	rplL	SAV0540	50S ribosomal protein L7/L12
RNM6 down	1.7	1.1	0.4	1183	532	-	SAV0680	lysine decarboxylase family protein
RNM6 down	1.4	1.2	0.3	1135	353	-	SAV0681	hypothetical protein SAV0681
RNM6 down	1.1	1.4	0.4	419	177	norA	SAV0695	quinolone resistance protein
RNM6 down	0.5	1.0	0.4	7157	2507	-	SAV0698	transcription repressor of fructose operon
RNM6 down	0.4	1.0	0.2	10034	2085	fruB	SAV0699	fructose 1-phosphate kinase
RNM6 down	0.5	0.9	0.2	6102	1105	fruA	SAV0700	fructose specific permease
RNM6 down	0.6	0.8	0.2	2027	498	nagA	SAV0701	N-acetylglucosamine-6-phosphate deacetylase
RNM6 down	1.1	1.5	0.4	1017	416	recQ	SAV0721	DNA helicase
RNM6 down	2.5	1.7	0.1	2584	265	-	SAV0736	lipoprotein
RNM6 down	0.7	1.1	0.4	33246	13834	-	SAV0752	ribosomal subunit interface protein
RNM6 down	0.7	1.2	0.4	795	352	clpB	SAV0975	ClpB chaperone-like protein
RNM6 down	1.3	0.9	0.4	873	359	-	SAV1022	toxic anion resistance protein
RNM6 down	1.6	1.3	0.4	2177	910	menD	SAV1043	menaquinone biosynthesis protein
RNM6 down	1.1	0.9	0.4	2883	1295	-	SAV1075	hypothetical protein SAV1075
RNM6 down	1.0	0.9	0.4	6531	2898	-	SAV1076	cation ABC transporter
RNM6 down	1.6	1.5	0.2	1605	330	-	SAV1086	cytochrome D ubiquinol oxidase subunit 1-like

RNM6 down	1.9	1.5	0.2	555	109	-	SAV1087	cytochrome D ubiquinol oxidase subunit II-like
RNM6 down	3.0	1.4	0.4	216	84	potB	SAV1100	spermidine/putrescine ABC transporter
RNM6 down	2.5	1.2	0.3	414	138	potC	SAV1101	spermidine/putrescine ABC transporter
RNM6 down	2.5	1.6	0.3	1206	379	potD	SAV1102	spermidine/putrescine-binding protein
RNM6 down	1.0	1.1	0.4	5060	2161	pheT	SAV1139	phenylalanyl-tRNA synthetase subunit beta
RNM6 down	0.9	0.9	0.4	1703	599	mutS2	SAV1144	recombination and DNA strand exchange
RNM6 down	1.0	1.2	0.4	5006	2025	murD	SAV1183	UDP-N-acetylmuramoyl-L-alanyl-D-glutamate
RNM6 down	1.4	1.1	0.4	1568	672	-	SAV1197	ribosomal large subunit psudouridine synthase D
RNM6 down	2.8	0.8	0.3	732	246	pyrP	SAV1199	uracil permease
RNM6 down	2.9	1.0	0.3	1459	410	pyrB	SAV1200	aspartate carbamoyltransferase catalytic subunit
RNM6 down	2.9	1.1	0.3	3380	1151	pyrC	SAV1201	dihydroorotase
RNM6 down	3.1	1.2	0.4	2056	761	pyrAA	SAV1202	carbamoyl phosphate synthase small subunit
RNM6 down	3.1	1.3	0.4	3468	1277	carB	SAV1203	carbamoyl phosphate synthase large subunit
RNM6 down	2.8	1.4	0.3	2409	714	pyrF	SAV1204	orotidine 5'-phosphate decarboxylase
RNM6 down	2.6	1.6	0.3	2220	665	pyrE	SAV1205	orotate phosphoribosyltransferase
RNM6 down	1.0	1.0	0.4	11461	4908	rplS	SAV1241	50S ribosomal protein L19
RNM6 down	1.1	1.0	0.4	13152	5347	rpsO	SAV1273	30S ribosomal protein S15
RNM6 down	0.9	1.1	0.4	22949	9098	glnA	SAV1310	glutamine-ammonia ligase
RNM6 down	1.2	1.3	0.4	209	84	trpB	SAV1372	tryptophan synthase subunit beta
RNM6 down	1.2	1.4	0.4	3182	1392	dnaK	SAV1580	molecular chaperone DnaK
RNM6 down	1.0	1.4	0.4	6277	2399	grpE	SAV1581	GrpE protein
RNM6 down	1.3	1.0	0.4	3064	1259	-	SAV1612	protease
RNM6 down	0.8	1.1	0.4	3277	1465	alaS	SAV1618	alanyl-tRNA synthetase
RNM6 down	2.0	1.3	0.4	6183	2621	tgt	SAV1639	queuine tRNA-ribosyltransferase
RNM6 down	1.0	1.3	0.4	4543	1900	valS	SAV1663	valyl-tRNA synthetase
RNM6 down	1.2	1.2	0.4	1444	534	metK	SAV1790	S-adenosylmethionine synthetase
RNM6 down	0.9	1.7	0.4	4546	1861	groEL	SAV2029	chaperonin GroEL
RNM6 down	0.5	1.8	0.4	1600	676	groES	SAV2030	co-chaperonin GroES
RNM6 down	0.9	1.1	0.4	223	100	-	SAV2095	SceD precursor
RNM6 down	1.2	1.2	0.4	5160	1983	rpmE2	SAV2120	50S ribosomal protein L31 type B
RNM6 down	1.3	0.9	0.2	8279	1854	pyrG	SAV2127	CTP synthetase
RNM6 down	0.4	0.8	0.4	252	95	lacG	SAV2189	6-phospho-beta-galactosidase
RNM6 down	1.5	1.1	0.4	11718	4442	rpsI	SAV2217	30S ribosomal protein S9
RNM6 down	1.0	1.1	0.4	18835	7901	rplQ	SAV2223	50S ribosomal protein L17
RNM6 down	0.9	1.0	0.4	27055	10608	rpoA	SAV2224	DNA-directed RNA polymerase subunit alpha
RNM6 down	1.0	1.0	0.4	32195	14028	rpsK	SAV2225	30S ribosomal protein S11
RNM6 down	0.9	1.0	0.4	39363	16624	rpsM	SAV2226	30S ribosomal protein S13
RNM6 down	1.1	1.0	0.4	39489	17436	rpsC	SAV2244	30S ribosomal protein S3
RNM6 down	1.1	1.0	0.4	43115	18294	rpsS	SAV2246	30S ribosomal protein S19
RNM6 down	1.2	0.9	0.4	44182	19203	rplD	SAV2249	50S ribosomal protein L4
RNM6 down	1.0	0.8	0.3	493	164	-	SAV2301	Na_ antiporter
RNM6 down	1.0	0.8	0.4	1164	417	-	SAV2302	D-octopine dehydrogenase
RNM6 down	0.2	1.1	0.3	951	284	-	SAV2395	nitrate reductase delta chain
RNM6 down	0.2	1.0	0.4	1634	693	narH	SAV2396	nitrate reductase beta chain
RNM6 down	3.8	1.4	0.4	2934	1314	ddh	SAV2524	D-lactate dehydrogenase
RNM6 down	0.3	0.8	0.3	7129	2026	ptsG	SAV2538	PTS system, glucose-specific II ABC component

APPENDIX B: CHARACTERIZATION OF SPM SPONTANEOUS RESISTANT MUTANTS

In addition to MuM as characterized in Chapter 2, nine more Spm-resistant mutants were independently isolated from agar containing Spm at 8x MIC or higher at a frequency of $1x10^{-8}$: three strains from RN4220 (MSSA; a common lab strain), one from Mu50 (MRSA) and five from COL (MRSA). To further investigate the molecular basis of Spm resistance, the phenotypes and genotypes of those Spm^R mutants were characterized and described below.

Increased resistance to β-lactam/Spm synergy among Spm^R mutants

MuM and nine more Spm^R mutants were further tested on their susceptibility to Spm and synergy. In comparison to the their parental strains, all mutants exhibited 32-64 fold increment on Spm MIC, regardless the growth conditions for MIC measurements (Table B.2). Notably, all these mutants also displayed greater resistance to Spm/β-lactam synergy although they were selected under Spm-only stress. The correlation between Spm resistance and synergy resistance existed universally among those Spm^R mutants regardless their strain background or genetic modification(s).

Growth phenotypes of the Spm^R mutants

The lack of PBP2 TPase domain impaired dramatically the growth/fitness of MuM. In order to see whether other Spm^R mutants shared similar characteristics, we analyzed the growth phenotypes in the following aspects: 1) the growth rate in Spm-free LB; 2) the growth behavior in response to Spm; 3) whether the supplement of glucose can restore, if any, the growth deficit; 4) whether the growth deficit, if any, is related to Spm resistance.

When incubated in theLB medium, three Spm^R mutants-RNM6, COLM2, and COLM7- showed impaired growth, with great reduction on final yield and slight decrease on growth rate (Table B.1). Glucose

supplement in the LB medium can improve the growth by reducing the doubling time and increasing the final yield (Figure B.1).

Next, growth kinetics in response to Spm were recorded in three RN4220 derived mutants (RNM2, RNM4, RNM6). In comparison to RN4220, the growth rate of RNM2 and RNM4 was hardly affected by Spm while RNM4 showed similar behavior as the parent. But even so, RNM4 still displayed high tolerance to Spm when incubated for long period as evidenced by the MIC measurement (Table B.2). This seemingly contradictory observation may indicate a unique defense mechanism of RNM4 to Spm toxicity.

Identification of mutation sites in Spm^R mutants

To further evaluate the molecular basis of Spm resistance, several Spm^R mutants derived from either RN4220 or Mu50 were subjected to genome sequencing . Genomic DNA was extracted by the phenol/chloroform method and DNA sequencing was conducted by 454 pyrosequencing. Plausible mutations were identified from sequence comparison and further confirmed by PCR-based sequencing aslisted in Table B.3.Interestingly, although those mutants were isolated independently, two mutations were shared between different variants: R153L at SigA, and D67E at RelA in both RNM2 and RNM4. For the Mu50 derivative, MuM3, only one mutation at the intergenic region of *mntC* and *tnp* (transposase) was identified in this study.

Complementation

In order to see whether the identified mutations are responsible for Spm resistance, each candidate gene (including its ORF and upstream regulatory region) was amplified from wt and mutant genome, individually cloned into *E. coli-S. aureus* shuttle vector pCN33 (copy number 10-15), and transformed into either wildtype or corresponding Spm^R mutants. Table B.4 showed the complementing plasmids

constructed so far, and most of these plasmids were successfully introduced in *S. aureus* strains. For *sigA* and *atpG*, even after many trials, no transformants can be obtained.

Next, to understand the role of the candidate genes in Spm resistance, the Spm MIC was determined in those recombinant strains. For those tested strains, as revealed by Table B.5, their susceptibility to Spm didn't show any changes regardless of the wt or mutant genes introduced. Since only one but not all mutations was complemented in those transformants, how the candidate genes contribute to the resistance remained unclear, and the possibility of combinational effects by multiple mutations cannot be ruled out.

Transcriptome analysis

To obtain a comprehensive view on how these mutations affect the transcriptome, the gene expression profiles of RNM2, RNM4, and RNM6 (derived from RN4220) -were analyzed by DNA microarrays (Affymetrix GeneChip). Incomparison to their parents, 178, 21, and 108 genes showed significant changes (with >2.5 fold change and signal intensity >200) in RNM2, RNM4, and RNM6, respectively. Notably, consistent with the similar growth behavior with its parent RN4220, the expression profile of RNM4 showed the least changes, with only 21genes down-regulated. Notably, unlike *sigA* and *relA* which were present in both RNM2 and RNM4, mutation on *trkA* was unique to RNM2 while the transcriptomes of RNM2 and RNM4 were vastly varied. Therefore, *trkA* may play an important role in regulating the transcriptional changes in RNM2, and possibly the resistance to Spm.

Table B. 1 Summary of Spm^R mutants selected from different lineage of *S. aureus*

Strain	Spm susceptibility	β-lactam/Spm susceptibility	Growth phenotype (LB)	
			generation time (min)	final yield (OD_{600})
Mu50	S	S	35	4.6
MuM	R	R	127	1.4
MuM3	R	R	37	4.5
RN4220	S	S	24	4.9
RNM2	R	R	30	5.1
RNM4	R	R	29	4.6
RNM6	R	R	33	2.1
COL	S	S	42	3.2
COLM1	R	R	45	3.1
COLM2	R	R	53	0.8
COLM5	R	R	40	3.1
COLM6	R	R	44	2.8
COLM7	R	R	56	0.9

Mu50 (MRSA), RN4220 (MSSA), and COL (MRSA) are parental strains sensitive to Spm and Spm/β-lactam synergy. S, sensitive; R, resistant.

Table B. 2 MICs of Spm or β-lactams in Spm^R mutants

	Spm			β-lactam[1]	
	broth, no shaking	broth, shaking	agar plate	no Spm	Spm[2]
Mu50	2	2	4	512	0.5
MuM	32	64	64	512	512
MuM3	>64	ND	ND	512	512
RN4220	4	4	4	8	<0.01
RNM2	8	64	64	8	16
RNM4	32	64	64	8	8
RNM6	16	64	64	8	16
COL	0.25	ND	ND	256	<0.5
COLM1	16	ND	ND	512	512
COLM2	16	ND	ND	512	512
COLM5	16	ND	ND	512	512
COLM6	16	ND	ND	512	512
COLM7	16	ND	ND	512	512

[1]β-lactams used in the combinational treat: oxacillin for Mu50 and its derivatives; ceftazidime for RN4220 and its derivatives. [2] Spm concentration used in the combinational treat: 0.5mM for Mu50, RNN4220 and their derivatives; 0.1mM for COL and its derivatives

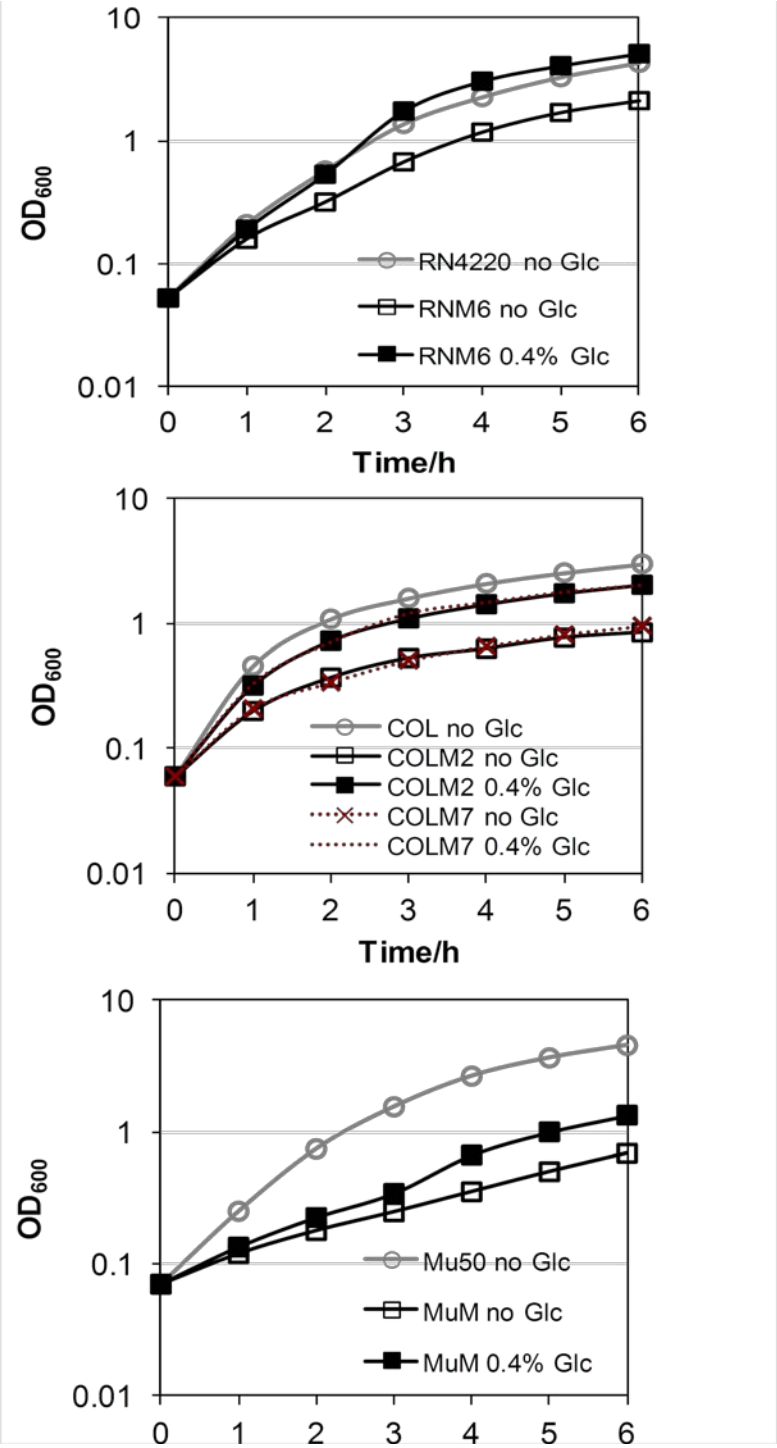

Figure B. 1 Glucose effects on the growth deficient Spm^R mutants.

Growth deficient mutants: MuM, RNM6, COLM2, and COLM7

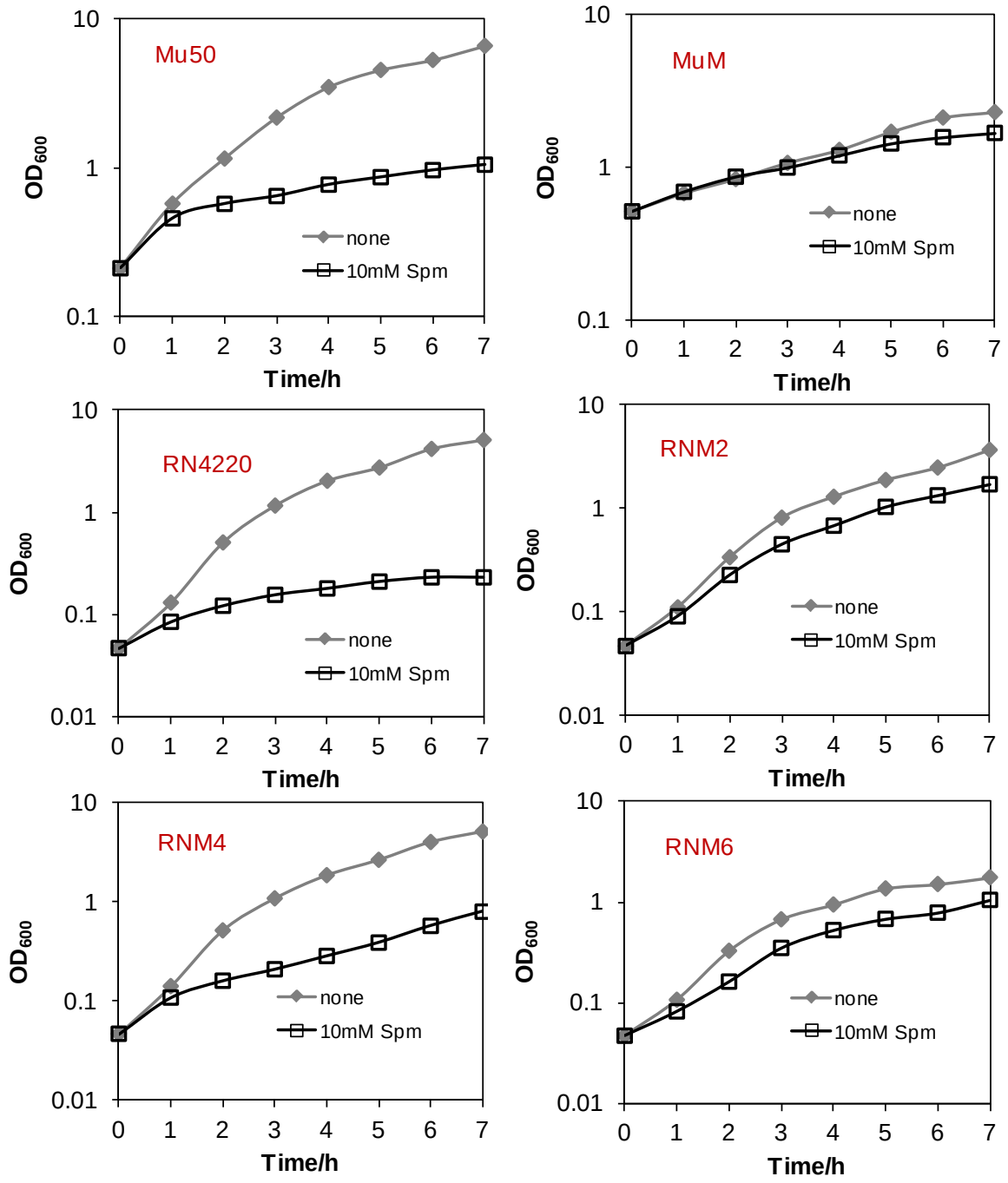

Figure B. 2 Growth kinetics of wildtype and Spm^R mutants on exposure to Spm

Wildtype: Mu50, RN4220; Spm^R mutants: MuM, RNM2, RNM4, RNM6

Table B. 3 Mutations identified in Spm^R mutants

ORF ID	Gene and Protein Name	Protein Sequence Length	Mutation Type	Mutation Presented Mutants	Parent Strain
SAV1450	*pbpB*, PBP2	727	7-bp deletion in TPase domain, after F455	MuM	Mu50
Intergenic region, downstream of SAV0631(*mntC*), upstream of SAV0630(*tnp*)		-	C to A	MuM3	Mu50
SAOUHSC_01034	*SA0939*, Hypothetical protein (similar to TrkA K^+ uptake family)	220	CAT to TAT(H47Y)	RNM2	RN4220
SAOUHSC_01662	*sigA*, RNA polymerase sigma factor RpoD	368	CGT to CTT(R153L)	RNM2,RNM4	RN4220
SAOUHSC_01742	*relA*, GTP pyrophosphokinase	736	GAC to GAA(D67E)	RNM2,RNM4	RN4220
SAOUHSC_02343	*atpG*, F0F1 ATP synthase gamma chain	288	ACT to CCT(T228P)	RNM6	RN4220
SAOUHSC_02822	*fbp*, Fructose-1,6-bisphosphatase class 3	654	ATG to ATA(M493I)	RNM6	RN4220

Table B. 4 Summary of complementation experiments.

	trkA		***sigA***		***relA***		***atpG***		***fbp***	
	wt	mt	wt	mt	wt	mt	wt	mt	wt	mt
Correct construct in *E.coli*	+	+	+	-	+	+	+	-	+	-
Transformed into *S. aureus*	+	+	-	-	+	+	-	-	+	- (in puc18)
Complemented	-	-	NA	NA	-	-	NA	NA	-	NA

wt, wildtype copy of candidate gene; mt, mutant copy of candidate gene
+, done or yes; -, not done or no.
e.g. the both wildtype and mutant copy of *trkA* have been cloned and transformed into either wildtype host or mutant host. The plasmid-borne wt *trkA* cannot restore Spm sensitivity in RNM2 (having *trkA* mutation on chromosome); likewise, the plasmid-borne mutant *trkA* was unable to make RN4220 become resistant to Spm.

Table B. 5 MICs of Spm in wildtype, Spm^R mutants and complementing strains.

Strain	Spm MIC (mM)
RN4220	4
RNM2	64
RNM4	64
RNM6	64
RN4220/m*trkA*	4-8
RN4220/m*relA*	4-8
RNM2/*trkA*	64
RNM2/*relA*	64
RNM4/*relA*	64
RNM6/*fbp*	64

m*trkA*, m*relA*, mutant copy of *trkA*, *relA*

Table B. 6 Statistics of 454 genome sequencing.

Performed using 454 GS FLX system (in 2009) or GS Junior (in 2012)

	Mu50	**MuM**	**MuM3**	**RN4220**	**RM2**	**RM4**	**RM6**
Sequencing system	GS FLX system		GS Junior	GS FLX system			
Reference sequence	NC_002758			NC_007795			
Num. Reads:	35180	39901	201155	26880	28333	35008	39915
Num. Bases:	13105328	15109299	83723458	9542418	10031840	13054399	13837616
Mapped Reads:	34398 (97.66%)	38927 (97.44%)	198178	26832 (99.67%)	28253 (99.53%)	34916 (99.57%)	39864 (99.75%)
Mapped Bases:	12819807 (97.81%)	14732960 (97.50%)	82914115	9506674 (99.61%)	9994602 (99.60%)	13010233 (99.64%)	13796679 (99.69%)
Ref genome size(bp)	2878529			2821361			
Avg. Map Length	373	379	418	355	354	373	347
# of contigs	509	353		842	757	448	372
Avg. contig size	5483	7953		3052	3410	5857	7093
Min. contig size	101	116		100	124	103	103
Max. contig size	42330	89033	2841620	20527	38706	38685	48360

APPENDIX C: SELECTED PUBLICATIONS

AAC Journals.ASM.org

A PBP 2 Mutant Devoid of the Transpeptidase Domain Abolishes Spermine–β-Lactam Synergy in *Staphylococcus aureus* Mu50

Xiangyu Yao[a] and Chung-Dar Lu[a,b]

Department of Biology, Georgia State University, Atlanta, Georgia, USA,[a] and Department of Medical Laboratory Sciences and Biotechnology, China Medical University, Taichung, Taiwan[b]

Exogenous spermine was reported to enhance the killing of methicillin-resistant *Staphylococcus aureus* (MRSA) by β-lactams through a strong synergistic effect of unknown nature. Spermine alone also exerts an antimicrobial activity against *S. aureus* in a pH-dependent manner. MIC measurements revealed stronger effects of spermine under alkaline conditions, suggesting the nucleophilic property of spermine instead of its positive charge as the cause of adverse effects. A spontaneous suppressor mutant (MuM) of MRSA Mu50 was selected for spermine resistance and conferred complete abolishment of spermine–β-lactam synergy. In comparison to that in Mu50, the spermine MIC in MuM remained constant (64 mM) at pH 6 to 8; however, MuM, a heat-sensitive mutant, also grew in a very narrow pH range. Furthermore, MuM acquired a unique phenotype of vancomycin-spermine synergy. Genome resequencing revealed a 7-bp deletion in *pbpB*, which results in a truncated penicillin-binding protein 2 (PBP 2) without the transpeptidase domain at the C terminus while the N-terminal transglycosidase domain remains intact. The results of fluorescent Bocillin labeling experiments confirmed the presence of this defective PBP 2 in MuM. All the aforementioned phenotypes of MuM were reverted to those of Mu50 after complementation by the wild-type *pbpB* carried on a recombinant plasmid. The anticipated changes in cell wall metabolism and composition in MuM were evidenced by observations that the cell wall of MuM was more susceptible to enzyme hydrolysis and that MuM exhibited a lower level of autolytic activities. Pleiotropic alterations in gene expression were revealed by microarray analysis, suggesting a remarkable flexibility of MuM to circumvent cell wall damage by triggering adaptations that are complex but completely different from that of the cell wall stress stimulon. In summary, these results reveal phenotypic changes and transcriptome adaptations in a unique *pbpB* mutant and provide evidence to support the idea that exogenous spermine may perturb normal cell wall formation through its interactions with PBP 2.

Methicillin-resistant *Staphylococcus aureus* (MRSA) constitutes a major health concern due to its numerous mechanisms of virulence and rapid acquisition of genes conferring resistance to β-lactams. New agents that can suppress or abrogate the emergence of resistance, therefore, are in great demand. Here we are interested in the potential application of biogenic polyamines, a group of small polycationic compounds widely distributed in prokaryotic and eukaryotic cells (8), to enhancing the bacterial susceptibility to β-lactam antibiotics. While spermine (a tetraamine) at high concentrations was reported to exert an intrinsic antibacterial activity in *S. aureus* (12), our previous studies have demonstrated the capability of exogenous spermine at low concentrations to reverse MRSA susceptibility to β-lactams (20). However, the molecular mechanism of this strong synergistic effect by spermine and β-lactams in *S. aureus* was still unclear.

β-Lactam antibiotics function by irreversibly occupying the serine residue at the active sites of penicillin-binding proteins (PBPs), and formation of this stable ester-linked acyl enzyme inhibits the transpeptidation step during cell wall cross-linking (11). In *S. aureus*, there are four native PBPs (PBPs 1 to 4) and one acquired PBP, PBP 2a, which is characteristic of MRSA. In contrast to other PBPs, PBP 2a, encoded by the *mecA* gene, shows low affinity to β-lactams due to inefficient formation of the acyl-PBP intermediate and thus ensures continued cell wall synthesis when normal PBPs are inactivated by β-lactams (13). Besides *mecA*, additional factors affecting cell wall architecture or synthesis are believed to have the potential to perturb or modulate β-lactam resistance in *S. aureus*, such as glycan chain length (27), stem peptide configuration (10), pentaglycine cross-bridges (3), and coordinated activity of peptidoglycan (PG) biosynthesis and autolysis (2). Particularly, one of the native PBPs, PBP 2, is essential for the high level of methicillin resistance in MRSA. PBP 2 belongs to the high-molecular-weight class A PBPs, with a transglycosidase (TG) domain and a transpeptidase (TP) domain. When exposed to β-lactams, PG synthesis in MRSA can be achieved at the division septum, mediated by the cooperative functioning of the TG domain of PBP 2 and the TP domain of PBP 2A, possibly as part of a multienzyme complex in cell wall synthesis (27, 29).

In the current study, we isolated an MRSA strain derivative (MuM) conferring spermine resistance by serial passages *in vitro* and compared its genetic basis as well as its phenotypic profiles with those of its parental strain Mu50. We found that this mutant not only shows a 32-fold increase in tolerance of growth inhibition by spermine but also has completely lost the spermine–β-lactam synergy. Furthermore, a 7-bp deletion within the *pbpB* gene, which encodes the essential PBP 2, was revealed by genome resequencing, through which the transpeptidase activity was deprived. Complementation of plasmid-borne wild-type *pbpB* to the mu-

Received 29 July 2011 **Returned for modification** 26 September 2011
Accepted 9 October 2011
Published ahead of print 17 October 2011
Address correspondence to Chung-Dar Lu, biocdl@gsu.edu.
Supplemental material for this article may be found at http://aac.asm.org/.

doi:10.1128/AAC.05415-11

tant can restore its sensitivity to both spermine and the synergy. In addition, reduced tolerance of the cell wall to hydrolysis and decreased autolytic activity were observed in this mutant, which may be due to changes in cell wall metabolism as a result of this *pbpB* lesion. This mutation also had a pleiotropic effect on gene expression as revealed by transcriptome analysis. Taken together, our results lend support to the idea that exogenous spermine may affect cell wall synthesis through its interactions with PBP 2 and/or PBP 2-assoicated multienzyme machineries to enhance the killing effects of β-lactam antibiotics.

MATERIALS AND METHODS

Bacterial strains, plasmids, and growth conditions. *S. aureus* Mu50 (ATCC 700699), COL (obtained from NARSA), and RN4220 (kindly provided by R. P. Novick) and *Escherichia coli* DH5α (Bethesda Research Laboratories) were employed in this study. Plasmid pCN38 (carrying ampicillin and chloramphenicol resistance), a shuttle vector of *E. coli* and *S. aureus* (6), was used for gene cloning. Both *E. coli* and *S. aureus* strains were routinely grown and maintained in the Luria-Bertani (LB) medium. When required, the LB medium was buffered with 20 mM Tris-HCl at the indicated pH. Antibiotics were added to the medium as necessary at the following concentrations: ampicillin, 100 μg/ml (for *E. coli*); chloramphenicol, 10 μg/ml (for *S. aureus*).

Isolation of spermine-resistant mutants. Spontaneous mutants of MRSA Mu50 (oxacillin MIC of 512 μg/ml and spermine MIC of 1 mM at pH 8.0) were isolated by spreading 1×10^8 CFU of log-phase cells onto spermine-containing plates (2 to 8 mM, pH 8.0) and incubated overnight at 37°C. One independent colony was recovered from plates with 8 mM spermine, and it remained resistant to spermine (up to 32 mM) in broth and on plates. This mutant strain was designated MuM in this study.

Genotypic characterization of spermine-resistant mutant MuM. The chromosomal mutation in MuM was identified by pyrosequencing carried out using the 454 Life Sciences Technology at the University of Florida. Genomic DNAs from both Mu50 and MuM were sent for sequencing, assembled, and compared to the published genomic sequence of *S. aureus* Mu50 (GenBank accession no. BA000017.4). The mutation unique to MuM identified in the *pbpB* gene was confirmed by PCR amplification and DNA sequencing with primers 5′-GGT TTA GTT GCT ATA TCT GGT GG-3′ and 5′-CGC GTT GTT ATA AGT ACC ACC G-3′.

Spermine and antibiotic susceptibility tests. MICs of antibiotics or spermine were determined by a liquid microdilution method according to the guidelines of the Clinical and Laboratory Standards Institute (7). Serial 2-fold dilutions of tested compounds were prepared in a 96-well microtiter tray, and fresh overnight cultures of each bacterial strain were diluted and inoculated with approximate 10^5 CFU/well. Cells were incubated without shaking at 37°C for 24 h (or for up to 36 h as specified). The lowest concentration of antimicrobial agent at which cells were not able to grow was defined as its MIC.

Transcriptome analysis. Mu50 and MuM were grown in Tris-buffered LB (pH 7.5), and cultures in the exponential phase (optical density at 600 nm [OD_{600}] of around 1.0) were immediately treated with the RNA protection reagent (Qiagen) before harvesting. RNA samples were extracted from cells with phenol (Fisher), digested with RNase-free DNase I (Roche) to remove genomic DNA, and purified with RNeasy minicolumns (Qiagen). cDNA synthesis, fragmentation, and terminal labeling were carried out according to the protocols of the manufacturer (Affymetrix). Labeled cDNA was hybridized to the GeneChip *S. aureus* genome array. After scanning, the images were processed with GCOS 1.4 software (Affymetrix). Data from three independent biological experiments were analyzed by comparing gene expression by MuM to that by Mu50, with a fold change of over 2.5 and signal intensity value of 200 as the threshold.

Complementation of *pbpB*. The *pbpB* gene was reported to be transcribed independently or as a polycistronic RNA from its upstream *prfA* promoter (28). To ensure optimal expression, a 3.2-kb fragment covering both *prfA* and *pbpB* was amplified by PCR from the Mu50 genomic DNA with the primers 5′-CGC GGA TCC ACA CAT ACT TGT ACT TGC CTC-3′ (forward and 5′-CGC GGC GCC GAG TGG ATT AGT TGA ATA TAC CTG TTA ATC CAC CGC TG-3′ (reverse). The resulting PCR product was cloned into the BamHI and NarI sites of the shuttle vector pCN38. The recombinant plasmid pYX9 was first cloned into and extracted from *E. coli* and then electroporated into *S. aureus* RN4220 (Bio-Rad Gene-Pulser Xcell) with parameters as described previously (19). Plasmid DNA isolated from recombinant strains of RN4220 was subsequently introduced into Mu50 and MuM by electroporation.

PBP profiling. Membrane fractions were prepared as described previously (25) for detection of PBPs. Protein samples (50 μg) were incubated with 5 μM Bocillin FL (Invitrogen) for 30 min, followed by SDS-PAGE on a 10% gel. The fluorescent Bocillin covalently bound to the PBPs was detected with excitation at 488 nm and emission at 520 nm (Typhoon 9400). Due to its low affinity to Bocillin, PBP 2a was detected by immunoblotting with mouse anti-PBP 2a antibodies (Abnova; 1:5,000 dilution), followed by rabbit anti-mouse IgG antibodies conjugated with alkaline phosphatase (Sigma; 1:30,000 dilution) and chromogenic substrates.

Triton X-100-induced autolysis assays. The Triton X-100-induced autolysis assay was conducted by following a protocol as described previously (9) with minor modifications. Briefly, cells were harvested, washed twice with ice-cold water, and then resuspended in the same volume of 50 mM Tris-HCl (pH 7.2) containing 0.05% Triton X-100. Cells were incubated at 30°C with shaking (~250 rpm) and checked for lysis by measuring the progressive decrease in absorbance (OD_{600}). Autolysis was quantified as a percentage of the initial OD_{600} remaining at each sampling point.

Preparation of autolytic enzyme extracts. Cellular extracts enriched with autolytic enzymes were prepared as previously described (16) with some modifications. Briefly, the cells were grown to mid-exponential phase in 20 ml of LB (20 mM Tris-Cl, pH 7.5) at 37°C with aeration to an OD_{600} of 1, chilled on ice, harvested by centrifugation, and washed twice with ice-cold 50 mM Tris-HCl (pH 7.5) buffer with 150 mM NaCl. The pellet was directly suspended in 80 μl of 4% SDS for 30 min at room temperature or in 400 μl of a solution containing 3 M LiCl and 0.1% Triton X-100 for 30 min at 4°C with stirring. After centrifugation at 10,000 × *g* for 10 min, the supernatants were collected as SDS extracts or LiCl extracts, which were used in zymographic analysis or *in vitro* enzymatic hydrolysis of crude cell walls, respectively.

Enzymatic hydrolysis of crude cell walls *in vitro*. Enzymatic hydrolysis of crude cell walls *in vitro* was performed as previously described (2). Briefly, crude cell walls were prepared from cells (10 ml) grown to mid-exponential phase (OD_{600} of around 1). Cell pellets were boiled in 8% SDS for 30 min and washed three times with hot water to remove SDS. The obtained pellets, as crude cell walls, were suspended in 50 mM Tris-HCl (pH 7.5) to an OD_{600} of 0.6, and LiCl extracts as described above were added to start hydrolysis. The reaction was conducted at 37°C with shaking (~250 rpm), and the hydrolysis rate was measured as a decrease of OD_{600}.

Zymographic analysis. Heat-killed cells of *S. aureus* RN4220 were prepared as the substrate for hydrolytic enzymes. Briefly, cells in mid-exponential phase were harvested, and the pellet was suspended in 2× Laemmli SDS sample buffer and heated for 5 min at 100°C. The heat-inactivated cells (with an OD_{600} equivalent to 10) in 1/10 volume of the resolving-gel (10%) solution was added to cast the gel, and the SDS extracts as described above were subjected to this SDS-PAGE to detect the hydrolytic activities. After electrophoresis, the gel was soaked for 30 min in distilled water at room temperature and then transferred into the renaturing buffer (25 mM Tris-HCl, 1% [vol/vol] Triton X-100, pH 8.0) with gentle shaking for 16 h at 37°C to allow for renaturation. The renatured autolysins appear as clear translucent bands on the opaque background, and the contrast can be enhanced for photography by staining the gels in 1% (wt/vol) methylene blue with 0.05% KOH.

Preparation and analysis of extracellular protein fraction. For the preparation of extracellular protein extracts, bacteria were grown in LB

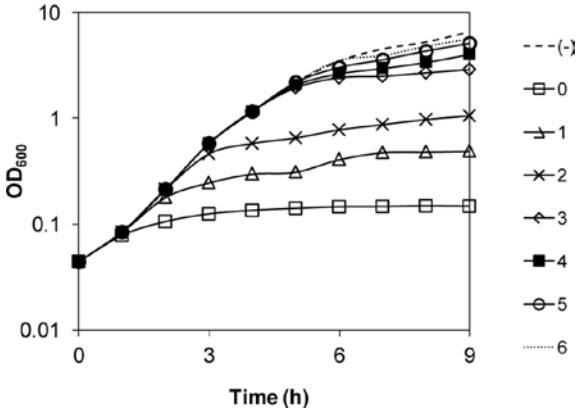

FIG 1 Growth inhibition by exogenous spermine. Cells from a fresh overnight seed culture were inoculated into prewarmed LB broth (pH 8.0). Spermine (10 mM) was added at the indicated time points after inoculation, and OD_{600} was monitored at 1-h intervals.

medium to exponential phase. After centrifugation, extracellular proteins in the supernatant (2 ml) were precipitated with 0.02% sodium deoxycholate at 4°C for 30 min followed by 10% (wt/vol) trichloroacetic acid at −20°C overnight. The precipitates were harvested by centrifugation at 4°C and 16,000 × *g* for 20 min, washed with 100% ice-cold acetone twice, and dried. The protein pellets were resolved in an appropriate volume of Laemmli SDS sample buffer, boiled, and separated by 10% SDS-PAGE. Bands showing different intensities in MuM and Mu50 samples were identified by matrix-assisted laser desorption ionization–time of flight tandem mass spectrometry (MALDI-TOF MS-MS).

ESI-MS. Solutions of spermine and oxacillin (2 mM), either alone or in combination, were prepared in ammonium acetate buffer (5 mM), and the final pH was adjusted with formic acid or ammonium hydroxide. All solutions were directly injected for electrospray ionization mass spectrometry (ESI-MS) analysis. Mass spectral acquisition was done in the positive-ion mode using the following parameters: capillary voltage, 3,000 V; sample cone voltage, 35 V; extraction cone voltage, 2.5 V; source temperature, 120°C; desolvation temperature, 150°C; gas flows desolvation, 500 liters/h; and pump flow rate, 5 μl/min.

RESULTS

Growth inhibition of Mu50 by spermine is pH dependent. While spermine and β-lactams exert a strong synergy effect on MRSA (20), spermine alone can cause growth inhibition of all tested strains of *S. aureus* (Mu50, N315, COL, and RN4220, with MICs of 1 mM, 1 mM, 0.5 mM, and 2 mM, respectively, at pH 8.0). To further understand the adverse effect of spermine, we first tested whether this effect is growth phase dependent. As shown in Fig. 1, growth of Mu50 in the buffered LB broth (20 mM Tris-Cl, pH 8.0) was immediately inhibited by the addition of spermine (10× MIC; 10 mM) regardless of the growth stage.

Spermine is a tetra-amine, and its four pK_a values were reported as 10.86, 10.05, 8.82, and 7.95 (4). At pH 7.4, the relative abundance of +4/+3 species was 3/1, and the ratio could be 1/1 at pH 8.0. If not protonated, the amino group would serve as a nucleophile for potential chemical reactions. To analyze the possible effect of spermine net charge on growth inhibition, the spermine MIC was determined for Mu50 suspended in buffered growth media with different pH values, as shown in Fig. 2A. When the pH was at 7.0 or lower, fully positively charged spermine did not have

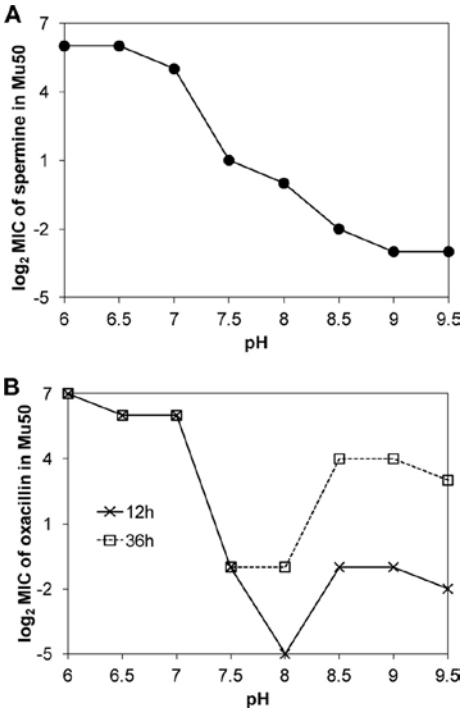

FIG 2 pH-dependent effects of spermine alone (A) or in combination with oxacillin (B). MICs of spermine or oxacillin for Mu50 were determined at different pHs. For measurements of oxacillin MICs, 0.25 times the MIC (for pH 8.0 to 9.5) or 0.5 mM (for pH 6.0 to 7.5) of spermine was included.

a strong inhibitory effect on growth, as reflected by MICs of 32 to 64 mM. Interestingly, the MIC was reduced to 2 mM at pH 7.5 and was decreased further to 0.125 mM at pH 9.0 or higher. Since the net positive charge of spermine is reduced when the pH is increased, these results strongly suggest that the growth inhibition effect of exogenous spermine may not be related to its positive charges and that instead its nucleophilic property may be the cause.

Effects of pH on oxacillin-spermine synergy in Mu50. We also analyzed the pH effect on oxacillin-spermine synergy by measuring the oxacillin MIC in the presence of spermine at different pHs (one-fourth of the MIC for pH 7.5 to 9.5 and 0.5 mM for pH 6 to 7). Like with spermine alone, such synergy also followed the same trend of pH dependence (Fig. 2B) but only when the pH was equal to or lower than 8.0. Unexpectedly, at pH 8.5 and higher, the oxacillin MIC showed the reverse trend and increased 16-fold from that at pH 8.0, and a further 32-fold increment was observed after 24 more hours of incubation. These results led us to propose oxacillin inactivation by a possible chemical reaction between nucleophilic spermine and the β-lactam ring of oxacillin (26).

To test this hypothesis, possible formation of spermine-oxacillin conjugates was analyzed by ESI-MS in the positive-ionization mode, as shown in Fig. 3. In comparison to the mass spectra for spermine and oxacillin (2 mM), a new peak corresponding to the proposed spermine-oxacillin conjugate (*m/z* 604.5) appeared in the mass spectrum of an equimolar mixture (2 mM) of spermine and oxacillin at pH 9.0 but not in that of a

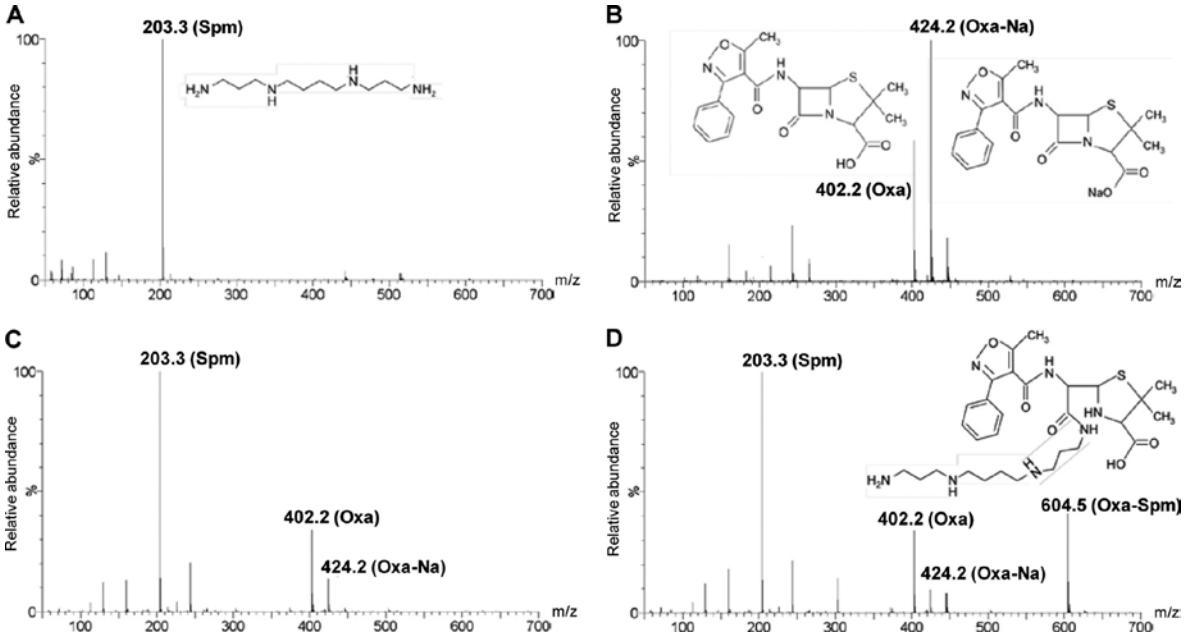

FIG 3 ESI-MS analysis. All compounds were dissolved in ammonium acetate buffer (5 mM), and mass spectra were acquired in positive-ionization mode. (A) Spermine (Spm); (B) oxacillin (Oxa); (C) equimolar mixture of spermine and oxacillin at pH 7; (D) equimolar mixture of spermine and oxacillin at pH 9.

mixture at pH 7.0. These data support pH-dependent formation of chemical conjugates between spermine and β-lactams and are consistent with the patterns of MIC readings in Fig. 2.

Selection and preliminary characterization of a spermine-resistant mutant, MuM. Strain MuM, a spermine-resistant mutant of Mu50, was isolated through selection on high concentrations of spermine as described in Materials and Methods. MuM exhibited resistance to spermine, with an MIC 32-fold higher than that of the parental Mu50 (Table 1). The genetic modification(s) in MuM was specific for spermine, as MICs of several tested antibiotics (streptomycin, tetracycline, gentamicin, erythromycin, chloramphenicol, kanamycin, and spectinomycin) for MuM were the same as those for Mu50. However, we observed significant changes in the growth behavior of MuM. In comparison, colonies of MuM on LB plates were homogeneously smaller than those of the parent strain, and these colonies required over 18 h to recover from the lag phase at 37°C when inoculated into the LB broth. Once in the logarithmic phase, the doubling time of MuM was over 3.5-fold longer than that of Mu50 (127 min versus 35 min) (Fig. 4A). However, fast-growing cells started to appear after continuous passage of MuM on LB plates, suggesting the rise of compensatory mutations from growth impairment (1). To maintain a stable MuM, we found that a glucose supplement in the LB medium was helpful, as evidenced by a reduced doubling time to 70 min with a shortened lag phase (Fig. 4A), and the spermine resistance phenotype as well as homogeneous colony size remained after passages. Another interesting phenotype of MuM was that this strain is a temperature-sensitive mutant; no apparent growth can be detected at 42°C.

Limitation of growth of MuM by pH. To examine the pH dependence of spermine effects on MuM, spermine MICs were measured under conditions of different pH. In contrast to the pH-dependent trend with its parental strain Mu50 (Fig. 2A), the spermine MIC for MuM was estimated to be 64 mM at pH 6.0 to 8.0 but, surprisingly, dropped to an undetectable level at pH 8.5 or higher. This prompted us to monitor the growth of MuM and Mu50 in buffered LB broth of pH 6.0 to 9.5 in the absence of exogenous spermine. Strain Mu50 grew comparably at pH 6.0 to

TABLE 1 MICs of oxacillin, vancomycin, and spermine for Mu50 and MuM

Antibiotic (MIC unit)	MIC[a] for strain: Mu50 Alone	Mu50 With spermine (0.5 mM)	MuM Alone	MuM With spermine (0.5 mM)	Mu50/pYX9 Alone	Mu50/pYX9 With spermine (0.5 mM)	MuM/pYX9 Alone	MuM/pYX9 With spermine (0.5 mM)
Oxacillin (μg/ml)	512	<1	1,024	1,024	512	<1	1,024	<1
Vancomycin (μg/ml)	4	4	2	<0.03	8	4	8	4
Spermine (mM)	2		64		2		2	

[a] MICs were determined in LB broth with the pH adjusted to 7.5. Plasmid pYX9 carries the wild-type *pbpB* gene.

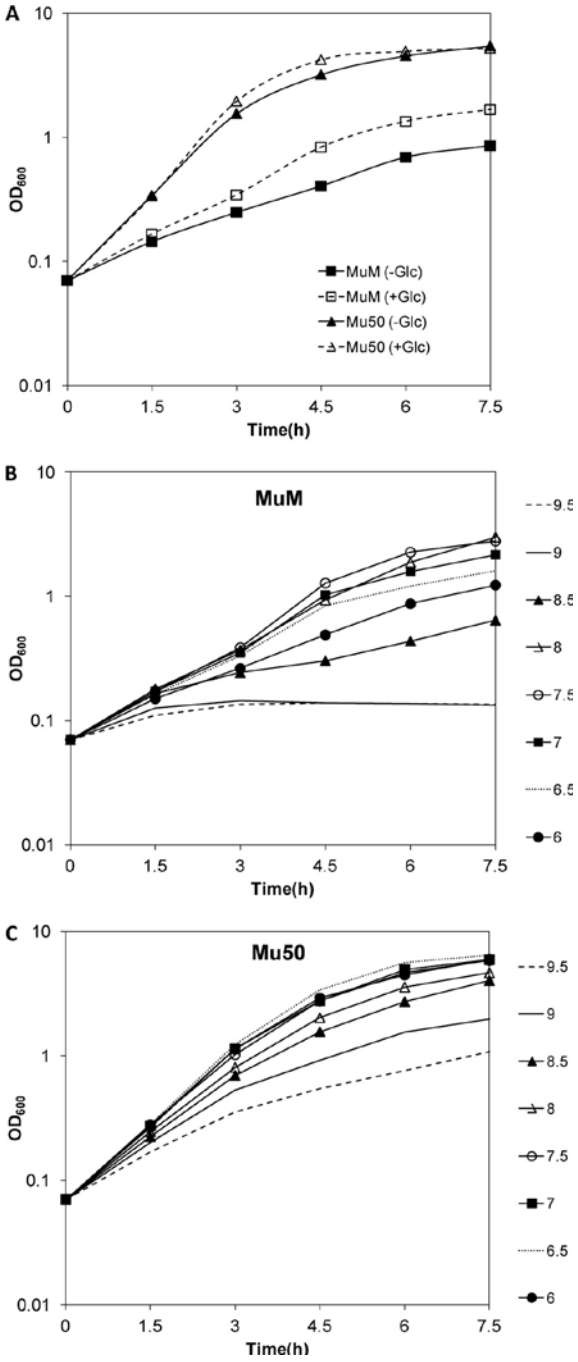

FIG 4 Growth behaviors of Mu50 and MuM. Growth of the cells in LB broth at 37°C with aeration was monitored by OD measurements. (A) Growth in the presence or absence of 0.4% glucose; (B) growth of MuM in LB buffered with 20 mM Tris-HCl at the indicated pH; (C) growth of Mu50 in LB buffered with 20 mM Tris-HCl at the indicated pH.

8.5, and the growth rate was significantly reduced at pH 9 and 9.5 (Fig. 4C). In comparison, MuM exhibited its optimal growth at pH 7.5 to 8.0 and basically showed no growth at pH 9.0 and higher (Fig. 4B).

Loss of spermine–β-lactam synergy and gain of spermine-vancomycin synergy in MuM. MICs of oxacillin and several different types of antibiotics in the presence and absence of spermine were determined for MuM and its parental stain Mu50. The results indicated that while the synergy effect of spermine was exclusively on β-lactams in Mu50, MuM behaved differently from Mu50 only on oxacillin (β-lactams in general) and vancomycin. As shown in Table 1, the MICs of oxacillin in the absence of exogenous spermine were comparable in MuM and Mu50. In the presence of 0.5 mM spermine, over a 500-fold reduction of the oxacillin MIC was observed in Mu50, whereas this sensitization effect was completely compromised in MuM. In the case of vancomycin, while its MIC was not affected by the presence of spermine in Mu50, MuM exhibited a considerable increase of susceptibility to this antibiotic when spermine (0.5 mM) was supplemented (Table 1). As an inhibitor of cell wall synthesis, vancomycin works by binding to the D-Ala-D-Ala moiety, and subsequently blocking cross-linkage, of the murein monomers during the transpeptidation reactions by PBPs (33). Such opposite responses of MuM to β-lactam and vancomycin in the presence of spermine raised the possibility that spermine may directly or indirectly inhibit cell wall synthesis.

Genome resequencing of MuM and Mu50 identifies a genetic defect in *pbpB*. To identify the mutation(s) responsible for spermine resistance, genome resequencing of MuM and Mu50 was conducted with the 454 Sequencer FLX system. On average, total base pair reads exceeded over six times the genome size, and the generated contigs covered more than 98% of the published genome sequence of Mu50. Through sequence comparison, only one sequence variation between Mu50 and MuM was identified: a 7-bp deletion in MuM which was located at nucleotides (nt) 1366 to 1372 within the *pbpB* gene, encoding an essential penicillin-binding protein (PBP) in *S. aureus*, PBP 2 (Fig. 5A). The presence of this deletion in MuM was confirmed by sequencing of a 461-bp fragment covering this region by PCR amplification from the genomic DNAs of Mu50 and MuM.

PBP 2 is composed of 727 amino acids (M_r of 80,236) with an N-terminal transglycosidase domain spanning residues 82 to 258 and a C-terminal transpeptidase domain spanning residues 361 to 629 (Fig. 5A) (UniProtKB/TrEMBL no. Q99U39). All PBPs share a penicillin-binding (PB) domain which binds β-lactam antibiotics due to the structural similarity between β-lactams and the D-Ala-D-Ala moiety of the nascent peptidoglycan, the natural substrate of PBPs. The PB domain is composed of two subdomains, and three motifs broadly conserved in PBPs lie at the interface of these two subdomains. In the case of *S. aureus* PBP 2, these three motifs comprise $SSLK_{401}$, SFN_{456}, and KTG_{585}, with S_{398} being the primary active residue (34). In MuM, a frameshift by the 7-bp deletion in *pbpB* creates an immediate stop codon that truncates the translated product from N_{456}, right at the second consensus motif, and removes the C-terminal transpeptidase domain of PBP 2 (Fig. 5A). As a result, the mutated PBP 2 was expected to lose its formation of an acyl linkage with β-lactams. To test this hypothesis, we conducted PBP labeling with Bocillin, a fluorescent derivative of penicillin. As shown in Fig. 5B, PBP 2 was not detectable in

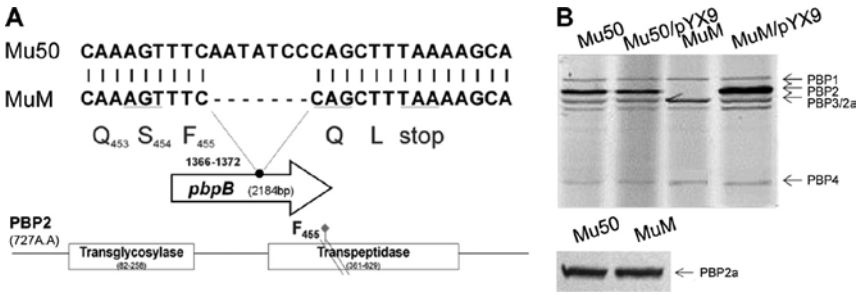

FIG 5 Identification of the *pbpB* lesion in spermine-resistant mutant MuM. (A) Sequence alignment of the *pbpB* genes from Mu50 and MuM at the mutation site. Also shown are the location of the 7-bp deletion (nt 1366 to 1372) in the *pbpB* gene of 2,184 bp, the amino acid sequence of the truncated PBP 2 of MuM, and the sizes and locations of the transglycosidase and transpeptidase domains of PBP 2. (B) The absence of PBP 2 in MuM and the presence of other penicillin-binding proteins were revealed by Bocillin labeling (top panel) or immunoblotting (bottom panel).

the membrane preparation of MuM, supporting the presence of a truncated PBP 2 in this mutant.

Complementation of the spermine-resistant MuM by *pbpB*. Plasmid pYX9 carrying *pbpB* of Mu50 was constructed for complementation tests. As shown in Table 1, in MuM carrying pYX9, spermine sensitivity and the synergy effect of spermine and β-lactams are restored. Plasmid pYX9 also restores the tolerance of MuM to vancomycin to the wild-type level in the presence of spermine. Vector alone (pCN38) does not rescue those phenotypes in MuM (data not shown). MuM/pYX9 grows much faster than MuM, with an estimated generation time comparable to that of Mu50 (data not shown). In addition, the pH sensitivity of growth was diminished in MuM/pYX9, indicating that a correct form of PBP 2 is required for the buildup of a rigid and strong cell wall to resist diverse environmental challenges.

It was suggested that different PBPs may work in concert or form a complex to coordinate PG synthesis (22). In order to see whether the sophisticated regulation of different PBPs can be affected by the addition of PBP 2, PBPs profile in Mu50 and MuM with or without pYX9 were compared. As shown in Fig. 5B, introduction of plasmid-borne wild-type PBP 2 did not have apparent effects on the production of other PBPs. MuM with vector pCN38 alone exhibited the same PBP pattern as observed in MuM (data not shown). Moreover, similar levels of PBP 2a were detected in MuM and Mu50 by immunoblotting (Fig. 5B), suggesting that the genetic lesion of *pbpB* did not affect *mecA* expression in MuM. As described below, we also conducted transcriptome analysis in MuM and Mu50; consistent with the results of Bocillin labeling and PBP 2a immunoblotting, we found comparable levels of expression for all genes encoding penicillin-binding proteins in these two strains (see Table S1 in the supplemental material).

Effects of the truncated PBP 2 in MuM on cell wall hydrolysis. The mutated *pbpB* gene of MuM may result in perturbation of cell wall synthesis and change the PG structure. To test this hypothesis, the sensitivity of MuM and Mu50 cell walls to hydrolytic enzymes was analyzed by incubation with a common source of autolytic enzyme extracts from strain COL. Degradation of the MuM cell wall materials was significantly faster than that for the Mu50 control (Fig. 6A), suggesting that cell walls of MuM may be less cross-linked and/or more susceptible to hydrolysis due to the defects in PBP 2.

It has been reported that enzymes for cell wall synthesis and hydrolysis may be coregulated and that the decreased expression of *pbpB* could repress the autolytic system in *S. aureus* (2). Here a similar situation may occur in the case of MuM. Whole-cell autolysis following exposure of MuM and Mu50 cells to Triton X-100 was assessed. As shown in Fig. 6B, the rate of Mu50 autolysis was significantly higher than that of MuM autolysis. Since the cell wall of MuM was more susceptible to degradation than that of

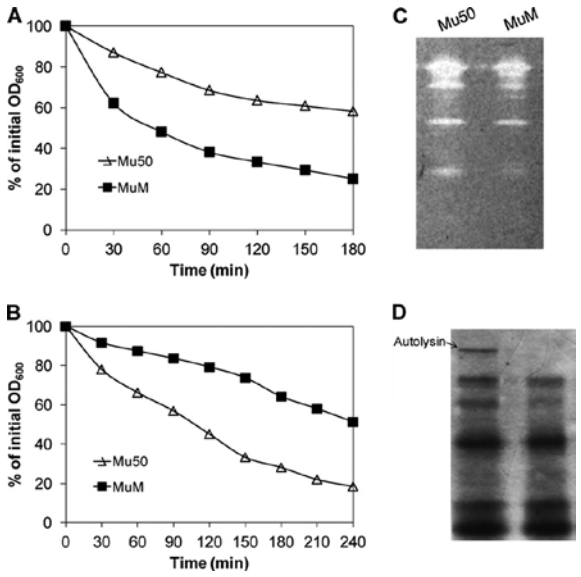

FIG 6 Analysis of cell wall hydrolysis. (A) *In vitro* susceptibility of cell walls. Crude cell walls of Mu50 or MuM were subjected to degradation by autolytic enzymes from *S. aureus* COL. Preparations of these samples are described in Materials and Methods. The experiments were reproduced several times, and data from a single representative experiment are shown. (B) Triton X-100-induced autolysis of Mu50 and MuM cells. Values indicate the average of two independent experiments. (C) Zymographic analysis of the autolysins in SDS cell extracts from Mu50 and MuM. Samples were analyzed in a 10% resolving gel containing heat-killed RN4220 cells. Lytic activity was detected by incubation of the gel with gentle agitation at 37°C in renaturing buffer. Equivalent amounts of protein samples were loaded. (D) Protein profiles in culture supernatants. Extracellular proteins from Mu50 and MuM were prepared as described in Materials and Methods. The gel was stained with Coomassie blue to detect the total secreted protein profile, and the protein band of autolysin was identified by MALDI-TOF MS-MS.

Mu50 (Fig. 6A), the lower rate of autolysis in MuM may be related to a decreased activity and/or quantity of autolytic enzymes, in addition to possible alterations in cell wall composition.

We also conducted zymographic analysis of autolytic enzymes from Mu50 and MuM. With crude cell walls of RN4220 as a substrate, several bacteriolytic bands caused by cell wall hydrolysis by the enzyme extract from MuM were less intense than those from Mu50 (Fig. 6C). Although the exact identities of these affected hydrolytic enzymes cannot be determined from this experiment, they may include the 138-kDa autolysin ATL and its proteolytic products of 62 and 51 kDa (16). In addition, the secreted protein profiles from the spent media of MuM and Mu50 in the logarithmic phase of growth were compared following SDS-PAGE. As shown in Fig. 6D, one polypeptide appeared preferentially in the protein sample of Mu50 but was completely absent in that of MuM, and this peptide was identified as autolysin ATL by MALDI-TOF MS-MS.

While the results in Fig. 6C suggest a reduced activity of cell wall hydrolytic enzymes in MuM, surprisingly, transcriptome analysis (see Table S1 in the supplemental material) revealed no apparent difference between MuM and Mu50 in expression of the major hydrolytic enzymes encoded by *atl*, *sle*, *lytM*, and *SA0620/SAV0665* (2). Since autolysin ATL requires proteolytic processing to reach its maximal activity, these somewhat contradictory results may be explained by a decreased level of ATL proteolytic processing and a greater degree of ATL retention within the cell wall of MuM, perhaps as a consequence of possible alterations in the PG composition due to the *pbpB* lesion.

Transcriptome analysis. The multiple phenotypic changes of MuM prompted us to evaluate the transcriptional profile caused by the defective PBP 2. Logarithmic-phase cells of MuM and Mu50 grown in LB alone without spermine supplement were subjected to transcriptome analysis as described in Materials and Methods. A total of 250 genes showing upregulation and 7 genes showing downregulation in MuM were identified and are listed in Table S1 in the supplemental material. In order to see whether the unique pattern of gene expression in MuM was due to the *pbpB* lesion, we also conducted transcriptome analysis of Mu50 and MuM carrying wild-type *pbpB* in *trans*. When sorted against MuM/pYX9 and Mu50/pYX9 expression profiles, the majority of the changes observed in MuM were greatly attenuated in MuM/pYX9, suggesting that the truncated PBP 2 is responsible for the complicated transcriptional adaptations in MuM. Nonetheless, it is worth noting that there are 10 genes (*czrAB*, *vraDE*, *gntPK*, *oppF*, *mtlF*, *SAV0069*, and *SAV0190*) showing up- or downregulation in MuM regardless of complementation by pYX9, and the fold change of expression of these genes in MuM/pYX9 was even greater than that in MuM.

While one might expect that the *pbpB* lesion of MuM could affect cell wall synthesis and trigger a specific stress response, the gene list in Table S1 in the supplemental material shows no overlap with the reported signature genes of the cell wall stress stimulon (17, 37). Instead, one intriguing observation was the upregulation of 67 genes associated with amino acid biosynthesis and transport that are members of the CodY regulon (23, 32). In *S. aureus*, like in many low-G+C Gram-positive bacteria, CodY is a central regulator mediating amino acid biosynthesis, nitrogen utilization, and transport of macromolecules.

Surprisingly, 67 genes residing in several genomic islands (GIs) were found to be activated in MuM (see Table S1 in the supplemental material), and this list could be expanded further if a less stringent fold change was applied in data analysis. These GIs include SCCmec, IS1181-1, SaPIm2, SaGlm, ϕMu50B, SaPIm3, and ϕMu50A (18). Although little was known about the nature of GI activation, similar activation of GIs was observed in a *murF* conditional mutant (35) in which the cell wall synthesis was perturbed in muropeptide maturation.

Other than the CodY regulon and GIs, genes that were differentially upregulated in MuM were clustered into potential operons: *ureABCEFGD* for urease synthesis, *sbnABCDRFGHI* for iron metabolism, *kdpABCDE* for an inducible potassium uptake system, *SAV2094-thiDME* for vitamin B_2 biosynthesis, and *bioFABD* for vitamin H biosynthesis. Specifically, degradation of urea by urease in *S. aureus* was thought to neutralize acidic microenvironments by generating NH_3 and CO_2 under acid stress (5). In addition, MuM also hosts the induced *arcABCD* operon for the arginine deiminase pathway, a major role of which is to alkalinize the medium by generating NH_3 and CO_2 as well as to energize the cells by production of ATP (36, 39). Together, these findings strongly suggest that MuM is primed to adjust its metabolic activities to increase the internal pH, which would imply that the defective cell wall may alter the membrane potential and somehow exert a mild acid stress on MuM.

DISCUSSION

Unique phenotypic behaviors and transcriptional adaptations of MuM. A spontaneous suppressor mutant of MRSA Mu50 with a mutation conferring resistance to β-lactams in the presence of spermine was isolated through spermine selection. This mutant possesses a unique *pbpB* lesion, in which a 7-bp deletion generates a truncated PBP 2 without the C-terminal transpeptidase (TP) domain while the transglycosidase (TG) domain at the N terminus remains intact. Although this *pbpB* mutant, MuM, still has β-lactam resistance, its physiological properties are very different from those of the parental strain Mu50, a clinical isolate of MRSA, in several aspects: gain of spermine resistance, loss of spermine–β-lactam synergy, gain of spermine-vancomycin synergy, a lower growth rate, a temperature-sensitive growth phenotype, a narrow pH range for growth, changes in cell wall composition and turnover, and a lower level of cell wall hydrolase activity. Furthermore, transcriptome analysis reveals a distinct pattern of gene expression, showing no overlap with that of the cell wall stress stimulon (17, 37).

Physiological functions of PBP 2. Our results indicate that the TP domain of PBP 2 is not essential for growth and β-lactam resistance of MRSA. These conclusions are consistent with a previous report (27) that a Ser_{398}Gly mutation at the TP domain has no effect on the MIC of methicillin but that loss of the TG activity as a result of a Glu_{114}Gln mutation causes a more-than-100-fold decrease in the methicillin MIC. In contrast, the TP activity of PBP 2 is essential for the growth of methicillin-susceptible *S. aureus* (MSSA) (30), and specific mutations at the TP domain (Pro_{458}Leu) can make MSSA resistant to β-lactam antibiotics (22). This discrepancy is due to the presence of a β-lactam-insensitive PBP 2a encoded by the *mecA* gene of MRSA. The TP activity of PBP 2a is able to sustain cell growth when that of PBP 2 is not available. Investigations from that study provide direct evidence that a mutated PBP 2 without the TP activity results in an altered cell wall composition with reduced amounts of highly

cross-linked oligomers. This is consistent with the increased cell wall degradation rate in MuM observed in our study.

In addition to the intrinsic TP and TG activities, PBP 2 may serve as scaffold for a multienzyme complex in cell wall synthesis. The presence of a multienzyme complex in cell wall synthesis was first proposed from studies of *E. coli* (14, 15). Later, Tomasz and coworkers (22, 27) reported evidence to support that PBP 2 forms a complex with PBP 2a, PBP 4, and perhaps other enzymes to coordinate cell wall synthesis and hydrolysis. Along this line, one hypothesis was that the TG and TP activities of PBP 2 are subjected to allosteric regulation within the complex and that the conformation of this complex could be affected by changes in the supporting scaffold of PBP 2. Based upon this model, we propose a working hypothesis for spermine effects on cell wall synthesis in *S. aureus*, as described below. This model may also provide an explanation of a somewhat contradictory report that insertion of a transposon at the 3′ end of *pbpB* (i.e., an intact TG domain and truncated TP domain) made the affected MRSA strain susceptible to β-lactams (31).

Proposed model of spermine–β-lactam synergy in *S. aureus*. Spermine was reported to exert a strong synergy effect with β-lactams on MRSA (20). In the current study, we present evidence that spermine alone also has a pH-dependent antibacterial activity against strains of *S. aureus* (MRSA and MSSA) and that this activity is most likely mediated by the nucleophilic property of spermine instead of its positive charges. In a search for the potential target of spermine by the genetic approach, the observed spermine-related phenotypes of MuM led us to propose that PBP 2 itself or enzymatic activities associated with the PBP 2-dependent complex in cell wall synthesis could be good candidates.

The working model we envisioned was as follows. Cell wall synthesis requires coordinated functions of a multienzyme complex to catalyze elongation of glycan chains and cross-linkage of peptide chains, and binding of spermine to this complex via PBP 2 elicits a conformational change to weaken interactions among enzymes in the complex and/or inhibit the TG activity of PBP 2. Given that a specific *pbpB* lesion confers resistance to spermine and spermine-oxacillin synergy to MuM, one would expect the TP domain of PBP 2 to be a potential target of spermine. However, we did not favor this hypothesis because TP-PBP 2 is not essential for growth of MRSA in the presence of PBP 2a. Moreover, the possibility of PBP 2a *per se* as target of spermine could also be excluded, because the spermine effects also exist in MSSA, in which PBP 2a is absent, and MuM possessing PBP 2a is resistant to spermine. Studies to elucidate the molecular mechanism for spermine effects based on the proposed model are currently in progress.

pH sensitivity of MuM. Because the TP domain of PBP 2 is truncated in MuM, it can grow in only a very limited pH range. The most striking difference between Mu50 and MuM in response to pH was under alkaline conditions (Fig. 4), which may be related to the cell wall turnover rate by the following rationale. It has been reported that the murein hydrolase exhibits a much lower level of activity under acidic conditions (38). Therefore, it is anticipated that alkaline conditions can speed up murein hydrolysis, which could have a more severe impact on MuM due to its weakened cell wall structure.

On the other hand, MuM also shows sensitivity to acidic pH. It is known that the transmembrane pH gradient is essential for the uptake of amino acids in *S. aureus* (24). The ability of MuM to adjust the transmembrane pH gradient may be reduced due to the PBP 2 mutation and concurrent cell wall anomaly, which could be a possible reason for its reduced growth rate when the pH is lower than 7. One explanation can be derived from the fact that PBP 2a is not detectable when growth is at pH 5.2 (13, 21), and therefore MuM without a functional TP of PBP 2 would encounter severe cell wall defects under acidic conditions.

In summary, several lines of evidence support PBP 2 as the potential target of spermine in sensitization of *S. aureus* to β-lactams. The absence of the TP domain in spermine-resistant MuM may liberate PBP 2 from spermine interference and concomitantly cooperate with PBP 2a to continue to be functional on exposure to β-lactams. The altered phenotypic properties and transcriptional adaptations could be the compensatory effects on cell wall composition triggered by mutated PBP 2. Future studies on the molecular mechanism of spermine interactions with the proposed PBP 2-associated multienzyme complex in cell wall synthesis hold great potential for the development of new therapeutics for MRSA infections.

ACKNOWLEDGMENTS

This work was supported in part by National Science Foundation grant NSF0950217 to C.-D. Lu and by a Molecular Basis of Disease Program fellowship from Georgia State University to X. Yao.

REFERENCES

1. Andersson DI, Hughes D. 2010. Antibiotic resistance and its cost: is it possible to reverse resistance? Nat. Rev. Microbiol. 8:260–271.
2. Antignac A, Sieradzki K, Tomasz A. 2007. Perturbation of cell wall synthesis suppresses autolysis in *Staphylococcus aureus*: evidence for co-regulation of cell wall synthetic and hydrolytic enzymes. J. Bacteriol. 189: 7573–7580.
3. Berger-Bächi B, Tschierske M. 1998. Role of fem factors in methicillin resistance. Drug Resist. Updat. 1:325–335.
4. Bergeron RJ, et al. 1995. The role of charge in polyamine analog recognition J. Med. Chem. 38:2278–2285.
5. Bore E, Langsrud S, Langsrud O, Rode TM, Holck A. 2007. Acid-shock responses in Staphylococcus aureus investigated by global gene expression analysis. Microbiology 153:2289–2303.
6. Charpentier E, et al. 2004. Novel cassette-based shuttle vector system for gram-positive bacteria. Appl. Environ. Microbiol. 70:6076–6085.
7. CLSI. 2011. Performance standards for antimicrobial susceptibility testing. M100–S21; 21st informational supplement. Clinical and Laboratory Standards Institute, Wayne, PA.
8. Cohen SS. 1997. A guide to the polyamines. Oxford University Press, New York, NY.
9. de Jonge BL, de Lencastre H, Tomasz A. 1991. Suppression of autolysis and cell wall turnover in heterogeneous Tn*551* mutants of a methicillin-resistant *Staphylococcus aureus* strain. J. Bacteriol. 173:1105–1110.
10. de Jonge BLM, Chang YS, Xu N, Gage D. 1996. Effect of exogenous glycine on peptidoglycan composition and resistance in a methicillin-resistant *Staphylococcus aureus* strain. Antimicrob. Agents Chemother. 40: 1498–1503.
11. Ghuysen JM. 1991. Serine beta-lactamases and penicillin-binding proteins. Annu. Rev. Microbiol. 45:37–67.
12. Gurevitch J, Rozansky R, Weber D, Brzezinsky A, Eckerling B. 1951. The role of spermine in the inhibition of Staphylococcus aureus by human semen. J. Clin. Pathol. 4:360–365.
13. Hartman BJ, Tomasz A. 1984. Low-affinity penicillin-binding protein associated with beta-lactam resistance in *Staphylococcus aureus*. J. Bacteriol. 158:513–516.
14. Holtje J-V. 1998. Growth of the stress-bearing and shape-maintaining murein sacculus of *Escherichia coli*. Microbiol. Mol. Biol. Rev. 62:181–203.
15. Höltje J-V. 1996. A hypothetical holoenzyme involved in the replication of the murein sacculus of Escherichia coli. Microbiology 142:1911–1918.
16. Komatsuzawa H, et al. 1997. Subcellular localization of the major autolysin, ATL and its processed proteins in Staphylococcus aureus. Microbiol. Immunol. 41:469–479.

17. **Kuroda M, et al.** 2003. Two-component system VraSR positively modulates the regulation of cell-wall biosynthesis pathway in Staphylococcus aureus. Mol. Microbiol. 49:807–821.
18. **Kuroda M, et al.** 2001. Whole genome sequencing of meticillin-resistant Staphylococcus aureus. Lancet 357:1225–1240.
19. **Kuwahara-Arai K, Kondo N, Hori S, Tateda-Suzuki E, Hiramatsu K.** 1996. Suppression of methicillin resistance in a *mecA*-containing pre-methicillin-resistant *Staphylococcus aureus* strain is caused by the mecI-mediated repression of PBP 2′ production. Antimicrob. Agents Chemother. 40:2680–2685.
20. **Kwon DH, Lu CD.** 2007. Polyamine effects on antibiotic susceptibility in bacteria. Antimicrob. Agents Chemother. 51:2070–2077.
21. **Lemaire S, Fuda C, Van Bambeke F, Tulkens PM, Mobashery S.** 2008. Restoration of susceptibility of methicillin-resistant Staphylococcus aureus to beta-lactam antibiotics by acidic pH: role of penicillin-binding protein PBP 2a. J. Biol. Chem. 283:12769–12776.
22. **Leski TA, Tomasz A.** 2005. Role of penicillin-binding protein 2 (PBP2) in the antibiotic susceptibility and cell wall cross-linking of *Staphylococcus aureus*: evidence for the cooperative functioning of PBP2, PBP4, and PBP2A. J. Bacteriol. 187:1815–1824.
23. **Majerczyk CD, et al.** 2010. Direct targets of CodY in *Staphylococcus aureus*. J. Bacteriol. 192:2861–2877.
24. **Niven DF, Hamilton WA.** 1974. Mechanisms of energy coupling to the transport of amino acids by Staphylococcus aureus. Eur. J. Biochem. 44: 517–522.
25. **Oku Y, Kurokawa K, Ichihashi N, Sekimizu K.** 2004. Characterization of the Staphylococcus aureus mprF gene, involved in lysinylation of phosphatidylglycerol. Microbiology 150:45–51.
26. **Palomo C, Oiarbide M.** 2010. β-Lactam ring opening: a useful entry to amino acids and relevant nitrogen-containing compounds, p 211–259. *In* Banik BK (ed), Heterocyclic scaffolds I, vol 22. Springer, Berlin, Germany.
27. **Pinho MG, de Lencastre H, Tomasz A.** 2001. An acquired and a native penicillin-binding protein cooperate in building the cell wall of drug-resistant staphylococci. Proc. Natl. Acad. Sci. U. S. A. 98:10886–10891.
28. **Pinho MG, de Lencastre H, Tomasz A.** 1998. Transcriptional analysis of the *Staphylococcus aureus* penicillin binding protein 2 gene. J. Bacteriol. 180:6077–6081.
29. **Pinho MG, Errington J.** 2005. Recruitment of penicillin-binding protein PBP2 to the division site of Staphylococcus aureus is dependent on its transpeptidation substrates. Mol. Microbiol. 55:799–807.
30. **Pinho MG, Filipe SR, de Lencastre H, Tomasz A.** 2001. Complementation of the essential peptidoglycan transpeptidase function of penicillin-binding protein 2 (PBP2) by the drug resistance protein PBP2A in *Staphylococcus aureus*. J. Bacteriol. 183:6525–6531.
31. **Pinho MG, Ludovice AM, Wu S, De Lencastre H.** 1997. Massive reduction in methicillin resistance by transposon inactivation of the normal PBP2 in a methicillin-resistant strain of Staphylococcus aureus. Microb. Drug Resist. 3:409–413.
32. **Pohl K, et al.** 2009. CodY in *Staphylococcus aureus*: a regulatory link between metabolism and virulence gene expression. J. Bacteriol. 191: 2953–2963.
33. **Pootoolal J, Neu J, Wright GD.** 2002. Glycopeptide antibiotic resistance. Annu. Rev. Pharmacol. Toxicol. 42:381–408.
34. **Sauvage E, Kerff F, Terrak M, Ayala JA, Charlier P.** 2008. The penicillin-binding proteins: structure and role in peptidoglycan biosynthesis. FEMS Microbiol. Rev. 32:234–258.
35. **Sobral RG, et al.** 2007. Extensive and genome-wide changes in the transcription profile of *Staphylococcus aureus* induced by modulating the transcription of the cell wall synthesis gene *murF*. J. Bacteriol. 189:2376–2391.
36. **Sonenshein AL, Hoch JA, Losick R.** 2002. *Bacillus subtilis* and its closest relatives: from genes to cells. ASM Press, Washington, DC.
37. **Utaida S, et al.** 2003. Genome-wide transcriptional profiling of the response of Staphylococcus aureus to cell-wall-active antibiotics reveals a cell-wall-stress stimulon. Microbiology 149:2719–2732.
38. **Yang SJ, Dunman PM, Projan SJ, Bayles KW.** 2006. Characterization of the Staphylococcus aureus CidR regulon: elucidation of a novel role for acetoin metabolism in cell death and lysis. Mol. Microbiol. 60: 458–468.
39. **Zuniga M, Perez G, Gonzalez-Candelas F.** 2002. Evolution of arginine deiminase (ADI) pathway genes. Mol. Phylogenet Evol. 25:429–444.

JOURNAL OF BACTERIOLOGY, Aug. 2011, p. 3923–3930 Vol. 193, No. 15
0021-9193/11/$12.00 doi:10.1128/JB.05105-11

Functional Characterization of Seven γ-Glutamylpolyamine Synthetase Genes and the *bauRABCD* Locus for Polyamine and β-Alanine Utilization in *Pseudomonas aeruginosa* PAO1[▽]

Xiangyu Yao,[1]† Weiqing He,[1,2]† and Chung-Dar Lu[1,3]*

Department of Biology, Georgia State University, Atlanta, Georgia 30303[1]; Institute of Medicinal Biotechnology, Chinese Academy of Medical Sciences and Peking Union Medical College, Beijing 100050, China[2]; and Department of Medical Laboratory Sciences and Biotechnology, China Medical University, Taichung, Taiwan 40402[3]

Received 16 April 2011/Accepted 13 May 2011

Pseudomonas aeruginosa **and many other bacteria can utilize biogenic polyamines, including diaminopropane (DAP), putrescine (Put), cadaverine (Cad), and spermidine (Spd), as carbon and/or nitrogen sources. Transcriptome analysis in response to exogenous Put and Spd led to the identification of a list of genes encoding putative enzymes for the catabolism of polyamines. Among them, *pauA1* to *pauA6*, *pauB1* to *pauB4*, *pauC*, and *pauD1* and *pauD2* (*p*olyamine *u*tilization) encode enzymes homologous to *Escherichia coli* PuuABCD of the γ-glutamylation pathway in converting Put into GABA. A series of unmarked *pauA* mutants was constructed for growth phenotype analysis. The results revealed that it requires specific combinations of *pauA* knockouts to abolish utilization of different polyamines and support the importance of γ-glutamylation for polyamine catabolism in *P. aeruginosa*. Another finding was that the list of Spd-inducible genes overlaps almost completely with that of Put-inducible ones except the *pauA3B2* operon and the *bauABCD* operon (β-*a*lanine *u*tilization). Mutation analysis led to the conclusion that *pauA3B2* participate in catabolism of DAP, which is related to the aminopropyl moiety of Spd, and that *bauABCD* are essential for growth on β-alanine derived from DAP (or Spd) catabolism via the γ-glutamylation pathway. Measurements of the *pauA3-lacZ* and *bauA-lacZ* expression indicated that these two promoters were differentially induced by Spd, DAP, and β-alanine but showed no apparent response to Put, Cad, and GABA. Induction of the *pauA3* and *bauA* promoters was abolished in the *bauR* mutant. The recombinant BauR protein was purified to demonstrate its interactions with the *pauA3* and *bauA* regulatory regions *in vitro*. In summary, the present study support that the γ-glutamylation pathway for polyamine utilization is evolutionarily conserved in *E. coli* and *Pseudomonas* spp. and is further expanded in *Pseudomonas* to accommodate a more diverse metabolic capacity in this group of microorganisms.**

Biogenic polyamines are a group of ubiquitous polycations found in all living organisms. They are essential for cell growth and participate in a variety of physiological functions (2, 30, 31). Depending on the specific biosynthetic pathways (12, 22, 26, 29), different bacteria possess a preferential set of polyamines, which include the diamines diaminopropane (DAP), putrescine (Put), and cadaverine (Cad); the triamines spermidine (Spd) and norspermidine; and the tetramine spermine. It is generally believed that polyamines form complexes with nucleic acid-containing macromolecules through charge interactions *in vivo* (8, 11, 16). *In vitro*, excess binding of polyamines to DNA was reported to form very condensed complexes (3), which might cause difficulties in DNA unwinding during replication or transcription. Therefore, the intracellular concentrations of polyamines need to be tightly monitored to prevent adverse effects on cell growth.

When released from the cells into environments, polyamines can be recycled by many bacteria or serve as sources of carbon and nitrogen. Studies conducted by Kurihara and coworkers on Put catabolism in *E. coli* (17, 19) established a novel γ-glutamylation pathway (Fig. 1), which is initiated by γ-glutamylputrescine synthetase PuuA, followed by three more reactions catalyzed by PuuB, PuuC, and PuuD in sequence, to convert Put into γ-aminobutyrate (GABA). These four enzymes, as well as the Put transporter PuuP and a transcriptional regulator PuuR, are encoded in a single *puu* gene cluster in *E. coli* (17).

Pseudomonas species, including *P. aeruginosa*, grow on several polyamine compounds as the sole source of carbon and nitrogen. However, the catabolic pathways for polyamine utilization in *Pseudomonas* were not clear. Characterization of the *spu* gene cluster identified four putative enzymes encoded by *spuIABC* for Spd/Put utilization and a Spd/Put uptake system by *spuDEFGH* (25). The impaired growth of *spuA* and *spuB* mutants on Spd and spermine suggests major roles of the SpuA and SpuB enzymes in the catabolism of these polyamines. Although the divergent *spuI* and *spuA* promoters were inducible by Put and Spd, most of the *spu* mutants grew normally on Put. Since the SpuI and SpuB enzymes are *E. coli* PuuA homologues based on sequence comparison, it is likely that the γ-glutamylation pathway plays a role on polyamine catabolism in *P. aeruginosa*.

Without γ-glutamylation, spermidine dehydrogenase encoded by the *spdH* gene was reported to catalyze oxidative cleavage of Spd into DAP and 4-aminobutyraldehyde, as well as spermine, into Spd and 3-aminopropanaldehyde (5). However, synthesis of this enzyme was not inducible by exogenous

* Corresponding author. Mailing address: Department of Biology, Georgia State University, 100 Piedmont Ave., Atlanta, GA 30303. Phone: (404) 413-5395. Fax: (404) 413-5301. E-mail: biocdl@gsu.edu.
† X.Y. and W.H. contributed equally to this study.
▽ Published ahead of print on 27 May 2011.

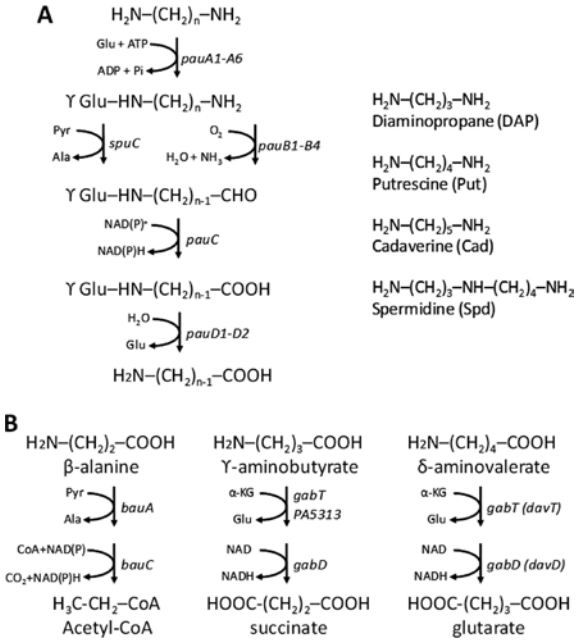

FIG. 1. Proposed diamine catabolic pathways of *P. aeruginosa*. (A) Oxidative deamination of diamines by the γ-glutamylation pathway. The *pau* genes coding enzymes for polyamine utilization in the pathway were marked. The chemical structures of three common diamines and the triamine spermidine are shown on the right. (B) Divergent catabolic pathways for β-alanine, γ-aminobutyrate, and δ-aminovalerate derived from diaminopropane, putrescine, and cadaverine. Also shown are genes encoding enzymes for the proposed reactions.

polyamines, and the *spdH* knockout mutant grew normally on Spd and spermine. It was concluded that *P. aeruginosa* PAO1 does not produce sufficient amounts of SpdH to support growth on these two polyamines.

In order to understand how *P. aeruginosa* responds to the presence of exogenous Put and Spd, DNA microarrays experiments had been conducted by our group to get snapshots of gene expression when the cells were exposed to these compounds in the exponential phase of growth (4, 20, 21). Analysis of these data has led us to report a connection of polyamine and antibiotic resistance through the PhoPQ two-component system, induction of the *dadRAX* operon for L-alanine catabolism by the putrescine-pyruvate transaminase SpuC, identification of genes that are essential for GABA utilization, and a set of redundant genes that might participate in the γ-glutamylation pathway for polyamine catabolism.

Although *E. coli* Puu homologues can be identified in the genome of PAO1 by sequence comparison, high redundancy of these homologues posed technical difficulties to conducting genetic analysis. In particular, there are seven *puuA* homologues in PAO1. In the present study, marker-less gene replacement was applied to construct a series of mutants with different combinations of *puuA* knockouts, and these mutants were tested for growth on polyamines. Transcriptome analysis indicated that genes inducible by exogenous Spd overlap with those by Put except six genes in two operons—the *pauA3B2* operon for γ-glutamylpolyamine synthetase and oxidoreductase and the *bauABCD* operon for β-alanine catabolism and uptake. Further analysis led to the conclusion that *pauA3B2* genes participate in the catabolism of DAP, the aminopropyl moiety of Spd, and that *bauABCD* genes are essential for growth on β-alanine derived from DAP (or Spd) catabolism via the γ-glutamylation pathway. A transcriptional regulator of the LysR family was identified in control of these two operons in response to β-alanine.

MATERIALS AND METHODS

Strains and growth conditions. Bacterial strains used in the study include *E. coli* DH5α and Top10 (Invitrogen) and *P. aeruginosa* PAO1. Mutants derived from PAO1 were constructed as described below or acquired from the strain stock center at University of Washington. Luria-Bertani (LB) medium was used for strain construction with the following supplements as required: ampicillin at 100 μg/ml for *E. coli* and carbenicillin at 100 μg/ml, streptomycin at 500 μg/ml, and gentamicin at 100 μg/ml for *P. aeruginosa*. Minimal medium P was used for the growth of *P. aeruginosa* supplemented with specific carbon (C) and nitrogen (N) sources, as indicated (9).

Construction of knockout mutants. For the *bauRABCD* locus, the flanking regions of the intended knockout gene were amplified by PCR, and restriction enzymes sites were introduced into the primers so that the PCR products possess configurations of 5′-BamHI-[left arm]-EcoRI-3′ and 5′-EcoRI-[right arm]-HindIII-3′. After restriction enzyme digestion, these two DNA fragments were ligated and cloned into the BamHI and HindIII sites of pRTP2 (24). The resulting plasmid was subjected to EcoRI digestion to insert a 1.6-kb EcoRI fragment containing the gentamicin resistance (Gm^r) cassette from plasmid pGMΩ1 (28). The final plasmid construct was introduced into *E. coli* SM10 to serve as the donor in the biparental conjugation (7), with a spontaneous streptomycin-resistant mutant of PAO1 as recipient. After incubation at 37°C for 6 h, the transconjugants were spread and selected on LB plates supplemented with streptomycin and gentamicin. For the construction of a series of *pauA* mutants, the protocol for gene replacement and *in vivo* excision by the Flp-FRT recombination system (10) was used to generate unmarked mutants of PAO1 with deletions on multiple genes. Expected deletions in these mutants were confirmed by PCR.

Construction of P*bauA*::*lacZ* and P*pauA3*::*lacZ* fusions. A DNA fragment of 429 bp covering the *bauR-bauA* intergenic region was amplified by PCR from the genomic DNA of PAO1 with the following two primers: 5′-TCTA GAG CGC AGG TTG AGT TCG CTG GAAC-3′ and 5′-TCT AGA CTC GCG GCC CTC GTC GGT CAG-3′. The PCR products were digested with XbaI restriction enzyme and cloned into the XbaI site of pQF50 (6), and the resulting plasmid pBAU1 was confirmed by nucleotide sequencing. For construction of the P*pauA3*::*lacZ* fusion plasmid pPAU3, the two primers (5′-CGC GGA TCC GCC GCT TTC CGG GCG TCT CT-3′ and 5′-CCC AAG CTT GGG GCT CTC TTG TCG GTC TTG-3′) were used to amplify a DNA fragment of 467 bp and clone it into the BamHI and HindIII sites of pQF50.

Electrophoretic mobility shift assays. DNA fragments covering the regulatory region of *bauA* and *pauA3* (Fig. 2) in pBAU1 and pPAU3 as described above were PCR amplified with specific pairs of oligonucleotide primers. For the binding reactions, the DNA probe (1.0 ng) was allowed to interact with different concentrations of purified BauR in a mixture of 20 μl containing 50 mM Tris-Cl (pH 7.5), 50 mM NaCl, 1 mM EDTA, 4 mM dithiothreitol, 5% (vol/vol) glycerol, negative-control DNA (1.0 ng), and 200 μg of acetylated bovine serum albumin/ml. After incubation for 20 min at room temperature, 10 μl of each reaction mixture was loaded onto a polyacrylamide gel (6%) in Tris-borate-EDTA buffer (pH 8.0). The gels were stained with SYBR green I solution (Invitrogen) for 20 min, washed twice with deionized H_2O, and scanned with an imaging system (Omega UltraLum) with excitation set at 473 nm and emission set at 520 nm.

For assays with crude extracts, the wild-type strain PAO1 and its BauR mutant were grown in glutamate minimal medium till mid-log phase. The cells were broken by Aminco French press followed by centrifugation, and the protein concentrations in the collected supernatants were determined by the Bradford method (1) using bovine serum albumin as standard. The probe covering the *bauA* regulatory region was amplified by PCR from pBAU1 and labeled with [γ-^{32}P]ATP and T4 DNA kinase according to standard protocols. The binding reactions were conducted under the conditions described above with the radioactive labeled probe and crude extracts.

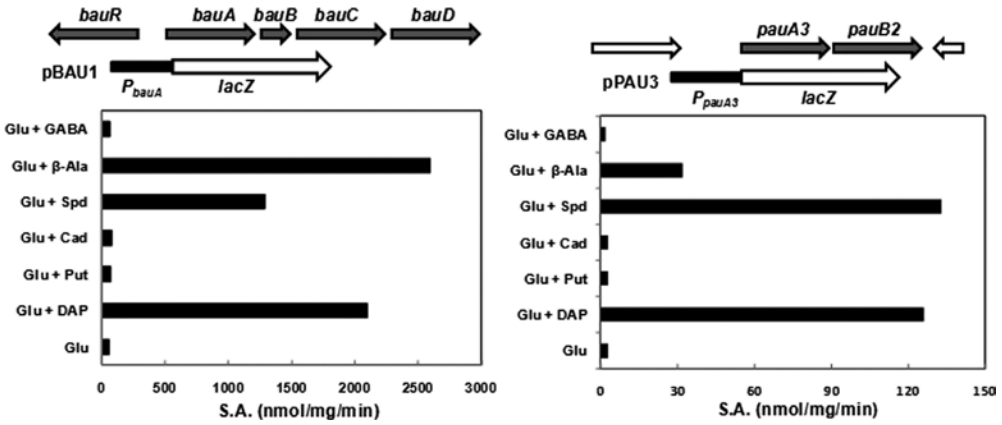

FIG. 2. Expression profile of the *bauA* and *pau3A* promoters in *P. aeruginosa* PAO1. The gene organizations of the *bauRABCD* and *pauA3B2* loci were depicted on top of each panel, followed by the schematic presentation of the respective promoter-*lacZ* fusions, pBAU1 and pPAU3. The expression of these two promoters from the fusion plasmids in strain PAO1 was monitored by measurements of the β-galactosidase activity. The cells were grown in glutamate (Glu) minimal medium in the absence or presence of diaminopropane (DAP), Put (Put), Cad (Cad), spermidine (Spd), β-alanine (β-Ala), and γ-aminobutyrate (GABA).

Expression of BauR in *E. coli*. The structural gene of *bauR* was amplified by PCR from the genomic DNA of PAO1 using the following primer pair: 5′-GCC AAA TCC CGC AAC CCG TC-3′ and 5′-GCC GAA TTC TCA CGA CAC CGC CAC CGC-3′. The resulting PCR product was digested with EcoRI and cloned into the SmaI and EcoRI sites of the expression vector pBAD-HisD (23) so that the N terminus of BauR was fused in-frame with the hexahistidine tag preceded by a ribosomal binding site and an arabinose-inducible promoter in the plasmid. The resulting plasmid, pBAUR, was introduced into *E. coli* Top10 (Invitrogen). For overexpression of BauR, the recombinant strain of *E. coli* was grown in LB medium containing ampicillin (100 μg/ml) at 37°C until the optical density at 600 nm reached 0.5, at which point 0.2% (wt/vol [final concentration]) arabinose was added to the culture for induction. Culture growth was continued for another 4 h under the same condition before harvest by centrifugation.

Purification of hexahistidine-tagged BauR. The cell pellets of *bauR* overexpression were suspended in phosphate buffer A (20 mM sodium phosphate, 0.5 M NaCl, 20 mM imidazole [pH 7.4]) plus protease inhibitors cocktail (Roche) as a protease inhibitor, and the cells were ruptured by an Aminco French press at 17,000 lb/in^2. Cell debris was removed by centrifugation at 20,000 × *g* for 30 min. The supernatant was applied to a HisTrap HP column (GE Healthcare) equilibrated with the same buffer. After the unbound proteins were washed off with equilibration buffer, His-tagged BauR was eluted at 50% of buffer B (20 mM sodium phosphate, 0.5 M NaCl, 1 M imidazole [pH 5.5]). The target fractions were pooled together and concentrated using an Aminco Ultra-15 centrifugal filter unit (molecular mass cutoff, 50 kDa; Millipore) to change the buffer to 20 mM potassium phosphate (pH 7.6) containing 1 mM EDTA.

Chemical cross-linkage of BauR (30 μg) was conducted in 10 mM HEPES buffer (pH 7.5) in a total volume of 50 μl with 10 μl of 2.3% freshly prepared solution of glutaraldehyde for 2 to 5 min at 37°C. The reaction is terminated by the addition of 5 μl of 1 M Tris-HCl (pH 8.0).

RESULTS

DNA microarrays analysis of polyamine utilization. The *puuABCD* genes (*put*rescine *u*tilization) of *E. coli* were recently reported (17) to encode four enzymes catalyzing the conversion of Put into GABA via the γ-glutamylation pathway (Fig. 1). In an attempt to explore polyamine metabolism in *P. aeruginosa*, we conducted DNA microarray experiments in strain PAO1 grown in glutamate minimal medium with or without the supplement Put or Spd (4, 21). Taking *E. coli* Puu polypeptides as templates, sequence comparison allowed us to identify Puu homologues in PAO1 genome that were found inducible by either Put or Spd from DNA microarrays experiments (Table 1). Synonymous to the nomenclature of *E. coli puu* genes, we thus designated identified six *puuA* homologues as *pauA1* to *pauA6* (*p*oly*a*mine *u*tilization), four *puuB* homologues as *pauB1* to *pauB4*, one *puuC* homologue as *pauC*, and two *puuD* homologues as *pauD1* and *pauD2* (Table 1).

The *pauA4* gene (PA2040) was not included in the original design of GeneChip due to >96% nucleotide sequence identity to *pauA1*; however, induction of its downstream PA2041 gene by Put and Spd (Table 1) led us to propose that *pauA4* is subjected to polyamine regulation. Gene PA5508 (*pauA7*) encodes the seventh and the last PuuA homologue in PAO1, and it is the only one that was not induced by Put or Spd (Table 1).

One interesting observation was that the list of Spd-inducible genes overlaps almost completely with that of Put-inducible ones, except for six genes in two putative operons, as shown in Table 1. The first operon is composed of *pauA3* and *pauB2* in polyamine catabolism, specifically for DAP as described in later sections. The second operon is composed of four genes, encoding two potential enzymes (PA0132 and PA0130), one small peptide of unknown function in the Cupin-2 super family (PA0131) with the conserved beta barrel domain, and an amino acid permease (PA0129). These four genes participate in utilization of β-alanine (pertinent data will be presented below), which is an intermediate compound of Spd and DAP degradation and hence were designated *bauABCD* (β-*a*lanine *u*tilization) for PA0132 to PA0129, respectively. In addition, PA0133 divergently transcribed from *bauA* encodes a possible transcriptional regulator of the LysR family and was designated *bauR* due to its function in control of the *bauA* promoter.

Growth phenotype analysis of *pauA* knockout mutants on polyamine utilization. In comparison to the single *puuA* gene in *E. coli*, there are seven *pauA* homologues in PAO1. To elucidate the physiological functions of these redundant genes in polyamine catabolism, a series of *pauA* mutants were constructed by the unmarked gene knockout approach as described in Materials and Methods, and the resulting mutants

TABLE 1. Selected genes from DNA microarrays analysis of putrescine and spermidine catabolism

PA ID[a]	Gene	Signal value[b]			Annotations
		Glu	Glu Put	Glu Spd	
PA0129*	*bauD*	166	85	2,311	Amino acid permease
PA0130*	*bauC*	147	210	4,498	3-Oxopropanoate dehydrogenase
PA0131*	*bauB*	124	134	3,783	Cupin-2 domain; unknown function
PA0132*	*bauA*	58	263	9,571	β-Alanine:pyruvate transaminase
PA0133	*bauR*	129	224	163	Transcriptional regulator; LysR family
PA0265	*gabD*	448	6,923	4,434	Succinate semialdehyde dehydrogenase
PA0266	*gabT*	721	9,244	6,136	GABA transaminase
PA0296	*pauA1* or *spuI*	1,113	7,613	5,044	Glutamylpolyamine synthetase
PA0297	*pauD1* or *spuA*	275	1,663	1,926	Peptidase C26 family; PFAM7722
PA0298	*pauA2* or *spuB*	582	2,625	4,244	Glutamylpolyamine synthetase
PA0299	*spuC*	1,203	6,179	7,115	Polyamine:pyruvate transaminase
PA0534	*pauB1*	26	683	34	FAD-dependent oxidoreductase
PA1565*	*pauB2*	58	42	2,111	FAD-dependent oxidoreductase
PA1566*	*pauA3*	23	13	2,057	Glutamylpolyamine synthetase
PA1742	*pauD2*	366	2,335	2,535	Glutamine amidotransferase class I
PA2040	*pauA4*	NA	NA	NA	Glutamylpolyamine synthetase
PA2041		107	1,245	971	Amino acid permease
PA2776	*pauB3*	194	3,674	2,397	FAD-dependent oxidoreductase
PA3356	*pauA5*	591	3,232	3,240	Glutamylpolyamine synthetase
PA5301	*pauR*	1,930	4,044	4,083	Transcriptional regulator; cupin-2 domain
PA5309	*pauB4*	398	1,363	1,872	FAD-dependent oxidoreductase
PA5312	*pauC* or *kauB*	922	7,744	5,540	Aldehyde dehydrogenase
PA5313	*gabT2*	144	4,226	2,095	Transaminase
PA5508	*pauA7*	118	140	79	Glutamylpolyamine synthetase homologue
PA5522	*pauA6*	116	591	566	Glutamylpolyamine synthetase

[a] The PA identification (ID) numbers were taken from the PAO1 genome annotation project (www.pseudomonas.com). Genes that are induced specifically by spermidine are marked with asterisks. These genes are divided by horizontal lines based on possible operon structures.
[b] GeneChip raw data are mean values from two independent sets of cultures. Cells were grown in minimal medium P supplemented with 20 mM concentrations of the following supplements as indicated: Glu, glutamate; Put, putrescine; or Spd, spermidine. NA, not available.

were tested for growth as the sole source of carbon and nitrogen on three diamines of different methylene chain length (DAP, Put, and Cad) and the triamine Spd.

As shown in Table 2, a single-knockout mutation on the *pauA2* gene was sufficient to block completely the growth on Spd, while the utilization of diamines remained normal. Single-knockout mutants of other six *pauA* genes grew normally on all tested polyamines (except *pauA3* on DAP as described below). Among PauA proteins, PauA1 and PauA4 exhibited >44% sequence identity to *E. coli* PuuA, and indeed growth of the *pauA1A4* double mutant on Put was severely retarded but not completely blocked. Combination of *pauA1A2A4* in strain M3A-124 and *pauA1A4A5* in strain M3A-145 were required to abolish growth on Put and Cad, respectively.

TABLE 2. Growth phenotypes of *pauA* and *pauB2* mutants on polyamines, β-alanine, and GABA

Strain	Genotype	Growth with various supplements[a]						
		Glu	Spd	Cad	Put	DAP	β-Ala	GABA
PAO1	Wild type	+	+	+	+	+	+	+
M7A	Δ*pauA1-pauA7*	+	−	−	−	−	+	+
M3A-124	Δ*pauA1A2A4*	+	−	+	−	+	+	+
M3A-145	Δ*pauA1A4A5*	+	−	−	+/−	+	+	+
M2A-14	Δ*pauA1A4*	+	+	+	+/−	+	+	+
M1A-1	Δ*pauA1*	+	+	+	+	+	+	+
M1A-2	Δ*pauA2*	+	−	+	+	+	+	+
M1A-3	Δ*pauA3*	+	+	+	+	+/−	+	+
M1A-4	Δ*pauA4*	+	+	+	+	+	+	+
M1B-2	Δ*pauB2*	+	+	+	+	−	+	+

[a] The cells were grown agar plates prepared in minimal medium with the indicated supplements as the sole source of carbon and nitrogen. Glu, glutamate; Spd, spermidine; Cad, cadaverine; Put; putrescine; DAP, diaminopropane; β-Ala, β-alanine; GABA, γ-aminobutyrate. All supplements were added to 10 mM except β-alanine to 2.5 mM. Growth on the plates was recorded in 48 h at 37°C. −, No growth after 48 h; +, growth after 24 h; +/−, growth after 48 h. All unmarked deletion mutants were derived from PAO1.

The *pauA3B2* operon was found to be inducible by Spd, as revealed from transcriptome analysis (Table 1). However, deletion of either of these two genes did not exert any apparent effect on Spd utilization. Instead, growth of the *pauA3* mutant on DAP was retarded, and the *pauB2* mutant cannot grow on DAP completely (Table 2). These results led us to propose that the *pauA3B2* operon encodes enzymes catalyzing the first two steps in DAP catabolism (Fig. 1). The presence of redundant PauA glutamylpolyamine synthetases in PAO1 likely accounts for the leaky growth phenotype of the *pauA3* mutant on DAP. In comparison, the M7 mutant deleting all seven *pauA* genes cannot grow on any tested polyamines including DAP; however, M7, as well as other *pau* mutants tested in the present study, grew normally on L-glutamate, β-alanine, and GABA.

Reminiscent of Put catabolism in *E. coli*, these results support γ-glutamylation as the first step of polyamine catabolism in *P. aeruginosa*. Via the γ-glutamylation pathway, the di-

TABLE 3. Growth phenotypes of *bauRABCD* mutants on polyamines, β-alanine, and GABA

Strain	Genotype	Growth with various supplements[a]						
		Glu	Spd	Cad	Put	DAP	β-Ala	GABA
PAO1	Wild type	+++	+++	+++	+++	+	+++	+++
	ΔbauD::GmΩ	+++	+++	+++	+++	+	++	+++
	ΔbauC::GmΩ	+++	++	+++	+++	−	−	+++
	ΔbauB::GmΩ	+++	+	+++	+++	−	−	+++
	ΔbauA::GmΩ	+++	+	+++	+++	−	−	+++
	ΔbauR::GmΩ	+++	+	+++	+++	−	−	+++
MPAO1	Wild type	+++	+++	ND	+++	+	+++	+++
	bauD::IS	+++	+++	ND	+++	+	++	+++
	bauC::IS	+++	+	ND	+++	−	−	+++
	bauA::IS	+++	++	ND	+++	−	−	+++
	bauR::IS	+++	++	ND	+++	−	−	+++

[a] The cells were grown in minimal medium with the indicated supplements as the sole source of carbon and nitrogen. Glu, glutamate; Spd, spermidine; Cad, cadaverine; Put, putrescine; DAP, 1, 3 diaminopropane; β-Ala, β-alanine; GABA, γ-aminobutyrate. All supplements were added to 10 mM except β-alanine to 2.5 mM. The optical density at 600 nm (OD_{600}) of each culture (2 ml in 15-ml culture tubes) was recorded after growth for 48 h at 37°C. −, $OD_{600} < 0.1$; +, $0.1 < OD_{600} < 0.3$; ++, $0.3 < OD_{600} < 0.8$; +++, $OD_{600} > 0.8$; ND, not determined. Deletion mutants with a gentamicin-resistant cassette (GmΩ) were derived from PAO1, and transposon insertion (IS) mutants were derived from MPAO1 and obtained from the stock center at University of Washington.

amines DAP, Put, and Cad are converted into β-alanine, GABA, and δ-aminovalerate, respectively (Fig. 1A). The situation for Spd was not clear since there are two terminal amino groups for γ-glutamylation and two possible internal C-N bonds to split the molecule into separate aminopropyl and aminobutyl moieties. Regardless, the hypothesis was that Spd could be split into β-alanine and GABA after γ-glutamylation.

Differential induction of the *bauA* and *pauA3* promoters by polyamines. The *bauABCD* and *pauA3B2* operons were found to be inducible by Spd but not by Put based on DNA microarray analysis. To substantiate this finding, the *bauA* and *pauA3* promoters in response to the presence of Spd and Put were monitored in PAO1 harboring pBAU1 (P*bauA*::*lacZ*) or pPAU3 (P*pauA3*::*lacZ*). As shown in Fig. 2, both promoters were specifically induced by exogenous Spd but not by Put. We also tested the potential effects of DAP and Cad on these promoters. Interestingly, DAP exerted an induction effect stronger than Spd did on the *bauA* promoter, whereas induction of the *pauA3* promoter by DAP was comparable to that by Spd. In comparison, Cad showed no effect on either promoter. Since Spd is composed of two methylene chains of three and four carbons (Fig. 1), these results support the view that the *bauABCD* and *pauA3B2* operons are related to DAP catabolism specifically.

β-Alanine but not GABA induces the *bauA* promoter. Polyamine catabolism is proposed to be initiated by γ-glutamylation of one terminal amino group, as first revealed in Put utilization of *E. coli*. After converting another terminal amino group into carboxyl group, the intermediate compound was catalyzed by hydrolase to release and recycle glutamate. In this scheme, GABA and β-alanine were generated from Put and DAP, respectively. Although the detailed pathway was still not clear, GABA and β-alanine were likely the intermediate compounds of Spd after splitting its aminobutyl and aminopropyl moieties, respectively.

The *bauA* and *bauC* genes have been predicted (5) to encode an β-alanine:pyruvate transaminase and a malonate semialdehyde dehydrogenase to convert β-alanine into acetyl coenzyme A (acetyl-CoA) (Fig. 1), and the proposed enzymatic activity of BauA has been reported (13). Along this line, we hypothesized that induction of the *bauABCD* operon by Spd and DAP was due to the common catabolic intermediate β-alanine and that GABA, the intermediate compound of Put catabolism, should have no effect on this operon. The activities of β-galactosidase expressed from the P*bauA*::*lacZ* fusion pBAU1 was measured in PAO1 grown in the presence or absence of GABA or β-alanine, and the results shown in Fig. 2 support this hypothesis of *bauA* induction by β-alanine.

Mutations in the *bauRABCD* genes affect β-alanine, DAP, and Spd utilization. A series of *bau*::GmΩ knockout mutants was constructed, and the growth phenotypes of these mutants on polyamines, β-alanine, and GABA as the sole source of carbon and nitrogen are shown in Table 3. All *bau* mutants grew normally on Put, Cad, and GABA, but growth on β-alanine was completely abolished when any of the *bauRABC* genes were deleted and was only partially retarded in the *bauD* mutant. These *bauRABC* mutants also exhibited different extents of growth handicap on Spd and DAP. Similar growth phenotypes were also observed in another set of mutants by transposon insertion from the University of Washington Genome Center (14). These results were in agreement with the proposed physiological functions of BauA and BauC in DAP and β-alanine catabolism and of BauD in β-alanine transport (Fig. 1) and provide a link of BauR and BauB to β-alanine catabolism.

Effects of *bauR* and *bauA* mutations on the *bauA* promoter. Since the *bauR* mutant cannot grow on β-alanine, we proposed that the expression of the *bauABCD* operon is controlled by BauR, a transcriptional regulator of the LysR family. As shown in Fig. 3, induction of the *bauA* promoter by β-alanine, DAP, and Spd was completely abolished in the *bauR* mutant, supporting BauR as transcriptional activator of the *bauABCD* operon.

The *bauA* promoter activity in response to exogenous β-alanine was also measured in the *bauA* mutant harboring pBAU1. Growth handicap of the *bauA* mutant on β-alanine (Table 3) indicates that BauA is the major, if not the only, source of β-alanine:pyruvate transaminase, and therefore β-al-

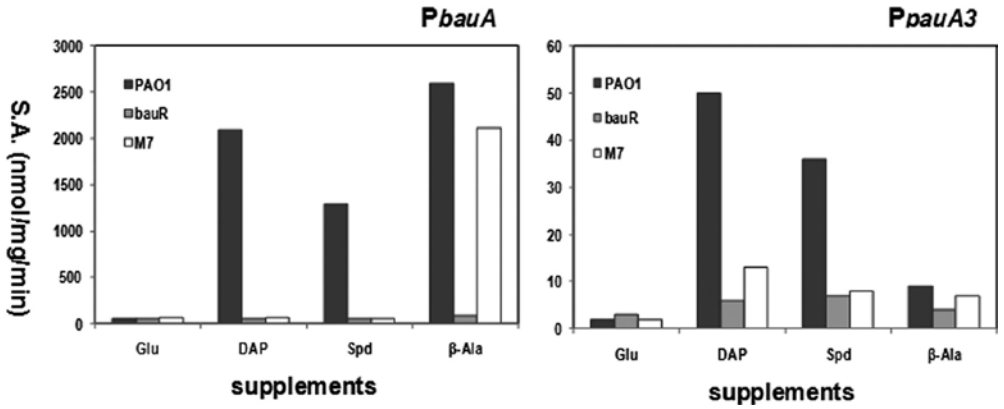

FIG. 3. Effects of *bauR* and γ-glutamylation on expression profiles of the *bauA* and *pauA3* promoters. The specific activities of β-galactosidase expressed from pBAU1 for the *bauA* promoter or pPAU3 for the *pauA3* promoter were measured from the host strains PAO1 (□), the *bauR* mutant (▨), and the M7 mutant (■) devoid of all seven *pauA* genes. The cells were grown in glutamate (Glu) minimal medium in the absence of presence of indicated supplements: diaminopropane (DAP), spermidine (Spd), and β-alanine (β-Ala).

anine was expected to accumulate without degradation in the *bauA* mutant. The *bauA* promoter was still inducible by exogenous β-alanine (data not shown), supporting β-alanine as the authentic signal compound for the *bauA* promoter activation.

γ-Glutamylation is essential for polyamine-dependent induction of the *bauA* and *pauA3* promoters. To convert into β-alanine and to induce the *bauABCD* operon, DAP or Spd needs to be glutamylated by γ-glutamylpolyamine synthetase as the first step in the proposed catabolic pathway. Therefore, one would expect abolishment of induction when there is no polyamine glutamylation and hence no β-alanine from catabolism. To test this hypothesis, the expression profile of the P_{bauA}::*lacZ* fusion was measured in strain M7, which has deletions of seven *pauA* genes. Consistent with this hypothesis, the *bauA* promoter was not subjected to induction by exogenous DAP or Spd in M7, while the induction effect of exogenous β-alanine remained (Fig. 3).

Similar experiments were also conducted in M7 harboring the P*pauA3*::*lacZ* fusion, and to our surprise polyamine-dependent induction of this promoter was significantly diminished in M7. These results prompted us to test whether BauR also plays a role in regulation of the *pauA3* promoter. As shown in Fig. 3, the *pauA3* promoter cannot be induced by DAP or Spd in the *bauR* mutant, supporting the pivotal role of BauR on *pauA3B2* expression.

Binding of BauR to the *bauA* and *pauA3* regulatory regions. Cell-free crude extracts were prepared from PAO1 and its *bauR* deletion mutant to conduct electrophoretic mobility shift assays with a ^{32}P-labeled probe covering the *bauR-bauA* intergenic region. As shown in Fig. 4A, one distinct nucleoprotein complex with slower mobility can be detected from the crude extract of PAO1 but not the *bauR* mutant. This result supports possible binding of BauR to the divergent *bauR-bauA* promoter region.

The recombinant BauR protein with a hexahistidine tag attached to its amino terminus (H-BauR) was expressed and purified from *E. coli* Top10. Although the majority of overexpressed H-BauR formed insoluble inclusion bodies, we have managed to purify this recombinant BauR protein from the remaining soluble fraction by column chromatography as described in Materials and Methods. To understand possible subunit configurations, BauR (0.5 mg/ml) was subjected to chemical cross-linkage with glutaraldehyde and monitored by SDS-PAGE. Additional polypeptides with higher molecular weights were detected (Fig. 4B), corresponding to the estimated sizes of dimers, trimers, and tetramers of BauR, plus other higher-order oligomers that were not able to resolve clearly on the gel. The inclusion of β-alanine (1 mM) in the reaction did not show any apparent effect on the distribution of these cross-linked products.

The purified H-BauR was used to demonstrate its specific interactions with the *bauA* and *pauA3* regulatory regions by electrophoretic mobility shift assays, as shown in Fig. 4C. Consistent with the conclusion from the genetic studies as described above, BauR formed specific nucleoprotein complexes with these DNA fragments, supporting BauR as a transcriptional regulator of the *bauA* and *pauA3* promoters. Although β-alanine was not required to demonstrate the DNA-binding activity of BauR, a marginal 2- to 3-fold increase on the estimated affinity of BauR to the *bauA* probe was observed by the presence of β-alanine in the reaction (Fig. 4D), as revealed from a plot of the percentage of free probe against BauR concentrations.

DISCUSSION

Redundancy and complexity of polyamine catabolism. In this study we were able to demonstrate that the M7 mutant strain of *P. aeruginosa* PAO1 devoid of seven *E. coli* PuuA homologues cannot grow on any tested polyamines as the sole source of carbon or nitrogen. In addition, it requires specific combinations of *pauA* knockouts to abolish utilization of different polyamines. These lines of genetic evidence support the functional redundancy of PauA enzymes and the importance of γ-glutamylation for polyamine catabolism in *P. aeruginosa*.

The complexity of polyamine catabolism is not limited to the

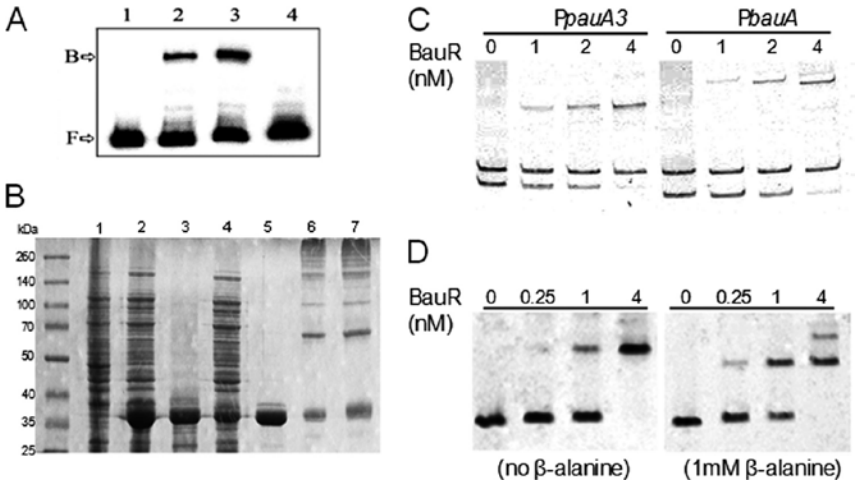

FIG. 4. Purification of BauR and demonstration of BauR-DNA interactions. (A) The presence of a nucleoprotein complex with the ^{32}P-labeled *bauA* promoter region as a probe was demonstrated by the electromobility shift assays. Lane 1, probe only; lane 2, PAO1 crude extract (4 μg); lane 3, PAO1 crude extract (9 μg); lane 4, crude extract of the *bauR* mutant (9 μg). (B) SDS-PAGE of protein fractions from BauR purification from *E. coli* Top10 harboring pBAUR. Lane 1, before arabinose induction; lane 2, after arabinose induction; lanes 3 and 4, pellet and supernatant, respectively, of the protein sample in lane 2 after 20,000 × *g* centrifugation; lane 5, eluted BauR from the nickel column; lanes 6 and 7, the purified BauR subjected to cross-linkage by glutaraldehyde without or with 1 mM β-alanine, respectively. (C) Electrophoretic mobility shift assays with the purified BauR. Two DNA probes covering the *bauA* or *pauA2* regulatory regions were used in the experiments in the presence of a nonspecific DNA fragment as negative control. (D) Binding of BauR to the *bauA* probe was analyzed in the presence or absence of 1 mM β-alanine in the reaction mixture and the running buffer.

presence of multiple *pauA* genes. After γ-glutamylation as the first step in the proposed pathway, the free amino group distal to the γ-glutamylation site is subjected to deamination, which can be accomplished either by oxidation or transamination (Fig. 1). There are four *pauB* genes for oxidative deamination (Table 1), which is supposed to operate under aerobic conditions. We have previously reported that mutants of *spuC* encoding a putrescine:alanine transaminase exhibited growth handicap on Put (25), and hence proposed the existence of a traditional transamination pathway for Put utilization (4). Since operation of the proposed traditional transamination pathway was excluded in the present study, it is likely that SpuC may participate in transamination of γ-glutamylated Put or other diamines regardless of the oxygen status.

After deamination, the aldehyde compounds were oxidized to carboxylates by PauC, an NAD(P)-dependent dehydrogenase of broad substrate specificity. The *pauC* gene was initially identified as the *kauB* gene for 4-guanidinobutyraldehyde dehydrogenase in ketoarginine utilization (15). The *kauB* mutant also cannot grow on Put, DAP, Spd, and spermine (5). Therefore, PauC (KauB) is the only entity for the proposed reaction without other redundant enzymes, even although many PauC homologues with very high sequence similarities exist in *P. aeruginosa* by BLAST search.

Two putative hydrolases were proposed (PauD1 and PauD2) to release and recycle glutamate in the last step of the γ-glutamylation pathway. The *E. coli* PuuD protein possesses the γ-glutamyl GABA hydrolase activity that is essential for Put utilization (18). PauD1 is the only *E. coli* PuuD homologue in *P. aeruginosa* PAO1 by sequence comparison (44% identity). However, we reported previously that a lesion in *pauD1* (*spuA*) causes a significant growth defect on Spd but not Put. Both PauD1 and PauD2 belong to the glutamine amidotransferase super family even though they bear no significant sequence homology. On the other hand, PauD1 was predicted by PFAM as peptidase C26 (PF07722) that has γ-glutamyl hydrolase activity. Among Put-inducible genes (4), PA2268 also encodes a polypeptide of the same predicted peptidase C26 function. Further studies are in progress to elucidate the biochemical and physiological functions of these putative enzymes.

Cleavage of Spd. Although the data represented here clearly demonstrate the importance of γ-glutamylation in Spd utilization, how Spd is cleaved into aminopropyl and aminobutyl units remains unknown. Genes that were specifically induced by Spd but not Put in DNA microarrays analysis and characterized in the present study are in fact designated for catabolism of DAP and β-alanine, which are two compounds related to the aminopropyl unit of Spd. It is possible that some PauB enzymes might be able to perform the oxidative cleavage of Spd in question.

Although the exact pathway for Spd degradation through γ-glutamylation was not clear, the fact that the *pauA3* and *pauB2* mutants exhibited growth defect on DAP but grew normally on Spd would strongly suggest that Spd catabolism does not generate DAP or glutamyl-DAP *per se*. Instead, we predicted that the cleaved products of Spd might be either glutamyl 3-aminopropan-aldehyde plus GABA or 3-aminopropan-aldehyde plus glutamyl Put.

Amino carboxylates derived from diamines. DAP, Put, and Cad are three natural diamines found in living organisms. Through the γ-glutamylation pathway, they are converted into β-alanine, GABA, and AMV, respectively. Different routes are

taken to further degrade these amino carboxylates into carbon and nitrogen sources in *Pseudomonas*. BauA and BauC catalyze two contiguous reactions to convert β-alanine into acetyl-CoA, and mutations in either of the cognate coding genes result in complete abolishment of growth on β-alanine. For GABA conversion into succinate, it involves two transaminases (GabT and PA5313) and one dehydrogenase (GabD) that are inducible by Put (4) in *P. aeruginosa*. Conversion of AMV to glutarate in *P. putida* requires DavT and DavD (27), which are orthologues of GabT and GabD of *P. aeruginosa*.

Regulation of polyamine catabolism. In *E. coli*, expression of the *puu* genes is subjected to regulation by the PuuR repressor. Due to the redundancy of *pau* genes, one would expect a more complicated regulatory system in *P. aeruginosa*. Based on sequence analysis and the physical proximity to several polyamine-inducible genes, there are at least three transcriptional regulators that likely participate in control of polyamine catabolism—PA0535, PA2267, and PA5301. In particular, PA5301 encodes a transcriptional regulator that exhibits 44% sequence identity to *E. coli* PuuR (17). Elucidating the potential functions of these regulators in control of *pau* gene expression is currently in progress.

The BauR protein was identified in the present study as a transcriptional activator for the *bauABCD* and *pauA3B2* operons in β-alanine and DAP catabolism, respectively. Induction of the *pauA3* promoter by DAP was abolished in the M7 mutant blocking all seven γ-glutamylpolyamine synthetases, suggesting that the signal molecule is the degradation product of DAP. The *bauR* gene is divergent from the *bauABCD* operon, and induction of the *bauA* promoter by β-alanine requires a functional BauR. Since β-alanine is considered as product of DAP degradation, these results suggest the presence of an unusual regulatory circuit in which an intermediate compound serves as a signal molecule for the induction of upstream and downstream genes of a catabolic pathway.

In summary, the results presented here show that the γ-glutamylation pathway for polyamine utilization is evolutionarily conserved in *E. coli* and *Pseudomonas* and is further expanded in *Pseudomonas* to accommodate the more diverse metabolic capacity in this group of microorganisms.

ACKNOWLEDGMENTS

This study was supported in part by National Science Foundation grant NSF0950217 to C.-D.L. and by a Molecular Basis of Disease Program fellowship from Georgia State University to X.Y.

REFERENCES

1. **Bradford, M. M.** 1976. A rapid and sensitive method for the quantitation of microgram quantities of protein utilizing the principle of protein-dye binding. Anal. Biochem. **72:**248–254.
2. **Casero, R. A., and A. E. Pegg.** 2009. Polyamine catabolism and disease. Biochem. J. **421:**323–338.
3. **Childs, A. C., D. J. Mehta, and E. W. Gerner.** 2003. Polyamine-dependent gene expression. Cell. Mol. Life Sci. **60:**1394–1406.
4. **Chou, H. T., D. H. Kwon, M. Hegazy, and C. D. Lu.** 2008. Transcriptome analysis of agmatine and putrescine catabolism in *Pseudomonas aeruginosa* PAO1. J. Bacteriol. **190:**1966–1975.
5. **Dasu, V. V., Y. Nakada, M. Ohnishi-Kameyama, K. Kimura, and Y. Itoh.** 2006. Characterization and a role of *Pseudomonas aeruginosa* spermidine dehydrogenase in polyamine catabolism. Microbiology **152:**2265–2272.
6. **Farinha, M. A., and A. M. Kropinski.** 1990. Construction of broad-host-range plasmid vectors for easy visible selection and analysis of promoters. J. Bacteriol. **172:**3496–3499.
7. **Gambello, M. J., and B. H. Iglewski.** 1991. Cloning and characterization of the *Pseudomonas aeruginosa lasR* gene, a transcriptional activator of elastase expression. J. Bacteriol. **173:**3000–3009.
8. **Ha, H. C., et al.** 1998. The natural polyamine spermine functions directly as a free radical scavenger. Proc. Natl. Acad. Sci. U. S. A. **95:**11140–11145.
9. **Haas, D., B. W. Holloway, A. Schambock, and T. Leisinger.** 1977. The genetic organization of arginine biosynthesis in *Pseudomonas aeruginosa*. Mol. Gen. Genet. **154:**7–22.
10. **Hoang, T. T., R. R. Karkhoff-Schweizer, A. J. Kutchma, and H. P. Schweizer.** 1998. A broad-host-range Flp-FRT recombination system for site-specific excision of chromosomally located DNA sequences: application for isolation of unmarked *Pseudomonas aeruginosa* mutants. Gene **212:**77–86.
11. **Huang, S. C., C. A. Panagiotidis, and E. S. Canellakis.** 1990. Transcriptional effects of polyamines on ribosomal proteins and on polyamine-synthesizing enzymes in *Escherichia coli*. Proc. Natl. Acad. Sci. U. S. A. **87:**3464–3468.
12. **Ikai, H., and S. Yamamoto.** 1997. Identification and analysis of a gene encoding L-2,4-diaminobutyrate:2-ketoglutarate 4-aminotransferase involved in the 1,3-diaminopropane production pathway in *Acinetobacter baumannii*. J. Bacteriol. **179:**5118–5125.
13. **Ingram, C. U., et al.** 2007. One-pot synthesis of amino-alcohols using a de-novo transketolase and beta-alanine: pyruvate transaminase pathway in *Escherichia coli*. Biotechnol. Bioeng. **96:**559–569.
14. **Jacobs, M. A., et al.** 2003. Comprehensive transposon mutant library of *Pseudomonas aeruginosa*. Proc. Natl. Acad. Sci. U. S. A. **100:**14339–14344.
15. **Jann, A., H. Matsumoto, and D. Haas.** 1988. The fourth arginine catabolic pathway of *Pseudomonas aeruginosa*. J. Gen. Microbiol. **134:**1043–1053.
16. **Khan, A. U., P. Di Mascio, M. H. Medeiros, and T. Wilson.** 1992. Spermine and spermidine protection of plasmid DNA against single-strand breaks induced by singlet oxygen. Proc. Natl. Acad. Sci. U. S. A. **89:**11428–11430.
17. **Kurihara, S., et al.** 2005. A novel putrescine utilization pathway involves gamma-glutamylated intermediates of *Escherichia coli* K-12. J. Biol. Chem. **280:**4602–4608.
18. **Kurihara, S., S. Oda, H. Kumagai, and H. Suzuki.** 2006. Gamma-glutamylgamma-aminobutyrate hydrolase in the putrescine utilization pathway of *Escherichia coli* K-12. FEMS Microbiol. Lett. **256:**318–323.
19. **Kurihara, S., et al.** 2008. γ-Glutamylputrescine synthetase in the putrescine utilization pathway of *Escherichia coli* K-12. J. Biol. Chem. **283:**19981–19990.
20. **Kwon, D. H., and C. D. Lu.** 2007. Polyamine effects on antibiotic susceptibility in bacteria. Antimicrob. Agents Chemother. **51:**2070–2077.
21. **Kwon, D. H., and C. D. Lu.** 2006. Polyamines induce resistance to cationic peptide, aminoglycoside, and quinolone antibiotics in *Pseudomonas aeruginosa* PAO1. Antimicrob. Agents Chemother. **50:**1615–1622.
22. **Lee, J., et al.** 2009. An alternative polyamine biosynthetic pathway is widespread in bacteria and essential for biofilm formation in *Vibrio cholerae*. J. Biol. Chem. **284:**9899–9907.
23. **Li, C., and C. D. Lu.** 2009. Arginine racemization by coupled catabolic and anabolic dehydrogenases. Proc. Natl. Acad. Sci. U. S. A. **106:**906–911.
24. **Li, C., and C. D. Lu.** 2009. Unconventional integration of the bla gene from plasmid pIT2 during ISlacZ/hah transposon mutagenesis in *Pseudomonas aeruginosa* PAO1. Curr. Microbiol. **58:**472–477.
25. **Lu, C. D., Y. Itoh, Y. Nakada, and Y. Jiang.** 2002. Functional analysis and regulation of the divergent *spuABCDEFGH-spuI* operons for polyamine uptake and utilization in *Pseudomonas aeruginosa* PAO1. J. Bacteriol. **184:**3765–3773.
26. **Nakada, Y., Y. Jiang, T. Nishijyo, Y. Itoh, and C. D. Lu.** 2001. Molecular characterization and regulation of the *aguBA* operon, responsible for agmatine utilization in *Pseudomonas aeruginosa* PAO1. J. Bacteriol. **183:**6517–6524.
27. **Revelles, O., M. Espinosa-Urgel, S. Molin, and J. L. Ramos.** 2004. The *davDT* operon of *Pseudomonas putida*, involved in lysine catabolism, is induced in response to the pathway intermediate delta-aminovaleric acid. J. Bacteriol. **186:**3439–3446.
28. **Schweizer, H. D.** 1993. Small broad-host-range gentamicin resistance gene cassettes for site-specific insertion and deletion mutagenesis. Biotechniques **15:**831–834.
29. **Tabor, C. W., and H. Tabor.** 1985. Polyamines in microorganisms. Microbiol. Rev. **49:**81–99.
30. **Walters, D. R.** 2003. Polyamines and plant disease. Phytochemistry **64:**97–107.
31. **Wortham, B. W., C. N. Patel, and M. A. Oliveira.** 2007. Polyamines in bacteria: pleiotropic effects yet specific mechanisms. Adv. Exp. Med. Biol. **603:**106–115.

AAC
Journals.ASM.org

γ-Glutamyl Spermine Synthetase PauA2 as a Potential Target of Antibiotic Development against *Pseudomonas aeruginosa*

Xiangyu Yao,[a] Congran Li,[b] Jianmei Zhang,[b] and Chung-Dar Lu[a,c]

Department of Biology, Georgia State University, Atlanta, Georgia, USA[a]; Institute of Medicinal Biotechnology, Chinese Academy of Medical Sciences and Peking Union Medical College, Beijing, People's Republic of China[b]; and Department of Medical Laboratory Sciences and Biotechnology, China Medical University, Taichung, Taiwan[c]

Polyamines are absolute requirements for cell growth. When in excess, *Pseudomonas aeruginosa* possesses six γ-glutamylpolyamine synthetases (GPSs) encoded by the *pauA1-pauA7* genes to initiate polyamine catabolism. Recently, the *pauA2* mutant was reported to lose the capability to grow on spermine (Spm) and spermidine (Spd) as sole carbon and nitrogen sources. Although this mutant grew normally in defined minimal medium and LB broth, growth was completely abolished by the addition of Spm or Spd. These two compounds exert a bactericidal effect (Spm > Spd) on the mutants as demonstrated by MIC measurements (over 500-fold reduction) and time-killing curves. Spm toxicity in the *pauA2* mutant was attenuated when the major uptake system was further deleted from the strain, suggesting cytoplasmic targets of toxicity. In addition, the synergistic effect of Spm and carbenicillin in the wild-type strain PAO1 was diminished in mutants without functional PauA2. Furthermore, Spm MIC was reduced by 8-fold when the Spm uptake system was deleted from the wild-type strain, suggesting a second target of Spm toxicity in the periplasm. Experiments were also conducted to test the hypothesis that native Spm and Spd in human serum may be sufficient to kill the *pauA2* mutant. Growth of the mutant was completely inhibited by 40% (vol/vol) human serum, whereas the parental strain required 80%. Colony counts indicated that the mutant but not the parent was in fact killed by human plasma. In addition, carbenicillin MIC against the mutant was reduced by 16-fold in the presence of 20% human serum while that of the parental strain remained unchanged. Taking PauA2 as the template, sequence comparison indicates that putative PauA2 homologues are widespread in a variety of Gram-negative bacteria. In summary, this study reveals the importance of GPS in alleviation of polyamine toxicity when in excess, and it provides strong support to the feasibility of GPS as a molecular target for new antibiotic development.

Spermine (Spm), along with spermidine (Spd) and putrescine (Put), is one of the three most common polyamines in human and other eukaryotic cells (3). Because of the positively charged nature, polyamines are believed to serve as ubiquitous structural components in cells through interactions with RNA and DNA macromolecules. Considerable attention has been paid to polyamine biosynthesis as a target for anti-tumor therapy because an elevated level of intracellular polyamine pools is a unique characteristic of tumor cells (21, 25). Spermine also participates in regulation of innate immunity. The tissue level of spermine is significantly increased at the inflammatory sites of infection. Released from dying cells, spermine can restrain macrophage activation in the anti-inflammatory process by inhibiting proinflammatory gene expression (24, 30).

Bacteria also need polyamines for growth. Unlike eukaryotes, most bacteria do not make spermine. It has been reported that mutant strains of *Escherichia coli* and *Pseudomonas aeruginosa* defective in polyamine biosynthesis exhibited a retarded growth phenotype (2, 17). Based on the studies in polyamine-requiring mutant strains of *E. coli*, the concept of "polyamine modulon" was proposed by Igarashi and Kashiwagi (7), referring to a group of genes whose expression requires intracellular polyamines for translational initiation. *In vitro*, exogenous polyamines have been reported to participate in many other aspects of bacterial physiology, including inhibition of swarming ability and chemotaxis (4), resistance to nitrosative stress (1), activation of biofilm formation (9), anti-mutagen activity (19, 20), and SOS induction of RecA and UvrA (11). Exogenous polyamines and the cognate uptake systems also play roles in bacterial virulence (31) and drug resistance. We have reported several significant effects of exogenous polyamines on antibiotics (13, 14). In particular, spermine increased the susceptibility of both Gram-negative *P. aeruginosa* and *E. coli* and Gram-positive methicillin-resistant *Staphylococcus aureus* (MRSA) to β-lactam antibiotics. However, molecular mechanisms for many of these multifaceted polyamine effects remain unknown.

Although polyamines are required for cell growth, these compounds could be very toxic if in excess. Depending on the pH value in the environments, polyamines can be highly positively charged molecules and potent nucleophiles. Through charge interactions, these compounds can cause DNA condensation *in vitro* (18), and as nucleophiles they are able to form covalent adducts with β-lactams (29) and potentially with other signal compounds or protein targets. To avoid these potential lethal effects, the cells need to maintain polyamine homeostasis through coordinated regulation on biosynthesis, catabolism, and uptake.

Polyamine catabolism can potentially attenuate the toxicity through modification on the amine groups and ultimately degrade the compounds. As shown in Fig. 1, polyamines are subjected to acetylation by spermidine/spermine acetyltransferase

Received 2 June 2012 **Returned for modification** 19 July 2012
Accepted 28 July 2012
Published ahead of print 6 August 2012
Address correspondence to Chung-Dar Lu, biocdl@gsu.edu.
X.Y. and C.L. contributed equally to this work.

doi:10.1128/AAC.01158-12

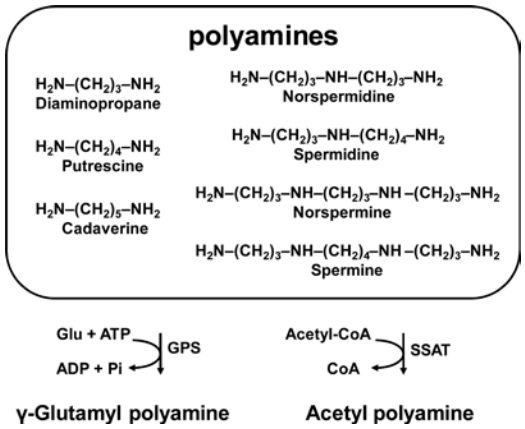

FIG 1 Schematic presentation of common polyamines and two polyamine modification reactions. GPS, glutamylpolyamine synthetase; SSAT, spermine/spermidine acetyltransferase; Glu, glutamate.

(SSAT) or γ-glutamylation by glutamylpolyamine synthetase (GPS) to initiate degradation. Human cells take the SSAT route to degrade and recycle spermidine and spermine or pump acetylated products out of the cells. In bacteria, the function of SSAT has been reported in *E. coli* (5, 15), *Bacillus subtilis* (26), and a specific strain lineage of *S. aureus* (8). *P. aeruginosa* and related bacteria do not seem to have an apparent SSAT homologue based on sequence comparison. Instead, our recent report (28) supports the presence of seven GPSs encoded by the *pauA1-pauA7* genes in polyamine catabolism. While some of these GPSs share common substrates, Spm and Spd catabolism requires absolutely the presence of a specific GPS: PauA2.

The PauA2 homologues are widely spread in Gram-negative bacteria. These enzymes were initially annotated as glutamine synthetase homologues based on sequence similarities. The first reported case of this family is PuuA of *E. coli*, which preferentially takes Put and other diamines as the substrate (12). Through the glutamylation pathway, one primary amine of putrescine, and presumably polyamines in general, is converted into carboxylic acid with the release of ammonium and recycling of glutamate. While *E. coli* was reported to possess one single set of genes for this pathway, the presence of redundant enzymes in a pseudomonad expands the capacity of these bacteria to utilize a variety of polyamines as carbon and nitrogen sources.

In this study, we further demonstrated the importance of PauA2 and Spm uptake against Spm toxicity and in Spm homeostasis of *P. aeruginosa*. Experiments were also conducted to test the hypothesis that mutants of *P. aeruginosa* without a functional PauA2 might be vulnerable to the intrinsic polyamine contents in human serum.

MATERIALS AND METHODS

Strains and growth conditions. Bacterial strains used in this study are *P. aeruginosa* PAO1 and mutants derived from PAO1. Construction and characterization of strains M1A2 (Δ*pauA2*), M7A (Δ*pauA1-pauA7*), and PAO5011 (*spuF*) have been reported (16, 28). To introduce the *spuF* allele into M1A2 and M7A, *E. coli* SM10 carrying the corresponding plasmid for allele exchange biparental conjugation was mated with the recipient strains following the protocol as described previously (16). The bacteria were routinely cultured in Luria-Bertani (LB) enriched medium at 37°C.

MIC determination. MICs of antibiotics or spermine were determined by the broth microdilution method in 96-well titer plates according to the CLSI guideline. Serial 2-fold dilutions of tested compounds were prepared in LB broth. When required, the LB medium was buffered with 20 mM Tris-HCl of the indicated pH. Fresh overnight cultures of each bacterial strain were diluted and inoculated with approximately 5×10^5 CFU/well. The plates were properly wrapped and incubated without shaking at 37°C for 16 to 18 h. The MIC was defined as the lowest concentration of the agent that inhibited the growth of the bacteria as detected by unaided eyes. The MICs were determined in triplicate.

Checkerboard testing. Checkerboard tests were performed in triplicate for the combination of carbenicillin plus spermine in LB broth (pH 8.0). The concentrations of antimicrobials ranged from approximately 4× the MIC to seven serial 2-fold dilutions below this amount. Each plate also contained a row and column in which a serial dilution of each agent was present alone. Bacteria with an inoculum of approximately 5×10^5 CFU were then added to each well, and the plates were incubated at 37°C for 18 h. Synergy was measured by determination of the fractional inhibitory concentration (FIC), which is the ratio of the MIC of a drug in combination and the MIC of the drug alone. For two interacting compounds A and B, the sum of the FICs ($\Sigma FIC = FIC_A + FIC_B$) indicates the extent of the interaction. When the ΣFIC is ≤0.5, there is a synergistic effect. A ΣFIC of 0.5 to 4.0 is defined as indifference, and a ΣFIC of ≥4.0 is defined as antagonism.

Time-killing assay. *In vitro* killing curve studies were performed as described previously. The bacterial culture was diluted in LB broth to an optical density at 600 nm (OD_{600}) reading of 0.15, and an aliquot of the diluted cells (final inoculum of approximately 1.5×10^5 CFU) was inoculated into the LB broth (pH 8.0) in the presence or absence of the indicated polyamines (10 mM Spm or 10 mM Spd). The culture was incubated at 37°C with shaking at 180 rpm. After 0, 1, 2, 4, and 6 h, samples were withdrawn and plated onto LB agar plates to obtain viable colony counts (serial dilutions were prepared when necessary). Bacterial colonies on the plates were counted after 18 to 24 h of incubation at 37°C. Experiments were performed in duplicate.

Measurements of human plasma and serum effects on bacterial growth. Pooled human plasma was obtained by anticoagulation with heparin and sterilized by filtration before use. Growth media containing the indicated percentages of plasma were prepared by mixing with appropriate proportions of cation-adjusted Mueller-Hinton broth (CAMH). The mixtures were aliquoted to 96-well plates, and inoculation of the three strains was performed as in MIC determination. The plates were properly wrapped and incubated at 35°C for 16 to 18 h. The growth of the cells in each well was recorded, and viable cells were counted for wells containing 0, 10, 50, 80, 90, and 100% human plasma. The effect of human serum on bacterial growth was also tested similarly to that of plasma. The effect of human serum on the antibacterial activity of carbenicillin against strains of *P. aeruginosa* was tested in serum concentrations of 0% to 50%.

TABLE 1 MICs of polyamines in *P. aeruginosa*

Strain (genotype)	MIC (mM) of polyamine[a]		
	Put	Spm	Spd
PAO1 (wild type)	>160	80	160
M1A2 (Δ*pauA2*)	>160	0.3	5
M7A (Δ*pauA1-pauA7*)	>160	0.3	5
PAO5011 (Δ*spuF*)	>160	10	160
M1A2F (Δ*pauA2*Δ*spuF*)	>160	1.2	40

[a] MICs were determined in LB broth with pH adjusted to 8. Put, putrescine; Spm, spermine; Spd, spermidine.

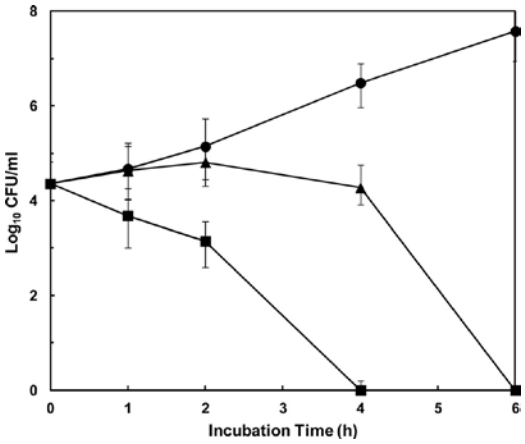

FIG 2 Time-killing curves for Δ*pauA2*. Time-killing curves were performed as described in Materials and Methods in LB broth alone (filled circle), with 10 mM spermine (filled square), or with 10 mM spermidine (filled triangle). Also shown are error bars for each data point, representing duplicate experiments.

RESULTS AND DISCUSSION

Enhanced spermidine and spermine toxicity in the mutant strains of *P. aeruginosa* devoid of PauA2. In *P. aeruginosa* PAO1 there are seven potential GPSs (PauA1-A7), which were proposed to participate in polyamine catabolism via the γ-glutamylation pathway (28). Growth of PAO1 on different polyamines requires a distinct set of PauA combinations, e.g., PauA1A2A4 for Put, PauA1A4A5 for cadaverine, and PauA2 for Spd and Spm (28). The M7A mutant devoid of seven PauA enzymes cannot grow on all tested polyamines as the sole source of carbon and nitrogen. However, the "no-growth" phenotype of the M7A or PauA2 mutant on Spd or Spm was not simply due to the lack of catabolism. We found that these mutants grew normally in the LB medium, but growth was arrested in LB supplemented with 10 mM Spm or Spd (data not shown). In comparison, addition of Put did not affect growth of M7A. The same pattern of growth phenotypes was also observed in the glutamate minimal medium with or without polyamine supplements. These results indicated that growth of these mutants without a functional PauA2 is subjected to inhibition by exogenous Spm and Spd.

To further differentiate the adverse effect of polyamines, MICs of these compounds were measured by the liquid microdilution method. As shown in Table 1, MICs of Spd and Spm reduce from 160 mM and 80 mM in the parental strain PAO1 to 5 mM and 0.3 mM, respectively, in the *pauA2* and M7A mutants. In contrast, Put MIC remains unchanged (>160 mM) even in the M7A mutant. These results support the function of PauA2 in detoxification of Spm and Spd through glutamylation, and they suggest the presence of an Spm-sensitive intracellular target of unknown nature.

Bactericidal effect of Spd and Spm. The inhibitory effect of Spd and Spm on growth was also assessed by time-killing assays. As shown in Fig. 2, growth of the *pauA2* mutant in the LB broth continues for at least 6 h. In contrast, Spd and Spm at 10 mM exert a killing effect on the *pauA2* mutant; no apparent viability of the inoculated cell population can be detected after a 6-hour exposure. The killing kinetics also revealed that Spm exerts a much stronger effect than Spd does. These results indicate that Spd and Spm, if not modified by PauA2-dependent glutamylation, have a potent bactericidal effect on *P. aeruginosa*.

Endogenous Spm and Spd were known to interact with the bacterial ribosome (22, 23). Under normal physiological conditions, one proposed function of Spm and Spd for cell viability is to ensure structural and functional integrity of the ribosome by binding to a specific region on the 23S rRNA of *E. coli* (27). In addition, Spm and Spd can also bind to tRNAs and result in acceleration of codon recognition on the ribosome (6). However, positive charges carried by polyamines have long been considered to have potential adverse effects if these essential compounds are accumulated to high concentrations inside the cells. To demonstrate the potential toxic effect of polyamines by their charge interactions with nucleic acid polymers, we tested the DNA-binding activity of Spm, Spd, and Put *in vitro*. When bound to DNA, polyamines are expected to contribute to the reduction of overall net negative charges of DNA-polyamine complexes and, hence, the mobility of these complexes on the native PAGE. Formation of these complexes would be reflected in decreased amounts of free-form DNA; no distinct retarded complex can be observed by this assay. As shown in Fig. 3, the intrinsic DNA-binding affinity of Spm is about 10-fold higher than that of Spd, and no apparent binding by Put can be detected even at a concentration of 5 mM. This trend of DNA affinity (Spm > Spd > Put) is consistent with that of toxicity by MIC measurements (Table 1).

Effects of uptake on Spm toxicity. Since *P. aeruginosa* does not make Spm through *de novo* synthesis, homeostasis of Spm would be mainly controlled by uptake and catabolism. As described above, PauA2 plays a pivotal role in Spm catabolism. Among potential uptake systems for polyamines in *P. aeruginosa* genome annotations (www.pseudomonas.com), we have reported that the *spuEFGH* operon encodes components of an ABC transport system for Spd in *P. aeruginosa* (16). Uptake of exogenous Spd was greatly diminished without a functional SpuEFGH transporter, the mutant form of which cannot grow on Spd as the sole carbon source. Based on the structural similarities, we proposed that the SpuEFGH transporter also serves for Spm uptake. To analyze the potential effects of uptake and catabolism in Spm homeostasis and, hence, Spm-dependent toxicity and synergy, a *spuF* knockout

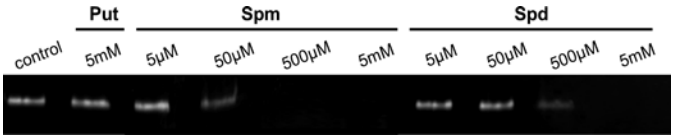

FIG 3 Binding of polyamines to DNA. Equal amounts of a DNA fragment were mixed without or with the indicated concentrations of polyamines before electrophoresis. Interactions of polyamine and DNA result in reduced intensity of the DNA fragments.

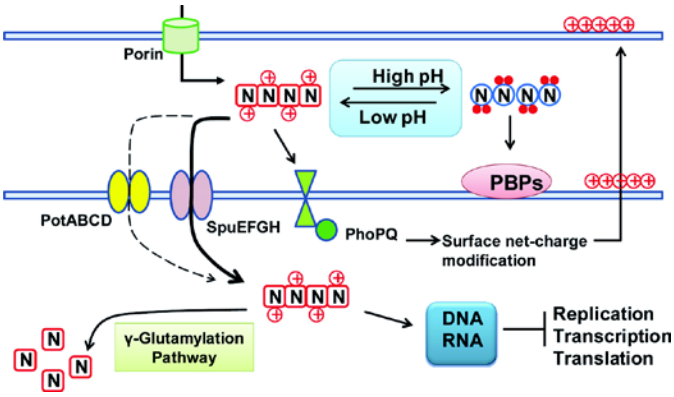

FIG 4 Summary of the "two-mode action" model of polyamines in *P. aeruginosa*. The tetra-amine spermine was used as a representative polyamine. PBPs, penicillin-binding proteins in cell wall synthesis.

lesion was introduced into the wild-type strain PAO1 and the *pauA2* mutant. Spm MICs of these strains are shown in Table 1.

If the *spuF* knockout lesion indeed blocked Spm uptake, one would expect an increased Spm MIC in the corresponding mutants regardless of the presence or absence of a functional PauA2. Surprisingly, in the presence of a functional PauA2, the Spm MIC for the *spuF* mutant was 8-fold lower than that of PAO1 (10 mM versus 80 mM). However, in the absence of PauA2, the *spuF pauA2* mutant indeed exhibited an Spm MIC 4-fold higher than that of the *pauA2* mutant (1.2 mM versus 0.3 mM). Information revealed by these somewhat contradictory results led to the following working model for the maintenance of Spm homeostasis in *P. aeruginosa*.

As shown in Fig. 4, two new molecular elements were proposed in this "two-mode action" model: (i) a second Spm transport system with uptake efficiency much lower than that of SpuEFGH and (ii) an Spm-dependent cytotoxic target in the periplasm. In the wild-type strain PAO1, exogenous Spm can pass the outer membrane barrier through unknown porins to reach the periplasm and subsequently be taken into the cytoplasm by specific transporters. Intracellular Spm will then be modified by PauA2-dependent γ-glutamylation and subjected to further degradation to support cell growth as carbon and nitrogen sources. In the *spuF* mutant, exogenous Spm accumulates in the periplasm to a level significantly higher than that in the wild-type strain PAO1 because of the absence of a high-efficiency transporter. Periplasmic Spm at a relatively high concentration may interact with and damage a molecular target essential for cell growth, perhaps through its strong nucleophilic property. Significant reduction of Spm MIC in the *spuF* mutant in comparison to PAO1 may be explained by adverse effects of Spm when accumulated in the periplasm of this mutant. In the *pauA2* mutant, a strong Spm influx into the cytoplasm but no attenuation by γ-glutamylation certainly makes this mutant more vulnerable to the Spm-dependent cytotoxic effect on an intracellular target. Without PauA2 and SpuF, the residual level of Spm uptake through the second transport system remains sufficient to cause accumulation of intracellular Spm to a level that leads to cell death. One likely candidate for the second transport system is encoded by PA3607-PA3610, which were annotated as *potABCD* based on sequence similarities to the *E. coli* counterparts (10) that encode components of an Spd transport system.

Dasu et al. have reported a periplasmic Spd/Spm dehydrogenase (3). Although this enzyme alone may not have any significant contribution to polyamine catabolism since its expression level was constitutively low and not inducible by polyamines, it may provide some degree of protection against Spm/Spd toxicity in the *spuF* mutant.

No synergy by Spm and β-lactam antibiotics in the *pauA2* mutant. Exogenous polyamines exert multiple effects on cell physiology, very likely mediated by interactions with different molecular targets. One particular effect of exogenous Spm that we have been interested in is the synergistic effect of Spm on β-lactam antibiotics. As proposed in the current working model, there are two Spm-dependent targets, one in the cytoplasm and another in the periplasm. To further understand the potential role of these two targets on synergy, we conducted checkerboard analysis in PAO1 and its mutants of *pauA2* and/or *spuF*. As shown in Fig. 5,

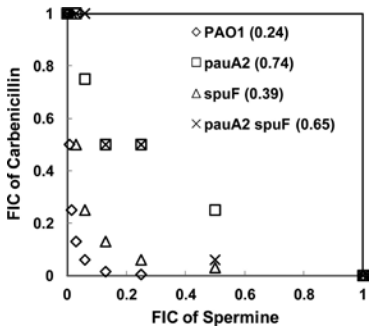

FIG 5 Isobolograms of spermine and carbenicillin FIC values against *P. aeruginosa*. Determination of FICs by checkerboard assays is described in Materials and Methods. Four strains of *P. aeruginosa* were used in this study, as indicated by different symbols, and the calculated average sum of the FICs in each strain is displayed in parentheses.

TABLE 2 Effects of human plasma and serum on growth of *P. aeruginosa*

Cell type and strain	Growth[a] of the strain in plasma or serum concn										
	100%	90%	80%	70%	60%	50%	40%	30%	20%	10%	0%
Plasma											
PAO1	−	+	+	+	+	+	+	+	+	+	+
M1A2	−	−	+	+	+	+	+	+	+	+	+
M7A	−	−	−	+	+	+	+	+	+	+	+
Serum											
PAO1	−	−	−	+	+	+	+	+	+	+	+
M1A2	−	−	−	−	−	−	−	+	+	+	+
M7A	−	−	−	−	−	−	−	+	+	+	+

[a] +, growth; −, no growth.

TABLE 3 Effect of human serum on antibacterial activity of carbenicillin against *P. aeruginosa*

Strain	MIC (μg/ml) of carbenicillin in serum concn					
	50%	40%	30%	20%	10%	0%
PAO1	16	16	16	16	32	64
M1A2	≤0.0001	≤0.0001	≤0.0001	1	32	64
M7A	≤0.0001	≤0.0001	≤0.0001	0.5	32	64

the calculated FIC index clearly indicated strong synergy with Spm and carbenicillin against the wild-type PAO1. In the *pauA2* mutant, only low concentrations of Spm can be applied because this mutant is much more sensitive to Spm than PAO1, and no synergy can be detected in this mutant. Without PauA2-dependent modification, exogenous Spm in low concentrations was sufficient to cause significant accumulation of free-form Spm inside this mutant through active uptake and resulted in cell death. The *pauA2 spuF* mutant also exhibited no synergy, as it can still take up and accumulate Spm through the second transport system as described above (Fig. 4). These results indicated that the intracellular Spm-sensitive target of unknown nature may not be required for synergy. Contrarily, synergy of carbenicillin and Spm persisted in the *spuF* mutant, of which growth inhibition by exogenous Spm was proposed to act on the second target in the periplasm. One possibility was that this Spm-dependent second target was related to cell wall synthesis. This hypothesis was consistent with our recent finding that in MRSA, a mutation in *pbpB* encoding the penicillin-binding protein 2 for cell wall synthesis can abolish the synergistic effect of exogenous Spm and β-lactams (29).

The *pauA2* mutants are more susceptible to human serum and plasma. Human cells, but not *P. aeruginosa* or many other bacteria, are able to synthesize Spm. Demand for Spm in cancer cells was found to be stronger than that in normal tissues, and Spm released from damaged tissues was reported to regulate innate immunity. Therefore, we proposed that circulating Spm in the human body may be sufficient to post adverse effects on bacteria of a loss of protective mechanisms. To test this hypothesis, survival rates of the *pauA2* mutants and the parental strain PAO1 after exposure to human plasma were measured and compared. The results demonstrated that viable cell counts of *pauA2* and PM7 were over 200-fold lower than the corresponding values of PAO1 when the concentrations of human plasma were ≥90% (data not shown).

It was noted that heparin, a highly negatively charged compound, was routinely used as an anticoagulant in preparation of plasma from pooled blood samples. Since Spm is a positively charged molecule at the physiological pH of human blood, it is conceivable that interactions of heparin and Spm by charge can reduce the working concentration of free Spm in the plasma. Therefore, pooled serum was prepared in the absence of heparin to test its effect on bacterial growth. As shown in Table 2, growth of PAO1 was more sensitive to the presence of serum than that of plasma: in 80% of bacteria, serum was sufficient to inhibit growth, whereas growth required plasma in 100% of bacteria. In comparison, the *pauA2* and M7A mutants were more susceptible than PAO1 to growth inhibition by plasma (in 80%) and even more so by serum (in 40%).

The potential effect of β-lactam antibiotics in the presence of serum was also analyzed by MIC measurements. As shown in Table 3, the carbenicillin MIC of PAO1 was reduced by 4-fold in the presence of 20 to 50% serum (64 versus 16 μg/ml), while that of the *pauA2* mutant was decreased 64-fold in the presence of 20% serum and was below 0.1 ng/ml when 30% serum was added to the growth medium. These results were surprising, as the synergistic effect of Spm and carbenicillin was lost in the *pauA2* mutant (Table 1) when tested in LB broth. Regardless, it is conceivable that PauA2 plays important roles in supporting the viability of *P. aeruginosa* in human serum. Molecular mechanisms of these PauA2-associated processes warrant further investigation.

In summary, spermine has multiple targets in *P. aeruginosa*. Our previous report indicated that they can block the outer membrane porin D and hence induce resistance to carbapenem (13) and that they can trigger the PhoPQ two-component system to modify lipopolysaccharides and result in resistance to polymyxin B (14). Through genetic studies, here we provide further evidence to support the presence and possible locations of two more targets. We demonstrated that the glutamyl polyamine synthetase PauA2 plays a major role in protection of *P. aeruginosa* against the bactericidal effect of spermine. The toxic effects of spermine may have two targets, one inside and the other outside the cells. While the intracellular target is more vulnerable without protection by PauA2, the synergistic effect of spermine and β-lactam antibiotics may come from the target in the periplasm. Although the *pauA2* mutants grew normally in rich or minimal medium, they exhibited a significant survival disadvantage as well as a pronounced synergistic effect with carbenicillin in the presence of human serum or plasma. These results support our hypothesis that circulating spermine in human bodies may potentially provide another layer of innate immunity against bacterial pathogens when the intrinsic spermine-modifying enzyme is inactivated. PauA and its homologues can be promising molecular targets for the development of new types of antibiotics against *P. aeruginosa* and related bacteria with multiple drug resistance.

ACKNOWLEDGMENTS

This work was supported in part by a National Science Foundation grant (NSF0950217) to C.-D. Lu and by the Molecular Basis of Disease Program fellowship of the Georgia State University to X. Yao.

REFERENCES

1. Bower JM, Mulvey MA. 2006. Polyamine-mediated resistance of uropathogenic Escherichia coli to nitrosative stress. J. Bacteriol. 188:928–933.
2. Chattopadhyay MK, Tabor CW, Tabor H. 2003. Polyamines protect

Escherichia coli cells from the toxic effect of oxygen. Proc. Natl. Acad. Sci. U. S. A. 100:2261–2265.
3. **Dasu VV, Nakada Y, Ohnishi-Kameyama M, Kimura K, Itoh Y.** 2006. Characterization and a role of Pseudomonas aeruginosa spermidine dehydrogenase in polyamine catabolism. Microbiology 152:2265–2272.
4. **Dela Vega AL, Delcour AH.** 1996. Polyamines decrease Escherichia coli outer membrane permeability. J. Bacteriol. 178:3715–3721.
5. **Fukuchi J, Kashiwagi K, Takio K, Igarashi K.** 1994. Properties and structure of spermidine acetyltransferase in Escherichia coli. J. Biol. Chem. 269:22581–22585.
6. **Hetrick B, et al.** 2010. Polyamines accelerate codon recognition by transfer RNAs on the ribosome. Biochemistry 49:7179–7189.
7. **Igarashi K, Kashiwagi K.** 2006. Polyamine Modulon in Escherichia coli: genes involved in the stimulation of cell growth by polyamines. J. Biochem. 139:11–16.
8. **Joshi GS, Spontak JS, Klapper DG, Richardson AR.** 2011. Arginine catabolic mobile element encoded speG abrogates the unique hypersensitivity of Staphylococcus aureus to exogenous polyamines. Mol. Microbiol. 82:9–20.
9. **Karatan E, Duncan TR, Watnick PI.** 2005. NspS, a predicted polyamine sensor, mediates activation of Vibrio cholerae biofilm formation by norspermidine. J. Bacteriol. 187:7434–7443.
10. **Kashiwagi K, Endo H, Kobayashi H, Takio K, Igarashi K.** 1995. Spermidine-preferential uptake system in Escherichia coli. ATP hydrolysis by PotA protein and its association with membrane. J. Biol. Chem. 270: 25377–25382.
11. **Kim IG, Oh TJ.** 2000. SOS induction of the recA gene by UV-, gamma-irradiation and mitomycin C is mediated by polyamines in Escherichia coli K-12. Toxicol. Lett. 116:143–149.
12. **Kurihara S, et al.** 2008. Gamma-glutamylputrescine synthetase in the putrescine utilization pathway of Escherichia coli K-12. J. Biol. Chem. 283:19981–19990.
13. **Kwon DH, Lu CD.** 2007. Polyamine effects on antibiotic susceptibility in bacteria. Antimicrob. Agents Chemother. 51:2070–2077.
14. **Kwon DH, Lu CD.** 2006. Polyamines induce resistance to cationic peptide, aminoglycoside, and quinolone antibiotics in Pseudomonas aeruginosa PAO1. Antimicrob. Agents Chemother. 50:1615–1622.
15. **Limsuwun K, Jones PG.** 2000. Spermidine acetyltransferase is required to prevent spermidine toxicity at low temperatures in Escherichia coli. J. Bacteriol. 182:5373–5380.
16. **Lu CD, Itoh Y, Nakada Y, Jiang Y.** 2002. Functional analysis and regulation of the divergent spuABCDEFGH-spuI operons for polyamine uptake and utilization in Pseudomonas aeruginosa PAO1. J. Bacteriol. 184: 3765–3773.
17. **Nakada Y, Itoh Y.** 2003. Identification of the putrescine biosynthetic genes in Pseudomonas aeruginosa and characterization of agmatine deiminase and N-carbamoylputrescine amidohydrolase of the arginine decarboxylase pathway. Microbiology 149:707–714.
18. **Pastre D, et al.** 2006. A new approach to DNA bending by polyamines and its implication in DNA condensation. Eur. Biophys. J. 35:214–223.
19. **Pillai SP, Shankel DM.** 1998. Effects of antimutagens on development of drug/antibiotic resistance in microorganisms. Mutat. Res. 402:139–150.
20. **Pillai SP, Shankel DM.** 1997. Polyamines and their potential to be antimutagens. Mutat. Res. 377:217–224.
21. **Seiler N.** 2004. Catabolism of polyamines. Amino Acids 26:217–233.
22. **Stevens L, Morrison MR.** 1968. Studies on the role of polyamines associated with the ribosomes from Bacillus stearothermophilus. Biochem. J. 108:633–640.
23. **Tabor CW, Kellogg PD.** 1967. The effect of isolation conditions on the polyamine content of Escherichia coli ribosomes. J. Biol. Chem. 242: 1044–1052.
24. **Wang H, et al.** 1998. Fetuin (alpha2-HS-glycoprotein) opsonizes cationic macrophagedeactivating molecules. Proc. Natl. Acad. Sci. U. S. A. 95: 14429–14434.
25. **Wang Y, and Casero RA, Jr.** 2006. Mammalian polyamine catabolism: a therapeutic target, a pathological problem, or both? J. Biochem. 139: 17–25.
26. **Woolridge DP, Martinez JD, Stringer DE, Gerner EW.** 1999. Characterization of a novel spermidine/spermine acetyltransferase, BltD, from Bacillus subtilis. Biochem. J. 340(Pt 3):753–758.
27. **Xaplanteri MA, Petropoulos AD, Dinos GP, Kalpaxis DL.** 2005. Localization of spermine binding sites in 23S rRNA by photoaffinity labeling: parsing the spermine contribution to ribosomal 50S subunit functions. Nucleic Acids Res. 33:2792–2805.
28. **Yao X, He W, Lu CD.** 2011. Functional characterization of seven gamma-glutamylpolyamine synthetase genes and the bauRABCD locus for polyamine and beta-alanine utilization in Pseudomonas aeruginosa PAO1. J. Bacteriol. 193:3923–3930.
29. **Yao X, Lu CD.** 2012. A PBP 2 mutant devoid of the transpeptidase domain abolishes spermine-beta-lactam synergy in Staphylococcus aureus Mu50. Antimicrob. Agents Chemother. 56:83–91.
30. **Zhang M, Wang H, Tracey KJ.** 2000. Regulation of macrophage activation and inflammation by spermine: a new chapter in an old story. Crit. Care Med. 28:N60–N66.
31. **Zhou L, Wang J, Zhang LH.** 2007. Modulation of bacterial type III secretion system by a spermidine transporter dependent signaling pathway. PLoS One 2:e1291. doi:10.1371/journal.pone.0001291.